Universidade do Minho
Escola de Ciências da Saúde

Andreia Cristiana Teixeira de Castro

Identification of modulators of ataxin-3 proteotoxicity in animal models of Machado-Joseph disease.

Identificação de modificadores da proteotoxicidade da ataxina-3 em modelos animais para a doença de Machado-Joseph.

Maio de 2011

Identification of modulators of ataxin-3 proteotoxicity in animal models of Machado-Joseph disease.
Identificação de modificadores da proteotoxicidade da ataxina-3 em modelos animais para a doença de Machado-Joseph.
Andreia Cristiana Teixeira de Castro
UMinho | 2011

Universidade do Minho
Escola de Ciências da Saúde

Andreia Cristiana Teixeira de Castro

Identification of modulators of ataxin-3 proteotoxicity in animal models of Machado-Joseph disease.

Identificação de modificadores da proteotoxicidade da ataxina-3 em modelos animais para a doença de Machado-Joseph.

Tese de Doutoramento em Ciências da Saúde
Especialidade de Ciências da Saúde

Trabalho efectuado sobre a orientação da
Professora Doutora Patrícia Espinheira de Sá Maciel
Professora Auxiliar da Escola de Ciências da Saúde,
Universidade do Minho, Braga, Portugal.

e co-orientação do
Professor Doutor Richard I. Morimoto
Bill and Gayle Cook Professor of Biology,
Director, Rice Institute for Biomedical Research,
Northwestern University, Evanston, USA.

Maio de 2011

Declaração

NOME: Andreia Cristiana Teixeira de Castro

ENDEREÇO ELECTRÓNICO: accastro@ecsaude.uminho.pt

TÍTULO DA TESE DE DOUTORAMENTO:
Identificação de modificadores da proteotoxicidade da ataxin-3 em modelos animais para a doença de Machado-Joseph.
Identification of modulators of ataxin-3 proteotoxicity in animal models of Machado-Joseph disease.

ORIENTADOR:
Professora Doutora Patrícia Maciel

CO-ORIENTADOR:
Professor Doutor Richard Morimoto

DOUTORAMENTO EM:
Ciências da Saúde

Universidade do Minho, ___/___/_____

Assinatura:

_____

À minha família e ao Pedro.

Agradecimentos/Acknowledgments

As últimas palavras (a serem escritas) de uma tese são provavelmente as de maior importância. Ao finalizar este trabalho gostaria de expressar o meu profundo agradecimento a todos os que de uma forma ou de outra contribuíram para a realização desta tese. A todos o meu MUITO OBRIGADA!

À Professora Patrícia Maciel, pelo apoio, pela paciência, pela confiança e pelas palavras de incentivo nos momentos mais difíceis da realização deste trabalho. Pelas ideias e pedido de experiências controlo que se tornam as verdadeiras experiências chave! Por NÃO querer ver cada gel, dando-nos assim liberdade e preparação para o futuro! Pela energia, pelas correções rápidas e eficientes, e por não mostrar que se chateia com o facto de ser tudo em cima da hora! Obrigada!

I would like to thank Professor Rick Morimoto for welcoming me in his laboratory and specially for challenging me scientifically and for giving me the freedom to pursue my goals. Thank you also for creating a scientifically critical but also helpful laboratory environment.

À Fundação para a Ciência e Tecnologia por me ter possibilitado a realização deste trabalho, através da concessão da bolsa (SFRH/BD/27258/2006).

À Professora Cecília Leão pelo papel determinante na criação de uma Escola (ECS) e Instituto (ICVS) de investigação (mais recentemente Laboratório Associado) com todas as condições para a realização de um bom trabalho. Por, assim como eu, acreditar que se podem marcar provas de doutoramento em 5 semanas.

Ao ginásio da UM por me ajudar a manter a sanidade mental e a ter ideias!

Aos NeRDs pelas discussões acesas e criticas construtivas!

Às meninas do piso 1 (pitos e pulmões) por não se chatearem com a redução da luz da sala e partilharem as lupas.

Aos "engenheiros" Nuno Dias, JoãoO, JoãoV, Pedro Rodrigues e Carlos Bessa por me facilitarem grandemente a vida com a vontade de automatizar!

Às meninas (e poucos meninos) da DMJ: Anabela, Ana João, Andreia Carvalho, Sara Silva, Carina, Márcio e Diogo, pela companhia, pela imprescindível ajuda e incentivo. Às meninas das *Terapias ratinho* por serem

pouco sucintas nas reuniões e me irritarem por isso! Aos membros da *Função* por me deixarem ser penetra! Às *minhas* meninas das *Terapias C. elegans* Ana Jalles, Adriana e Sara Carvalho muito obrigada pela vossa ajuda, pelas perguntas que me ajudam a evoluir cada dia, pela entrega ao trabalho e por gostarem tanto disto como eu! Jalles obrigada pela ajuda incondicional! Espero poder retribuir!

À Fernanda pela amizade, sinceridade, por poder sempre contar contigo sempre e por poder dizer tudo o que penso e gostares de mim na mesma. Pelas conversas na passadeira!

To all my Morimoto lab mates, past and present (I'm sorry I cannot mention you all individually) for the help, support, discussions and excellent company during my short term visits to the lab. For all the great insights into American culture! It was great to work with all of you! Uma palavra especial para a Catarina, pela amizade, boa disposição, companhia, pelo optimismo científico e pela partilha de experiências. Sue, for understanding may stress and for being always there! I miss you all!

To Diane, for all the friendship and support. For the late night kitchen conversations and snacks... for letting me share the Portuguese culture and for making me feel that I was at "home"! I will never forget you....

À D. Emília e ao Sr. José, ao Rui e à Luísa, à Xanda e ao Jony, à Ani, ao Fred e à Kikas pelas palavras de carinho e de força. À Beatriz por me fazer esquecer o trabalho e pela companhia aos domingos á tarde durante a escrita desta tese.

Aos meus pais, por me apoiarem incondicionalmente, e a quem devo tudo o que sou e o que construí. Por ficarem mais felizes do que eu com as NOSSAS vitórias! Ao Nuno, pelo exemplo de sucesso e pelo apoio sempre presente e por perguntares *qual é o Impact Factor?*

Por fim, ao Pedro por todo o amor e compreensão. Pelo incondicional apoio e pela frase constante: "Tu vais conseguir, eu tenho a certeza!". Por ouvires os meus desabafos e os pores em perspectiva. Pela compreensão na minha falta de tempo! Pela paciência quando finjo que percebo de informática. E por mais tudo aquilo que aqui não pode ser escrito, esta tese também é tua! Prometo que é a ultima!

"Identification of modulators of ataxin-3 proteotoxicity in animal models of Machado-Joseph disease"

Abstract

At least nine human neurodegenerative diseases are caused by the expansion of CAG repeats within otherwise unrelated genes. In these diseases, including Machado-Joseph disease (MJD), polyglutamine (polyQ) expansions cause the appearance of misfolded protein species, that ultimately lead to the formation of aggregates and neuronal loss. Along with the pathogenic motif, all these diseases have in common the fact that the associated gene products are widely expressed but affect only specific subsets of neurons. This specificity suggests that protein misfolding and its toxic outcomes may be determined by the polyQ-flanking sequences of the specific disease-associated proteins. Ataxin-3 (ATXN3) is a polyQ protein and expansion of its repetitive glutamine tract causes MJD. MJD is characterized by the formation of ubiquitylated intra-neuronal inclusions but the mechanism underlying mutant ATXN3-mediated neuronal dysfunction still remains unsolved.

Caenorhabditis elegans offers unique advantages for examining the aggregation dynamics of aggregation-prone proteins and its toxic effects on individual neurons, since the transparency of all 959 cells allows easy detection of fluorescent proteins in live animals. Despite having relatively few neurons, *C. elegans* display a wide array of complex behaviors and a clear link exists between the behavior and the function of neuronal subsets.

In this study, we established a novel pan-neuronal *C. elegans* model for the study of ATXN3 pathogenesis. Pan-neuronal expression of mutant ATXN3 leads to a polyQ-length dependent, neuron subtype-specific aggregation and neuronal dysfunction. Analysis of different neurons revealed a pattern of dorsal nerve cord and sensory neuron processes susceptibility to mutant ATXN3 that was distinct from the aggregation and toxicity profiles of polyQ-alone proteins. This suggests that the sequences flanking the polyQ-stretch in ATXN3 have a dominant influence on cell-intrinsic neuronal factors that modulate polyQ-mediated pathogenesis.

We investigated the role of the wild-type (WT) ATXN3 in polyQ-related pathogenesis and found that WT ATXN3 is irreversibly recruited into polyQ-containing cellular aggregates, aggravating the animals' motor dysfunction. In contrast, genetic ablation of endogenous *C. elegans* ATX-3 did not modulate MJD pathogenesis. Our findings support the idea that, unlike what happens in other polyQ disorders, WT ATXN3 does not seem to display a neuroprotective role in MJD.

We have also found that in *C. elegans* mutations reducing insulin/insulin growth factor (IGF)-1-like signaling (IIS) pathway partially rescues mutant ATXN3-mediated aggregation and toxicity. Strikingly, other longevity-related pathways showed different effects on ATXN3 proteotoxicity: dietary restricted animals succumbed to neuronal ATXN3 pathogenesis at similar rates to those of regularly fed animals. In turn, mutations leading to altered mitochondrial function and known to lead to increased longevity showed heterogeneous effects: *clk-1* mutation severely aggravated mutant ATXN3 pathogenesis, whereas *isp-1* mutation caused a significant delay in the appearance of aggregates. These results suggest that, in spite of improving global organism survival, aging-related pathways may not always show a positive effect on conformational disorders.

Heat shock factor 1 (HSF-1) plays a neuroprotective role in ATXN3-mediated pathology in *C. elegans.* However, in mice, genetic reduction of *Hsf-1* resulted in comparable motor uncoordination and pathology, when compared with MJD transgenic mice with two copies of *Hsf-1* gene, suggesting that one copy of *Hsf-1* is sufficient to cope with ATXN3(Q94) proteotoxicity in mice.

Lastly, we validated our novel *C. elegans* model as a tool for identification of potential therapeutic compounds for MJD and established five compounds, potentially involved in heat shock response, autophagy, transcription regulation and longevity, as good candidates to test in higher model organisms for MJD.

In summary, this work provided new clues for the study of ATXN3 pathogenesis and the role of the WT protein in disease. It raised new hypotheses regarding the mechanistic link(s) between aging determinants and proteotoxicity. It also made available a valuable *C. elegans* model/tool for drug discovery and target identification that can be very useful in future therapy development in MJD.

"Identificação de moduladoras da proteotoxicidade da ataxina-3 em modelos animais para a doença de Machado-Joseph"

Resumo

Diferentes doenças neurodegenerativas humanas são causadas por uma expansão de uma repeticão CAG em genes que, de outra forma, não estão relacionados. Neste tipo de doenças, nomeadamente na doença de Machado-Joseph (DMJ), a expansão de poliglutaminas (poliQ) está associada a uma alteração da conformação das proteínas, com consequente formação de agregados e perda de células neuronais. Além do domínio patogénico, todas estas doenças têm em comum o facto de as suas proteínas causadoras terem uma expressão ubíqua, mas somente afectarem populações específicas de neurónios características de cada uma das doenças. Esta especificidade sugere que a agregação proteica e os seus efeitos tóxicos podem ser determinados pela sequência aminoacídica de cada proteína. A ataxina-3 (ATXN3) contém um segmento de poliQ cuja expansão está na origem da DMJ. A DMJ, assim como outras doenças de poliQ, é caracterizada pela formação de inclusões intraneuronais ubiquitiladas, mas o mecanismo associado à disfunção neuronal causada pela expressão da ATXN3 mutante não é totalmente compreendido.

O nemátode *Caenorhabditis elegans* proporciona grandes vantagens no estudo dos efeitos tóxicos de proteínas poliQ em neurónios, uma vez que a transparência das suas 959 células facilita a detecção de proteínas fluorescentes *in vivo*. Apesar de apresentarem um número reduzido de neurónios, os *C. elegans* apresentam inúmeros comportamentos complexos, existindo uma relação clara entre a função de determinados subtipos neuronais e o comportamentos regulados por esses grupos de neurónios.

Neste estudo, estabelecemos um novo modelo animal com expressão da ATXN3 humana em todas as células do sistema nervoso dos *C. elegans*, para o estudo da patogénese da DMJ. A expressão da ATXN3 mutada resulta no aparecimento de agregados e em disfunção neurológica. Ambos os fenótipos dependem do tamanho da sequência de poliQ da ATXN3. A análise de neurónios específicos revelou que os processos de neurónios sensoriais e do cordão nervoso dorsal são especificamente afectados em animais que expressam a ATXN3 mutante e não em animais que expressam proteínas poliQ. Estes resultados sugerem que o efeito das sequências flanqueantes da ATXN3 se sobrepõe a factores intrínsecos ao ambiente neuronal, modulando a patogénese mediada pelo tracto de poliQ.

O papel da ATXN3 normal na patogénese da DMJ foi também investigado. Verificámos que a proteína normal é irreversivelmente recrutada para agregados de poliQ, provocando um agravamento do fenótipo motor destes animais. Em contraste, a deleção da ataxina-3 endógena (ATX-3) não modifica o

fenótipo do modelo da DMJ em *C. elegans*. Estes resultados sugerem que, ao contrário do que acontece noutras doenças de poliQ, a ATXN3 WT não parece ter um papel neuroprotector na DMJ.

Em *C. elegans*, mutações que reduzem a sinalização da via da insulina/factor de crescimento da insulina 1 (IIS) revertem parcialmente a agregação e toxicidade causada pela ATXN3 mutante. Surpreendentemente, outras vias que afectam a longevidade de organismos mostraram efeitos diversos na proteotoxicidade da ATXN3: animais em restrição calórica não apresentaram diferenças na patogénese da mediada pela ATXN3 mutada relativamente a animais com uma dieta *ad libitum.* Mutações que alteram a função mitocondrial e causam aumento da longevidade em *C. elegans* apresentaram efeitos heterogéneos: a mutação do gene *clk-1* agravou o fenótipo de agregação, enquanto que a mutação do gene *isp-1* atrasou o aparecimento dos agregados. Estes resultados sugerem que as vias da longevidade, embora aumentem a sobrevivência global dos organismos, nem sempre têm um impacto positivo no tratamento de doenças associadas a conformações proteicas.

O factor de choque térmico 1 (HSF-1) desempenha um papel neuro-protector relativamente à proteotoxicidade da ATXN3 em *C. elegans*. Contudo, em ratinhos esse efeito não é claro. A redução dos níveis do gene *Hsf-1* em ratinho resultou num fenótipo de descoordenação motora semelhante ao de ratinhos contendo duas cópias do gene. Este resultado sugere que uma cópia do *Hsf-1* é suficiente para combater a proteotoxicidade causada pela ATXN3 quando mutada.

Finalmente, validámos o nosso modelo em *C. elegans* como uma ferramenta para a identificação de potenciais compostos terapêuticos para a DMJ e identificámos cinco compostos, potencialmente envolvidos na regulação da resposta ao choque térmico nas células, na autofagia, na regulação da transcrição e na longevidade, como bons candidatos para testar em modelos da DMJ desenvolvidos em organismos evolutivamente mais próximos do humano, como é o caso do ratinho.

Em resumo, este trabalho trouxe novas pistas para o estudo da patogénese da DMJ e para o papel da ATXN3 normal na doença. Também levantou novas possíveis hipóteses no que diz respeito a ligações mecanísticas entre factores que determinam a longevidade dos organismos e a proteotoxicidade. Este novo modelo passou a estar disponível para a comunidade como uma ferramenta para a potencial descoberta de novas drogas e identificação de alvos que podem ser úteis para o desenvolvimento de terapias para a DMJ.

Table of Contents:

List of Abbreviations:

µL: Microliter
Ab: Antibody
AD: Alzheimer's Disease
AH: Anterior Horn
ALS: Amyotrophic Lateral Sclerosis
AR: Androgen receptor
ATXN3: Ataxin-3 protein
AT3Q(n): Ataxin-3 protein containing n glutamine residues
***ATXN3*:** Ataxin-3 gene
BDNF: Brain-Derived Neurotrophic Factor
bp: Base pairs
***C. elegans*:** *Caenorhabditis elegans*
C/P: Caudate/Putamen
CAG: Trinucleotide codon for glutamine
CBP: CREB binding protein
cDNA: complementary DNA
CFP: Cyan Fluorescent Protein
CJD: Creutzfeldt-Jakob Disease
CREB: cyclic AMP-response element binding protein
Ctx: Cerebral cortex
DN: Dentate Nucleus
DNA: Deoxyribonucleic acid
DNC: Dorsal nerve cord
DRPLA: Dentatorubral-pallidoluysian Atrophy
ECL: Enhanced ChemiLuminescence
FRAP: Fluorescence Recovery After Photobleaching
GABA: Gamma-Amino butyric acid
GFP: Green Fluorescent Protein
GP: Globus Pallidus
HAP1: Hutingtin interacting protein 1
HD: Huntington's Disease
HDAC: Histone deacetylase
Hdj-1: 40-kDa heat-shock protein
Hdj2: Constitutive form of 40-kDa heat-shock protein
HHR23A/B: Human homolog of yeast RAD23 protein
Hprt: Hypoxanthine-guanine phosphoribosyl transferase
Hsc-70: Heat shock cognate 70
HSF1: Heat Shock Factor 1
Hsp: Heat shock protein
Htt: Huntingtin Protein
JD: Josephin domain
kDa: kiloDalton
L: Liter
LCN: Lateral Cuneate Nucleus

min: Minute
MJD: Machado-Joseph Disease
mL: Milliliter
mM: Milimolar
MMP-2: Matrix metalloproteinase-2
mRNA: Messenger RNA
n: Number of samples in the study
N2: Bristol Laboratory *C. elegans* strain (wild-type strain)
NCoR: Nuclear receptor co-receptor
NEDD8: Neural developmental down-regulated gene 8
ng: Nanogram
NGM: Nematode Growth Medium
NI: Neuronal inclusion
NLS: Nuclear localization signal
nm: namometer
OD: Optical Density
O/E: Over-expression
OSM: Osmotic avoidance abnormal
PAGE: Polyacrilamide Gel Electrophoresis
pCAF: Protein-associated factor
PCR: Polymerase Chain Reaction
PD: Parkinson's Disease
PN: Pontine Nucleus
polyQ: Polyglutamine
Q(n): Q stretch of n residues
Q: Glutamine
RFI: Relative Fluorescence Intensity
RN: Red Nucleus
RNA: Ribonucleic acid
RNAi: RNA interference
ROI: Region of interest
rpm: Rotations per minute
RT-PCR: Reverse transcription- PCR
SCA: Spinocerebellar Ataxia
SD: Standard Deviation
SDS: Sodium dodecyl sulphate
SDS-PAGE: Sodium dodecyl sulphate- Polyacrilamide Gel Electrophoresis
SEM: Standard Error of the Mean
SMBA: Spinal and Bulbar Muscular Atrophy
SN: Substantia Nigra
SP1: Specificity Protein 1
STN: Subthalamic Nucleus
$TAF_{II}130$: TBP-associated factor
TBP: TATA box binding protein
***t-test*:** Student's *t* test
ub: Ubiquitin

UBL: Ubiquitin-Like domain
UIM: Ubiquitin-interacting motifs
UPS: Ubiquitin-proteasome system
VCP: Valosin-containing protein
VL: Ventrolateral Thalamic nucleus
VNC: Ventral nerve cord
WT: Wild-type
YAC: Yeast Artificial Chromosome
YFP: Yellow Fluorescent Protein

Thesis Outline

Protein folding is an essential cellular process and is recognized as the basis for several human diseases, collectively known as conformational disorders. In the cellular context, misfolding of a protein may result in aberrant protein interactions, abnormal subcellular localization, degradation and aggregation, ultimately leading to a decrease in availability of the functional protein, as in Cystic Fibrosis, or gain-of-toxic function, as in many neurodegenerative diseases. These comprise Parkinson's disease, Alzheimer's disease, amyotrophic lateral sclerosis, and polyglutamine expansion disorders, among others. The polyglutamine diseases constitute a class of nine genetically distinct disorders, which include Machado-Joseph disease (MJD), and are caused by expansion of a translated CAG repeat. Although the disease causing proteins are widely expressed in the central nervous system (CNS), specific populations of neurons are vulnerable in each disease, resulting in characteristic patterns of neurodegeneration and clinical features. This specificity suggests that protein misfolding and its toxic outcomes may be determined by the amino acid sequence of the particular protein. It still remains poorly understood how ATXN3 protein context modifies the phenotypic effect of the expanded polyQ-tract, and therefore this was one of the questions that we addressed in this work.

The main goal of the work performed in this thesis was to identify modulators (genetic and pharmacologic) of MJD pathogenesis in a multicellular organism. We used the nematode *C. elegans* to express fluorescently tagged ATXN3 specifically in neuronal cells, as a model to study proteostasis in the context of MJD.

The present dissertation is organized in 7 different chapters. Chapter 1 is the general introduction, the chapters concerning the experimental work are presented in Chapter 2 to 6 (in the format of research articles) and Chapter 7 is the general discussion of the work. The manuscript presented in Chapter 2 is *in press*, whereas Chapters 4 and 6 are *in preparation*.

An overview of the literature relevant for the studies described here is given in **Chapter 1**. It focuses on the relevance of protein folding in the cellular environment and the consequences of disruptions in this process. A description of diseases caused by protein misfolding and aggregation follows, with particular focus on polyglutamine disorders and MJD. The pathogenic mechanisms underlying theses diseases, as well as the role played by aging in protein homeostasis and aggregation, are also discussed. Finally, a brief review of *C. elegans* models of polyQ diseases and their contribution to the field is presented.

Chapter 2 describes the generation of a novel *C. elegans* model of ataxin-3-mediated pathogenesis, as well as its extensive characterization regarding expression, aggregation, neuron subtype- specific susceptibility and impact on the animals' behavior. We found that ATXN3 flanking sequences greatly modulate polyQ-mediated

aggregation and neuronal dysfunction; the neuronal cell-type-specific susceptibility to expression of mutant ATXN3 proteins was not stochastic, and was distinct from that observed by expression of polyQ-alone.

In spite of having dissimilar clinical presentations, and the identities of proteins involved being distinct, polyQ diseases display certain features suggestive of a common underlying mechanism of toxicity. The fact that all diseases have delayed onset, with symptoms appearing in late adulthood suggests that aging is a major risk factor. Our work shows that mutant ATXN3-related phenotypes in *C. elegans* are aggravated with aging, and pinpoints the protective roles of the DAF-16 and HSF-1 pathways in the suppression of proteotoxicity.

One of the great advantages of the model here generated is the fact that presents quantifiable phenotypes, namely mutant ATXN3-mediated aggregation and motility defects; which can be relevant in therapeutic studies (see Appendix 3). **Chapter 2.1** describes the details regarding the imaging processing application that we have developed specifically to quantify fluorescent protein aggregates *in vivo* in our model; this application is currently under further development and customization. This is the result of a highly collaborative work between biology and engineering fields.

An emerging question arising from chapter 2 is how aging-related pathways, other than the Insulin/Insulin Growth Factor 1 (IGF-1)-like signaling, can influence proteotoxicity. **Chapter 3** reports our surprising preliminary observations pointing to opposing effects of distinct aging-related pathways on mutant ATXN3-mediated pathogenesis. Mutation in *clk-1*, which catalyzes the final step of ubiquinone biosynthesis and confers a long lived phenotype to the animals, causes an increase in mutant ATXN3 aggregation; whereas mutation in *isp-1*, a subunit of the Complex III of the electron transporter chain that also increases lifespan, suppresses it. Dietary restriction-mediated increased lifespan showed no effect in the aggregation and toxicity of ataxin-3 in neuronal cells. Differences in proteostasis and folding capacity could underlie these findings. However, we are aware that a number of important experiments will be needed to further support or reject our hypothesis.

One prominent question in the polyQ field is to understand the influence of the wild-type (WT) proteins in the disease context. **Chapter 4** gives further insight into the role of normal ATXN3 in polyQ-mediated pathogenesis. Here, we found that WT ATXN3 is recruited into neuronal polyQ cellular aggregates and aggravates motor neuron dysfunction of a *C. elegans* model expressing polyQ-alone proteins. Endogenous *atx-3* knock-out has no major influence in mutant ataxin-3-mediated pathogenesis. These findings contradict the idea that WT ATXN3 plays a neuroprotective role, as has been suggested for MJD and other polyQ diseases.

Chapter 5, "Searching for therapeutic strategies in a *C. elegans* model of MJD", presents a candidate-based approach for the development of new therapeutic approaches in MJD. The main goal was to validate our novel *C. elegans* model expressing full-length mutant ATXN3 as a good platform for screening of small

molecules. Results of the candidate drugs presented here constitute the proof-of-concept for future high throughput hypothesis-free testing of compound libraries (see Appendix 3).

Results from our *C. elegans* model (Chapter 2) indicate HSF-1 as a potent suppressor of mutant ATXN3 proteotoxicity. Based on this, we have tested the effects of HSF-1 in a higher model organism, namely a mouse model of MJD pathogenesis. However, **Chapter 6** shows that genetic reduction of HSF-1 in mice had limited influence in pathogenesis.

Chapter 7 integrates the results and describes their relevance in the field, as well as future perspectives.

Two **appendices** are included in this thesis; one is a book chapter, written in Portuguese "Doenças de expansão de poliglutaminas – o paradigma das doenças de Huntington e de Machado-Joseph", that will be included in the book *Neurociências* from LIDEL editorial. Appendix 2 shows the outline of the ongoing project *Screening of therapeutic compounds in a C. elegans model of Machado-Joseph disease*. Our specific goal in this project is to screen a library of 1200 FDA-approved out-of-patent small molecules for their ability to prevent or delay the formation of fluorescent mutant ataxin-3 aggregates (Chapter 2.1) and/or suppress motor neuron dysfunction (using automated motility analysis, currently under development in collaboration with *Noldus Information Technology*).

Chapter 1

General introduction

1.1 Protein folding, misfolding and conformational disorders

Proteins are nearly the most abundant molecules in cells and constitute important effectors of cellular function. Upon synthesis, the majority of the nascent polypeptide chains does not acquire spontaneously its native conformation, but needs to be converted into compact folded structures in order to become functionally active. It is now widely accepted that within live cells there are a number of auxiliary factors that assist and promote the folding process. Those include folding enzymes and molecular chaperones (reviewed in (3).

Molecular chaperones are important in the cell's crowded environment that favors non-specific and folding-disruptive intermolecular interactions between hydrophobic amino acids of non-native proteins (4).

An imbalance in protein homeostasis, whether caused by aging-associated cellular changes, cell stress, expression of mutant aggregation-prone proteins or by a combination of these factors results in the appearance of proteins with alternative conformations that can self-associate to form cellular aggregates. The cell has developed a highly efficient protein folding quality control machinery to regulate protein homeostasis and to avoid accumulation of misfolded proteins (5-7). However, under some pathological conditions, the capacity of this machinery is exceed and misfolded proteins may accumulate to deleterious levels. In fact, protein misfolding is recognized as the basis of numerous human diseases, collectively known as *conformational disorders* (8). The mechanisms underlying the majority of these disorders are yet to be unveiled, but the subsequent lack of proper protein folding results in the accumulation of both intra and extra-cellular misfolded proteins and is the cause of various neurological and systemic diseases of striking social impact. These include Alzheimer's disease (AD), Parkinson's disease (PD), Huntington's disease (HD), spinocerebellar ataxias (SCA), including SCA3/Machado-Joseph disease (MJD), type II diabetes, amyotrophic lateral sclerosis (ALS) and prion diseases such as Creutzfeld-Jakob disease (9, 10).

1.2 Polyglutamine (PolyQ) diseases

Pathogenic mutations that affect nucleotide repeats were first described in the early 1990s when the causative mutations in fragile X syndrome (FRAXA; also known as fragile site mental retardation 1, FMR1) (11) and spinal and bulbar muscular atrophy (SBMA) (12) were identified as trinucleotide repeat expansions. In the following years, this group of disorders has expanded also to tetra- (13) and pentanucleotide (14) repeat disorders.

Nine disorders are caused by expanded (CAG)n repeats within the coding regions of the related genes, producing extended polyQ tracts in the expressed protein. These include: dentatorubral-pallidoluysian atrophy (DRPLA), which is caused by mutations in atrophin-1, a transcriptional regulator (15, 16); SBMA or Kennedy disease, associated with mutations in the androgen receptor (12), Huntington's disease (HD), caused by a CAG expansion on the N-terminal of huntingtin (Htt) protein (17) and several forms of spinocerebellar ataxias (SCAs): SCA1, caused by mutations in ataxin-1 (18), SCA2, mutation in ataxin-2 (19), SCA3 also known as Machado-Joseph disease (MJD) and caused by CAG-repeat expansion in the C-terminus of ataxin-3 (20), SCA6 caused by

a mutation in the α1A calcium channel (21), SCA7 (22) and SCA17 associated with a CAG expansion in TATA-binding transcription factor (23, 24) (see Table 1.1).

Table 1.1- Molecular traits of polyglutamine diseases.

Disease	Gene mutated	Gene product	Putative function	Normal (CAG)n	Expanded (CAG)n
Huntington's Disease (HD)	*HD*	Huntingtin	Signalling, transport, transcription	6-35	36-121
Spinocerebellar ataxia type-1 (SCA1)	*ATXN1*	Ataxin-1	Transcription	6-39	39-83
Spinocerebellar ataxia type-2 (SCA2)	*ATXN2*	Ataxin-2	RNA metabolism	14-31	32-200
Spinocerebellar ataxia type-3 (SCA3; Machado-Joseph Disease)	*ATXN3*	Ataxin-3	De-ubiquitylating activity	12-40	54-86
Spinocerebellar ataxia type-6 (SCA6)	*CACNA1A*	CACNA1A	a1A-voltage-dependent-calcium channel subunit	4-20	20-30
Spinocerebellar ataxia type-7 (SCA7)	*ATXN7*	Ataxin-7	Transcription	4-35	37-306
Spinocerebellar ataxia type-17 (SCA17)	*TBP*	TBP	Transcription factor	25-42	47-63
Dentatorubral-pallidoluysian atrophy (DRPLA)	*DRPLA*	Atrophin-1	Transcriptional regulator	3-35	49-88
Spinal and bulbar muscukar atrophy (SMBA; Kenedy disease)	*AR*	Androgen receptor	Streoid-hormone receptor	9-36	38-62

Adapted from (1).

Besides the polyQ tract, these proteins share no homologies, are unrelated to each other, vary in size and contain the polyQ tract at distinct locations of the protein sequence. It is thought that this common expanded polyQ tract highly contributes to the toxic properties of the proteins. These proteins are expressed in the central nervous system (CNS) as well as in the peripheral tissues. However, each polyQ containing protein originates a disease-specific neurodegeneration pattern (24-27). Eight of the nine characterized diseases are autosomal dominant (with the exception of SBMA, which is X-linked), completely penetrant and progressive. The Q-length is highly polymorphic and expansion of the CAG tract above a certain length threshold confers toxicity. In general, the pathological threshold length varies between 35-50 Qs (with the exception of SCA6). Within the expanded ranges, there is an inverse correlation between the number of CAG repeats and the age of disease onset (1) (Figure 1.1). Finally, for lengths above the threshold there is a striking intergenerational CAG instability. The expanded CAG repeats may expand or contract, but more often their instability manifests trough expansion of the polyQ tract (28). This causes earlier age at onset in successive generations, a phenomenon that was called anticipation (29-31).

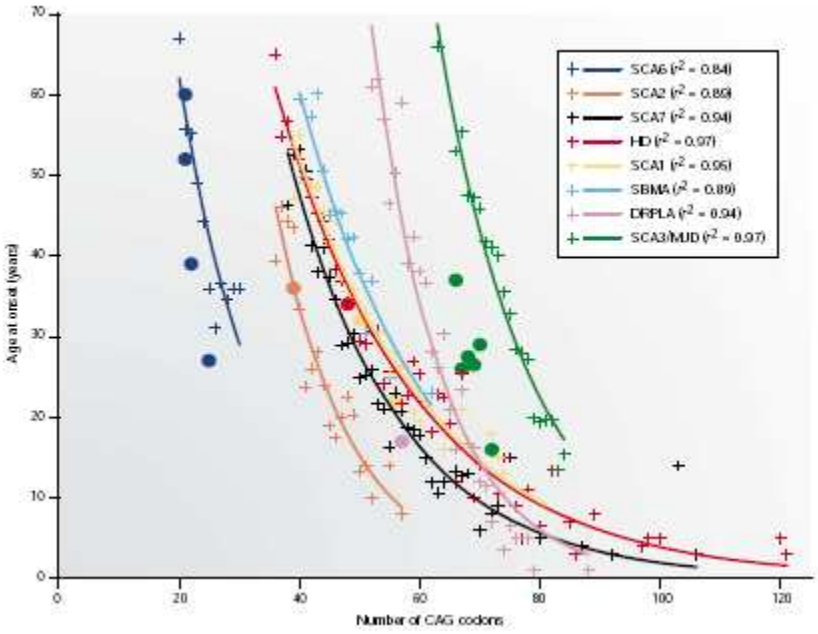

Figure 1.1- Correlation between age at onset and CAG-repeat length for polyglutamine disorders. '+' represent age at onset associated with various CAG repeats lengths. The age at onset for homozygotes for the various disorders is also shown (filled circles), plotted according to the longer of their two expanded CAG repeats. Figure adapted from (1).

1.3 PolyQ diseases: specificity and commonalities

1.3.1 Protein aggregation is a unifying feature

The direct evidence for an altered conformation of expanded polyQ-containing proteins comes from the fact that certain antibodies specifically recognize expanded, but not normal, polyQ stretches in proteins (27). Expanded polyQ proteins are susceptible to misfolding and aggregation. The natural propensity for aggregation is conferred by the formation of highly stable β-sheet structures. This β-sheet conformation is further stablilized by intermolecular interactions, which may underlie the formation of oligomers and aggregates (27, 32).

Nuclear inclusions (NIs) or aggregates were first observed in the late 1990s in the brain of mouse models of polyQ pathogenesis as well as in post-mortem brain tissue of patients. Davies and colleagues detected NIs in the brain of a HD mouse model and suggested that the inclusions were formed through self aggregation of the polyQ repeat (33). In 1997, DiFiglia *et al* reported that the polyQ length influenced the extent of htt aggregation and accumulation in the HD cortex and striatum (34). In the same year, Paulson and colleagues found intranuclear inclusions in post-mortem brain tissue of MJD patients (35). Since this foundation, several studies have confirmed that aggregation occurs in post-mortem tissues (36-41) and in animal models of polyQ diseases, such as *C. elegans* (42-44), flies (45, 46), mice (33, 47-50) and cellular models (40, 51-56).

Aggregation of expanded polyQ proteins was therefore established as an unifying feature of polyQ and other neurodegenerative diseases such as AD, PD and prion diseases. The aggregates are usually detergent-insoluble and exhibit several features of amyloids, like reactivity with anti-amyloid antibodies, Congo-red birefringence and binding to thioflavine T (51, 57, 58). Aggregates also show reduced mobility in the cell

environment, which can be measured using dynamic imaging techniques of fluorescently tagged proteins (reviewed in (59).

The function of the polyQ repeats in proteins is mostly unknown, however, when the whole human genome is considered, Q repeats are more frequent than any other type of amino acid repeats (60).

Role of aggregates in disease: toxic or beneficial?

A causal role for aggregation in polyQ pathology was proposed when different polyQ transgenic mice expressing large polyQ expansions were seen to develop progressive degeneration in the presence of inclusion bodies. However, aggregate formation could be instead a cellular attempt to trap these toxic species and prevent deleterious consequences to cell homeostasis.

When NIs were initially described, several reports described a significant correlation between the presence of aggregates and cellular death (33, 61-64). It has been also observed that soluble polyQ proteins are efficiently cleared by the proteasome. However, once captured into aggregates, they become resistant to proteolysis and accumulate (65). Moreover, reduction of polyQ aggregation by over-expression of chaperones is associated with a decrease in cell death (66, 67). These observations led to a conceptual model in which the presence of aggregates was thought to be indicative of disease progression, and aggregation clearance was beneficial.

Although these data suggest a link between aggregation and pathogenesis, the toxic species could be either the aggregates themselves, or the intermediates in the aggregation pathway, or there could be a contribution from both.

In support to this idea, some researchers argue that NI may be inert or even protective to cells and point the intermediate misfolded oligomeric protein forms, as the pathogenic entity able to disrupt cellular function. Saudou and co-workers proposed that the inclusions were neither essential nor sufficient to trigger neuronal dysfunction in HD (68); an idea that was advanced also for SMBA (54). Another finding that supports this theory is the fact that the NI localization does not always match the disease pathology, namely in SBMA, HD, SCA2 and SCA7 (38, 69-73). Similarly in MJD, thalamic neurodegeneration occurs independently from ATXN3 immunopositive neuronal intranuclear inclusions (74). Recent data has contributed more directly to this hypothesis. In a HD cell culture model, it was observed that the presence of inclusion bodies predicted better neuronal survival whereas diffuse huntingtin correlated significantly with cell death (75).

It is possible that the monomers, soluble intermediates and insoluble aggregates have distinct deleterious effects upon neuronal function and act in different phases of the disease pathogenesis.

1.3.2 Gain-of-function in polyQ disorders

The presence of polyQ expansions in several functionally unrelated genes is a strong clue suggesting that expanded polyQ tracts confer by themselves a toxic gain-of-function. Several additional lines of evidence

support to this hypothesis. For most of these disorders heterozygous and homozygous individuals display similar age at onset and symptoms. In contrast, individuals with loss of a single allele of the HD gene do not show any abnormal phenotype (76). Also, it was reported that mice null for huntingtin were embryonic lethal and when null for ataxin-1, mice were viable but showed decreased exploratory behavior and pronounced deficits in the spatial version of the Morris water maze test, none of which are features of HD or SCA1 (77, 78). ATXN3 knock-out mice are also viable, and do not show defects in locomotion or major pathological hallmarks (79). In all cases, the loss of function of the endogenous protein did not recapitulate the neurodegeneration observed when polyQ expansions are present. Furthermore, the expression of mutant huntingtin, ataxin-1 or ataxin-3 causes neurodegeneration in mouse (and humans) even in the presence of normal endogenous protein (33, 48, 50, 80). Finally, expanded polyQ tracts are also toxic when introduced in a gene that does not normally contain them. Insertion of 146 glutamines into the mouse hypoxanthine-guanine phosphoribosyl transferase (Hprt) gene resulted in neurodegeneration and premature death (81). The expression of a simple polyQ tract, in the absence of any additional protein context is also toxic, as shown in cell culture, mouse, *Drosophila* and *C. elegans* (49, 82-84). Taken together, these data suggest that the polyQ expanded tract confers a toxic gain-of-function to the protein that bears it, which appears to be sufficient to cause neuropathology. However, the pathogenesis caused by the expression of the polyQ-stretch alone does not recapitulate all the disease features, suggesting additional determinant factors.

1.3.3 Contribution of the protein context to polyQ toxicity: role of the wild-type allele

Although neurodegeneration in CAG-repeat diseases is the result of a toxic gain-of-function, some evidences suggest that a partial loss-of-function might also contribute to the overall pathology (85), producing disease-specific characteristics.

Post natal elimination of Htt protein expression yielded striatal degeneration in Htt conditional knock-out mice (86). Moreover, in the HD yeast artificial chromosome (YAC) 128 mouse, absence of endogenous Htt expression accentuated HD neuropathology (87, 88). Several studies *in vitro* found that cells with depressed levels of Htt showed increased sensitivity to polyQ toxicity (89, 90).

Absence of endogenous AR protein in AR100Tfm mice (91) (AR YAC transgenic mouse model with 100Qs (AR100) (92) in an AR null (testicular feminization; Tfm) background) had profound effects upon neuromuscular and endocrine-reproductive features of this SBMA mouse model, as AR100Tfm mice displayed accelerated neurodegeneration and severe androgen insensitivity in comparison to AR100 littermates. Reduction in size and number of androgen-sensitive motor neurons in the spinal cord of AR100Tfm mice underscored the importance of AR action for neuronal health and survival (91). These studies suggest that SBMA disease pathogenesis involves two simultaneous pathways: gain-of-function misfolded protein toxicity and loss of normal protein function.

The importance of protein context and also of subcellular localization has been highlighted in SCA1, since the presence of the polyQ tract is necessary but not sufficient to explain the neurodegeneration phenotype in mice. Overexpression of expanded ATXN1 with a single serine mutated to alanine (S776A) does not lead to Punkinje cell degeneration. Moreover, lack of a functional nuclear localization signal or of the AXN domain in expanded ATXN1 is not toxic in mice (50, 93, 94). These data suggested that key domains in ATXN1, other that the polyQ tract, are critical for SCA1 pathogenesis.

Furthermore, overexpression of polyQ-alone chains in fly neuronal and non-neuronal tissue causes cellular degeneration. However, the presence of other amino acids together with the expanded polyQ tract was seen to modify and reduce polyQ toxicity (82). Similar results were obtained in our *C. elegans* model of ATXN3 pathogenesis (Capter 2).

In MJD, it was shown that overexpression of the WT protein in the disease context (in mice and fly models) suppressed mutant-ATXN3 mediated pathogenesis (48, 95). Surprisingly, these observations were not replicated in other disease models and are still under debate. This issue will be addressed in Chapter 4.

A model for CAG disorders is emerging in which the presence of polyQ expansions within the disease protein causes a change in conformation leading to a proteotoxic state that may be modulated, to a certain extent, by protein context. The loss of the normal protein function also contributes to the disease pathogenesis and might be involved in the neuronal specificity observed.

1.3.4 Neuron-specific toxicity

The CAG-repeat diseases show distinct pathologies in terms of neurodegeneration and symptoms. In HD, for example, neuronal death is most prevalent in the striatum and cerebral cortex, whereas in SCA1 degeneration of neurons occurs in the inferior olivary nuclei, cerebellar dentate nuclei, red nuclei and Purkinje neurons in the cerebellum (reviewed in (2, 24). The cause of neuron-specific toxicity is a major unanswered question in the polyQ field. Early studies showed that the distinct neuropathologies of CAG-repeat diseases were not due to (i) neuron-specific expression pattern of polyQ proteins, (ii) neuron-specific protein levels or (iii) heterogeneity in CAG repeat-length among distinct neurons.

(i) In fact, all of the proteins associated with CAG-repeat diseases are ubiquitously expressed (2, 24). In patients, both WT and expanded Htt have been found in brain and non-neuronal tissues including skeletal muscle, lung, kidney, lymphoblasts, testis and ovary (15, 27, 31, 96, 97). Similarly, there are (ii) no dramatic differences in expression levels of Htt between types of neurons or after disease onset (98). Nor were significant differences found between expression levels of WT or expanded polyQ tract Htt in heterozygous patients or animals models (96). (iii) A third possibility for neuron-specific pathogenesis was cell-specific heterogeneity of the polyQ length resulting in the loss of neurons with expanded polyQ tract and survival of neurons with fewer CAG repeats. Widespread heterogeneity of the CAG-repeat in the brain has been described for SCA1, HD and DRPLA but no correlation to selective brain pathology has been found (96, 99-102), in studies using macroscopic brain

dissection. Laser-capture microscopy studies in DRPLA have shown that range of CAG repeats in the cerebellar granular cells is smaller than those in cerebellar glial cells (103). While there is some evidence of heterogeneity in the CAG-repeat length in juvenile HD cases (104) no correlation was observed between the mosaicism pattern and pathology (24). All this studies however, made use of post mortem tissue or at advanced ages, increasing the possibility that cells holding increased CAG repeats were no longer available for analysis. The use of animal models allowed longitudinal studies, but lack of correlation between increased CAG length and affected brain regions was also detected in a mouse model for MJD (105).

Together, these studies show that neuron-specific toxicity in CAG-repeat diseases does not result from tissue-specific expression, neuron-specific differences in protein levels, or heterogeneity in polyQ length.

Additional proposed mechanisms fall into two general classes: cell autonomous and non-autonomous mechanisms. Cell autonomous or intracellular mechanisms include any factors that determine sensitivity to polyQ-mediated pathology independently of neighboring cells or extracellular signals. PolyQ proteins, such as Htt, are known to be expressed ubiquitously in both neuronal and non-neuronal tissues. Given that polyQ pathogenesis is only observed in neurons, it seems likely that some 'intracellular' characteristic differentiates neurons from non-neuronal tissues and increases neuronal susceptibility. Further support for the possibility of cell autonomous factors acting in neurons comes from studies showing that a significant proportion of mammalian genes are only expressed in the nervous system (106). In contrast, the absence of HSF1 in rat hippocampal neurons (affected in AD) and an higher threshold for HSF-1 activation in motor neurons suggests the possibility that neurons may be selectively vulnerable to stresses that active the heat shock response in other cells (107, 108). Other proteins may be under-represented in brains regions affected in human polyQ-associated disorders and perhaps unveiling the neuron-specific proteome could be of great importance.

Cell non-autonomous mechanisms imply interactions between different groups of cells. In the case of CAG repeat diseases, it has been suggested that pathogenesis is affected by interactions between types of neurons. For example, brain-derived neurotrophic factor (BDNF) is transported from the cortex to neurons in the striatum; a subset of neurons particularly susceptible to degeneration in HD. It has been shown that WT Htt enhances the rate of vesicular transport of BDNF along microtubules and that function is compromised in the presence of expanded Htt. This study predicts that polyQ-mediated dysfunction in neurons of the cortex provides one of the intercellular signals leading to degeneration of the striatum (109).

Extensive efforts are ongoing to understand how polyQ tracts, expressed within the context of disease-associated protein sequences, may mediate neuron-specific degeneration.

1.3.5 Aging as a major risk factor for neurodegenerative diseases

Advances in medicine, nutrition, and public health have significantly increased the average human lifespan in the last century. The average lifespan has increased more than 50% since the early 1900s and today, living well into the seventh decade is common. Life expectancy in developed countries is now predicted to

exceed 85 years by the year of 2050 (110). In Portugal, life expectancy at birth is of 78.54 years in 2011 (http://www.indexmundi.com/pt/portugal/expectativa_de_vida_no_nascimento.html).

In the United States alone 12% of the population, approximately 37 million people, are over the age of 65 (Agency, 2005). As the number of aged individuals increases, so does the prevalence of age-associated diseases. The lifetime risk of developing some form of dementia, one of the most common symptoms of neurodegenerative disease, is estimated to be 6-10% for men and 12-19% for women. The prevalence of dementia doubles every additional five years after 65, reaching 25-50% in those 85 or older (111). The number of deaths due to neurodegenerative disease has risen consistently in the past decades. This trend is expected to continue since the population over the age of 75 in the United States is expected to double within the next 50 years (Statistics, 2005). Because lifespan continues to increase, understanding and treating neurodegenerative disease will become even more critical.

With the discovery in the 1980s that mutations in single genes can significantly extend lifespan in the nematode *Caenorhabditis elegans* (112, 113), aging started to be viewed as a malleable physiologic phenomenon that could be modified by methods also used to understand development and disease. At present, hundreds of mutant genes are known that can increase longevity in model organisms, like yeast, nematodes, fruitflies and mice. Most act in evolutionarily conserved pathways that regulate growth, energy metabolism, food sensing and/or reproduction (114). Examples include genes encoding components of the insulin/insulin-like growth factor 1 (IGF-1) signaling (IIS) pathway, the target of rapamycin (TOR) pathway, and the mitochondrial electron transport chain. Interestingly, lifespan extension occurs when activity of the component is diminished, suggesting reduced somatic damage and/or increase in maintenance and repair, as a mechanism for prolonged life (114, 115). Increased activity of molecular chaperones and of folding capacity has been associated with increased longevity in worms (116).

Although disrupting/activating conserved aging pathways identified in model organisms seems a plausible starting point for human lifespan extension, it must be first determined whether these pathways modulate aging and protect against aging-associated diseases in *Homo sapiens*. An initial approach was to identify associations between polymorphisms in or surrounding conserved genes and human longevity, since extreme longevity seems to be genetically controlled. Indeed, siblings of centenarians have increased probability to survive beyond 100 years, when compared with the regular population (117). However, so far linkage analyses have been inconclusive, possibly because studies were underpowered (118).

Attempts to associate candidate genes with extreme human longevity have mainly identified gene variants in lipoprotein metabolism as overrepresented in centenarians (119), and variants in the FOXO1 and 3 (120) genes; specifically in females, gene variants were found that reduce insulin/IGF-1 signaling (121). Recently, heterozygous mutations in the IGF-1R were also shown to be overrepresented in centenarians (122). Although these results are promising, growth hormone (GH) and IGF-1 deficiencies in humans are in some cases associated with major defects and diseases (reviewed in (123). However, the normal and possible longer

lifespan of a few individuals with mutations analogous to those that extend longevity in mice suggest that it may be possible to extend human longevity by reducing plasma GH and IGF-1 levels.

1.4 Proteostasis networks and challenges

Disease-associated aggregation-prone proteins undergo misfolding and cause a disruption in protein homeostasis in the cellular environment. In 2008, Balch, Morimoto, Dillin and Kelly introduced the term *proteostasis* as the *state of dynamic equilibrium in which protein synthesis and folding are balanced with protein degradation*. Proteins are maintained *functionally active*, *thus leading to a healthy proteome* (124, 125). Although the exact players that constitute and help to maintain functional proteostasis networks in cells are not yet totally known, they play an important role in the interaction between disease-associated proteins and their cellular environment. In several unbiased genetic screens using animal models of proteotoxicity, common factors were identified that may be critical to maintain proteostasis. Molecular chaperones and components of the cells degradation machinery are the most consistent modifier genes found, suggesting that assistance in folding, aggregation prevention and clearance of the non-functional aggregated species are crucial *in vivo*. Importantly, the hits obtained by screening for suppressors of polyQ or SOD1 aggregation in *C. elegans* showed a significant overlap with genes that are involved in the response to osmotic stress-induced protein damage (126-128). Moreover, many suppressor genes of ATXN3 neurodegeneration in Drosophila also suppressed toxicity in a hypomorphic Hsp70 fly strain (129). The hits of the aforementioned screens include proteins involved in RNA processing and protein synthesis in addition to protein folding and degradation hits. The data suggests a core set of genes that function both in stress-induced protein damage and in response to the expression of disease-associated proteins. This core set of proteostasis networks factors may become compromised under disease conditions and during aging. Under physiological growth conditions, aging is accompanied by an increase in the amount and quality of aggregated proteins (130). Unfortunately, cells are unable to cope with the challenging of the proteostasis robustness that occurs during aging. The aging-related decline in the functionality of proteostasis networks is well documented at least in HD, with the levels of functional chaperones and the capacity of the clearance mechanisms diminished during aging. Increase in protein damage, transcriptional and translational dysregulation, aberrant signaling, and other changes also follow this decline. If this is the case cell-type-specific differences in the proteostasis networks and the robustness of adaptive stress responses may underlie disease-specific proteotoxicity.

1.5 Polyglutamine pathogenic mechanisms

As discussed above, several cellular and molecular mechanisms have been proposed for polyQ pathology, which suggest a gain-of-toxic function to the expanded polyQ tract, in some cases associated with loss-of-function mechanisms of the disease-specific proteins. Figure 1.2 summarizes the pathogenic

mechanisms that have been proposed for polyQ disorders. Nevertheless, it is important to highlight that not all the putative pathogenic mechanisms represented in Figure 1.2 were specifically tested for each disorder.

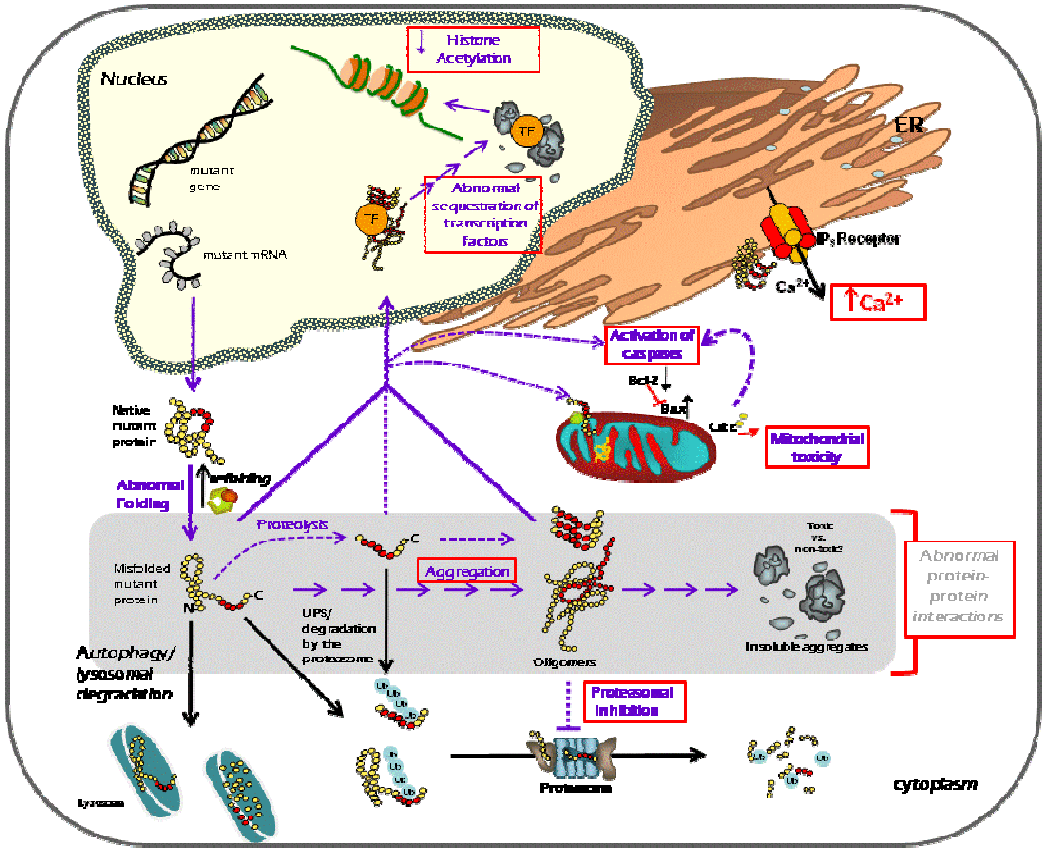

Figure 1.2. Mechanisms of polyglutamine pathogenesis. Various pathogenic pathways have been suggested. The pathogenic process (blue arrows) begins with the synthesis of a protein with an expanded polyQ tract. The expanded polyQ tract alters the native conformation of the protein, modulated by the presence of molecular chaperones and co-chaperones. At least a fraction of the abnormally folded protein is subjected to lysosomal-dependent proteolysis, and another portion of the abnormal protein is ubiquitylated (Ub) and degraded via the proteasome. Cleavage of the abnormally folded mutant protein produces polyQ-containing fragments that favour the aggregation process. The mutant proteins shift, in part, from a monomeric random coil or β-sheet into oligomeric β-sheets and eventually into insoluble aggregates. These might contribute to pathology through abnormal interactions with cellular proteins, or might represent a mechanism for reducing the toxicity of aggregation intermediates. Aggregation intermediates inhibit proteasomal processing. The monomers or oligomers directly activate caspases or disrupt mitochondrial function, leading to indirect activation of caspases. Mutant polyQ proteins also bind to inositol-(1,4,5)-tri-phosphate receptor (IP_3R) and increasing calcium release into the cytoplasm. Aggregation intermediates translocate into the nucleus (by an unknown mechanism) and recruit specific nuclear factors, co-activators and co-repressors, inhibiting their normal activities and resulting in altered gene transcription. As a simplification, mutant proteins are depicted as originating in the cytoplasm, although some of them might also be located in the nucleus or cycle between the cytoplasm and nucleus.

1.5.1 Disruption of proteostasis

The mutant polyQ-containing proteins undergo ubiquitylation and recruit proteasome subunits and molecular chaperones into the aggregates (35, 131, 132). In several cellular and organism models, the overexpression of chaperones was found to modify the toxicity phenotype (132-134). This finding suggests the involvement of the ubiquitin-proteasome system (UPS) in these pathologies, and of the heat shock response machinery in order to either refold or degrade the mutant polyQ proteins. The mislocalization of chaperones and proteasome subunits may underlie the progress of the disease. Molecular chaperones were shown to associate

with the aggregates only transiently and to move freely (135). In contrast, the proteasome subunits were irreversibly recruited into the aggregates, possibly "caught" when attempting to degrade the misfolded proteins (136). Furthermore, it was shown that the proteasome is unable to efficiently degrade polyQ proteins due to their intrinsic properties (137), and there is a physical blocking of the proteasome by oligomers/aggregates of polyQ proteins. Conversely, the accumulation and aggregation of the polyQ proteins was shown to be promoted by inhibition of proteasome activity (138). Proteasome activity was also found to decrease both in brains of aged rats (139) and mice (140). These observations are particularly relevant since age-dependency is characteristic of polyQ disorders. A decline in proteasomal activity associated with both the accumulation of misfolded proteins and aging would initiate a deleterious cascade: less free proteasome means a slower clearance of proteins, leading to enhancement of protein aggregation (136).

In spite of all this compelling data demonstrating the impairment of the UPS in polyQ expansion disorders, this topic is controversial since some groups showed an increase in proteasome activity (141, 142) .

Moreover, impairments in the autophagy process have more recently also been associated with neurodegeneration (143). Evidence of the involvement of autophagy in conformational disorders arises mainly from the observation that autophagic bodies accumulate in AD (144), PD (145) and MJD (146) brains.

Autophagy is the process by which intracellular proteins or organelles are degraded through the formation of double membrane structures, the autophagosomes. They fuse with primary lysosomes, where their contents are degraded, being later disposed or recycled back for cellular use (147-149).

It is not completely understood which proteins are degraded by the UPS or by autophagy, nor how or when the cells decide to use one pathway in detriment of the other. In 2007 Pandey and colleagues described autophagy also as a compensatory mechanism in circumstances of proteasome impairment (150). Moreover, the size and tridimensional conformation of the aggregates and oligomeric intermediates may also determine the chosen degradation pathway: once the mutant proteins are organized in oligomers, they may be degraded by certain types of autophagy rather than the by UPS, or by chaperone-mediated autophagy (CMA). In 2004, Cuervo *et al* has shown that only WT α-synuclein was degraded by CMA and that the mutant protein blocked the degradation of other CMA substrates and activated macroautophagy (145).

In summary, impairment of proteasome/autophagy function(s) and reduction of available molecular chaperones in the cellular environment may compromise degradation and folding of the disease-associated proteins and possibly also of other proteins that play important roles in the cells, causing a general disruption in proteostasis.

1.5.2 Perturbations in transcriptional regulation

Non-specific recruitment of cellular proteins into nascent polyQ aggregates is thought to contribute to cellular dysfunction. Co-localization of WT proteins to polyQ aggregates may be transient or may reflect an

irreversible sequestration that depletes cellular factors from their normal localization and thus compromises their function, and ultimately may lead to toxicity (151).

In addition to molecular chaperones and proteasome subunits, polyQ aggregates co-localize with critical cellular components such as the transcription factors (TFs) TATA-Binding Protein (TBP), CREB (cyclic AMP-responsive element binding protein) Binding Protein (CBP), Specificity Protein 1 (SP1) and TAFII130 (which encodes a TBP-Associated Factor). The recruitment of TFs together with other essential cellular components would be expected to have important cellular consequences (152).

Deletion of CREB or SP1 genes in mice resulted in an HD-like phenotype (153). Also, CBP recruitment into the aggregates was shown to be associated with neuronal toxicity, and downregulation of CRE-regulated genes was detected in HD patients (154). In addition, levels of soluble CBP are known to be reduced in cells expressing expanded polyQ despite increased levels of CBP mRNA. CBP overexpression rescued the reduced transcription of CBP-dependent genes and was sufficient to suppress polyQ toxicity (155, 156). Also, histone deacetylase inhibitors, which globally increase transcription, ameliorate polyQ-mediated neurodegeneration in cell culture, fly and mouse models of HD, presumably by altering gene expression patterns (157).

Atrophin-1 is known to be involved in transcription regulation by association with the nuclear receptor co-repression complex ETO/MTG8 (158) and to act as a member of a co-repressor complex in Drosophila (159). ATXN3 also seems to inhibit the acetyltransferase activity of several transcriptional coactivators such as CBP, p300 and p300/CBP-Associated Factor (pCAF) (160). Changes in transcriptional regulation activities of these proteins induced by the polyQ expanded might be relevant in disease.

Either by sequestration of TFs or by aberrant interactions, a common aspect of polyQ disorders is the transcriptional de-regulation, which highlights the importance of studying this pathway for the development of potential therapies.

1.5.3 Role of proteolysis and other post-translation modifications in polyQ diseases

One hypothesis concerning the mechanisms of neurotoxicity of polyQ proteins states that this toxicity depends on the cleavage of the mutant protein, releasing a toxic polyQ-containing fragment, which is required for initiation of the aggregation process and for harmful effects to the neurons. It is suggested that these polyQ-bearing fragments may translocate into the nucleus, where they exert toxic effects (161-163). Such cleavage- and nuclear translocation-dependent toxicity have been demonstrated for atrophin-1 (164). Whether cleavage is an important step in disease pathogenesis or is a normal event in degradation of polyQ-containing proteins remains in question. Initial evidence for Htt cleavage in human HD brain was obtained using a panel of antibodies to different epitopes of the protein (39). Only antibodies specific for the N-terminal of Htt (including the CAG-tract) were able to detect NIs. Similarly, in SMBA brain tissue, only antibodies to the N-terminal, which includes the Q tract, were able to detect AR NIs (72). According to Schmidt *et al.* (1998) and to *Goti et al.*

(2004), in MJD/SCA3, only antibodies to the polyQ-bearing C-terminus region of ataxin-3 were able to detect NIs (36, 165).

Extensive evidence has been collected regarding *in vitro* cleavage of several polyQ proteins, especially by caspases. The earliest indication that proteolysis might play a role in HD was the discovery that Htt could be cleaved by extracts from apoptotic cells, specifically by caspase-3 (166). A more recent study has also shown that inclusions from HD brains contain N-terminal fragments of mutant Htt rather than the full-length protein (167). Although these fragments may result from unspecific proteolytic activities, it has been demonstrated that specific cleavage of the mutant protein is an early event in HD pathogenesis, supporting the idea that the smaller products of specific cleavage may seed the formation of inclusions, being followed by the recruitment of larger non-specific fragments (168). Interestingly, nuclear translocation of expanded Htt was delayed in mice expressing mutant Htt resistant to caspase-6 cleavage (169).

In MJD/SCA3, Berke and colleagues showed that ATXN3 is a target for caspase-mediated cleavage in cell culture. Full-length ATXN3 is cleaved in staurosporine- induced apoptosis and this leads to the appearance of a C-terminal ATXN3 fragment of 28-kDa. This proteolysis may be predominantly mediated by caspase-1 (170). It has also been suggested that ATXN3 is cleaved by calpains in cell culture, but *in vivo* evidence is still lacking (171). The putative C-terminal ATXN3 fragment was also found in a transgenic mouse model (165). Brains from sick Q71 transgenic mice contained an abundant mutant ATXN3 mjd1a putative cleavage fragment, which was scarce in normal Q71 transgenic mice. Reactivity of the fragment with a panel of antibodies and co-migration with truncated versions of mutant ataxin-3 revealed that it contained residues C-terminal to amino acid 221, which is in accordance with the studies in cell culture. This fragment was more abundant in two affected brain regions of MJD patients (165).

These data support a model in which proteolysis of polyQ expanded proteins, formation of protein aggregates and subsequent sequestration of crucial cell proteins (including normal polyQ protein) are required for disease onset.

Besides proteolytic cleavage, other post-translational modifications of mutant polyQ proteins, such as phosphorylation, have been shown to play a role in pathogenesis. Phosphorylation of the mutant protein Htt has an impact in the proteolytic cleavage, change in conformation and in nuclear transport, which are key steps for the disease manifestation (172). It has been demonstrated *in vitro*, that the toxicity of mutant Htt could be decreased or inhibited by phosphorylation of Htt at S421 (173), at S434 (174), and at S536 (175). These results suggest a neuroprotective role of this phosphorylation in HD (176).

A similar effect has been observed in MJD, in which ATXN3 phosphorylation at S256 by glycogen synthase kinase 3β reduced mutant ATXN3 aggregation *in vitro* (177). CK2-dependent phosphorylation of ATXN3 at S236 and S340/S352 decreased the appearance of NIIs and controlled the nuclear translocation of ATXN3 providing a reasonable therapeutic approach for MJD (178). In contrast, phosphorylation of mutant ATXN1 at S776 is associated with the formation of aggregates and neurodegeneration (179). Together, these observations

suggest that post-translational modification play an important role in the manifestation and/or progression of the disease, reinforcing the idea that the protein context in which the polyQ-stretch is located influences the pathology.

1.5.4 Role of nuclear versus cytoplasmic localization of mutant proteins

The presence of polyQ aggregates in the nucleus of cells is thought to play an important role in the disease pathogenesis by at least two main mechanisms: (i) by disrupting nuclear organization and function (180) and/or (ii) by affecting gene expression (24). In mammalian cells, aggregated polyQ peptides were shown to be highly toxic when target to the nuclei and less so in the cytoplasm (163). Some studies revealed that nuclear accumulation of mutant proteins are predominant in HD, SCA1, 3, 7 and 17, DRPLA, and SBMA patients (181); however, inclusions in the cytoplasm are also found in affected brain regions of HD, SCA2, MJD, DRPLA and SBMA patients (182-184). In disease models, the presence of aggregates in the nucleus seems to cause more severe phenotypes. Specifically in MJD, studies in mice revealed that nuclear localization of ATXN3 is required for the manifestation of symptoms (185). More recently, one putative ATXN3 nuclear localization signal (NLS) was proven to be functional in yeast and mammalian cells. The NLS is located at the N-terminus of ATXN3 may have implications in pathogenesis (186).

1.5.5 Defects in axonal transport

At the axon level, it has also been suggested that defects in the axonal transport may underlie pathology of some of the polyQ diseases (reviewed in (187). The exact mechanism is not known but it has been proposed that (i) disease-causing proteins may have normal functions in the axonal transport system and cause axonal blockages when mutated; and that (ii) protein aggregates may physically block transport within the narrow axonal processes. Moreover, Gallarza and collaborators showed that Htt is both anterogradely and retrogradely transported in rat sciatic nerve axons (188). It has been suggested Htt may interact with motor proteins (a subunit of dynactin) via HAP1 (189). ATXN3 was also shown to interact with dynein intermediate chain 2 (190) and to be a microtubule associated protein (191). Pathological evidence for axonal transport problems in HD comes from observations in transgenic HD mouse models and human patient brains. Several groups have demonstrated that dystrophic striatal and corticostriatal neurites in HD exhibit characteristics of blocked axons, namely, accumulations of vesicles and organelles in swollen axonal projections and termini in association with Htt aggregates (34, 192). Huntingtin accumulations have been found in axons of striatal projection neurons in R6/2 and knock-in mouse models of HD and also in human patient brains (67).

1.5.6 Mitochondrial dysfunction

Impairment of mitochondrial function is one of the key events in polyQ diseases leading to cell death via activation of apoptotic cascades. The process of mitochondrial dysfunction is accompanied by impaired

respiration, stress induced mitochondrial depolarization, increased ROS production leading to oxidative damage, and abnormal energy metabolism in polyQ diseases (193, 194). The importance of mitochondria in polyQ disease pathogenesis and related cell death had been suggested by mimicking the HD phenotype using the complex II respiratory chain inhibitors 3-nitropropionic acid or malonate (195, 196). In toxin models of HD, the activities of complex II and III were reduced and energy metabolism was impaired, as observed in human HD brains and in cells derived from HD model mice, respectively (197, 198). Electron microcopy studies localized mutant Htt into membranes and the incubation of normal mitochondria with the purified expanded polyQ protein reduced their Ca^{2+} retention capacity (194). It has been demonstrated that recombinant mutant htt directly induced mitochondrial permeability transition (MPT) pore opening in isolated mouse liver mitochondria. Mutant Htt decreased the Ca^{2+} threshold necessary to trigger MPT pore opening accompanied by a significant release of cytochrome c (199). In a cellular and a *Caenorhabditis elegans* HD model, it has been shown that the over-expression of mutant htt diminished the normal dynamics of mitochondria fusion and fission interfering with mitochondrial ATP generation (200).

The expression of mutant AR caused mitochondrial abnormalities leading to caspase activation. Surprisingly, a polyQ-dependent decrease in mitochondrial number and impaired mitochondrial membrane potential was observed with increased ROS. Mutant AR also altered the expression of genes important for mitochondrial function including one of the key regulators of mitochondrial biogenesis and function, peroxisome proliferator-activated receptor c coactivator-1 (PGC-1b), and its target genes peroxisome proliferator-activated receptor c, and mitochondrial transcription factor A. The mitochondrial genes regulated by mitochondrial transcription factor A and several cellular antioxidant genes were also down-regulated suggesting a profound role of mitochondrial dysfunction in SBMA pathogenesis (201).

Similarly to previously cited studies, PGC-1a, another member of PGC-1 complex, is a mitochondrial biogenesis and function co-activator, which regulates mitochondria response to oxidative stress (202). Mutant htt was reported to directly bind to PGC-1a and interfere with its function (203), supporting the connection between oxidative stress and mitochondrial dysfunction in HD. Moreover, PGC-1a is regulated by cAMP response element (CRE)-binding protein (CREB), a transcription factor down-regulated by expanded polyQ htt (152) and mutant htt was shown to interfere with transcription of PGC-1a (204).

Mutant ataxin-3 has been recently reported to decrease the activities of antioxidant enzyme causing increased damage of mitochondrial DNA (205). Oxidative stress also induces nuclear localization of mutant ATXN3 proteins (206), which has been associated to pathology. Moreover, mutant ATXN3 expressing cells are more sensitive to treatment with the apoptosis inducer staurosporin, probably because the cells present lower levels of bcl-2. Mitochondria from MJD patients were also found to release increased levels of cytochrome c (207). Based on a number of studies, it can be suggested that mitochondrial impairment is also a common feature in the pathogenesis of polyQ diseases.

1.6 Therapeutic approaches

Potential treatments of polyQ diseases could be divided into two classes: (i) those targeting the mutant proteins directly or indirectly; and into (ii) those targeting downstream cellular deterioration caused by the mutant proteins.

(i)**Therapies aimed at the polyQ proteins** themselves include:

(a) ***gene silencing*****.** Down-regulating the expression of the abnormal gene has been demonstrated to be an effective approach to therapy in Tet-Off mice systems of HD (208) and MJD (209), and in a doxycycline-regulated SCA1 mouse model (210). The amount of nuclear inclusions was reduced and the behavioral phenotype was ameliorated upon shutting-down of mutant Htt and ATXN3 protein expression, respectively. Several techniques targeting polyQ protein expression have been explored including small interference RNA or short hairpin RNA (211). In particular cases, this strategy makes use of single nucleotide polymorphisms allowing the siRNA to specifically target the mutant allele, sparing the RNA of the normal copy of the gene (212-214). The gene silencing approach is very suitable for diseases with pathology at limited localizations such as the retina in SCA7, however targeting wide CNS pathology in other polyQ diseases is currently still very challenging.

(b) attempts to ***enhance protein degradation*** through autophagic clearance of the mutant proteins. This strategy resulted in reduced toxicity in N171-82Q Htt, in ATXN3 transgenic mice and in *Drosophila* and zebrafish models of HD treated with lithium, calpain inhibitors or rapamacyn analog CCI-779 (215-217). Increased degradation of polyQ proteins through increased UPS activity has not been achieved yet because less compounds are available to manipulate this system. Amiloride and benzamil have been reported to reduce polyQ aggregation and toxicity in HD models (218). Y-27632, a rho-associated kinase inhibitor, seems to have a unique double effect since it has been shown to modulate both main cellular degradation pathways. The small molecule increases both UPS activity and activates macroautophagy and led to reduced levels and aggregation of mutant Htt, ATXN3, AR and atrophin-1 in cell models (219).

(c) ***inhibition/prevention of aggregation*****.** This was one of the fist therapeutic strategies used in the polyQ field. Certain small molecules like Congo red and trehalose can bind directly to and prevent the formation of aggregated species. In the R6/2 mice, these compounds significantly increased survival (220, 221). Cystamine may also reduce expanded polyQ aggregation by inhibition of transglutaminases that are thought to crosslink expanded polyQ proteins and to facilitate their aggregation. Cystamine treatment was effective, by decreasing Htt aggregation and improving survival in mice (222). Moreover, cysteamine, the FDA-approved reduced form of cystamine, was shown to be neuroprotective in HD mice by increasing BDNF levels in the brain (223), since experimental evidence derived from both clinical as well as basic research suggests a close association between BDNF deficiency and HD pathogenesis (reviewed in (224). Another approach to reduce misfolding and aggregation is to increase the cellular levels of molecular chaperones. Oral administration of geranylgeranylacetone enhanced expression of Hsp70, Hsp90 and Hsp105 through induction of Heat-shock

factor-1 (HSF-1) in the CNS, where it inhibited nuclear accumulation of mutant AR, leading to an improved motor behavior and increased survival of transgenic SBMA mice (225). An Hsp90 inhibitor, 17-(allylamino)-17-demethoxigeldanamycin (17-AAG) has also been demonstrated to reduce neurodegeneration in SBMA mice (226). Treatment with 17-AAG increased proteasomal degradation of mutant AR and sustained the cellular heat shock response (HSR). 17-AAG has also an effect for other polyQ-induced types of degeneration, whose proteins are not direct Hsp90-client proteins. Recently, has been shown that in *Drosophila* models of MJD and HD, 17-AAG suppressed polyQ-induced pathogenesis via activation of HSF-1 (227).

(ii)**Therapies aimed at the downstream effects of the mutant polyQ proteins** include:

(a) ***modulation of transcription.*** Normalization of transcription, in particular by targeting histone methylation and acetylation using different compounds, has been tested in different models of polyQ diseases. Histone deacetylase inhibitors such as suberoylanilide hydroxamic acid (SAHA), sodium butyrate (SB) and phenylbutyrate have been demonstrated to improve the motor phenotype in mouse models of HD, DRPLA and SBMA (228-232). On the other hand, inhibition of histone H3 methylation by mithramycin led to an increase of the lifespan, improvement in motor performance and striatal pathology in R6/2 mice (233). Rolipram also alleviated transcriptional dysregulation by increasing the phosphorylation and activity of CREB. R6/2 HD mice treated with rolipram presented an increase in lifespan as well as an improvement of the neuropathology and a slower progression of neurological phenotype. Interestingly, the expression of BDNF, which is impaired in HD (234), was induced in treated mice via restored function of CREB (235). In a *C. elegans* model, resveratrol-mediated Sir2 activation specifically rescued early neuronal function phenotypes induced by the expression of mutant Htt proteins (236).

(b) ***mitochondrial stabilization and reduction of oxidative stress***. Reduced concentration of creatine and phosphocreatine have been observed in the brain of HD patients, reinforcing the idea that mitochondrial dysfunction and energy depletion could be implicated in polyQ pathogenesis (237). Creatine treatment stabilized the MPT, prevented ATP depletion and increased protein synthesis. Creatine treatment also ameliorated brain pathology and motor symptoms in mouse models of HD (238, 239). Moreover, antioxidants such as α-lipoic acid, coenzyme Q10, clioquinol, tauroursodeoxycholic acid or BN82451 have proven to be effective in R6/2 mouse lines (240). Specifically, coenzyme Q10, a cofactor of mitochondrial electron transport chain and inhibitor of MPT, extended survival of R6/2 mice, improved motor performance and reduced inclusions (241). Clioquinol treatment reduced striatal atrophy, decreased nuclear inclusions formation, improved development delay and enhanced lifespan in R6/2 mice (242).

(c) ***excitotoxicity blockage***. Excessive activation of N-methyl D-aspartate (NMDA) glutamate receptors and the subsequent excitotoxicity in striatum neurons, has been implicated in HD pathogenesis (243). Interestingly, the use of compounds that block the excessive glutamate release, like riluzole, has proven to be effective in a HD mouse model (244). Similar to riluzole, two drugs affecting the levels of glutamate in the

synaptic cleft, LY379268 and 2- methyl-6-(phenylethynyl)-pyridine, have significantly increased the lifespan of R6/2 mice (245). Administration of remacemide (NMDA antagonist) and/or coenzyme Q10 significantly prolonged the survival rates of the mice (246). However, the clinical trial using these drugs individually or in combination, displayed no significant effects in HD patients (Huntington Study Group, 2001).

(d) *apoptosis inhibition*. Minocycline, an antiapoptotic drug, was shown to inhibit the mitochondrial release of apoptosis inducing factor, proapoptotic protein Smac/Diablo, and cytochrome c, while decreasing the cleavage of proapoptotic factor Bid and activating certain caspases (247). Minocycline treatment extended the lifespan of R6/2 mice and the combination of minocycline and coenzyme Q10 has further improved survival, neuropathology and motor phenotype when compared with any of the treatments alone (248, 249). Although the results of the clinical studies using minocycline produced promising data, a long-term clinical trial should be conducted to clearly evaluate the benefits of minocycline in HD patients. Another strategy for apoptosis blockade is the inhibition of caspases that could have a second beneficial effect by decreased generation of caspase-cleaved fragments of mutant proteins. Indeed, a broad caspase inhibitor, z-Val-Ala-Asp-fluoromethylketone, was shown to improve the rotarod performance of R6/2 mice and extended the lifespan by 25% (250).

1.7 Machado-Joseph disease (MJD)

The official history of MJD started is the 1970s with the description of three families originally from Azores living in the United States of America. The disease was first described in a patient with Portuguese ancestors, William Machado, by Nakano and collaborators, as an *autosomal dominant ataxia* and they named it as *Machado disease* (251). The Thomas family was reported in 1972 by Woods and Schaumburg, and displayed similar characteristics to those described previously but with some particular clinical features. The disease was entitled *Nigro-spino-dentatal degeneration with nuclear ophthalmoplegia* (252). Later on, Rosenberg and colleagues described a particular type of autosomal dominant hereditary ataxia in the family of Antone Joseph, which was designated as *Joseph disease* (253). The authors described the diseases as distinct clinical entities and the controversy lasted for several years. In 1978, Andrade and Coutinho traveled to the Azores islands, where they undertook extensive studies in a large number of families (254-256). In the 1980, Coutinho e Sequeiros proposed for the first time the name Machado-Joseph disease (MJD) for a clinical entity encompassing many of the previously described phenotypes, and some clinical criteria for diagnosis were introduced (257). They defined MJD as a single disorder characterized by high clinical variability, proposing the clinical classification of patients into three types that accommodated variability. The ultimately disease unification was achieved in 1983-84, when Rosenberg and Barbeau examined several patients and found siblings that presented characteristics of different types of MJD (258, 259).

In our days, MJD is also known as spinocerebellar ataxia type 3 (SCA3), and is known to be the most common autosomal dominant ataxia worldwide (15-45% of all forms in distinct populations) (181, 260, 261). In Portugal, the disease prevalence is of 3.1:100.000 habitants, including a total of 108 MJD families (262).

1.7.1 MJD clinical symptoms and sub-types

Motor function is highly affected in MJD. This progressive disease is characterized by ataxia, weakness in the arms and legs, spasticity, difficulty with speech articulation and with swallowing, imapaired involuntary eye movements and dystonia. Some patients have twitchings of the face or tongue, or bulging eyes (255, 257, 259, 263).

The difficulty to accommodate all disease presentations in a unique identity could be partially justified by the phenotypic variability of MJD that lead to the organization of the disease sub-types, sorted by the age of clinical onset and major symptoms of the disorder (257). MJD type I includes the MJD forms with early age at onset (10-30 years of age), faster progression and more severe pyramidal and extra-pyramidal signs. MJD type II is the most frequent, and is characterized by intermediate age-at-onset (20-50 years of age) and a moderate progression rate, with patients exhibiting mainly ataxia and ophthalmoplegia. MJD patients with MJD type III present the latest age at onset (40-70 years of age), slow disease progression and more peripheral signs. In 1983, Rosenberg added a fourth type, which is the rarest and includes MJD patients exhibiting Parkinsonic symptoms associated with the most representative symptoms of MJD (258, 260).

1.7.2 MJD pathology

Pathological examination of post-mortem brains from MJD patients revealed neuronal degeneration of specific brain regions, such as the cerebellar dentate nucleus, pallidum, substantia nigra, subthalamic, red and pontine nuclei, select cranial nerve nuclei and the anterior horn and Clarke's column of the spinal cord (Fig. 1.3) (36, 264-268).

The majority of the brains of MJD patients with disease duration of more than 15 years presented reduced weight when compared with individuals without medical histories of neurological or psychiatric diseases (265).

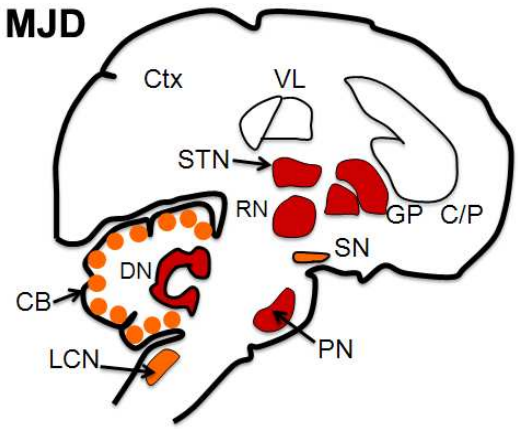

Figure 1.3. Classical brain regions affected in MJD are showed in orange. Adapted from (2). STN: subtalamic nucleus, GP: globus pallidus, RN: red nucleus, SN: substantia nigra, PN: pontine nucleus, DN: dentate nucleus, LCN: lateral cuneate nucleus, CB: cerebellar cortex.

Later on, pathoanatomical investigations using thicker tissue sections (which allow observation of an increased number of neural cells per section) demonstrated widespread damage to the cerebellum, thalamus, midbrain, pons, medulla oblongata and spinal cord in MJD (74, 269-275). Recently, a systematic immunohistochemical study of serial thick sections of MJD patients revealed axonal ATXN3 aggregates in fiber tracts known to undergo neurodegeneration in MJD (276).

MJD, as other polyQ diseases, is characterized by the presence of neuronal ubiquitylated inclusions; within the inclusions other proteins have been found, such as molecular chaperones, proteasomal components, TFs and both normal and pathogenic ATXN3 (35, 45, 277). As in the neuronal cell bodies, the axonal aggregates in MJD were ubiquitylated and immunopositive for the proteasome- and autophagy-associated protein p62 (276).

1.7.3 MJD genetics

Like other polyQ diseases, MJD is transmitted in an autosomal dominant manner and is characterized by intergenerational instability of the expanded CAG repeat. The expanded repeats may expand or retract, but often during paternal transmissions, expansion is more common. As a result, there is an early age-at-onset in successive generations (anticipation) (29, 278). In general, longer CAG tracts underlie more severe symptoms and premature disease onset (29).

MJD is caused by a mutation in the *MJD1/ATXN3* gene, mapped to the long arm of chromosome 14 (14q24.3-q32) in 1993 (279). Cloning of the gene was achieved one year later by Kawaguchi and collaborators (20). Molecular diagnosis of MJD became possible, and the mutation was then confirmed in families of diverse origins (29, 280-282). As expected, the presence of mutation (expansion) of the CAG tract was verified only in patients.

The *MJD1/ATXN3* gene is composed by 11 exons, spanning a genomic region of about 48 kb, the (CAG)n tract being located at exon 10 (283). In the WT alleles, the CAG repeat ranges between 12-44; the expanded alleles, with full penetrance, range between 52-86 repeats (284, 285). Individuals carrying intermediate CAG repeats length (45-51) may or may not manifest the disease (284-286).

Northern blot analysis revealed ubiquitous *ATXN3* expression and the existence of four different transcripts (1.4, 1.8, 4.5 and 7.5 Kb), probably arising from differential splicing and polyadenylation signals (283). Five cDNA variants were described: MJD1a, MJD1-1, MJD5-1, MJD2-1 and H2 (20, 287). The MJD1-1 and MJD5-1 variants only differ in the size of their 3' UTR, and employ exon 11 as 3'-terminal sequence. MJD1a was the first one to be described and uses exon 10 to provide the 3'-terminal sequence. MJD2-1 is identical to MJD1a except for the single nucleotide substitution in the exon 10 stop codon (287). In H2, exon 2 is absent (283).

Recently, the occurrence of additional alternative splicing at the *MJD1/ATXN3* gene was investigated. Two novel exons and 50 additional alternative splicing variants were described (288). However, the physiological and clinical relevance of these variants remains to be determined.

1.7.4 MJD protein: ataxin-3 (ATXN3)

Protein homology. The *ATXN3* gene encodes for a 42 KDa protein, ataxin-3 (ATXN3). ATXN3 is evolutionarily conserved in mice (289), rat (290), chicken (291), *C. elegans* (292) and other organisms. Interestingly, the long polyQ tract is specific to humans, since it is nearly absent in other species such as mouse (6 Q) and *C. elegans* (1 Q).

Domains. The human ATXN3 protein has a conserved N-terminal Josephin domain, containing the putative catalytic triad of aminoacids: cysteine (C14), histidine (H119) and asparagine (N134). This domain is followed by two or three ubiquitin-interacting motifs (UIMs), depending on the protein isoform. ATXN3 also contains a conserved nuclear-localization signal (NLS) (293). The polyQ stretch of variable length is located at the C-terminus of the protein (294, 295).

Isoforms. Until now, at least four ATXN3 isoforms were described: isoform 1 (NP_004984) has 361 aa, with a hydrophilic C-terminal and corresponds to the clones MJD1-1 and MJD5-1; isoform 2 (P54252) has a distinct C-terminal region when comparing with the first one and it has a hydrophobic nature. It is formed by 365 aa and matches the MJD2-1 clone (287); the third isoform, MJD1a (S50830), contains 349 aa (it lacks 16 aa within the C- terminus region comparatively to isoform 2, due to a premature stop codon) (20). Finally, the isoform 4 (NP_1093376) contains less 55 aa than isoform 1 due to the lack of exon 2 in the H2 clone (283). This ATXN3 variant lacks the catalytic aminoacid (C14), essential for ATXN3 deubiquitylating *in vitro* activity against poly-ubiquitin chains (see **Function**).

Expression and subcellular localization. Ataxin-3 is highly present in the cytoplasm of most cells, but may be present also in the nucleus and has been associated with the nuclear matrix, endoplasmic reticulum (ER) and mitochondria (35, 36, 293, 296, 297). As in other CAG repeat diseases, the abnormal and normal allele products were shown to be similarly expressed in lymphoblastoid cells and in the brain of MJD patients (35, 298). Isoform 1 (3 UIMs) is the most abundant ATXN3 isoform in brain of patients and transgenic mice (299). Paulson *et al* demonstrated that in patients, both the normal and mutant ataxin-3 proteins were expressed throughout the body and in all regions of the brain examined, including areas generally spared by the disease. In *C. elegans* and mouse, the homologous ataxin-3 proteins are also widely expressed since embryonic life stages (289, 292).

Molecular partners. The ATXN3 interactome includes proteins involved in (i) transcriptional regulation, (ii) cell structure and motility, and (iii) in the ubiquitin-proteasome pathway (UPP) and molecular chaperones (reviewed in (300).

(i) The interaction of ATXN3 with transcriptional repressors, activators and HDACs suggests a putative role in transcription regulation (160, 301), however the relevance of these interactions *in vivo* are still not clear;

(ii) ATXN3 binds to alpha- and beta-tubulin and also to dynein (190, 302, 303). ATXN3 plays a role in muscle cell differentiation by interacting with and regulating the levels of alpha5

integrin and other proteins (300, 304). Moreover, the absence of ATXN3 causes cytoskeleton disorganization (191), suggesting a role for ATXN3 in cytoskeleton and maintenance of cell structure;

(iii) A significant number of ATXN3 molecular partners are components or regulators of UPP and cell surveillance: ATXN3 binds to ubiquitin, proteasomal subunits, parkin (E3 ubiquitin ligase), C-terminus of Hsp70-interacting protein (CHIP), Valosin-containing protein (VCP), UBXN5, ubiquitin-like proteins such as HHR23A/B, NEDD8 and components of the SCF (Skp1, Cullin, F-box) complex (190, 294, 295, 302, 305-309). ATXN3 also binds to Hsp90 and Hsp60 (300).

Function. A crucial breakthrough in the understanding of ataxin-3 function was the discovery of its deubiquitylating (DUB) activity *in vitro* (294, 295, 310). There are five main classes of DUBs, and ATXN3 is included in the MJD domain group (311). The primary role of DUB proteins is to deubiquitylate the substrate facilitating its degradation. However, some authors have suggested that DUBs can also have a polyubiquitin *proof reading* activity (E4) or even rescue off-target proteins from the proteasome (312).

Expression of WT ATXN3 and not of the catalytic inactive form (C14A) in cells diminishes the ubiquitylation level of VCP substrates, suggesting that ATXN3 is capable of removing ubiquitin from proteins *in vivo* (302). Even though DUBs are often promiscuous, specific substrates have been suggested for ATXN3, namely proteins involved in endoplasmic reticulum-associated degradation (ERAD). ATXN3 increases the level of CD3delta by decreasing its degradation, but does not alter the levels of several non-ERAD substrates (302). Recently, Alpha5 integrin subunit (304) and parkin (313, 314) were also found to be specific substrates of ATXN3. Of note, the putative role in transcriptional regulation suggested for ATXN3 can also be related to its DUB activity, since removal of ubiquitin molecules from TFs and/or histones can modulate transcription. Nevertheless, this hypothesis remains to be tested.

1.7.5 Animal models of MJD pathogenesis

Since the description of the disease-causing gene in MJD, several *in vitro* and *in vivo* models were generated in order to gain insight into the pathogenic mechanism(s) and to assess therapeutic approaches. So far, there are MJD models in cell culture, *C. elegans*, Drosophila, mouse and rat. A brief description of these models will follow (Table 1.2).

Cell culture. Studies in cell lines brought new insights to the study of MJD (35, 45, 49, 56, 155, 277, 315, 316), some of which were then tested in animals models of the disease. In general, it was found that (i) mutant ATXN3 toxicity is influenced by the length of the polyQ tract; (ii) the polyQ-containing truncated form of the protein displays higher toxicity than its full-length counterpart; (iii) causes increased cell death; (iv) mutant ATXN3 recruits non-pathological ATXN3 into the aggregates; (v) the aggregates are an early event in disease and

finally (vi) relevant cell function components like proteasome subunits, molecular chaperones and TFs are find sequestered into ATXN3 aggregates.

***C. elegans*.** In a model developed by Khan *et al* using unc-119 promoter, animals expressing full-length ATXN3 (variant MJD1a) with 130 glutamines (and not with 17Q or 91Q) in all neuronal cells did not present significant aggregation or toxicity phenotype (only in 7 day-old or older animals) (44). In contrast, expression of a truncated form of ATXN3 (containing only the polyQ domain and C-terminal region) caused polyQ length-dependent aggregation and toxicity. Also, expanded polyQ proteins caused interruption of the synaptic transmission and induced swelling and abnormal branching of neuronal processes. In this model all neurons showed equal susceptibility to the expression of expanded polyQ proteins.

Drosophila. The majority of the work in MJD using flies as a model system comes from the lab of N. Bonini. Initially, Warrick and collaborators recreated glutamine repeat disease by expressing a segment of ATXN3 containing the polyQ tract. The wide expression of the truncated form of ATXN3 revealed that the neurons were the most affected cell types; it caused the formation of nuclear inclusions (NI) and late-onset cellular degeneration (46). The authors also showed that overexpression of Hsp70 suppressed polyQ-induced neurodegeneration *in vivo*, without major effects on NI formation (133). In 2005, they found that human WT ATXN3 is a striking suppressor of polyQ neurodegeneration *in vivo*, and that this suppressor activity of ATXN3 was dependent upon its ubiquitin-associated activities (DUB) and on proteasome function (95). Later on, a genome-wide screen for modifiers of ataxin-3 neurodegeneration was performed in this model. The authors found 25 modifiers encoding 18 genes, most of which affected protein misfolding. The modifiers affected ATXN3 accumulation in cells in a proteasome- or autophagy-dependent manner (129). MicroRNA pathways were also found to modulate MJD induced neurodegeneration downstream of ATXN3 toxicity (317).

Mouse. Eight mouse models have been generated since 1996 (48, 49, 105, 165, 185, 209, 318, 319), all of which show expression of mutant ATXN3 in the mouse brain, however displaying considerable differences regarding affected brain regions and neuronal sub-types, as well as distinct rates of disease progression. Table 1.2 summarizes the features of the models generated so far. These dissimilarities may arise from the use of different promoters to drive the expression of mutant ATXN3 proteins, and from variations in the transgene copy number. Moreover, mice have reduced lifespan and increased metabolic activity when compared to humans. Although no model has yet completely reproduced the pathological and clinical symptoms observed in MJD patients, these mouse models have provided important insights into the mechanisms involved in MJD pathogenesis.

Rat. Overexpression of mutant ATXN3 in the rat brain using lentiviral vectors (LV) led to neuropathological abnormalities: formation of ubiquitylated ATXN3 aggregates, alpha-synuclein immunoreactivity and loss of dopaminergic markers (TH and VMAT2). Alves and collaborators suggested striatal pathology as contributing factors for the dystonia and chorea observed in some MJD patients (320).

1.7.6 ATXN3 loss-of-function models

The first knockout (KO) models for ATXN3 were generated in *C. elegans* by the *Caenorhabditis Genetics Center* (CGC) and by National Bioresource Project (NBRP) for the Experimental Animal "Nematode *C. elegans*"; and the characterization of these animals was performed by our group (292). No overt phenotype was observed at 20°C in the KO animals, which were viable and showed no obvious abnormalities. Nevertheless, gene expression analysis uncovered a molecular phenotype with significant dysregulation of genes involved in the UPP, structure/motility and signal transduction (292). More recently, our group has found that at 25°C ataxin-3 KOs do present an uncoordination phenotype (321). Surprisingly, these animals also show an increased resistance to heat stress, which was further enhanced by pre-exposure to a mild heat shock. At a molecular level, ATX-3 mutants have a distinct transcriptomic and proteomic profile with several molecular chaperones abnormally up-regulated during heat shock and recovery. The improved thermotolerance in *atx-3* mutants is dependent on *DAF-16*, a critical stress responsive transcription factor involved in longevity and stress resistance (300).

ATXN3 null mice are also viable, fertile and display normal development and lifespan, with no major coordination problems (79). Although no morphological signs of pathogenesis were found in several areas of the CNS of mice lacking ATXN3, there were increased levels of ubiquitylated proteins in Atxn3 KO tissues, providing the first *in vivo* cue of the deubiquitylating function of ataxin-3.

These observations support the idea that MJD is not solely caused by the loss-of-function of ATXN3, and constitute important tools to investigate the contribution of WT ATXN3 in MJD pathogenesis.

Tabela 1.2- Animal models for the pathogenesis of MJD.

Model organism	Transgene	Promoter	CAG-repeat length	Expression pattern	Aggregation	Neurodegeneration/Pathology	Disease onset	Phenotype
C. elegans								
e.g. Khan *et al.*, 2006	Full-length and C-terminal truncated MJD1a cDNA	*unc-119*	17, 19, 63, 127 and 130	pan-neuronal	yes	no/inclusions	ND	uncoordination
Drosophila								
e.g. Warrick *et al.,* 2005	Full-length and C-terminal truncated MJD1a cDNA	gmr-/ elav-GAL4	27,78 and 84	eye and nervous system	yes	yes	ND	eye morphology and photoreceptor disrupted; premature death
Mus musculus								
Ikeda *et al.,* 1996	Full-length and C-terminal truncated MJD1a cDNA	L7	79	Purkinje cells	no	yes (three layers of the cerebellum)	4 W	ataxia; gait disturbance; absence of rearings
Cemal *et al.,* 2002	ATXN3 YAC	*ATXN3*	64, 67, 72, 76 and 84	ubiquitous	yes	pontine and dentate nuclei	4 W	weight loss; lowered pelvis and limb clasping; hypotonia; tremor; negative geotaxis deficit
Goti *et al.,* 2004	Full-length MJD1a cDNA	PrP	71	ubiquitous	yes	↓ number of TH-positive neurons in the SN	8 W	weight loss and progressive impaired grip strength by forelimbs and hindlimbs; deficit to remain on an accelerating rod
Bichelmeier U *et al.,* 2007	Full-length MJD1-1 cDNA	PrP	15, 70 and 148	ubiquitous	yes	ATXN3 and Ub-positive inclusions	6 W	weight loss, increased base-width of the posterior pons; reduced activity and grooming; tremor; premature death
Chou *et al.,* 2008	Full-length and C-terminal truncated MJD1a cDNA	PrP	79	ubiquitous	yes	neuronal loss in the cerebellum/intranuclear inclusions in pontine and dentate nuclei and SN	5 W	motor uncoordination; hypoactivity; ataxia; weight loss; deficit in the ability to correct body posture
Boy J *et al.,* 2009	Full-length MJD1-1 cDNA	PrP/Tet-Off	77	ubiquitous	yes	Purkinje cells	9 W	reduced ansiety, hyperactivity, motor uncoordination. reduced weight gain
Boy *et al.,* 2010	Full-length MJD1-1 cDNA	rat huntingtin	148	ubiquitous	no	Purkinje cells	48 W	hyperactivity at early disease stages, motor uncoordination and motor learning impairment in old mice
Silva-Fernandes et al., 2010	Full-length MJD1-1 cDNA	CMV	83 and 94	ubiquitous	yes	astrogliosis (SN and vestibular) and neuronal atrophy (pontine and dentate nuclei)	16 W	motor uncoordination
Rattus norvegicus								
e.g. Alves *et al.,* 2008	full-length MJD1a cDNA	Lentivirus (PGK)	27 and 72	Cortex, striatum or SN (injection)	yes	↓ number of TH-positive neurons in the SN, striatal degeneration, cellular death	ND	ND

Legend: ND- Not Determined; W- weeks; CMV-cytomegalovirus; PrP-Prion promoter; SN- Substantia Nigra; Ub-ubiquitin

1.8 *Caenorhabditis elegans* as a model system

As a model system, *C. elegans* provides a good compromise between the complexity of vertebrates (e.g. mouse) and the simplicity of yeast models. It has many useful characteristics for lab use. In particular, a 2,5-day life cycle (when animals are grown at 25°C) and ~2 week lifespan are very convenient in studying diseases of aging (Fig. 1.4). It is economic and easy to maintain, allowing long term storage as glycerol stocks. In a normal population, *C. elegans* are more than 99% self-fertilizing hermaphrodites making it possible to maintain and study large clonal populations. Males do arise spontaneously, though infrequently, due to meiotic chromosomal non-disjunction, which facilitates genetic studies.

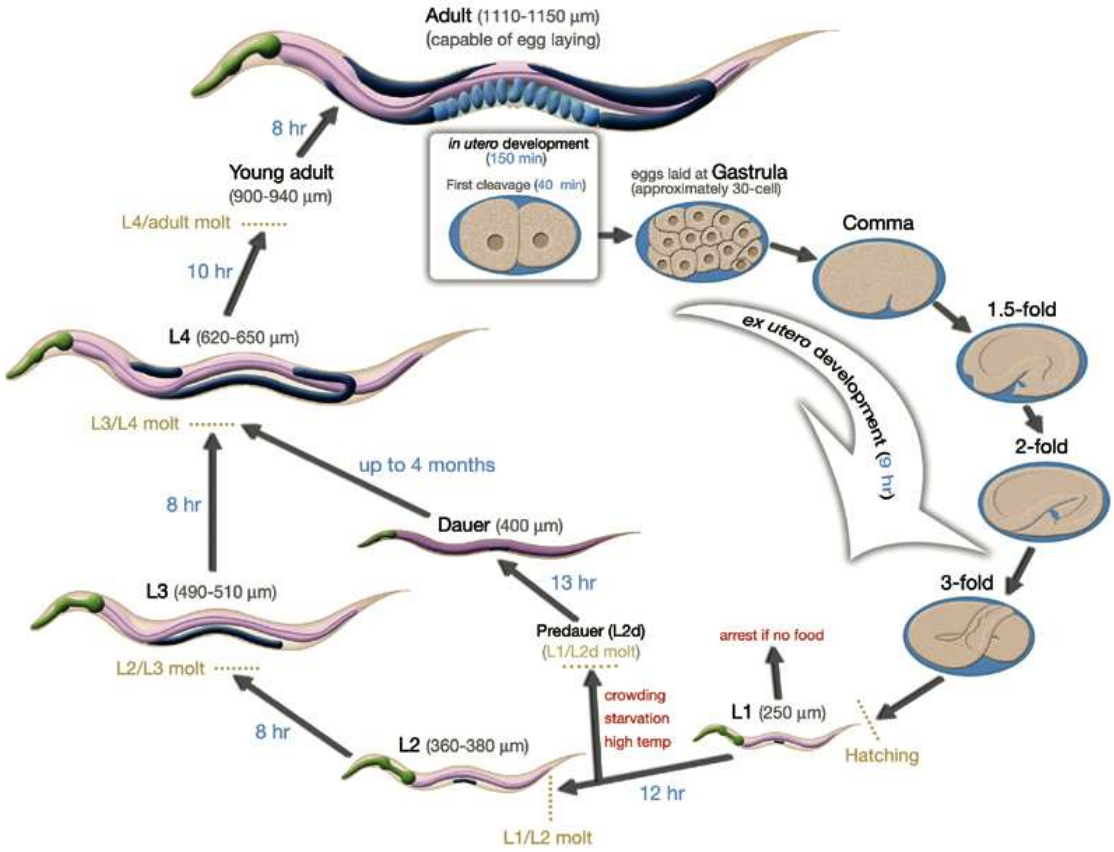

Figure 1.4. *C. elegans* life cycle. *C. elegans* proceed through their complete life cycle, from egg to reproductive adult stage, in about two and a half days at 25°C. The times indicated in blue are the duration of each stage of development. *C. elegans* can enter in dauer stage, an alternate developmental step in which they are extremely resistant to environmental stresses such as starvation. Upon entering in this stage, *C. elegans* life span is significantly extended from weeks to months. Figure adapted from Wormatlas (www.wormatlas.org/handbook/fig.s/IntroFIG6.jpg).

C. elegans constitutes a great model for investigating how polyQ proteins cause neuron-specific pathogenesis because is a multicellular organism with multiple tissue types that can be examined noninvasively as the animal aged. It has a fully functioning nervous system of 302 neurons, with multiple neuron sub-types in which polyQ proteins can be conditionally expressed either in all neurons or in subsets. Moreover, it is possible to identify and assay the function of individual neurons while they remain part of the functioning nervous system and organism. Although the nervous system of *C. elegans* is small, animals display complex behaviors that are good indicators of neuronal function (322). Examples of behaviors that can be measured in *C. elegans*, most of which are neuron-regulated, are given in Table 1.3 (323).

The developmental lineage of neurons and that of the remaining 687 cells in the hermaphrodite animal have been mapped (324, 325). The morphology of all 302 neurons has been defined by electron microscopy and much is known about their synaptic connectivity (326, 327). Behavioral analyses of *C. elegans* with laser-ablated neurons have provided data about the function of small groups or even individual neurons such as chemosensory, mechanosensory, and motor neurons (322, 328). Fig. 1.5 shows the *C. elegans* ventral nerve cord neurons and locomotory circuit.

Since *C. elegans* are transparent animals, behavioral analysis can be combined with *in vivo* imaging and biophysical assays to examine protein solubility and protein interactions in neurons of interest (84, 126).

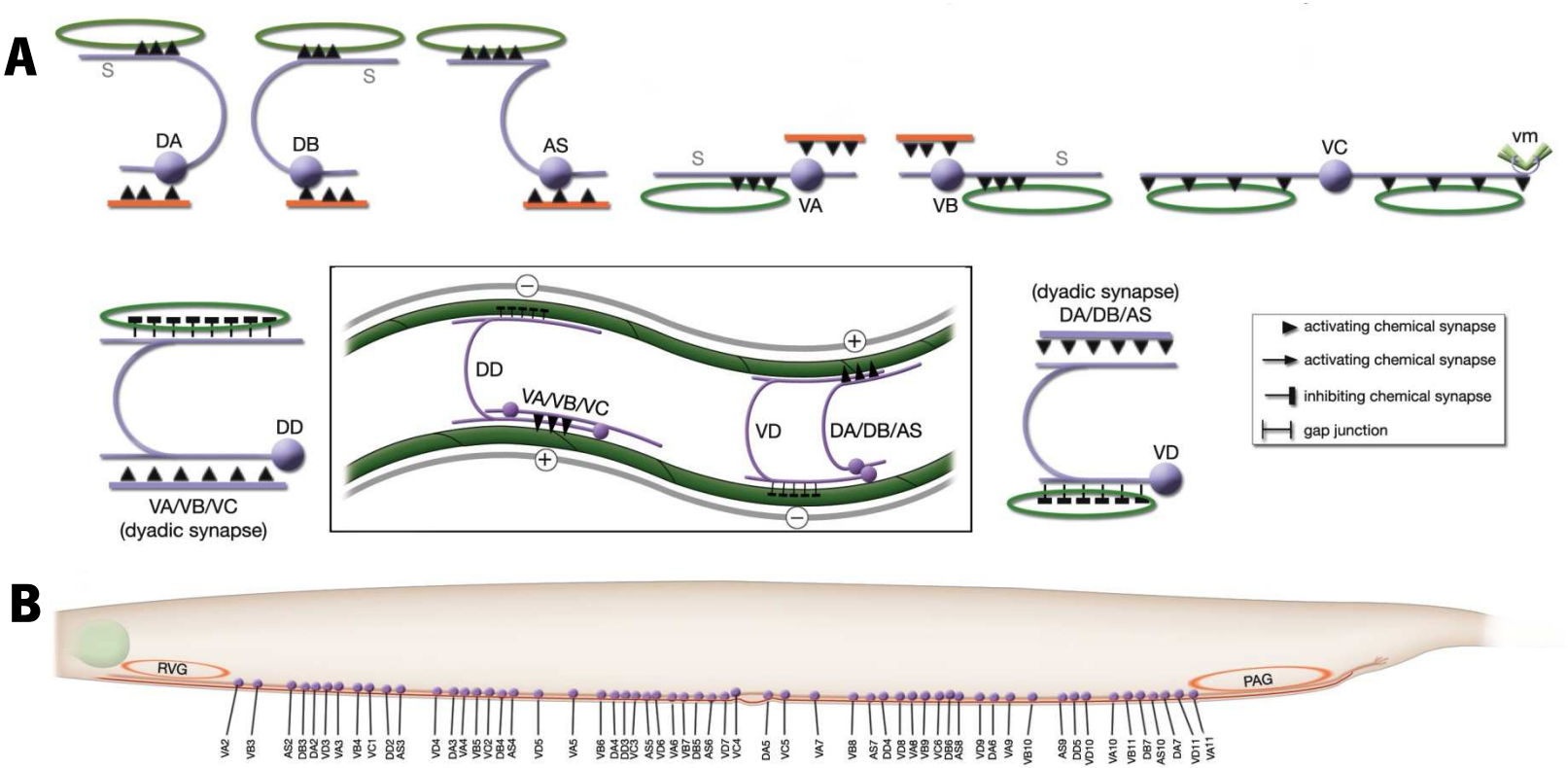

Figure 1.5. VNC motor neurons and locomotory circuit. A. The A motor neurons control backward locomotion and B motor neurons control forward locomotion. D motor neurons, which receive synapses from A and B motor neurons and function as cross-inhibitory on the body wall muscles, are required for both forward and backward locomotion. On the dorsal side, VDs are exclusively post-synaptic, receiving input from DA, DB, and AS neurons as co-recipients at neuromuscular junctions (NMJs) (dyadic synapse). On the ventral side, VD neurons are presynaptic to body wall muscle. DDs are exclusively post-synaptic on the ventral side, where they receive input from VA, VB, and VC neurons as corecipients at NMJs (dyadic synapse). DDs are predominantly presynaptic to body wall muscle on the dorsal side. The synaptic zones for the members of each class do not overlap, creating a clearly defined fate map of neuromuscular activity for each class (327). VC neurons are an exception to this rule. Active zones of members of different classes overlap; however, the transition regions among members are not generally the same for every class (White et al., 1976; Von Stetina et al., 2006). Neurons of a given class, except for VA, are electrically coupled to one another via gap junctions in both the VNC and DC. Similarly, muscle cells in each row of a muscle quadrant are also electrically coupled to their neighbors. The boxed model shows how reciprocal inhibitors (DD, VD) receive inputs diametrically opposite to their zone of innervation, so that contracting muscle quadrants (+) are matched by relaxing quadrants (–) on the opposite side of the body. (S) Synapse-free stretch-sensitive regions; (vm) vulval muscle; (green ovals) muscle; (red lines) interneurons; (black arrows and arrowheads) excitatory chemical synapses; (T-shaped lines) inhibitory chemical synapses; (straight lines with bars on each side) gap junctions. B. Schematic representation of positions of motor neurons between RVG and PAG along the VNC (Adapted from *Wormatlas*, based on (327).

Table 1.3- Examples of behaviors that can be measured in *C. elegans*.

Behavior	Assay
Mechanosensation	Gentle touch to the body
	Harsh touch to the body
	Precipice response
	Nictation
	Head withdrawal and foraging
	Tap reflex and habituation to tap (including tap reflex)
	Nose touch
Osmotic avoidance	Osmotic ring assay
Chemosensation	Chemotaxis, chemoaversion and plasticity-quadrant plate
	Drop assay
	Chemotaxis to volatile point source
	Distinguishing between odorants during cross-saturation
	Decreased response after chronic exposure to attractant
	Oxygen sensing
	Polyunsaturated fatty acids avoidance; liquid drop assay
	Males attraction to hermaphrodites
	Interaction of two chemosensory stimuli (interaction assay)
Learning, adaptation and habituation	Learning, habituation and adaptation to tap
	State-dependent adaptation to volatile odorants
	Ethanol intoxication
	Attraction to chemicals previously paired with attractive stimuli and avoidance of chemicals previously paired with starvation
	Chemotaxis to soluble point source
	Plasticity in chemotaxis using NaCl
	Context dependency in olfactory adaptation
Thermal responses	Thermotaxis-tracking themoclines
	Microdroplet assay for thermotaxis
	Linear thermal gradient assay for thermotaxis assay
	Point source heat avoidance
Locomotion	Quantitation of locomotion rate by counting body bends/Thrashing
	Motility
	Decreased locomotion on food
	Bordering at edges of bacterial lawns
	Spontaneous reversals
	Ivermectin sensitivity assays
	Pirouettes
	Dauer lethargy and molting lethargy
	Duration and velocity of spontaneous forward or backward locomotion
	Suppression of head oscillations during backwards locomotion
	Immobilization in serotonin (liquid)
Feeding	Electropharyngeogram recordings
	Pharyngeal pumping rate
	Foraging
Egg-laying, males and mating	Assessing defective or constitutive egg-laying
	Quantitation of constitutive egg-laying
	Modulation of egg-laying in response by bacteria
	Stimulation of egg-laying with serotonin and other drugs
	Quantification of egg-laying with chitinase assays
	Analyzing the temporal dynamics of egg-laying
	Male mating behaviors
	Nicotine adaptation with or without levamisole induction
Assays of *C. elegans* reproductive behavior	Hermaphrodite sexual behavior
	Sprinting assay
	Sperm expulsion assay
	Male sexual behavior
Defecation	Assaying the defecation motor program (DMP)

Major outcomes of research using *C. elegans*

The genes regulating programmed cell death (ced) were initially identified and the pathway characterized in *C. elegans* (329). In humans, caspases, which play a major role in regulating programmed cell death, were identified on the basis of their similarity to the *C. elegans* ced genes. The discovery of these genes was of such significance that the three scientists who worked to establish the model, mapped the cell lineage, identified cells undergoing programmed cell death and the genes regulating the process, were awarded the Nobel prize in 2002.

Interest in *C. elegans* as a genetic model led to another scientific milestone in 1996 when *C. elegans* was the first multicellular organism to have a completely sequenced genome (330). Researchers have taken full advantage of the available genome and developed numerous forward and reverse genetics techniques. Andrew Fire and Craig Mello were also awarded with the Nobel Prize in Medicine (2006) for their discovery and use of RNA interference (RNAi), gene silencing by double stranded RNA in *C. elegans*.

Today's studies in *C. elegans* continue to influence and direct studies in mammalian models as well as in humans due to their relative speed and simplicity. The benefits of *C. elegans* as a model has led to the development of multiple *C. elegans* systems designed for studying the effect of aggregation-prone proteins. The following sections summarize the most important findings using *C. elegans* as a model system for the study of polyQ diseases.

1.8.1 *C. elegans* models of polyglutamine expansions

Consistent with observations in human disorders, polyQ proteins expressed in the *C. elegans* body wall muscle cells exhibited a polyQ length-dependent aggregate formation and cellular toxicity (43, 83). Furthermore, the threshold of Q35-Q40 for aggregation and motility defects observed in the *C. elegans* muscle cells was within the Q-length range observed in human neurons. For each polyQ length tested, the development of a motility defect correlated with the rate of aggregate accumulation. Near the threshold, animals showed a high degree of variation in the appearance of aggregates and this correlated with toxicity. Like in human polyQ-associated diseases, which shows a progressive exacerbation of the disease symptoms with age, the phenotypes observed in the animals expressing expanded polyQ tracts (and not normal polyQ-lengths) aggravated as the animals aged (83). A link between aggregation onset and age-associated cellular changes was established for the first time in polyQ *C. elegans* models (83, 116, 331). Q82 proteins in the background of the long lived age-1(hx546) mutant exhibit reduced aggregate formation in embryos relatively to the WT background (83).

In order to identify the protein factors that protect cells against the formation of protein aggregates, besides proteins involved in the aging pathway, Nollen and collaborators tested transgenic *C. elegans* strains expressing Q35::YFP, the Q-length threshold associated with the age-dependent appearance of protein aggregation. From a genome-wide RNAi screening 186 genes were identified that, when suppressed, resulted in the premature appearance of protein aggregates. Those genes were classified into five principal groups of polyQ

regulators: genes involved in RNA metabolism, protein synthesis, protein folding, and protein degradation; and those involved in protein trafficking (126).

In order to study the effect of polyQ pathogenic motifs in neuronal cells and to determine if the expression of the same toxic species would affect differently distinct neuronal subtypes, Brignull and colleagues expressed polyQ expanded proteins throughout the *C. elegans* nervous system (84). By the expression of a range of polyQ lengths, the authors showed, similarly to the polyQ *C. elegans* body wall muscle cells model, a polyQ length dependent threshold of Q40 for the formation of protein aggregates (Fig. 1.6). Moreover, at the threshold Q-length, distinct neuronal subtypes were differently susceptible to the expression of expanded polyQ protein. Specifically, ventral nerve cord (VNC) neurons showed aggregated Q40-proteins, whereas certain lateral neurons such as the HSN, CAN and BDU neurons were resistant to aggregation. This model provided a basis for the present work and will be further used and discussed in Chapters 2, 3 and 4.

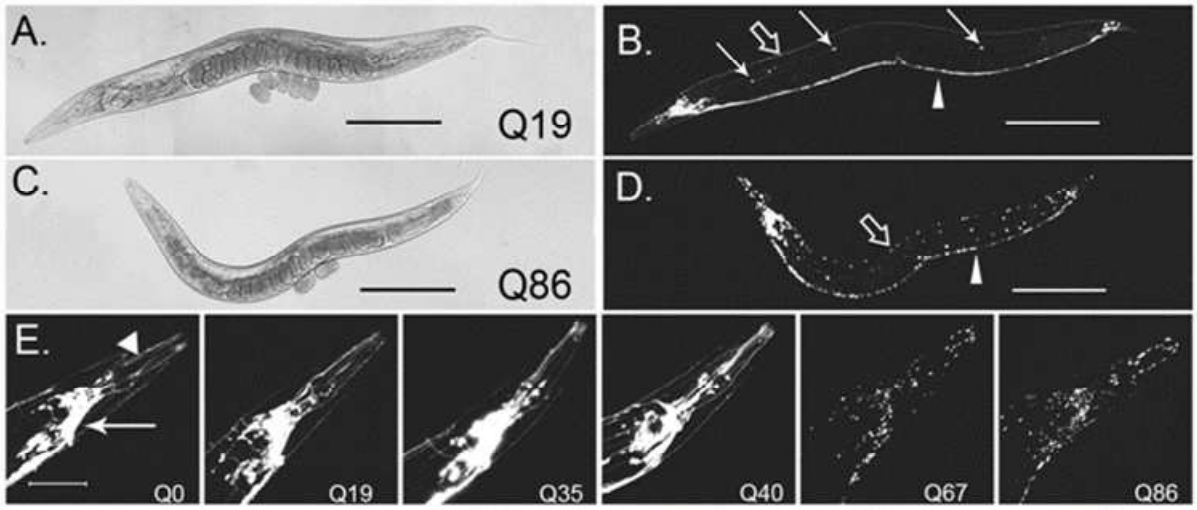

Figure 1.6. Pan-neuronal expression of polyQ proteins results in length-dependent foci formation. Pan-neuronal Q19::CFP has a soluble distribution pattern (A,B), whereas Q86::CFP is distributed into neuronal foci (C,D). Scale bar, 100 μm. Flatenned z-stacks *of C. elegans* head expressiong YFP-alone protein (Q0) (E). Expression of a range of polyQ lengths reveals that proteins with tracts less than that of Q40 maintain a soluble distribution pattern, whereas those expressing Q40 proteins contain aggregates. Scale bar, 50 μm. All animals depicted are young adults (4 days post hatch). Image adapted from (84).

1.8.2 *C. elegans* models of polyglutamine expansions in a protein context

At least three *C. elegans* model systems were generated in which polyQ expansions were expressed in the context of Htt protein fragments (42, 332, 333).

C. elegans lines expressing GFP-Htt fusion proteins in body wall muscle displayed a polyQ repeat-length dependent decrease in body movement compared with WT animals (332). In this model, expression of a normal repeat-length within Htt flanking sequences (GFP-Htt(Q28) already results in a significant loss in motility, suggesting that Htt protein is toxic to the nematodes. Increases in Q-length to pathogenic sizes worsened the phenotype. RNAi of the *C. elegans* ubiquilin gene (implicated in autophagy), exacerbated the motility defect, whereas overexpression rescued loss of worm movement induced by overexpression of GFP-Htt(Q55) (332).

Truncated Htt proteins with different Q-lengths were also expressed in distinct neuronal subsets (42, 333). Two different types of constructs were built: (1) Parker model - chimeras containing the first 57 amino acids of Htt, the polyQ stretch and GFP under regulation of the mec-3 gene promoter, used to drive the expression of the GFP fusion protein in a group of 10 neurons, including six of the touch receptor neurons (333, 334). In this model, neuronal dysfunction was assessed by the analysis of touch sensitivity in the tail, mediated by the PLM mechanosensory neurons. These neurons showed a polyQ length-dependent dysfunction, although this phenotype was not 100% penetrant. In fact, a fraction of the population of transgenic animals expressing expanded polyQ proteins, 88 or 128 Qs, showed touch insensitivity. Consistently with the body wall muscle cell model, the PML neurons exhibited protein deposits for all polyQ lengths expressed, from short to long Qs. For the longer expansions, both protein deposits as well as morphological abnormalities were detected in the PLM cell axons. The cellular dysfunction and morphological abnormalities were not accompanied by cell death in this strain. These data suggested that significant polyQ-associated dysfunction may occur without cell death.

(2) Faber model - proteins containing the first 171 amino acids of Htt followed by the polyQ stretch, under regulation of the osm-10 promoter, driving expression of the 171Htt::polyQ proteins in sensory neurons (42, 335, 336). A polyQ length-dependent cellular degeneration was observed in the two ASH neurons in strains containing the longest polyQ expansion, 150 Qs but not for shorter Q-lengths. However, co-expression of a subthreshold toxic OSM::GFP was necessary for apoptotic cell death to occur. The presence of discrete foci of Htt, reminiscent of protein aggregates, was detected for the Htt::150Qs, but not for shorter polyQ lengths. Also, the number of foci in this strain increased as the animals aged. Interestingly, the ASH sensory neurons expressing 171Htt150Qs were functionally impaired before neurodegeneration, foci formation or cell death was detected.

All the models described the presence of protein aggregation and a toxic phenotype associated to the expression of polyQ repeats. The different cells tested however, seemed to have different sensitivities to polyQ toxicity; these data would support the neuron-specific toxicity described for polyQ disorders.

When comparing and interpreting the results of these models, it should be considered that the distinct phenotypes and sensitivities found may be explained based on (i) differences in protein expression levels as a result of the distinct promoters used and protein the stability of the different proteins; or (ii) differences associated to protein context, as it has been suggested that longer protein sequences, surrounding the polyQ stretch, are associated to a decreased toxicity (82). Also relevant are the aggregation and toxicity thresholds described for these models that do not always mimic what is known for humans or for other model systems.

When we first started this work, *C. elegans* models expressing polyQ tracts under the regulation of a pan-neuronal promoter (F25B3.3 promoter) had been recently characterized (84). In these strains, similarly to what was seen by Morley and colleagues (2002), a length-dependent aggregation was observed, similar to the described for humans. Furthermore, using this promoter, distinct neurons displayed different sensitivities to

polyQ expression. As such, we thought that it would be interesting to test in this pan-neuronal model system the effect of protein context in polyQ-mediated toxicity. We chose ATXN3, the protein involved in MJD.

1.9 Aims of the Study

Bearing in mind (i) the impact of neurodegenerative diseases in the society, (ii) that the mechanisms by which the expansion of the CAG-repeat of ATXN3 cause neurological dysfunction and disease are still unclear and (iii) taking into account the advantages of *C. elegans* as a model for the study of neurodegenerative diseases, we aimed:

1. To **establish a novel *C. elegans* model for the *in vivo* study of the misfolding and aggregation of ATXN3**, the protein involved in Machado-Joseph disease (Chapters 2, 4);

2. To **characterize the *C. elegans* models** at the biochemical, cellular and phenotypic level (Chapters 2, 2.1, 4);

3. To **understand how the protein sequence flanking the polyQ tract modulates aggregation and animals' behavior** (Chapter 2);

4. To **validate our novel *C. elegans* model as a tool for the identification of potential new therapies** for MJD (Chapter 5);

5. To **understand how aging-related pathways modify MJD pathogenesis** (Chapters 2, 3);

6. To test **heat shock factor-1 (HSF-1)**, the major regulator of the heat shock response in cells, **as a candidate modifier of mutant ATXN3-mediated pathogenesis in a mouse model** (Chapter 6).

1.10 References

1 Gusella, J.F. and MacDonald, M.E. (2000) Molecular genetics: unmasking polyglutamine triggers in neurodegenerative disease. *Nat Rev Neurosci*, **1**, 109-115.

2 Ross, C.A. (1995) When more is less: pathogenesis of glutamine repeat neurodegenerative diseases. *Neuron*, **15**, 493-496.

3 Gething, M.J. and Sambrook, J. (1992) Protein folding in the cell. *Nature*, **355**, 33-45.

4 Ellis, R.J. and Minton, A.P. (2006) Protein aggregation in crowded environments. *Biol Chem*, **387**, 485-497.

5 Horwich, A.L. and Weissman, J.S. (1997) Deadly conformations--protein misfolding in prion disease. *Cell*, **89**, 499-510.

6 Morimoto, R.I. (2002) Dynamic remodeling of transcription complexes by molecular chaperones. *Cell*, **110**, 281-284.

7 Nollen, E.A. and Morimoto, R.I. (2002) Chaperoning signaling pathways: molecular chaperones as stress-sensing 'heat shock' proteins. *J Cell Sci*, **115**, 2809-2816.

8 Carrell, R.W. and Lomas, D.A. (1997) Conformational disease. *Lancet*, **350**, 134-138.

9 Dobson, C.M. (1999) Protein misfolding, evolution and disease. *Trends Biochem Sci*, **24**, 329-332.

10 Soto, C. (2003) Unfolding the role of protein misfolding in neurodegenerative diseases. *Nat Rev Neurosci*, **4**, 49-60.

11 Verkerk, A.J., Pieretti, M., Sutcliffe, J.S., Fu, Y.H., Kuhl, D.P., Pizzuti, A., Reiner, O., Richards, S., Victoria, M.F., Zhang, F.P. *et al.* (1991) Identification of a gene (FMR-1) containing a CGG repeat coincident with a breakpoint cluster region exhibiting length variation in fragile X syndrome. *Cell*, **65**, 905-914.

12 La Spada, A.R., Wilson, E.M., Lubahn, D.B., Harding, A.E. and Fischbeck, K.H. (1991) Androgen receptor gene mutations in X-linked spinal and bulbar muscular atrophy. *Nature*, **352**, 77-79.

13 Liquori, C.L., Ricker, K., Moseley, M.L., Jacobsen, J.F., Kress, W., Naylor, S.L., Day, J.W. and Ranum, L.P. (2001) Myotonic dystrophy type 2 caused by a CCTG expansion in intron 1 of ZNF9. *Science*, **293**, 864-867.

14 Matsuura, T., Yamagata, T., Burgess, D.L., Rasmussen, A., Grewal, R.P., Watase, K., Khajavi, M., McCall, A.E., Davis, C.F., Zu, L. *et al.* (2000) Large expansion of the ATTCT pentanucleotide repeat in spinocerebellar ataxia type 10. *Nat Genet*, **26**, 191-194.

15 Li, S.H., McInnis, M.G., Margolis, R.L., Antonarakis, S.E. and Ross, C.A. (1993) Novel triplet repeat containing genes in human brain: cloning, expression, and length polymorphisms. *Genomics*, **16**, 572-579.

16 Nagafuchi, S., Yanagisawa, H., Sato, K., Shirayama, T., Ohsaki, E., Bundo, M., Takeda, T., Tadokoro, K., Kondo, I., Murayama, N. *et al.* (1994) Dentatorubral and pallidoluysian atrophy expansion of an unstable CAG trinucleotide on chromosome 12p. *Nat Genet*, **6**, 14-18.

17 Gusella, J.F., Wexler, N.S., Conneally, P.M., Naylor, S.L., Anderson, M.A., Tanzi, R.E., Watkins, P.C., Ottina, K., Wallace, M.R., Sakaguchi, A.Y. *et al.* (1983) A polymorphic DNA marker genetically linked to Huntington's disease. *Nature*, **306**, 234-238.

18 Orr, H.T., Chung, M.Y., Banfi, S., Kwiatkowski, T.J., Jr., Servadio, A., Beaudet, A.L., McCall, A.E., Duvick, L.A., Ranum, L.P. and Zoghbi, H.Y. (1993) Expansion of an unstable trinucleotide CAG repeat in spinocerebellar ataxia type 1. *Nat Genet*, **4**, 221-226.

19 Pulst, S.M., Nechiporuk, A., Nechiporuk, T., Gispert, S., Chen, X.N., Lopes-Cendes, I., Pearlman, S., Starkman, S., Orozco-Diaz, G., Lunkes, A. *et al.* (1996) Moderate expansion of a normally biallelic trinucleotide repeat in spinocerebellar ataxia type 2. *Nat Genet*, **14**, 269-276.

20 Kawaguchi, Y., Okamoto, T., Taniwaki, M., Aizawa, M., Inoue, M., Katayama, S., Kawakami, H., Nakamura, S., Nishimura, M., Akiguchi, I. *et al.* (1994) CAG expansions in a novel gene for Machado-Joseph disease at chromosome 14q32.1. *Nat Genet*, **8**, 221-228.

21 Zhuchenko, O., Bailey, J., Bonnen, P., Ashizawa, T., Stockton, D.W., Amos, C., Dobyns, W.B., Subramony, S.H., Zoghbi, H.Y. and Lee, C.C. (1997) Autosomal dominant cerebellar ataxia (SCA6)

associated with small polyglutamine expansions in the alpha 1A-voltage-dependent calcium channel. *Nat Genet*, **15**, 62-69.
22 David, G., Abbas, N., Stevanin, G., Durr, A., Yvert, G., Cancel, G., Weber, C., Imbert, G., Saudou, F., Antoniou, E. *et al.* (1997) Cloning of the SCA7 gene reveals a highly unstable CAG repeat expansion. *Nat Genet*, **17**, 65-70.
23 Nakamura, K., Jeong, S.Y., Uchihara, T., Anno, M., Nagashima, K., Nagashima, T., Ikeda, S., Tsuji, S. and Kanazawa, I. (2001) SCA17, a novel autosomal dominant cerebellar ataxia caused by an expanded polyglutamine in TATA-binding protein. *Hum Mol Genet*, **10**, 1441-1448.
24 Zoghbi, H.Y. and Orr, H.T. (2000) Glutamine repeats and neurodegeneration. *Annu Rev Neurosci*, **23**, 217-247.
25 Burright, E.N., Clark, H.B., Servadio, A., Matilla, T., Feddersen, R.M., Yunis, W.S., Duvick, L.A., Zoghbi, H.Y. and Orr, H.T. (1995) SCA1 transgenic mice: a model for neurodegeneration caused by an expanded CAG trinucleotide repeat. *Cell*, **82**, 937-948.
26 Sharp, A.H., Loev, S.J., Schilling, G., Li, S.H., Li, X.J., Bao, J., Wagster, M.V., Kotzuk, J.A., Steiner, J.P., Lo, A. *et al.* (1995) Widespread expression of Huntington's disease gene (IT15) protein product. *Neuron*, **14**, 1065-1074.
27 Trottier, Y., Lutz, Y., Stevanin, G., Imbert, G., Devys, D., Cancel, G., Saudou, F., Weber, C., David, G., Tora, L. *et al.* (1995) Polyglutamine expansion as a pathological epitope in Huntington's disease and four dominant cerebellar ataxias. *Nature*, **378**, 403-406.
28 Duyao, M., Ambrose, C., Myers, R., Novelletto, A., Persichetti, F., Frontali, M., Folstein, S., Ross, C., Franz, M., Abbott, M. *et al.* (1993) Trinucleotide repeat length instability and age of onset in Huntington's disease. *Nat Genet*, **4**, 387-392.
29 Maciel, P., Gaspar, C., DeStefano, A.L., Silveira, I., Coutinho, P., Radvany, J., Dawson, D.M., Sudarsky, L., Guimaraes, J., Loureiro, J.E. *et al.* (1995) Correlation between CAG repeat length and clinical features in Machado-Joseph disease. *Am J Hum Genet*, **57**, 54-61.
30 Rubinsztein, D.C., Leggo, J., Coles, R., Almqvist, E., Biancalana, V., Cassiman, J.J., Chotai, K., Connarty, M., Crauford, D., Curtis, A. *et al.* (1996) Phenotypic characterization of individuals with 30-40 CAG repeats in the Huntington disease (HD) gene reveals HD cases with 36 repeats and apparently normal elderly individuals with 36-39 repeats. *Am J Hum Genet*, **59**, 16-22.
31 Vonsattel, J.P. and DiFiglia, M. (1998) Huntington disease. *J Neuropathol Exp Neurol*, **57**, 369-384.
32 Tanaka, M., Morishima, I., Akagi, T., Hashikawa, T. and Nukina, N. (2001) Intra- and intermolecular beta-pleated sheet formation in glutamine-repeat inserted myoglobin as a model for polyglutamine diseases. *J Biol Chem*, **276**, 45470-45475.
33 Davies, S.W., Turmaine, M., Cozens, B.A., DiFiglia, M., Sharp, A.H., Ross, C.A., Scherzinger, E., Wanker, E.E., Mangiarini, L. and Bates, G.P. (1997) Formation of neuronal intranuclear inclusions underlies the neurological dysfunction in mice transgenic for the HD mutation. *Cell*, **90**, 537-548.
34 DiFiglia, M., Sapp, E., Chase, K.O., Davies, S.W., Bates, G.P., Vonsattel, J.P. and Aronin, N. (1997) Aggregation of huntingtin in neuronal intranuclear inclusions and dystrophic neurites in brain. *Science*, **277**, 1990-1993.
35 Paulson, H.L., Das, S.S., Crino, P.B., Perez, M.K., Patel, S.C., Gotsdiner, D., Fischbeck, K.H. and Pittman, R.N. (1997) Machado-Joseph disease gene product is a cytoplasmic protein widely expressed in brain. *Ann Neurol*, **41**, 453-462.
36 Schmidt, T., Landwehrmeyer, G.B., Schmitt, I., Trottier, Y., Auburger, G., Laccone, F., Klockgether, T., Volpel, M., Epplen, J.T., Schols, L. *et al.* (1998) An isoform of ataxin-3 accumulates in the nucleus of neuronal cells in affected brain regions of SCA3 patients. *Brain Pathol*, **8**, 669-679.
37 Holmberg, M., Duyckaerts, C., Durr, A., Cancel, G., Gourfinkel-An, I., Damier, P., Faucheux, B., Trottier, Y., Hirsch, E.C., Agid, Y. *et al.* (1998) Spinocerebellar ataxia type 7 (SCA7): a neurodegenerative disorder with neuronal intranuclear inclusions. *Hum Mol Genet*, **7**, 913-918.

38 Koyano, S., Uchihara, T., Fujigasaki, H., Nakamura, A., Yagishita, S. and Iwabuchi, K. (1999) Neuronal intranuclear inclusions in spinocerebellar ataxia type 2: triple-labeling immunofluorescent study. *Neurosci Lett*, **273**, 117-120.
39 Sieradzan, K.A., Mechan, A.O., Jones, L., Wanker, E.E., Nukina, N. and Mann, D.M. (1999) Huntington's disease intranuclear inclusions contain truncated, ubiquitinated huntingtin protein. *Exp Neurol*, **156**, 92-99.
40 Chai, Y., Koppenhafer, S.L., Shoesmith, S.J., Perez, M.K. and Paulson, H.L. (1999) Evidence for proteasome involvement in polyglutamine disease: localization to nuclear inclusions in SCA3/MJD and suppression of polyglutamine aggregation in vitro. *Hum Mol Genet*, **8**, 673-682.
41 Duyckaerts, C., Durr, A., Cancel, G. and Brice, A. (1999) Nuclear inclusions in spinocerebellar ataxia type 1. *Acta Neuropathol*, **97**, 201-207.
42 Faber, P.W., Alter, J.R., MacDonald, M.E. and Hart, A.C. (1999) Polyglutamine-mediated dysfunction and apoptotic death of a Caenorhabditis elegans sensory neuron. *Proc Natl Acad Sci U S A*, **96**, 179-184.
43 Satyal, S.H., Schmidt, E., Kitagawa, K., Sondheimer, N., Lindquist, S., Kramer, J.M. and Morimoto, R.I. (2000) Polyglutamine aggregates alter protein folding homeostasis in Caenorhabditis elegans. *Proc Natl Acad Sci U S A*, **97**, 5750-5755.
44 Khan, L.A., Bauer, P.O., Miyazaki, H., Lindenberg, K.S., Landwehrmeyer, B.G. and Nukina, N. (2006) Expanded polyglutamines impair synaptic transmission and ubiquitin-proteasome system in Caenorhabditis elegans. *J Neurochem*, **98**, 576-587.
45 Perez, M.K., Paulson, H.L., Pendse, S.J., Saionz, S.J., Bonini, N.M. and Pittman, R.N. (1998) Recruitment and the role of nuclear localization in polyglutamine-mediated aggregation. *J Cell Biol*, **143**, 1457-1470.
46 Warrick, J.M., Paulson, H.L., Gray-Board, G.L., Bui, Q.T., Fischbeck, K.H., Pittman, R.N. and Bonini, N.M. (1998) Expanded polyglutamine protein forms nuclear inclusions and causes neural degeneration in Drosophila. *Cell*, **93**, 939-949.
47 Martindale, D., Hackam, A., Wieczorek, A., Ellerby, L., Wellington, C., McCutcheon, K., Singaraja, R., Kazemi-Esfarjani, P., Devon, R., Kim, S.U. *et al.* (1998) Length of huntingtin and its polyglutamine tract influences localization and frequency of intracellular aggregates. *Nat Genet*, **18**, 150-154.
48 Cemal, C.K., Carroll, C.J., Lawrence, L., Lowrie, M.B., Ruddle, P., Al-Mahdawi, S., King, R.H., Pook, M.A., Huxley, C. and Chamberlain, S. (2002) YAC transgenic mice carrying pathological alleles of the MJD1 locus exhibit a mild and slowly progressive cerebellar deficit. *Hum Mol Genet*, **11**, 1075-1094.
49 Ikeda, H., Yamaguchi, M., Sugai, S., Aze, Y., Narumiya, S. and Kakizuka, A. (1996) Expanded polyglutamine in the Machado-Joseph disease protein induces cell death in vitro and in vivo. *Nat Genet*, **13**, 196-202.
50 Klement, I.A., Skinner, P.J., Kaytor, M.D., Yi, H., Hersch, S.M., Clark, H.B., Zoghbi, H.Y. and Orr, H.T. (1998) Ataxin-1 nuclear localization and aggregation: role in polyglutamine-induced disease in SCA1 transgenic mice. *Cell*, **95**, 41-53.
51 Scherzinger, E., Lurz, R., Turmaine, M., Mangiarini, L., Hollenbach, B., Hasenbank, R., Bates, G.P., Davies, S.W., Lehrach, H. and Wanker, E.E. (1997) Huntingtin-encoded polyglutamine expansions form amyloid-like protein aggregates in vitro and in vivo. *Cell*, **90**, 549-558.
52 Cooper, J.K., Schilling, G., Peters, M.F., Herring, W.J., Sharp, A.H., Kaminsky, Z., Masone, J., Khan, F.A., Delanoy, M., Borchelt, D.R. *et al.* (1998) Truncated N-terminal fragments of huntingtin with expanded glutamine repeats form nuclear and cytoplasmic aggregates in cell culture. *Hum Mol Genet*, **7**, 783-790.
53 Ishikawa, K., Owada, K., Ishida, K., Fujigasaki, H., Shun Li, M., Tsunemi, T., Ohkoshi, N., Toru, S., Mizutani, T., Hayashi, M. *et al.* (2001) Cytoplasmic and nuclear polyglutamine aggregates in SCA6 Purkinje cells. *Neurology*, **56**, 1753-1756.

54 Stenoien, D.L., Cummings, C.J., Adams, H.P., Mancini, M.G., Patel, K., DeMartino, G.N., Marcelli, M., Weigel, N.L. and Mancini, M.A. (1999) Polyglutamine-expanded androgen receptors form aggregates that sequester heat shock proteins, proteasome components and SRC-1, and are suppressed by the HDJ-2 chaperone. *Hum Mol Genet*, **8**, 731-741.
55 Piccioni, F., Pinton, P., Simeoni, S., Pozzi, P., Fascio, U., Vismara, G., Martini, L., Rizzuto, R. and Poletti, A. (2002) Androgen receptor with elongated polyglutamine tract forms aggregates that alter axonal trafficking and mitochondrial distribution in motor neuronal processes. *FASEB J*, **16**, 1418-1420.
56 Evert, B.O., Wullner, U., Schulz, J.B., Weller, M., Groscurth, P., Trottier, Y., Brice, A. and Klockgether, T. (1999) High level expression of expanded full-length ataxin-3 in vitro causes cell death and formation of intranuclear inclusions in neuronal cells. *Hum Mol Genet*, **8**, 1169-1176.
57 Chen, S., Berthelier, V., Hamilton, J.B., O'Nuallain, B. and Wetzel, R. (2002) Amyloid-like features of polyglutamine aggregates and their assembly kinetics. *Biochemistry*, **41**, 7391-7399.
58 Huang, C.C., Faber, P.W., Persichetti, F., Mittal, V., Vonsattel, J.P., MacDonald, M.E. and Gusella, J.F. (1998) Amyloid formation by mutant huntingtin: threshold, progressivity and recruitment of normal polyglutamine proteins. *Somat Cell Mol Genet*, **24**, 217-233.
59 Lippincott-Schwartz, J., Altan-Bonnet, N. and Patterson, G.H. (2003) Photobleaching and photoactivation: following protein dynamics in living cells. *Nat Cell Biol*, **Suppl**, S7-14.
60 Green, H. and Wang, N. (1994) Codon reiteration and the evolution of proteins. *Proc Natl Acad Sci U S A*, **91**, 4298-4302.
61 Lunkes, A. and Mandel, J.L. (1998) A cellular model that recapitulates major pathogenic steps of Huntington's disease. *Hum Mol Genet*, **7**, 1355-1361.
62 Moulder, K.L., Onodera, O., Burke, J.R., Strittmatter, W.J. and Johnson, E.M., Jr. (1999) Generation of neuronal intranuclear inclusions by polyglutamine-GFP: analysis of inclusion clearance and toxicity as a function of polyglutamine length. *J Neurosci*, **19**, 705-715.
63 de Cristofaro, T., Affaitati, A., Feliciello, A., Avvedimento, E.V. and Varrone, S. (2000) Polyglutamine-mediated aggregation and cell death. *Biochem Biophys Res Commun*, **272**, 816-821.
64 Davies, S.W., Turmaine, M., Cozens, B.A., Raza, A.S., Mahal, A., Mangiarini, L. and Bates, G.P. (1999) From neuronal inclusions to neurodegeneration: neuropathological investigation of a transgenic mouse model of Huntington's disease. *Philos Trans R Soc Lond B Biol Sci*, **354**, 981-989.
65 Verhoef, L.G., Lindsten, K., Masucci, M.G. and Dantuma, N.P. (2002) Aggregate formation inhibits proteasomal degradation of polyglutamine proteins. *Hum Mol Genet*, **11**, 2689-2700.
66 Ho, L.W., Carmichael, J., Swartz, J., Wyttenbach, A., Rankin, J. and Rubinsztein, D.C. (2001) The molecular biology of Huntington's disease. *Psychol Med*, **31**, 3-14.
67 Li, H., Li, S.H., Yu, Z.X., Shelbourne, P. and Li, X.J. (2001) Huntingtin aggregate-associated axonal degeneration is an early pathological event in Huntington's disease mice. *J Neurosci*, **21**, 8473-8481.
68 Saudou, F., Finkbeiner, S., Devys, D. and Greenberg, M.E. (1998) Huntingtin acts in the nucleus to induce apoptosis but death does not correlate with the formation of intranuclear inclusions. *Cell*, **95**, 55-66.
69 Kuemmerle, S., Gutekunst, C.A., Klein, A.M., Li, X.J., Li, S.H., Beal, M.F., Hersch, S.M. and Ferrante, R.J. (1999) Huntington aggregates may not predict neuronal death in Huntington's disease. *Ann Neurol*, **46**, 842-849.
70 Huynh, D.P., Del Bigio, M.R., Ho, D.H. and Pulst, S.M. (1999) Expression of ataxin-2 in brains from normal individuals and patients with Alzheimer's disease and spinocerebellar ataxia 2. *Ann Neurol*, **45**, 232-241.
71 Gutekunst, C.A., Li, S.H., Yi, H., Mulroy, J.S., Kuemmerle, S., Jones, R., Rye, D., Ferrante, R.J., Hersch, S.M. and Li, X.J. (1999) Nuclear and neuropil aggregates in Huntington's disease: relationship to neuropathology. *J Neurosci*, **19**, 2522-2534.

72 Li, M., Miwa, S., Kobayashi, Y., Merry, D.E., Yamamoto, M., Tanaka, F., Doyu, M., Hashizume, Y., Fischbeck, K.H. and Sobue, G. (1998) Nuclear inclusions of the androgen receptor protein in spinal and bulbar muscular atrophy. *Ann Neurol*, **44**, 249-254.
73 Li, M., Nakagomi, Y., Kobayashi, Y., Merry, D.E., Tanaka, F., Doyu, M., Mitsuma, T., Hashizume, Y., Fischbeck, K.H. and Sobue, G. (1998) Nonneural nuclear inclusions of androgen receptor protein in spinal and bulbar muscular atrophy. *Am J Pathol*, **153**, 695-701.
74 Rub, U., de Vos, R.A., Brunt, E.R., Sebesteny, T., Schols, L., Auburger, G., Bohl, J., Ghebremedhin, E., Gierga, K., Seidel, K. *et al.* (2006) Spinocerebellar ataxia type 3 (SCA3): thalamic neurodegeneration occurs independently from thalamic ataxin-3 immunopositive neuronal intranuclear inclusions. *Brain Pathol*, **16**, 218-227.
75 Arrasate, M., Mitra, S., Schweitzer, E.S., Segal, M.R. and Finkbeiner, S. (2004) Inclusion body formation reduces levels of mutant huntingtin and the risk of neuronal death. *Nature*, **431**, 805-810.
76 Ambrose, C.M., Duyao, M.P., Barnes, G., Bates, G.P., Lin, C.S., Srinidhi, J., Baxendale, S., Hummerich, H., Lehrach, H., Altherr, M. *et al.* (1994) Structure and expression of the Huntington's disease gene: evidence against simple inactivation due to an expanded CAG repeat. *Somat Cell Mol Genet*, **20**, 27-38.
77 Duyao, M.P., Auerbach, A.B., Ryan, A., Persichetti, F., Barnes, G.T., McNeil, S.M., Ge, P., Vonsattel, J.P., Gusella, J.F., Joyner, A.L. *et al.* (1995) Inactivation of the mouse Huntington's disease gene homolog Hdh. *Science*, **269**, 407-410.
78 Matilla, A., Roberson, E.D., Banfi, S., Morales, J., Armstrong, D.L., Burright, E.N., Orr, H.T., Sweatt, J.D., Zoghbi, H.Y. and Matzuk, M.M. (1998) Mice lacking ataxin-1 display learning deficits and decreased hippocampal paired-pulse facilitation. *J Neurosci*, **18**, 5508-5516.
79 Schmitt, I., Linden, M., Khazneh, H., Evert, B.O., Breuer, P., Klockgether, T. and Wuellner, U. (2007) Inactivation of the mouse Atxn3 (ataxin-3) gene increases protein ubiquitination. *Biochem Biophys Res Commun*, **362**, 734-739.
80 Hodgson, J.G., Agopyan, N., Gutekunst, C.A., Leavitt, B.R., LePiane, F., Singaraja, R., Smith, D.J., Bissada, N., McCutcheon, K., Nasir, J. *et al.* (1999) A YAC mouse model for Huntington's disease with full-length mutant huntingtin, cytoplasmic toxicity, and selective striatal neurodegeneration. *Neuron*, **23**, 181-192.
81 Ordway, J.M., Tallaksen-Greene, S., Gutekunst, C.A., Bernstein, E.M., Cearley, J.A., Wiener, H.W., Dure, L.S.t., Lindsey, R., Hersch, S.M., Jope, R.S. *et al.* (1997) Ectopically expressed CAG repeats cause intranuclear inclusions and a progressive late onset neurological phenotype in the mouse. *Cell*, **91**, 753-763.
82 Marsh, J.L., Walker, H., Theisen, H., Zhu, Y.Z., Fielder, T., Purcell, J. and Thompson, L.M. (2000) Expanded polyglutamine peptides alone are intrinsically cytotoxic and cause neurodegeneration in Drosophila. *Hum Mol Genet*, **9**, 13-25.
83 Morley, J.F., Brignull, H.R., Weyers, J.J. and Morimoto, R.I. (2002) The threshold for polyglutamine-expansion protein aggregation and cellular toxicity is dynamic and influenced by aging in Caenorhabditis elegans. *Proc Natl Acad Sci U S A*, **99**, 10417-10422.
84 Brignull, H.R., Moore, F.E., Tang, S.J. and Morimoto, R.I. (2006) Polyglutamine proteins at the pathogenic threshold display neuron-specific aggregation in a pan-neuronal Caenorhabditis elegans model. *J Neurosci*, **26**, 7597-7606.
85 Cattaneo, E., Rigamonti, D., Goffredo, D., Zuccato, C., Squitieri, F. and Sipione, S. (2001) Loss of normal huntingtin function: new developments in Huntington's disease research. *Trends Neurosci*, **24**, 182-188.
86 Dragatsis, I., Levine, M.S. and Zeitlin, S. (2000) Inactivation of Hdh in the brain and testis results in progressive neurodegeneration and sterility in mice. *Nat Genet*, **26**, 300-306.
87 Leavitt, B.R., Guttman, J.A., Hodgson, J.G., Kimel, G.H., Singaraja, R., Vogl, A.W. and Hayden, M.R. (2001) Wild-type huntingtin reduces the cellular toxicity of mutant huntingtin in vivo. *Am J Hum Genet*, **68**, 313-324.

88 Van Raamsdonk, J.M., Pearson, J., Rogers, D.A., Bissada, N., Vogl, A.W., Hayden, M.R. and Leavitt, B.R. (2005) Loss of wild-type huntingtin influences motor dysfunction and survival in the YAC128 mouse model of Huntington disease. *Hum Mol Genet*, **14**, 1379-1392.
89 Leavitt, B.R., van Raamsdonk, J.M., Shehadeh, J., Fernandes, H., Murphy, Z., Graham, R.K., Wellington, C.L., Raymond, L.A. and Hayden, M.R. (2006) Wild-type huntingtin protects neurons from excitotoxicity. *J Neurochem*, **96**, 1121-1129.
90 Rigamonti, D., Bauer, J.H., De-Fraja, C., Conti, L., Sipione, S., Sciorati, C., Clementi, E., Hackam, A., Hayden, M.R., Li, Y. *et al.* (2000) Wild-type huntingtin protects from apoptosis upstream of caspase-3. *J Neurosci*, **20**, 3705-3713.
91 Thomas, P.S., Jr., Fraley, G.S., Damian, V., Woodke, L.B., Zapata, F., Sopher, B.L., Plymate, S.R. and La Spada, A.R. (2006) Loss of endogenous androgen receptor protein accelerates motor neuron degeneration and accentuates androgen insensitivity in a mouse model of X-linked spinal and bulbar muscular atrophy. *Hum Mol Genet*, **15**, 2225-2238.
92 Sopher, B.L., Thomas, P.S., Jr., LaFevre-Bernt, M.A., Holm, I.E., Wilke, S.A., Ware, C.B., Jin, L.W., Libby, R.T., Ellerby, L.M. and La Spada, A.R. (2004) Androgen receptor YAC transgenic mice recapitulate SBMA motor neuronopathy and implicate VEGF164 in the motor neuron degeneration. *Neuron*, **41**, 687-699.
93 Tsuda, H., Jafar-Nejad, H., Patel, A.J., Sun, Y., Chen, H.K., Rose, M.F., Venken, K.J., Botas, J., Orr, H.T., Bellen, H.J. *et al.* (2005) The AXH domain of Ataxin-1 mediates neurodegeneration through its interaction with Gfi-1/Senseless proteins. *Cell*, **122**, 633-644.
94 Emamian, E.S., Kaytor, M.D., Duvick, L.A., Zu, T., Tousey, S.K., Zoghbi, H.Y., Clark, H.B. and Orr, H.T. (2003) Serine 776 of ataxin-1 is critical for polyglutamine-induced disease in SCA1 transgenic mice. *Neuron*, **38**, 375-387.
95 Warrick, J.M., Morabito, L.M., Bilen, J., Gordesky-Gold, B., Faust, L.Z., Paulson, H.L. and Bonini, N.M. (2005) Ataxin-3 suppresses polyglutamine neurodegeneration in Drosophila by a ubiquitin-associated mechanism. *Mol Cell*, **18**, 37-48.
96 Aronin, N., Chase, K., Young, C., Sapp, E., Schwarz, C., Matta, N., Kornreich, R., Landwehrmeyer, B., Bird, E., Beal, M.F. *et al.* (1995) CAG expansion affects the expression of mutant Huntingtin in the Huntington's disease brain. *Neuron*, **15**, 1193-1201.
97 DiFiglia, M., Sapp, E., Chase, K., Schwarz, C., Meloni, A., Young, C., Martin, E., Vonsattel, J.P., Carraway, R., Reeves, S.A. *et al.* (1995) Huntingtin is a cytoplasmic protein associated with vesicles in human and rat brain neurons. *Neuron*, **14**, 1075-1081.
98 Landwehrmeyer, G.B., McNeil, S.M., Dure, L.S.t., Ge, P., Aizawa, H., Huang, Q., Ambrose, C.M., Duyao, M.P., Bird, E.D., Bonilla, E. *et al.* (1995) Huntington's disease gene: regional and cellular expression in brain of normal and affected individuals. *Ann Neurol*, **37**, 218-230.
99 Chong, S.S., McCall, A.E., Cota, J., Subramony, S.H., Orr, H.T., Hughes, M.R. and Zoghbi, H.Y. (1995) Gametic and somatic tissue-specific heterogeneity of the expanded SCA1 CAG repeat in spinocerebellar ataxia type 1. *Nat Genet*, **10**, 344-350.
100 MacDonald, M.E., Barnes, G., Srinidhi, J., Duyao, M.P., Ambrose, C.M., Myers, R.H., Gray, J., Conneally, P.M., Young, A., Penney, J. *et al.* (1993) Gametic but not somatic instability of CAG repeat length in Huntington's disease. *J Med Genet*, **30**, 982-986.
101 Ueno, S., Kondoh, K., Kotani, Y., Komure, O., Kuno, S., Kawai, J., Hazama, F. and Sano, A. (1995) Somatic mosaicism of CAG repeat in dentatorubral-pallidoluysian atrophy (DRPLA). *Hum Mol Genet*, **4**, 663-666.
102 Zuhlke, C., Riess, O., Schroder, K., Siedlaczck, I., Epplen, J.T., Engel, W. and Thies, U. (1993) Expansion of the (CAG)n repeat causing Huntington's disease in 352 patients of German origin. *Hum Mol Genet*, **2**, 1467-1469.
103 Watanabe, H., Tanaka, F., Doyu, M., Riku, S., Yoshida, M., Hashizume, Y. and Sobue, G. (2000) Differential somatic CAG repeat instability in variable brain cell lineage in dentatorubral pallidoluysian atrophy (DRPLA): a laser-captured microdissection (LCM)-based analysis. *Hum Genet*, **107**, 452-457.

104 Telenius, H., Kremer, H.P., Theilmann, J., Andrew, S.E., Almqvist, E., Anvret, M., Greenberg, C., Greenberg, J., Lucotte, G., Squitieri, F. *et al.* (1993) Molecular analysis of juvenile Huntington disease: the major influence on (CAG)n repeat length is the sex of the affected parent. *Hum Mol Genet*, **2**, 1535-1540.
105 Silva-Fernandes, A., Costa, M.D., Duarte-Silva, S., Oliveira, P., Botelho, C.M., Martins, L., Mariz, J.A., Ferreira, T., Ribeiro, F., Correia-Neves, M. *et al.* Motor uncoordination and neuropathology in a transgenic mouse model of Machado-Joseph disease lacking intranuclear inclusions and ataxin-3 cleavage products. *Neurobiol Dis*.
106 He, X. and Rosenfeld, M.G. (1991) Mechanisms of complex transcriptional regulation: implications for brain development. *Neuron*, **7**, 183-196.
107 Marcuccilli, C.J., Mathur, S.K., Morimoto, R.I. and Miller, R.J. (1996) Regulatory differences in the stress response of hippocampal neurons and glial cells after heat shock. *J Neurosci*, **16**, 478-485.
108 Batulan, Z., Shinder, G.A., Minotti, S., He, B.P., Doroudchi, M.M., Nalbantoglu, J., Strong, M.J. and Durham, H.D. (2003) High threshold for induction of the stress response in motor neurons is associated with failure to activate HSF1. *J Neurosci*, **23**, 5789-5798.
109 Gauthier, L.R., Charrin, B.C., Borrell-Pages, M., Dompierre, J.P., Rangone, H., Cordelieres, F.P., De Mey, J., MacDonald, M.E., Lessmann, V., Humbert, S. *et al.* (2004) Huntingtin controls neurotrophic support and survival of neurons by enhancing BDNF vesicular transport along microtubules. *Cell*, **118**, 127-138.
110 Kinsella, K.G. (2005) Future longevity-demographic concerns and consequences. *J Am Geriatr Soc*, **53**, S299-303.
111 Berr, C., Wancata, J. and Ritchie, K. (2005) Prevalence of dementia in the elderly in Europe. *Eur Neuropsychopharmacol*, **15**, 463-471.
112 Klass, M.R. (1983) A method for the isolation of longevity mutants in the nematode Caenorhabditis elegans and initial results. *Mech Ageing Dev*, **22**, 279-286.
113 Friedman, D.B. and Johnson, T.E. (1988) A mutation in the age-1 gene in Caenorhabditis elegans lengthens life and reduces hermaphrodite fertility. *Genetics*, **118**, 75-86.
114 Kenyon, C. (2005) The plasticity of aging: insights from long-lived mutants. *Cell*, **120**, 449-460.
115 Vijg, J. and Campisi, J. (2008) Puzzles, promises and a cure for ageing. *Nature*, **454**, 1065-1071.
116 Hsu, A.L., Murphy, C.T. and Kenyon, C. (2003) Regulation of aging and age-related disease by DAF-16 and heat-shock factor. *Science*, **300**, 1142-1145.
117 Perls, T., Kohler, I.V., Andersen, S., Schoenhofen, E., Pennington, J., Young, R., Terry, D. and Elo, I.T. (2007) Survival of parents and siblings of supercentenarians. *J Gerontol A Biol Sci Med Sci*, **62**, 1028-1034.
118 Beekman, M., Blauw, G.J., Houwing-Duistermaat, J.J., Brandt, B.W., Westendorp, R.G. and Slagboom, P.E. (2006) Chromosome 4q25, microsomal transfer protein gene, and human longevity: novel data and a meta-analysis of association studies. *J Gerontol A Biol Sci Med Sci*, **61**, 355-362.
119 Barzilai, N., Atzmon, G., Schechter, C., Schaefer, E.J., Cupples, A.L., Lipton, R., Cheng, S. and Shuldiner, A.R. (2003) Unique lipoprotein phenotype and genotype associated with exceptional longevity. *JAMA*, **290**, 2030-2040.
120 Kuningas, M., Magi, R., Westendorp, R.G., Slagboom, P.E., Remm, M. and van Heemst, D. (2007) Haplotypes in the human Foxo1a and Foxo3a genes; impact on disease and mortality at old age. *Eur J Hum Genet*, **15**, 294-301.
121 Capri, M., Salvioli, S., Sevini, F., Valensin, S., Celani, L., Monti, D., Pawelec, G., De Benedictis, G., Gonos, E.S. and Franceschi, C. (2006) The genetics of human longevity. *Ann N Y Acad Sci*, **1067**, 252-263.
122 Suh, Y., Atzmon, G., Cho, M.O., Hwang, D., Liu, B., Leahy, D.J., Barzilai, N. and Cohen, P. (2008) Functionally significant insulin-like growth factor I receptor mutations in centenarians. *Proc Natl Acad Sci U S A*, **105**, 3438-3442.

123 Longo, V.D. and Finch, C.E. (2003) Evolutionary medicine: from dwarf model systems to healthy centenarians? *Science*, **299**, 1342-1346.
124 Balch, W.E., Morimoto, R.I., Dillin, A. and Kelly, J.W. (2008) Adapting proteostasis for disease intervention. *Science*, **319**, 916-919.
125 Gidalevitz, T., Kikis, E.A. and Morimoto, R.I. A cellular perspective on conformational disease: the role of genetic background and proteostasis networks. *Curr Opin Struct Biol*, **20**, 23-32.
126 Nollen, E.A., Garcia, S.M., van Haaften, G., Kim, S., Chavez, A., Morimoto, R.I. and Plasterk, R.H. (2004) Genome-wide RNA interference screen identifies previously undescribed regulators of polyglutamine aggregation. *Proc Natl Acad Sci U S A*, **101**, 6403-6408.
127 Wang, J., Farr, G.W., Hall, D.H., Li, F., Furtak, K., Dreier, L. and Horwich, A.L. (2009) An ALS-linked mutant SOD1 produces a locomotor defect associated with aggregation and synaptic dysfunction when expressed in neurons of Caenorhabditis elegans. *PLoS Genet*, **5**, e1000350.
128 Lamitina, T., Huang, C.G. and Strange, K. (2006) Genome-wide RNAi screening identifies protein damage as a regulator of osmoprotective gene expression. *Proc Natl Acad Sci U S A*, **103**, 12173-12178.
129 Bilen, J. and Bonini, N.M. (2007) Genome-wide screen for modifiers of ataxin-3 neurodegeneration in Drosophila. *PLoS Genet*, **3**, 1950-1964.
130 David, D.C., Ollikainen, N., Trinidad, J.C., Cary, M.P., Burlingame, A.L. and Kenyon, C. Widespread protein aggregation as an inherent part of aging in C. elegans. *PLoS Biol*, **8**, e1000450.
131 Becher, M.W., Kotzuk, J.A., Sharp, A.H., Davies, S.W., Bates, G.P., Price, D.L. and Ross, C.A. (1998) Intranuclear neuronal inclusions in Huntington's disease and dentatorubral and pallidoluysian atrophy: correlation between the density of inclusions and IT15 CAG triplet repeat length. *Neurobiol Dis*, **4**, 387-397.
132 Cummings, C.J., Mancini, M.A., Antalffy, B., DeFranco, D.B., Orr, H.T. and Zoghbi, H.Y. (1998) Chaperone suppression of aggregation and altered subcellular proteasome localization imply protein misfolding in SCA1. *Nat Genet*, **19**, 148-154.
133 Warrick, J.M., Chan, H.Y., Gray-Board, G.L., Chai, Y., Paulson, H.L. and Bonini, N.M. (1999) Suppression of polyglutamine-mediated neurodegeneration in Drosophila by the molecular chaperone HSP70. *Nat Genet*, **23**, 425-428.
134 Chan, H.Y., Warrick, J.M., Gray-Board, G.L., Paulson, H.L. and Bonini, N.M. (2000) Mechanisms of chaperone suppression of polyglutamine disease: selectivity, synergy and modulation of protein solubility in Drosophila. *Hum Mol Genet*, **9**, 2811-2820.
135 Kim, S., Nollen, E.A., Kitagawa, K., Bindokas, V.P. and Morimoto, R.I. (2002) Polyglutamine protein aggregates are dynamic. *Nat Cell Biol*, **4**, 826-831.
136 Bence, N.F., Sampat, R.M. and Kopito, R.R. (2001) Impairment of the ubiquitin-proteasome system by protein aggregation. *Science*, **292**, 1552-1555.
137 Holmberg, C.I., Staniszewski, K.E., Mensah, K.N., Matouschek, A. and Morimoto, R.I. (2004) Inefficient degradation of truncated polyglutamine proteins by the proteasome. *EMBO J*, **23**, 4307-4318.
138 Zhou, H., Cao, F., Wang, Z., Yu, Z.X., Nguyen, H.P., Evans, J., Li, S.H. and Li, X.J. (2003) Huntingtin forms toxic NH2-terminal fragment complexes that are promoted by the age-dependent decrease in proteasome activity. *J Cell Biol*, **163**, 109-118.
139 Keller, J.N., Huang, F.F. and Markesbery, W.R. (2000) Decreased levels of proteasome activity and proteasome expression in aging spinal cord. *Neuroscience*, **98**, 149-156.
140 Zhou, H., Li, S.H. and Li, X.J. (2001) Chaperone suppression of cellular toxicity of huntingtin is independent of polyglutamine aggregation. *J Biol Chem*, **276**, 48417-48424.
141 Diaz-Hernandez, M., Hernandez, F., Martin-Aparicio, E., Gomez-Ramos, P., Moran, M.A., Castano, J.G., Ferrer, I., Avila, J. and Lucas, J.J. (2003) Neuronal induction of the immunoproteasome in Huntington's disease. *J Neurosci*, **23**, 11653-11661.

142 Bett, J.S., Goellner, G.M., Woodman, B., Pratt, G., Rechsteiner, M. and Bates, G.P. (2006) Proteasome impairment does not contribute to pathogenesis in R6/2 Huntington's disease mice: exclusion of proteasome activator REGgamma as a therapeutic target. *Hum Mol Genet*, **15**, 33-44.
143 Garcia-Arencibia, M., Hochfeld, W.E., Toh, P.P. and Rubinsztein, D.C. Autophagy, a guardian against neurodegeneration. *Semin Cell Dev Biol*, **21**, 691-698.
144 Yu, W.H., Cuervo, A.M., Kumar, A., Peterhoff, C.M., Schmidt, S.D., Lee, J.H., Mohan, P.S., Mercken, M., Farmery, M.R., Tjernberg, L.O. *et al.* (2005) Macroautophagy--a novel Beta-amyloid peptide-generating pathway activated in Alzheimer's disease. *J Cell Biol*, **171**, 87-98.
145 Cuervo, A.M., Stefanis, L., Fredenburg, R., Lansbury, P.T. and Sulzer, D. (2004) Impaired degradation of mutant alpha-synuclein by chaperone-mediated autophagy. *Science*, **305**, 1292-1295.
146 Nascimento-Ferreira, I., Santos-Ferreira, T., Sousa-Ferreira, L., Auregan, G., Onofre, I., Alves, S., Dufour, N., Colomer Gould, V.F., Koeppen, A., Deglon, N. *et al.* Overexpression of the autophagic beclin-1 protein clears mutant ataxin-3 and alleviates Machado-Joseph disease. *Brain*.
147 Ravikumar, B., Duden, R. and Rubinsztein, D.C. (2002) Aggregate-prone proteins with polyglutamine and polyalanine expansions are degraded by autophagy. *Hum Mol Genet*, **11**, 1107-1117.
148 Qin, Z.H., Wang, Y., Kegel, K.B., Kazantsev, A., Apostol, B.L., Thompson, L.M., Yoder, J., Aronin, N. and DiFiglia, M. (2003) Autophagy regulates the processing of amino terminal huntingtin fragments. *Hum Mol Genet*, **12**, 3231-3244.
149 Mizushima, N. (2007) Autophagy: process and function. *Genes Dev*, **21**, 2861-2873.
150 Pandey, U.B., Nie, Z., Batlevi, Y., McCray, B.A., Ritson, G.P., Nedelsky, N.B., Schwartz, S.L., DiProspero, N.A., Knight, M.A., Schuldiner, O. *et al.* (2007) HDAC6 rescues neurodegeneration and provides an essential link between autophagy and the UPS. *Nature*, **447**, 859-863.
151 Chai, Y., Shao, J., Miller, V.M., Williams, A. and Paulson, H.L. (2002) Live-cell imaging reveals divergent intracellular dynamics of polyglutamine disease proteins and supports a sequestration model of pathogenesis. *Proc Natl Acad Sci U S A*, **99**, 9310-9315.
152 Steffan, J.S., Kazantsev, A., Spasic-Boskovic, O., Greenwald, M., Zhu, Y.Z., Gohler, H., Wanker, E.E., Bates, G.P., Housman, D.E. and Thompson, L.M. (2000) The Huntington's disease protein interacts with p53 and CREB-binding protein and represses transcription. *Proc Natl Acad Sci U S A*, **97**, 6763-6768.
153 Mantamadiotis, T., Lemberger, T., Bleckmann, S.C., Kern, H., Kretz, O., Martin Villalba, A., Tronche, F., Kellendonk, C., Gau, D., Kapfhammer, J. *et al.* (2002) Disruption of CREB function in brain leads to neurodegeneration. *Nat Genet*, **31**, 47-54.
154 Glass, M., Dragunow, M. and Faull, R.L. (2000) The pattern of neurodegeneration in Huntington's disease: a comparative study of cannabinoid, dopamine, adenosine and GABA(A) receptor alterations in the human basal ganglia in Huntington's disease. *Neuroscience*, **97**, 505-519.
155 McCampbell, A., Taylor, J.P., Taye, A.A., Robitschek, J., Li, M., Walcott, J., Merry, D., Chai, Y., Paulson, H., Sobue, G. *et al.* (2000) CREB-binding protein sequestration by expanded polyglutamine. *Hum Mol Genet*, **9**, 2197-2202.
156 Nucifora, F.C., Jr., Sasaki, M., Peters, M.F., Huang, H., Cooper, J.K., Yamada, M., Takahashi, H., Tsuji, S., Troncoso, J., Dawson, V.L. *et al.* (2001) Interference by huntingtin and atrophin-1 with cbp-mediated transcription leading to cellular toxicity. *Science*, **291**, 2423-2428.
157 Steffan, J.S., Bodai, L., Pallos, J., Poelman, M., McCampbell, A., Apostol, B.L., Kazantsev, A., Schmidt, E., Zhu, Y.Z., Greenwald, M. *et al.* (2001) Histone deacetylase inhibitors arrest polyglutamine-dependent neurodegeneration in Drosophila. *Nature*, **413**, 739-743.
158 Wood, J.D., Nucifora, F.C., Jr., Duan, K., Zhang, C., Wang, J., Kim, Y., Schilling, G., Sacchi, N., Liu, J.M. and Ross, C.A. (2000) Atrophin-1, the dentato-rubral and pallido-luysian atrophy gene product, interacts with ETO/MTG8 in the nuclear matrix and represses transcription. *J Cell Biol*, **150**, 939-948.
159 Zhang, C.X., Chen, A.D., Gettel, N.J. and Hsieh, T.S. (2000) Essential functions of DNA topoisomerase I in Drosophila melanogaster. *Dev Biol*, **222**, 27-40.

160 Li, F., Macfarlan, T., Pittman, R.N. and Chakravarti, D. (2002) Ataxin-3 is a histone-binding protein with two independent transcriptional corepressor activities. *J Biol Chem*, **277**, 45004-45012.
161 Peters, M.F., Nucifora, F.C., Jr., Kushi, J., Seaman, H.C., Cooper, J.K., Herring, W.J., Dawson, V.L., Dawson, T.M. and Ross, C.A. (1999) Nuclear targeting of mutant Huntingtin increases toxicity. *Mol Cell Neurosci*, **14**, 121-128.
162 Martin-Aparicio, E., Avila, J. and Lucas, J.J. (2002) Nuclear localization of N-terminal mutant huntingtin is cell cycle dependent. *Eur J Neurosci*, **16**, 355-359.
163 Yang, W., Dunlap, J.R., Andrews, R.B. and Wetzel, R. (2002) Aggregated polyglutamine peptides delivered to nuclei are toxic to mammalian cells. *Hum Mol Genet*, **11**, 2905-2917.
164 Nucifora, F.C., Jr., Ellerby, L.M., Wellington, C.L., Wood, J.D., Herring, W.J., Sawa, A., Hayden, M.R., Dawson, V.L., Dawson, T.M. and Ross, C.A. (2003) Nuclear localization of a non-caspase truncation product of atrophin-1, with an expanded polyglutamine repeat, increases cellular toxicity. *J Biol Chem*, **278**, 13047-13055.
165 Goti, D., Katzen, S.M., Mez, J., Kurtis, N., Kiluk, J., Ben-Haiem, L., Jenkins, N.A., Copeland, N.G., Kakizuka, A., Sharp, A.H. *et al.* (2004) A mutant ataxin-3 putative-cleavage fragment in brains of Machado-Joseph disease patients and transgenic mice is cytotoxic above a critical concentration. *J Neurosci*, **24**, 10266-10279.
166 Goldberg, Y.P., Nicholson, D.W., Rasper, D.M., Kalchman, M.A., Koide, H.B., Graham, R.K., Bromm, M., Kazemi-Esfarjani, P., Thornberry, N.A., Vaillancourt, J.P. *et al.* (1996) Cleavage of huntingtin by apopain, a proapoptotic cysteine protease, is modulated by the polyglutamine tract. *Nat Genet*, **13**, 442-449.
167 Hoffner, G., Island, M.L. and Djian, P. (2005) Purification of neuronal inclusions of patients with Huntington's disease reveals a broad range of N-terminal fragments of expanded huntingtin and insoluble polymers. *J Neurochem*, **95**, 125-136.
168 Wellington, C.L., Ellerby, L.M., Gutekunst, C.A., Rogers, D., Warby, S., Graham, R.K., Loubser, O., van Raamsdonk, J., Singaraja, R., Yang, Y.Z. *et al.* (2002) Caspase cleavage of mutant huntingtin precedes neurodegeneration in Huntington's disease. *J Neurosci*, **22**, 7862-7872.
169 Graham, R.K., Deng, Y., Slow, E.J., Haigh, B., Bissada, N., Lu, G., Pearson, J., Shehadeh, J., Bertram, L., Murphy, Z. *et al.* (2006) Cleavage at the caspase-6 site is required for neuronal dysfunction and degeneration due to mutant huntingtin. *Cell*, **125**, 1179-1191.
170 Berke, S.J., Schmied, F.A., Brunt, E.R., Ellerby, L.M. and Paulson, H.L. (2004) Caspase-mediated proteolysis of the polyglutamine disease protein ataxin-3. *J Neurochem*, **89**, 908-918.
171 Haacke, A., Hartl, F.U. and Breuer, P. (2007) Calpain inhibition is sufficient to suppress aggregation of polyglutamine-expanded ataxin-3. *J Biol Chem*, **282**, 18851-18856.
172 Warby, S.C., Doty, C.N., Graham, R.K., Shively, J., Singaraja, R.R. and Hayden, M.R. (2009) Phosphorylation of huntingtin reduces the accumulation of its nuclear fragments. *Mol Cell Neurosci*, **40**, 121-127.
173 Humbert, S., Bryson, E.A., Cordelieres, F.P., Connors, N.C., Datta, S.R., Finkbeiner, S., Greenberg, M.E. and Saudou, F. (2002) The IGF-1/Akt pathway is neuroprotective in Huntington's disease and involves Huntingtin phosphorylation by Akt. *Dev Cell*, **2**, 831-837.
174 Luo, S., Vacher, C., Davies, J.E. and Rubinsztein, D.C. (2005) Cdk5 phosphorylation of huntingtin reduces its cleavage by caspases: implications for mutant huntingtin toxicity. *J Cell Biol*, **169**, 647-656.
175 Gafni, J., Hermel, E., Young, J.E., Wellington, C.L., Hayden, M.R. and Ellerby, L.M. (2004) Inhibition of calpain cleavage of huntingtin reduces toxicity: accumulation of calpain/caspase fragments in the nucleus. *J Biol Chem*, **279**, 20211-20220.
176 Pardo, R., Colin, E., Regulier, E., Aebischer, P., Deglon, N., Humbert, S. and Saudou, F. (2006) Inhibition of calcineurin by FK506 protects against polyglutamine-huntingtin toxicity through an increase of huntingtin phosphorylation at S421. *J Neurosci*, **26**, 1635-1645.

177 Fei, E., Jia, N., Zhang, T., Ma, X., Wang, H., Liu, C., Zhang, W., Ding, L., Nukina, N. and Wang, G. (2007) Phosphorylation of ataxin-3 by glycogen synthase kinase 3beta at serine 256 regulates the aggregation of ataxin-3. *Biochem Biophys Res Commun*, **357**, 487-492.
178 Mueller, T., Breuer, P., Schmitt, I., Walter, J., Evert, B.O. and Wullner, U. (2009) CK2-dependent phosphorylation determines cellular localization and stability of ataxin-3. *Hum Mol Genet*, **18**, 3334-3343.
179 Chen, H.K., Fernandez-Funez, P., Acevedo, S.F., Lam, Y.C., Kaytor, M.D., Fernandez, M.H., Aitken, A., Skoulakis, E.M., Orr, H.T., Botas, J. *et al.* (2003) Interaction of Akt-phosphorylated ataxin-1 with 14-3-3 mediates neurodegeneration in spinocerebellar ataxia type 1. *Cell*, **113**, 457-468.
180 Sun, J., Xu, H., Negi, S., Subramony, S.H. and Hebert, M.D. (2007) Differential effects of polyglutamine proteins on nuclear organization and artificial reporter splicing. *J Neurosci Res*, **85**, 2306-2317.
181 Schols, L., Bauer, P., Schmidt, T., Schulte, T. and Riess, O. (2004) Autosomal dominant cerebellar ataxias: clinical features, genetics, and pathogenesis. *Lancet Neurol*, **3**, 291-304.
182 DiFiglia, M. (2002) Huntingtin fragments that aggregate go their separate ways. *Mol Cell*, **10**, 224-225.
183 Gatchel, J.R. and Zoghbi, H.Y. (2005) Diseases of unstable repeat expansion: mechanisms and common principles. *Nat Rev Genet*, **6**, 743-755.
184 Heng, M.Y., Duong, D.K., Albin, R.L., Tallaksen-Greene, S.J., Hunter, J.M., Lesort, M.J., Osmand, A., Paulson, H.L. and Detloff, P.J. Early autophagic response in a novel knock-in model of Huntington disease. *Hum Mol Genet*, **19**, 3702-3720.
185 Bichelmeier, U., Schmidt, T., Hubener, J., Boy, J., Ruttiger, L., Habig, K., Poths, S., Bonin, M., Knipper, M., Schmidt, W.J. *et al.* (2007) Nuclear localization of ataxin-3 is required for the manifestation of symptoms in SCA3: in vivo evidence. *J Neurosci*, **27**, 7418-7428.
186 Macedo-Ribeiro, S., Cortes, L., Maciel, P. and Carvalho, A.L. (2009) Nucleocytoplasmic shuttling activity of ataxin-3. *PLoS One*, **4**, e5834.
187 Gunawardena, S. and Goldstein, L.S. (2005) Polyglutamine diseases and transport problems: deadly traffic jams on neuronal highways. *Arch Neurol*, **62**, 46-51.
188 Block-Galarza, J., Chase, K.O., Sapp, E., Vaughn, K.T., Vallee, R.B., DiFiglia, M. and Aronin, N. (1997) Fast transport and retrograde movement of huntingtin and HAP 1 in axons. *Neuroreport*, **8**, 2247-2251.
189 Li, S.H., Gutekunst, C.A., Hersch, S.M. and Li, X.J. (1998) Interaction of huntingtin-associated protein with dynactin P150Glued. *J Neurosci*, **18**, 1261-1269.
190 Burnett, B.G. and Pittman, R.N. (2005) The polyglutamine neurodegenerative protein ataxin 3 regulates aggresome formation. *Proc Natl Acad Sci U S A*, **102**, 4330-4335.
191 Rodrigues, A.J., do Carmo Costa, M., Silva, T.L., Ferreira, D., Bajanca, F., Logarinho, E. and Maciel, P. Absence of ataxin-3 leads to cytoskeletal disorganization and increased cell death. *Biochim Biophys Acta*, **1803**, 1154-1163.
192 Sapp, E., Penney, J., Young, A., Aronin, N., Vonsattel, J.P. and DiFiglia, M. (1999) Axonal transport of N-terminal huntingtin suggests early pathology of corticostriatal projections in Huntington disease. *J Neuropathol Exp Neurol*, **58**, 165-173.
193 Grunewald, T. and Beal, M.F. (1999) Bioenergetics in Huntington's disease. *Ann N Y Acad Sci*, **893**, 203-213.
194 Panov, A.V., Gutekunst, C.A., Leavitt, B.R., Hayden, M.R., Burke, J.R., Strittmatter, W.J. and Greenamyre, J.T. (2002) Early mitochondrial calcium defects in Huntington's disease are a direct effect of polyglutamines. *Nat Neurosci*, **5**, 731-736.
195 Brouillet, E., Hantraye, P., Ferrante, R.J., Dolan, R., Leroy-Willig, A., Kowall, N.W. and Beal, M.F. (1995) Chronic mitochondrial energy impairment produces selective striatal degeneration and abnormal choreiform movements in primates. *Proc Natl Acad Sci U S A*, **92**, 7105-7109.

196 Beal, M.F., Brouillet, E., Jenkins, B., Henshaw, R., Rosen, B. and Hyman, B.T. (1993) Age-dependent striatal excitotoxic lesions produced by the endogenous mitochondrial inhibitor malonate. *J Neurochem*, **61**, 1147-1150.
197 Gu, M., Gash, M.T., Mann, V.M., Javoy-Agid, F., Cooper, J.M. and Schapira, A.H. (1996) Mitochondrial defect in Huntington's disease caudate nucleus. *Ann Neurol*, **39**, 385-389.
198 Milakovic, T. and Johnson, G.V. (2005) Mitochondrial respiration and ATP production are significantly impaired in striatal cells expressing mutant huntingtin. *J Biol Chem*, **280**, 30773-30782.
199 Choo, Y.S., Johnson, G.V., MacDonald, M., Detloff, P.J. and Lesort, M. (2004) Mutant huntingtin directly increases susceptibility of mitochondria to the calcium-induced permeability transition and cytochrome c release. *Hum Mol Genet*, **13**, 1407-1420.
200 Wang, H., Lim, P.J., Karbowski, M. and Monteiro, M.J. (2009) Effects of overexpression of huntingtin proteins on mitochondrial integrity. *Hum Mol Genet*, **18**, 737-752.
201 Ranganathan, S., Harmison, G.G., Meyertholen, K., Pennuto, M., Burnett, B.G. and Fischbeck, K.H. (2009) Mitochondrial abnormalities in spinal and bulbar muscular atrophy. *Hum Mol Genet*, **18**, 27-42.
202 St-Pierre, J., Drori, S., Uldry, M., Silvaggi, J.M., Rhee, J., Jager, S., Handschin, C., Zheng, K., Lin, J., Yang, W. *et al.* (2006) Suppression of reactive oxygen species and neurodegeneration by the PGC-1 transcriptional coactivators. *Cell*, **127**, 397-408.
203 Weydt, P., Pineda, V.V., Torrence, A.E., Libby, R.T., Satterfield, T.F., Lazarowski, E.R., Gilbert, M.L., Morton, G.J., Bammler, T.K., Strand, A.D. *et al.* (2006) Thermoregulatory and metabolic defects in Huntington's disease transgenic mice implicate PGC-1alpha in Huntington's disease neurodegeneration. *Cell Metab*, **4**, 349-362.
204 Cui, L., Jeong, H., Borovecki, F., Parkhurst, C.N., Tanese, N. and Krainc, D. (2006) Transcriptional repression of PGC-1alpha by mutant huntingtin leads to mitochondrial dysfunction and neurodegeneration. *Cell*, **127**, 59-69.
205 Yu, Y.C., Kuo, C.L., Cheng, W.L., Liu, C.S. and Hsieh, M. (2009) Decreased antioxidant enzyme activity and increased mitochondrial DNA damage in cellular models of Machado-Joseph disease. *J Neurosci Res*, **87**, 1884-1891.
206 Reina, C.P., Zhong, X. and Pittman, R.N. Proteotoxic stress increases nuclear localization of ataxin-3. *Hum Mol Genet*, **19**, 235-249.
207 Tsai, H.F., Tsai, H.J. and Hsieh, M. (2004) Full-length expanded ataxin-3 enhances mitochondrial-mediated cell death and decreases Bcl-2 expression in human neuroblastoma cells. *Biochem Biophys Res Commun*, **324**, 1274-1282.
208 Yamamoto, A., Lucas, J.J. and Hen, R. (2000) Reversal of neuropathology and motor dysfunction in a conditional model of Huntington's disease. *Cell*, **101**, 57-66.
209 Boy, J., Schmidt, T., Wolburg, H., Mack, A., Nuber, S., Bottcher, M., Schmitt, I., Holzmann, C., Zimmermann, F., Servadio, A. *et al.* (2009) Reversibility of symptoms in a conditional mouse model of spinocerebellar ataxia type 3. *Hum Mol Genet*, **18**, 4282-4295.
210 Zu, T., Duvick, L.A., Kaytor, M.D., Berlinger, M.S., Zoghbi, H.Y., Clark, H.B. and Orr, H.T. (2004) Recovery from polyglutamine-induced neurodegeneration in conditional SCA1 transgenic mice. *J Neurosci*, **24**, 8853-8861.
211 Bonini, N.M. and La Spada, A.R. (2005) Silencing polyglutamine degeneration with RNAi. *Neuron*, **48**, 715-718.
212 Lombardi, M.S., Jaspers, L., Spronkmans, C., Gellera, C., Taroni, F., Di Maria, E., Donato, S.D. and Kaemmerer, W.F. (2009) A majority of Huntington's disease patients may be treatable by individualized allele-specific RNA interference. *Exp Neurol*, **217**, 312-319.
213 Pfister, E.L., Kennington, L., Straubhaar, J., Wagh, S., Liu, W., DiFiglia, M., Landwehrmeyer, B., Vonsattel, J.P., Zamore, P.D. and Aronin, N. (2009) Five siRNAs targeting three SNPs may provide therapy for three-quarters of Huntington's disease patients. *Curr Biol*, **19**, 774-778.
214 Alves, S., Nascimento-Ferreira, I., Auregan, G., Hassig, R., Dufour, N., Brouillet, E., Pedroso de Lima, M.C., Hantraye, P., Pereira de Almeida, L. and Deglon, N. (2008) Allele-specific RNA silencing of

mutant ataxin-3 mediates neuroprotection in a rat model of Machado-Joseph disease. *PLoS One*, **3**, e3341.
215 Sarkar, S., Perlstein, E.O., Imarisio, S., Pineau, S., Cordenier, A., Maglathlin, R.L., Webster, J.A., Lewis, T.A., O'Kane, C.J., Schreiber, S.L. *et al.* (2007) Small molecules enhance autophagy and reduce toxicity in Huntington's disease models. *Nat Chem Biol*, **3**, 331-338.
216 Williams, A., Sarkar, S., Cuddon, P., Ttofi, E.K., Saiki, S., Siddiqi, F.H., Jahreiss, L., Fleming, A., Pask, D., Goldsmith, P. *et al.* (2008) Novel targets for Huntington's disease in an mTOR-independent autophagy pathway. *Nat Chem Biol*, **4**, 295-305.
217 Menzies, F.M., Huebener, J., Renna, M., Bonin, M., Riess, O. and Rubinsztein, D.C. Autophagy induction reduces mutant ataxin-3 levels and toxicity in a mouse model of spinocerebellar ataxia type 3. *Brain*, **133**, 93-104.
218 Wong, H.K., Bauer, P.O., Kurosawa, M., Goswami, A., Washizu, C., Machida, Y., Tosaki, A., Yamada, M., Knopfel, T., Nakamura, T. *et al.* (2008) Blocking acid-sensing ion channel 1 alleviates Huntington's disease pathology via an ubiquitin-proteasome system-dependent mechanism. *Hum Mol Genet*, **17**, 3223-3235.
219 Bauer, P.O., Wong, H.K., Oyama, F., Goswami, A., Okuno, M., Kino, Y., Miyazaki, H. and Nukina, N. (2009) Inhibition of Rho kinases enhances the degradation of mutant huntingtin. *J Biol Chem*, **284**, 13153-13164.
220 Sanchez, I., Mahlke, C. and Yuan, J. (2003) Pivotal role of oligomerization in expanded polyglutamine neurodegenerative disorders. *Nature*, **421**, 373-379.
221 Tanaka, M., Machida, Y., Niu, S., Ikeda, T., Jana, N.R., Doi, H., Kurosawa, M., Nekooki, M. and Nukina, N. (2004) Trehalose alleviates polyglutamine-mediated pathology in a mouse model of Huntington disease. *Nat Med*, **10**, 148-154.
222 Dedeoglu, A., Kubilus, J.K., Jeitner, T.M., Matson, S.A., Bogdanov, M., Kowall, N.W., Matson, W.R., Cooper, A.J., Ratan, R.R., Beal, M.F. *et al.* (2002) Therapeutic effects of cystamine in a murine model of Huntington's disease. *J Neurosci*, **22**, 8942-8950.
223 Borrell-Pages, M., Canals, J.M., Cordelieres, F.P., Parker, J.A., Pineda, J.R., Grange, G., Bryson, E.A., Guillermier, M., Hirsch, E., Hantraye, P. *et al.* (2006) Cystamine and cysteamine increase brain levels of BDNF in Huntington disease via HSJ1b and transglutaminase. *J Clin Invest*, **116**, 1410-1424.
224 Wu, C.L., Hwang, C.S., Chen, S.D., Yin, J.H. and Yang, D.I. Neuroprotective mechanisms of brain-derived neurotrophic factor against 3-nitropropionic acid toxicity: therapeutic implications for Huntington's disease. *Ann N Y Acad Sci*, **1201**, 8-12.
225 Katsuno, M., Sang, C., Adachi, H., Minamiyama, M., Waza, M., Tanaka, F., Doyu, M. and Sobue, G. (2005) Pharmacological induction of heat-shock proteins alleviates polyglutamine-mediated motor neuron disease. *Proc Natl Acad Sci U S A*, **102**, 16801-16806.
226 Waza, M., Adachi, H., Katsuno, M., Minamiyama, M., Sang, C., Tanaka, F., Inukai, A., Doyu, M. and Sobue, G. (2005) 17-AAG, an Hsp90 inhibitor, ameliorates polyglutamine-mediated motor neuron degeneration. *Nat Med*, **11**, 1088-1095.
227 Fujikake, N., Nagai, Y., Popiel, H.A., Okamoto, Y., Yamaguchi, M. and Toda, T. (2008) Heat shock transcription factor 1-activating compounds suppress polyglutamine-induced neurodegeneration through induction of multiple molecular chaperones. *J Biol Chem*, **283**, 26188-26197.
228 Ferrante, R.J., Kubilus, J.K., Lee, J., Ryu, H., Beesen, A., Zucker, B., Smith, K., Kowall, N.W., Ratan, R.R., Luthi-Carter, R. *et al.* (2003) Histone deacetylase inhibition by sodium butyrate chemotherapy ameliorates the neurodegenerative phenotype in Huntington's disease mice. *J Neurosci*, **23**, 9418-9427.
229 Hockly, E., Richon, V.M., Woodman, B., Smith, D.L., Zhou, X., Rosa, E., Sathasivam, K., Ghazi-Noori, S., Mahal, A., Lowden, P.A. *et al.* (2003) Suberoylanilide hydroxamic acid, a histone deacetylase inhibitor, ameliorates motor deficits in a mouse model of Huntington's disease. *Proc Natl Acad Sci U S A*, **100**, 2041-2046.

230 Minamiyama, M., Katsuno, M., Adachi, H., Waza, M., Sang, C., Kobayashi, Y., Tanaka, F., Doyu, M., Inukai, A. and Sobue, G. (2004) Sodium butyrate ameliorates phenotypic expression in a transgenic mouse model of spinal and bulbar muscular atrophy. *Hum Mol Genet*, **13**, 1183-1192.
231 Ying, M., Xu, R., Wu, X., Zhu, H., Zhuang, Y., Han, M. and Xu, T. (2006) Sodium butyrate ameliorates histone hypoacetylation and neurodegenerative phenotypes in a mouse model for DRPLA. *J Biol Chem*, **281**, 12580-12586.
232 Gardian, G., Browne, S.E., Choi, D.K., Klivenyi, P., Gregorio, J., Kubilus, J.K., Ryu, H., Langley, B., Ratan, R.R., Ferrante, R.J. *et al.* (2005) Neuroprotective effects of phenylbutyrate in the N171-82Q transgenic mouse model of Huntington's disease. *J Biol Chem*, **280**, 556-563.
233 Ferrante, R.J., Ryu, H., Kubilus, J.K., D'Mello, S., Sugars, K.L., Lee, J., Lu, P., Smith, K., Browne, S., Beal, M.F. *et al.* (2004) Chemotherapy for the brain: the antitumor antibiotic mithramycin prolongs survival in a mouse model of Huntington's disease. *J Neurosci*, **24**, 10335-10342.
234 Zuccato, C., Tartari, M., Crotti, A., Goffredo, D., Valenza, M., Conti, L., Cataudella, T., Leavitt, B.R., Hayden, M.R., Timmusk, T. *et al.* (2003) Huntingtin interacts with REST/NRSF to modulate the transcription of NRSE-controlled neuronal genes. *Nat Genet*, **35**, 76-83.
235 DeMarch, Z., Giampa, C., Patassini, S., Bernardi, G. and Fusco, F.R. (2008) Beneficial effects of rolipram in the R6/2 mouse model of Huntington's disease. *Neurobiol Dis*, **30**, 375-387.
236 Parker, J.A., Arango, M., Abderrahmane, S., Lambert, E., Tourette, C., Catoire, H. and Neri, C. (2005) Resveratrol rescues mutant polyglutamine cytotoxicity in nematode and mammalian neurons. *Nat Genet*, **37**, 349-350.
237 Sanchez-Pernaute, R., Garcia-Segura, J.M., del Barrio Alba, A., Viano, J. and de Yebenes, J.G. (1999) Clinical correlation of striatal 1H MRS changes in Huntington's disease. *Neurology*, **53**, 806-812.
238 Ferrante, R.J., Andreassen, O.A., Jenkins, B.G., Dedeoglu, A., Kuemmerle, S., Kubilus, J.K., Kaddurah-Daouk, R., Hersch, S.M. and Beal, M.F. (2000) Neuroprotective effects of creatine in a transgenic mouse model of Huntington's disease. *J Neurosci*, **20**, 4389-4397.
239 Andreassen, O.A., Dedeoglu, A., Ferrante, R.J., Jenkins, B.G., Ferrante, K.L., Thomas, M., Friedlich, A., Browne, S.E., Schilling, G., Borchelt, D.R. *et al.* (2001) Creatine increase survival and delays motor symptoms in a transgenic animal model of Huntington's disease. *Neurobiol Dis*, **8**, 479-491.
240 Giampa, C., Patassini, S., Borreca, A., Laurenti, D., Marullo, F., Bernardi, G., Menniti, F.S. and Fusco, F.R. (2009) Phosphodiesterase 10 inhibition reduces striatal excitotoxicity in the quinolinic acid model of Huntington's disease. *Neurobiol Dis*, **34**, 450-456.
241 Smith, K.M., Matson, S., Matson, W.R., Cormier, K., Del Signore, S.J., Hagerty, S.W., Stack, E.C., Ryu, H. and Ferrante, R.J. (2006) Dose ranging and efficacy study of high-dose coenzyme Q10 formulations in Huntington's disease mice. *Biochim Biophys Acta*, **1762**, 616-626.
242 Nguyen, T., Hamby, A. and Massa, S.M. (2005) Clioquinol down-regulates mutant huntingtin expression in vitro and mitigates pathology in a Huntington's disease mouse model. *Proc Natl Acad Sci U S A*, **102**, 11840-11845.
243 Cepeda, C., Hurst, R.S., Flores-Hernandez, J., Hernandez-Echeagaray, E., Klapstein, G.J., Boylan, M.K., Calvert, C.R., Jocoy, E.L., Nguyen, O.K., Andre, V.M. *et al.* (2003) Morphological and electrophysiological characterization of abnormal cell types in pediatric cortical dysplasia. *J Neurosci Res*, **72**, 472-486.
244 Schiefer, J., Landwehrmeyer, G.B., Luesse, H.G., Sprunken, A., Puls, C., Milkereit, A., Milkereit, E. and Kosinski, C.M. (2002) Riluzole prolongs survival time and alters nuclear inclusion formation in a transgenic mouse model of Huntington's disease. *Mov Disord*, **17**, 748-757.
245 Schiefer, J., Sprunken, A., Puls, C., Luesse, H.G., Milkereit, A., Milkereit, E., Johann, V. and Kosinski, C.M. (2004) The metabotropic glutamate receptor 5 antagonist MPEP and the mGluR2 agonist LY379268 modify disease progression in a transgenic mouse model of Huntington's disease. *Brain Res*, **1019**, 246-254.

246 Ferrante, R.J., Andreassen, O.A., Dedeoglu, A., Ferrante, K.L., Jenkins, B.G., Hersch, S.M. and Beal, M.F. (2002) Therapeutic effects of coenzyme Q10 and remacemide in transgenic mouse models of Huntington's disease. *J Neurosci*, **22**, 1592-1599.
247 Wang, X., Zhu, S., Drozda, M., Zhang, W., Stavrovskaya, I.G., Cattaneo, E., Ferrante, R.J., Kristal, B.S. and Friedlander, R.M. (2003) Minocycline inhibits caspase-independent and -dependent mitochondrial cell death pathways in models of Huntington's disease. *Proc Natl Acad Sci U S A*, **100**, 10483-10487.
248 Chen, M., Ona, V.O., Li, M., Ferrante, R.J., Fink, K.B., Zhu, S., Bian, J., Guo, L., Farrell, L.A., Hersch, S.M. *et al.* (2000) Minocycline inhibits caspase-1 and caspase-3 expression and delays mortality in a transgenic mouse model of Huntington disease. *Nat Med*, **6**, 797-801.
249 Stack, E.C., Smith, K.M., Ryu, H., Cormier, K., Chen, M., Hagerty, S.W., Del Signore, S.J., Cudkowicz, M.E., Friedlander, R.M. and Ferrante, R.J. (2006) Combination therapy using minocycline and coenzyme Q10 in R6/2 transgenic Huntington's disease mice. *Biochim Biophys Acta*, **1762**, 373-380.
250 Ona, V.O., Li, M., Vonsattel, J.P., Andrews, L.J., Khan, S.Q., Chung, W.M., Frey, A.S., Menon, A.S., Li, X.J., Stieg, P.E. *et al.* (1999) Inhibition of caspase-1 slows disease progression in a mouse model of Huntington's disease. *Nature*, **399**, 263-267.
251 Nakano, K.K., Dawson, D.M. and Spence, A. (1972) Machado disease. A hereditary ataxia in Portuguese emigrants to Massachusetts. *Neurology*, **22**, 49-55.
252 Woods, B.T. and Schaumburg, H.H. (1972) Nigro-spino-dentatal degeneration with nuclear ophthalmoplegia. A unique and partially treatable clinico-pathological entity. *J Neurol Sci*, **17**, 149-166.
253 Rosenberg, R.N., Nyhan, W.L., Bay, C. and Shore, P. (1976) Autosomal dominant striatonigral degeneration. A clinical, pathologic, and biochemical study of a new genetic disorder. *Neurology*, **26**, 703-714.
254 Coutinho, P., Calheiros, J.M. and Andrade, C. (1977) Sobre uma nova doenca degenerativa do sistema nervoso central transmitida de modo autossomico dominante e afectando familias originarias dos Acores *O Medico*, **82**, 446-448.
255 Coutinho, P. and Andrade, C. (1978) Autosomal dominant system degeneration in Portuguese families of the Azores Islands. A new genetic disorder involving cerebellar, pyramidal, extrapyramidal and spinal cord motor functions. *Neurology*, **28**, 703-709.
256 Coutinho, P., Almeida, R. and Andrade, C. (1980) Estudo clinico e genetico de 25 familias dos Acores com uma forma particular de heredoataxia. *Livro de Homenagem ao Professor Arnaldo Sampaio* 287-300.
257 Lima, L. and Coutinho, P. (1980) Clinical criteria for diagnosis of Machado-Joseph disease: report of a non-Azorena Portuguese family. *Neurology*, **30**, 319-322.
258 Rosenberg, R.N. (1983) Dominant ataxias. *Res Publ Assoc Res Nerv Ment Dis*, **60**, 195-213.
259 Barbeau, A., Roy, M., Cunha, L., de Vincente, A.N., Rosenberg, R.N., Nyhan, W.L., MacLeod, P.L., Chazot, G., Langston, L.B., Dawson, D.M. *et al.* (1984) The natural history of Machado-Joseph disease. An analysis of 138 personally examined cases. *Can J Neurol Sci*, **11**, 510-525.
260 Margolis, R.L. (2002) The spinocerebellar ataxias: order emerges from chaos. *Curr Neurol Neurosci Rep*, **2**, 447-456.
261 Paulson, H.L. (2007) Dominantly inherited ataxias: lessons learned from Machado-Joseph disease/spinocerebellar ataxia type 3. *Semin Neurol*, **27**, 133-142.
262 Coutinho, P. (2009) Machado-Joseph Disease Revisited. *V International Workshop on Machado-Joseph disease*.
263 Coutinho, P. (1992) Doenca de Machado-Joseph. *Grande Premio Bial de Medicina.*
264 Robitaille, Y., Lopes-Cendes, I., Becher, M., Rouleau, G. and Clark, A.W. (1997) The neuropathology of CAG repeat diseases: review and update of genetic and molecular features. *Brain Pathol*, **7**, 901-926.

265 Iwabuchi, K., Tsuchiya, K., Uchihara, T. and Yagishita, S. (1999) Autosomal dominant spinocerebellar degenerations. Clinical, pathological, and genetic correlations. *Rev Neurol (Paris)*, **155**, 255-270.
266 Gilman, S. (2000) The spinocerebellar ataxias. *Clin Neuropharmacol*, **23**, 296-303.
267 Yamada, M., Tan, C.F., Inenaga, C., Tsuji, S. and Takahashi, H. (2004) Sharing of polyglutamine localization by the neuronal nucleus and cytoplasm in CAG-repeat diseases. *Neuropathol Appl Neurobiol*, **30**, 665-675.
268 Koeppen, A.H. (2005) The pathogenesis of spinocerebellar ataxia. *Cerebellum*, **4**, 62-73.
269 Rub, U., Brunt, E.R., Del Turco, D., de Vos, R.A., Gierga, K., Paulson, H. and Braak, H. (2003) Guidelines for the pathoanatomical examination of the lower brain stem in ingestive and swallowing disorders and its application to a dysphagic spinocerebellar ataxia type 3 patient. *Neuropathol Appl Neurobiol*, **29**, 1-13.
270 Rub, U., Brunt, E.R., Gierga, K., Schultz, C., Paulson, H., de Vos, R.A. and Braak, H. (2003) The nucleus raphe interpositus in spinocerebellar ataxia type 3 (Machado-Joseph disease). *J Chem Neuroanat*, **25**, 115-127.
271 Rub, U., Del Turco, D., Del Tredici, K., de Vos, R.A., Brunt, E.R., Reifenberger, G., Seifried, C., Schultz, C., Auburger, G. and Braak, H. (2003) Thalamic involvement in a spinocerebellar ataxia type 2 (SCA2) and a spinocerebellar ataxia type 3 (SCA3) patient, and its clinical relevance. *Brain*, **126**, 2257-2272.
272 Rub, U., Brunt, E.R., de Vos, R.A., Del Turco, D., Del Tredici, K., Gierga, K., Schultz, C., Ghebremedhin, E., Burk, K., Auburger, G. *et al.* (2004) Degeneration of the central vestibular system in spinocerebellar ataxia type 3 (SCA3) patients and its possible clinical significance. *Neuropathol Appl Neurobiol*, **30**, 402-414.
273 Rub, U., Gierga, K., Brunt, E.R., de Vos, R.A., Bauer, M., Schols, L., Burk, K., Auburger, G., Bohl, J., Schultz, C. *et al.* (2005) Spinocerebellar ataxias types 2 and 3: degeneration of the pre-cerebellar nuclei isolates the three phylogenetically defined regions of the cerebellum. *J Neural Transm*, **112**, 1523-1545.
274 Rub, U., Brunt, E.R., Petrasch-Parwez, E., Schols, L., Theegarten, D., Auburger, G., Seidel, K., Schultz, C., Gierga, K., Paulson, H. *et al.* (2006) Degeneration of ingestion-related brainstem nuclei in spinocerebellar ataxia type 2, 3, 6 and 7. *Neuropathol Appl Neurobiol*, **32**, 635-649.
275 Rub, U., Seidel, K., Ozerden, I., Gierga, K., Brunt, E.R., Schols, L., de Vos, R.A., den Dunnen, W., Schultz, C., Auburger, G. *et al.* (2007) Consistent affection of the central somatosensory system in spinocerebellar ataxia type 2 and type 3 and its significance for clinical symptoms and rehabilitative therapy. *Brain Res Rev*, **53**, 235-249.
276 Seidel, K., den Dunnen, W.F., Schultz, C., Paulson, H., Frank, S., de Vos, R.A., Brunt, E.R., Deller, T., Kampinga, H.H. and Rub, U. Axonal inclusions in spinocerebellar ataxia type 3. *Acta Neuropathol*.
277 Chai, Y., Koppenhafer, S.L., Bonini, N.M. and Paulson, H.L. (1999) Analysis of the role of heat shock protein (Hsp) molecular chaperones in polyglutamine disease. *J Neurosci*, **19**, 10338-10347.
278 Rubinsztein, D.C., Leggo, J., Coetzee, G.A., Irvine, R.A., Buckley, M. and Ferguson-Smith, M.A. (1995) Sequence variation and size ranges of CAG repeats in the Machado-Joseph disease, spinocerebellar ataxia type 1 and androgen receptor genes. *Hum Mol Genet*, **4**, 1585-1590.
279 Takiyama, Y., Nishizawa, M., Tanaka, H., Kawashima, S., Sakamoto, H., Karube, Y., Shimazaki, H., Soutome, M., Endo, K., Ohta, S. *et al.* (1993) The gene for Machado-Joseph disease maps to human chromosome 14q. *Nat Genet*, **4**, 300-304.
280 Higgins, J.J., Nee, L.E., Vasconcelos, O., Ide, S.E., Lavedan, C., Goldfarb, L.G. and Polymeropoulos, M.H. (1996) Mutations in American families with spinocerebellar ataxia (SCA) type 3: SCA3 is allelic to Machado-Joseph disease. *Neurology*, **46**, 208-213.
281 Lopes-Cendes, I., Maciel, P., Kish, S., Gaspar, C., Robitaille, Y., Clark, H.B., Koeppen, A.H., Nance, M., Schut, L., Silveira, I. *et al.* (1996) Somatic mosaicism in the central nervous system in spinocerebellar ataxia type 1 and Machado-Joseph disease. *Ann Neurol*, **40**, 199-206.

282 Gaspar, C., Lopes-Cendes, I., Hayes, S., Goto, J., Arvidsson, K., Dias, A., Silveira, I., Maciel, P., Coutinho, P., Lima, M. *et al.* (2001) Ancestral origins of the Machado-Joseph disease mutation: a worldwide haplotype study. *Am J Hum Genet*, **68**, 523-528.
283 Ichikawa, Y., Goto, J., Hattori, M., Toyoda, A., Ishii, K., Jeong, S.Y., Hashida, H., Masuda, N., Ogata, K., Kasai, F. *et al.* (2001) The genomic structure and expression of MJD, the Machado-Joseph disease gene. *J Hum Genet*, **46**, 413-422.
284 Maciel, P., Costa, M.C., Ferro, A., Rousseau, M., Santos, C.S., Gaspar, C., Barros, J., Rouleau, G.A., Coutinho, P. and Sequeiros, J. (2001) Improvement in the molecular diagnosis of Machado-Joseph disease. *Arch Neurol*, **58**, 1821-1827.
285 Padiath, Q.S., Srivastava, A.K., Roy, S., Jain, S. and Brahmachari, S.K. (2005) Identification of a novel 45 repeat unstable allele associated with a disease phenotype at the MJD1/SCA3 locus. *Am J Med Genet B Neuropsychiatr Genet*, **133B**, 124-126.
286 Gu, W., Ma, H., Wang, K., Jin, M., Zhou, Y., Liu, X., Wang, G. and Shen, Y. (2004) The shortest expanded allele of the MJD1 gene in a Chinese MJD kindred with autonomic dysfunction. *Eur Neurol*, **52**, 107-111.
287 Goto, J., Watanabe, M., Ichikawa, Y., Yee, S.B., Ihara, N., Endo, K., Igarashi, S., Takiyama, Y., Gaspar, C., Maciel, P. *et al.* (1997) Machado-Joseph disease gene products carrying different carboxyl termini. *Neurosci Res*, **28**, 373-377.
288 Bettencourt, C., Santos, C., Montiel, R., Costa Mdo, C., Cruz-Morales, P., Santos, L.R., Simoes, N., Kay, T., Vasconcelos, J., Maciel, P. *et al.* Increased transcript diversity: novel splicing variants of Machado-Joseph disease gene (ATXN3). *Neurogenetics*, **11**, 193-202.
289 do Carmo Costa, M., Gomes-da-Silva, J., Miranda, C.J., Sequeiros, J., Santos, M.M. and Maciel, P. (2004) Genomic structure, promoter activity, and developmental expression of the mouse homologue of the Machado-Joseph disease (MJD) gene. *Genomics*, **84**, 361-373.
290 Schmitt, I., Brattig, T., Gossen, M. and Riess, O. (1997) Characterization of the rat spinocerebellar ataxia type 3 gene. *Neurogenetics*, **1**, 103-112.
291 Linhartova, I., Repitz, M., Draber, P., Nemec, M., Wiche, G. and Propst, F. (1999) Conserved domains and lack of evidence for polyglutamine length polymorphism in the chicken homolog of the Machado-Joseph disease gene product ataxin-3. *Biochim Biophys Acta*, **1444**, 299-305.
292 Rodrigues, A.J., Coppola, G., Santos, C., Costa Mdo, C., Ailion, M., Sequeiros, J., Geschwind, D.H. and Maciel, P. (2007) Functional genomics and biochemical characterization of the C. elegans orthologue of the Machado-Joseph disease protein ataxin-3. *FASEB J*, **21**, 1126-1136.
293 Tait, D., Riccio, M., Sittler, A., Scherzinger, E., Santi, S., Ognibene, A., Maraldi, N.M., Lehrach, H. and Wanker, E.E. (1998) Ataxin-3 is transported into the nucleus and associates with the nuclear matrix. *Hum Mol Genet*, **7**, 991-997.
294 Burnett, B., Li, F. and Pittman, R.N. (2003) The polyglutamine neurodegenerative protein ataxin-3 binds polyubiquitylated proteins and has ubiquitin protease activity. *Hum Mol Genet*, **12**, 3195-3205.
295 Doss-Pepe, E.W., Stenroos, E.S., Johnson, W.G. and Madura, K. (2003) Ataxin-3 interactions with rad23 and valosin-containing protein and its associations with ubiquitin chains and the proteasome are consistent with a role in ubiquitin-mediated proteolysis. *Mol Cell Biol*, **23**, 6469-6483.
296 Trottier, Y., Cancel, G., An-Gourfinkel, I., Lutz, Y., Weber, C., Brice, A., Hirsch, E. and Mandel, J.L. (1998) Heterogeneous intracellular localization and expression of ataxin-3. *Neurobiol Dis*, **5**, 335-347.
297 Fujigasaki, H., Uchihara, T., Koyano, S., Iwabuchi, K., Yagishita, S., Makifuchi, T., Nakamura, A., Ishida, K., Toru, S., Hirai, S. *et al.* (2000) Ataxin-3 is translocated into the nucleus for the formation of intranuclear inclusions in normal and Machado-Joseph disease brains. *Exp Neurol*, **165**, 248-256.

298 Wang, G., Ide, K., Nukina, N., Goto, J., Ichikawa, Y., Uchida, K., Sakamoto, T. and Kanazawa, I. (1997) Machado-Joseph disease gene product identified in lymphocytes and brain. *Biochem Biophys Res Commun*, **233**, 476-479.
299 Harris, G.M., Dodelzon, K., Gong, L., Gonzalez-Alegre, P. and Paulson, H.L. Splice isoforms of the polyglutamine disease protein ataxin-3 exhibit similar enzymatic yet different aggregation properties. *PLoS One*, **5**, e13695.
300 Rodrigues, A.J. (2008) C. elegans ataxin-3: function, loss of funcion and molecular partners. *Doctoral Thesis. University of Minho.*
301 Evert, B.O., Araujo, J., Vieira-Saecker, A.M., de Vos, R.A., Harendza, S., Klockgether, T. and Wullner, U. (2006) Ataxin-3 represses transcription via chromatin binding, interaction with histone deacetylase 3, and histone deacetylation. *J Neurosci*, **26**, 11474-11486.
302 Zhong, X. and Pittman, R.N. (2006) Ataxin-3 binds VCP/p97 and regulates retrotranslocation of ERAD substrates. *Hum Mol Genet*, **15**, 2409-2420.
303 Mazzucchelli, S., De Palma, A., Riva, M., D'Urzo, A., Pozzi, C., Pastori, V., Comelli, F., Fusi, P., Vanoni, M., Tortora, P. *et al.* (2009) Proteomic and biochemical analyses unveil tight interaction of ataxin-3 with tubulin. *Int J Biochem Cell Biol*, **41**, 2485-2492.
304 do Carmo Costa, M., Bajanca, F., Rodrigues, A.J., Tome, R.J., Corthals, G., Macedo-Ribeiro, S., Paulson, H.L., Logarinho, E. and Maciel, P. Ataxin-3 plays a role in mouse myogenic differentiation through regulation of integrin subunit levels. *PLoS One*, **5**, e11728.
305 Boeddrich, A., Gaumer, S., Haacke, A., Tzvetkov, N., Albrecht, M., Evert, B.O., Muller, E.C., Lurz, R., Breuer, P., Schugardt, N. *et al.* (2006) An arginine/lysine-rich motif is crucial for VCP/p97-mediated modulation of ataxin-3 fibrillogenesis. *EMBO J*, **25**, 1547-1558.
306 Jana, N.R., Dikshit, P., Goswami, A., Kotliarova, S., Murata, S., Tanaka, K. and Nukina, N. (2005) Co-chaperone CHIP associates with expanded polyglutamine protein and promotes their degradation by proteasomes. *J Biol Chem*, **280**, 11635-11640.
307 Ferro, A., Carvalho, A.L., Teixeira-Castro, A., Almeida, C., Tome, R.J., Cortes, L., Rodrigues, A.J., Logarinho, E., Sequeiros, J., Macedo-Ribeiro, S. *et al.* (2007) NEDD8: a new ataxin-3 interactor. *Biochim Biophys Acta*, **1773**, 1619-1627.
308 Tsai, Y.C., Fishman, P.S., Thakor, N.V. and Oyler, G.A. (2003) Parkin facilitates the elimination of expanded polyglutamine proteins and leads to preservation of proteasome function. *J Biol Chem*, **278**, 22044-22055.
309 Matsumoto, M., Yada, M., Hatakeyama, S., Ishimoto, H., Tanimura, T., Tsuji, S., Kakizuka, A., Kitagawa, M. and Nakayama, K.I. (2004) Molecular clearance of ataxin-3 is regulated by a mammalian E4. *EMBO J*, **23**, 659-669.
310 Mao, Y., Senic-Matuglia, F., Di Fiore, P.P., Polo, S., Hodsdon, M.E. and De Camilli, P. (2005) Deubiquitinating function of ataxin-3: insights from the solution structure of the Josephin domain. *Proc Natl Acad Sci U S A*, **102**, 12700-12705.
311 Nijman, S.M., Luna-Vargas, M.P., Velds, A., Brummelkamp, T.R., Dirac, A.M., Sixma, T.K. and Bernards, R. (2005) A genomic and functional inventory of deubiquitinating enzymes. *Cell*, **123**, 773-786.
312 Lam, Y.A., Xu, W., DeMartino, G.N. and Cohen, R.E. (1997) Editing of ubiquitin conjugates by an isopeptidase in the 26S proteasome. *Nature*, **385**, 737-740.
313 Durcan, T.M., Kontogiannea, M., Thorarinsdottir, T., Fallon, L., Williams, A.J., Djarmati, A., Fantaneanu, T., Paulson, H.L. and Fon, E.A. The Machado-Joseph disease-associated mutant form of ataxin-3 regulates parkin ubiquitination and stability. *Hum Mol Genet*, **20**, 141-154.
314 Durcan, T.M. and Fon, E.A. Mutant ataxin-3 promotes the autophagic degradation of parkin. *Autophagy*, **7**, 233-234.
315 Haacke, A., Broadley, S.A., Boteva, R., Tzvetkov, N., Hartl, F.U. and Breuer, P. (2006) Proteolytic cleavage of polyglutamine-expanded ataxin-3 is critical for aggregation and sequestration of non-expanded ataxin-3. *Hum Mol Genet*, **15**, 555-568.

316 Yoshizawa, T., Yamagishi, Y., Koseki, N., Goto, J., Yoshida, H., Shibasaki, F., Shoji, S. and Kanazawa, I. (2000) Cell cycle arrest enhances the in vitro cellular toxicity of the truncated Machado-Joseph disease gene product with an expanded polyglutamine stretch. *Hum Mol Genet*, **9**, 69-78.
317 Bilen, J., Liu, N., Burnett, B.G., Pittman, R.N. and Bonini, N.M. (2006) MicroRNA pathways modulate polyglutamine-induced neurodegeneration. *Mol Cell*, **24**, 157-163.
318 Chou, A.H., Yeh, T.H., Ouyang, P., Chen, Y.L., Chen, S.Y. and Wang, H.L. (2008) Polyglutamine-expanded ataxin-3 causes cerebellar dysfunction of SCA3 transgenic mice by inducing transcriptional dysregulation. *Neurobiol Dis*, **31**, 89-101.
319 Boy, J., Schmidt, T., Schumann, U., Grasshoff, U., Unser, S., Holzmann, C., Schmitt, I., Karl, T., Laccone, F., Wolburg, H. *et al.* A transgenic mouse model of spinocerebellar ataxia type 3 resembling late disease onset and gender-specific instability of CAG repeats. *Neurobiol Dis*, **37**, 284-293.
320 Alves, S., Regulier, E., Nascimento-Ferreira, I., Hassig, R., Dufour, N., Koeppen, A., Carvalho, A.L., Simoes, S., de Lima, M.C., Brouillet, E. *et al.* (2008) Striatal and nigral pathology in a lentiviral rat model of Machado-Joseph disease. *Hum Mol Genet*, **17**, 2071-2083.
321 Rodrigues, A.J., Neves-Carvalho, A., Ferro, A., Rokka, A., Corthals, G., Logarinho, E. and Maciel, P. (2009) ATX-3, CDC-48 and UBXN-5: a new trimolecular complex in Caenorhabditis elegans. *Biochem Biophys Res Commun*, **386**, 575-581.
322 Bargmann, C.I. and Kaplan, J.M. (1998) Signal transduction in the Caenorhabditis elegans nervous system. *Annu Rev Neurosci*, **21**, 279-308.
323 Hart, A.C. (2006) Behavior. *WormBook, ed. The C. elegans Research Community, WormBook, doi/10.1895/wormbook.1.87.1, http://www.wormbook.org.*, 1-67.
324 Sulston, J.E. (1983) Neuronal cell lineages in the nematode Caenorhabditis elegans. *Cold Spring Harb Symp Quant Biol*, **48 Pt 2**, 443-452.
325 Sulston, J.E., Schierenberg, E., White, J.G. and Thomson, J.N. (1983) The embryonic cell lineage of the nematode Caenorhabditis elegans. *Dev Biol*, **100**, 64-119.
326 Albertson, D.G. and Thomson, J.N. (1976) The pharynx of Caenorhabditis elegans. *Philos Trans R Soc Lond B Biol Sci*, **275**, 299-325.
327 White, J.G., Southgate, E., Thomson, J.N. and Brenner, S. (1976) The structure of the ventral nerve cord of Caenorhabditis elegans. *Philos Trans R Soc Lond B Biol Sci*, **275**, 327-348.
328 Rankin, C.H. (2002) From gene to identified neuron to behaviour in Caenorhabditis elegans. *Nat Rev Genet*, **3**, 622-630.
329 Hedgecock, E.M., Sulston, J.E. and Thomson, J.N. (1983) Mutations affecting programmed cell deaths in the nematode Caenorhabditis elegans. *Science*, **220**, 1277-1279.
330 (1998) Genome sequence of the nematode C. elegans: a platform for investigating biology. *Science*, **282**, 2012-2018.
331 Morley, J.F. and Morimoto, R.I. (2004) Regulation of longevity in Caenorhabditis elegans by heat shock factor and molecular chaperones. *Mol Biol Cell*, **15**, 657-664.
332 Wang, H., Lim, P.J., Yin, C., Rieckher, M., Vogel, B.E. and Monteiro, M.J. (2006) Suppression of polyglutamine-induced toxicity in cell and animal models of Huntington's disease by ubiquilin. *Hum Mol Genet*, **15**, 1025-1041.
333 Parker, J.A., Connolly, J.B., Wellington, C., Hayden, M., Dausset, J. and Neri, C. (2001) Expanded polyglutamines in Caenorhabditis elegans cause axonal abnormalities and severe dysfunction of PLM mechanosensory neurons without cell death. *Proc Natl Acad Sci U S A*, **98**, 13318-13323.
334 Way, J.C. and Chalfie, M. (1989) The mec-3 gene of Caenorhabditis elegans requires its own product for maintained expression and is expressed in three neuronal cell types. *Genes Dev*, **3**, 1823-1833.
335 Kaplan, J.M. and Horvitz, H.R. (1993) A dual mechanosensory and chemosensory neuron in Caenorhabditis elegans. *Proc Natl Acad Sci U S A*, **90**, 2227-2231.
336 Hart, A.C., Kass, J., Shapiro, J.E. and Kaplan, J.M. (1999) Distinct signaling pathways mediate touch and osmosensory responses in a polymodal sensory neuron. *J Neurosci*, **19**, 1952-1958.

Chapter 2

Neuron-specific proteotoxicity of mutant ataxin-3 in *C. elegans*: rescue by the DAF-16 and HSF-1 pathways

HMG Advance Access published May 23, 2011

Human Molecular Genetics, 2011 **1–14**
doi:10.1093/hmg/ddr203

Neuron-specific proteotoxicity of mutant ataxin-3 in *C. elegans*: rescue by the DAF-16 and HSF-1 pathways

Andreia Teixeira-Castro[1,2], Michael Ailion[3], Ana Jalles[1], Heather R. Brignull[2,†], João L. Vilaça[1,4], Nuno Dias[1,4], Pedro Rodrigues[1], João F. Oliveira[1], Andreia Neves-Carvalho[1], Richard I. Morimoto[2,‡] and Patrícia Maciel[1,*,‡]

[1]Life and Health Sciences Research Institute (ICVS), School of Health Sciences, University of Minho, Campus de Gualtar, 4710-057 Braga, Portugal, [2]Department of Molecular Biosciences, Northwestern University Institute for Neuroscience, Rice Institute for Biomedical Research, Northwestern University, Evanston, IL 60208, [3]Department of Biology, University of Utah, Salt Lake City, UT 84112, USA and [4]DIGARC, Polytechnic Institute of Cávado and Ave, 4750-810 Barcelos, Portugal

Received February 23, 2011; Revised and Accepted May 1, 2011

The risk of developing neurodegenerative diseases increases with age. Although many of the molecular pathways regulating proteotoxic stress and longevity are well characterized, their contribution to disease susceptibility remains unclear. In this study, we describe a new *Caenorhabditis elegans* model of Machado–Joseph disease pathogenesis. Pan-neuronal expression of mutant ATXN3 leads to a polyQ-length dependent, neuron subtype-specific aggregation and neuronal dysfunction. Analysis of different neurons revealed a pattern of dorsal nerve cord and sensory neuron susceptibility to mutant ataxin-3 that was distinct from the aggregation and toxicity profiles of polyQ-alone proteins. This reveals that the sequences flanking the polyQ-stretch in ATXN3 have a dominant influence on cell-intrinsic neuronal factors that modulate polyQ-mediated pathogenesis. Aging influences the ATXN3 phenotypes which can be suppressed by the downregulation of the insulin/insulin growth factor-1-like signaling pathway and activation of heat shock factor-1.

INTRODUCTION

Machado–Joseph disease (MJD) (or spinocerebellar ataxia type 3) is the most common dominantly inherited ataxia worldwide (1,2). This adult-onset neurodegenerative disorder is characterized by ataxia, ophthalmoplegia and pyramidal signs, associated in variable degree with dystonia, spasticity, peripheral neuropathy and amyotrophy (3), but with no cognitive decline. Pathologically, the disorder is associated with the degeneration of the deep nuclei of the cerebellum, pontine and subthalamic nuclei, substantia nigra and spinocerebellar nuclei. Similar to Huntington's disease (HD), spinobulbar muscular atrophy and other ataxias, MJD is caused by a translated unstable CAG trinucleotide-repeat expansion. The resulting polyglutamine (polyQ) expansions render the affected proteins susceptible to abnormal conformations that promote the formation of neuronal inclusions (4–6). Despite this unifying feature, specific populations of neurons are affected in different polyQ disorders, suggesting that protein domains outside the polyQ tract contribute to the pathological signature of each disease. In MJD, it is known that this neuron-specific susceptibility is not the result of the mutant ataxin-3 (ATXN3) expression pattern, as this protein, like all the other polyQ-containing proteins, is widely expressed from very early stages of development (7,8). ATXN3 is a small protein that contains a cysteine protease-like domain, the Josephin domain and two or three ubiquitin-interacting motifs (UIMs). Among the polyQ-containing proteins, ATXN3 is

*To whom correspondence should be addressed at: Life and Health Sciences Research Institute (ICVS), School of Health Sciences, University of Minho, Campus de Gualtar, 4710-057 Braga, Portugal. Tel: +351 253604824; Fax: +351 253604820; Email: pmaciel@ecsaude.uminho.pt
†Present address: Department of Biological Structure, University of Washington, Seattle, WA 98915, USA.
‡Research was shared equally among the two laboratories.

unique because it has been implicated in cellular protein degradation pathways, through its deubiquitylase (9–12) and deneddylase (13) activities.

The mean age at onset of MJD is 37 years (14) and correlates significantly with the number of CAG/polyQ repeats, with earlier onset in individuals with larger repeat sizes. However, there is considerable individual variation of age at onset within a given repeat-length range (reviewed in 15, highlighting the role of other genetic and environmental factors. Correlative evidence suggests aging as a major risk factor for the development of many neurodegenerative diseases (16). Typically, individuals that carry neurodegeneration-linked mutations develop the disease during their fifth decade, whereas sporadic cases appear during the seventh decade or later (17). It is still unclear why distinct neurodegenerative diseases occur late in life with overlapping temporal inceptions. One likely possibility is that the aging process interferes with the cellular proteostasis machinery, enabling misfolding, aggregation and initiating neurodegeneration (18,19). Recent studies point to the insulin/insulin growth factor (IGF)-1-like signaling (IIS) pathway, facilitated by heat shock factor-1 (HSF-1), as major candidates that link aging, proteotoxicity and neurodegenerative diseases (20–22).

MJD pathogenesis has been recapitulated *in vivo* in a variety of invertebrate and rodent model systems (23–29). *Caenorhabditis elegans* has been successfully used to model neurodegeneration *in vivo*, mainly due to the conservation of basic cellular mechanisms, such as those coupled with neuronal signaling, cell death/survival and the maintenance of proteostasis and aging. The morphology of all 302 neurons has been defined by electron microscopy, and much is known about their synaptic connectivity and functional properties (30,31). Despite having relatively few neurons, *C. elegans* exhibit complex behaviors that can be assayed to monitor neuronal dysfunction, which can be combined with biophysical assays to examine protein solubility in neurons of interest (32). Previous studies using *C. elegans* to investigate polyQ pathology, in subsets of neurons or in body-wall muscle cells, have found a polyQ length-dependent aggregation and toxicity (33–36). Recent studies have introduced the possibility of studying the impact of the expression of a single species of a misfolded polyQ protein on the *C. elegans* nervous system and its toxic behavioral outcome. These studies have shown neuronal subtype-specific vulnerability to the expression of polyQ segments at the threshold Q-length for aggregation and neuronal dysfunction (32).

Here, we have established a new *C. elegans* model of MJD in which ataxin-3 was expressed throughout the nervous system. The comparison of these ATXN3 models with the previously characterized polyQ-alone models (32) should also shed light on the modulatory effects of protein context in pathogenesis. In our model, the expression of both full-length and truncated forms of ataxin-3, with different Q-lengths, results in a consistent pattern of neuronal cell-type-specific aggregation, with the ventral and dorsal nerve-cord neurons being highly affected, while some lateral interneuron cell bodies are resistant. Certain sensory processes in the head contain aggregated foci, but only when the polyQ stretch is within the ATXN3 protein-flanking sequences, and not when expressed alone. We have also studied the impact of aging and of reprogramming animals' survival in our model, and we found that reducing IIS and activating HSF-1 pathways (genetically or pharmacologically) reduced pathogenesis, supporting the mechanistic links between the aging process and neuronal toxic-protein aggregation, which are common hallmarks of many neurodegenerative disorders.

RESULTS

Expression of full-length ataxin-3 in live neuronal cells causes polyQ length-dependent aggregation

The pathogenesis of ATXN3 was studied in transgenic *C. elegans* strains expressing human wild-type (WT) or pathological full-length ATXN3 throughout the nervous system. Normal-length (q14) and mutant (q75 and q130) ATXN3 were tagged at the C-terminus with YFP and expressed in neuronal cells under the control of the promoter of the *F25B3.3* gene (Supplementary Material, Fig. S1A). This gene encodes a *C. elegans* ortholog of the Ca^{2+}-regulated Ras nucleotide exchange factor, RasGRP, that is expressed widely throughout the nervous system. The *F25B3.3* gene promoter ($P_{F25B3.3}$) becomes active in the comma stage of embryogenesis and expression persists after the terminal division of neurons (37). Expression of YFP-alone (Q0) and Q(*n*)::YFP (Q*n*, $n =$ number of glutamines) under the control of the *F25B3.3* promoter occurs throughout the nervous system (32), demonstrating that $P_{F25B3.3}$ is an appropriate tool to evaluate the response of different neurons to pathological ATXN3.

We verified that the levels of WT or mutant ATXN3 mRNA and protein expressed in transgenic lines were equivalent and at the expected molecular size (Supplementary Material, Fig. S2A and B). Only transgenic lines expressing levels of ATXN3 mutant proteins similar to or lower than the WT ATXN3 were selected for further study, as higher expression levels could influence aggregation and toxicity (Supplementary Material, Fig. S2A).

Analysis of the transgenic animals expressing ATXN3 proteins revealed that pan-neuronal expression of WT AT3q14 resulted in diffuse neuronal distribution (Fig. 1, panel 1), similar to that observed for Q0 animals (32). Uniform diffuse expression of AT3q14 was detected in the nucleus and the cytoplasm of neuronal cell bodies and processes along the entire length of the ventral nerve cord (VNC) (Fig. 1, panel 1, thin arrow) and the dorsal nerve cord (DNC) (Fig. 1, panel 1, thick arrow). Likewise, animals expressing AT3q75 also showed diffuse YFP fluorescence, similar to WT AT3q14 animals in the cell bodies and processes throughout the nervous system (Fig. 1, panel 2). However, AT3q130 animals show heterogeneity with discrete foci detected in some neurons and diffuse protein in other neurons. Foci formation was clearly evident in both the nucleus and the cytoplasm of cell bodies and in neuronal processes of VNC (Fig. 1, panel 3, thin arrow and Supplementary Material, Fig. S3A, C and D, respectively), DNC (Fig. 1, panel 3, thick arrow), commissures (Supplementary Material, Fig. S3B) and certain nerve ring cells (Fig. 1, panel 3, arrow head). AT3q130 foci were observed in the first larval stage

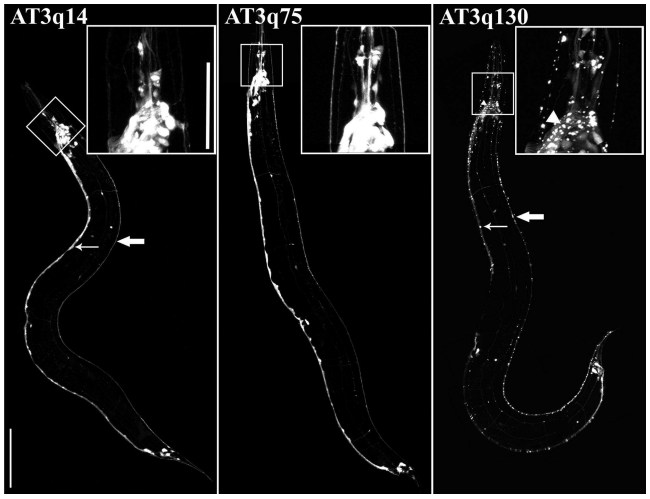

Figure 1. Pan-neuronal expression of full-length ATXN3 in *C. elegans* causes polyQ length-dependent changes in protein distribution. Expression of AT3q14 and AT3q75 proteins displayed a smooth and diffuse distribution pattern (left and middle panels, respectively), whereas AT3q130 proteins are found in discrete foci in certain neurons and are soluble in others (right panel). In the left panel, AT3q14 protein expression could be visualized in cell bodies (thin arrow) and in neuronal processes (thick arrow). In panel 3, the distribution of AT3q130 proteins was strikingly different: foci formation was clearly evident in VNC (thin arrow), DNC (thick arrow) and in certain cells of the circumpharyngeal nerve ring (arrow head). All animals depicted are young adults (4 days post-hatching). Scale bar, 100 μm. White boxes indicate magnified regions. The images were obtained using a Zeiss LSM 510 confocal microscope.

(L1) (Supplementary Material, Fig. S4A) and persisted throughout the lifespan.

We further characterized the AT3q130 foci by dynamic imaging and fluorescence recovery after photobleaching (FRAP) techniques to distinguish between foci of soluble or aggregated protein. As shown in Figure 2, the recovery rate after photobleaching observed for WT ATXN3 (AT3q14) and AT3q75 proteins in neurons was indistinguishable from the soluble Q0 control. In contrast, the AT3q130 foci exhibited only partial recovery (30% recovery over 150 s) [AT3q130 (A)], consistent with the properties of an immobile aggregated species and similar to that observed for the well-characterized Q67::YFP (Q67) aggregates (Fig. 2A and B) (32). We therefore employed the FRAP analysis to examine the foci in discrete neurons located in the head and tail of the animals, as well as in the VNC (adjoining the vulva) and DNC (opposing the vulva). The diffuse AT3q130 expressed in certain VNC, DNC and lateral neurons by comparison showed rapid FRAP recovery indicating that proteins in these neurons [AT3q130(S)] were soluble. Consistent with this, all soluble proteins analyzed by FRAP showed significant recovery rates at the first time point measured (2.27 s) (Fig. 2).

Phenotypic characterization of ATXN3-expressing animals showed that AT3q14 or AT3q75 animals were similar to WT N2 animals for lifespan and movement, whereas AT3q130 animals were lethargic and had slightly reduced lifespan (Supplementary Material, Fig. S5). Nevertheless, AT3q130 animals developed to adulthood and had similar brood sizes (data not shown).

Expression of a C-terminal cleavage fragment of ataxin-3 forms polyQ length-dependent aggregates in *C. elegans* neurons

A common feature of many proteins associated with neurodegenerative disease is proteolytic fragmentation. Likewise, there is evidence to support the proteolysis of ATXN3 in mammalian cells, transgenic mice and MJD brain tissue (25,38–40). To gain additional insight into the biochemical and cell biological properties of truncated ATXN3, we expressed a C-terminal fragment of ATXN3 lacking the amino terminal 257 amino acids of the protein (257cAT3) and retaining the polyQ expansion (q14, q75, q80 and q128) and the UIM3 domain of ATXN3 (Supplementary Material, Fig. S1B) (41). For each of these lines, the neuronal expression of 257cAT3 was at the expected molecular size for mRNA and protein, and at comparable or lower levels than WT controls, indicating that this C-terminal ATXN3 fragment is stably expressed (Supplementary Material, Fig. S2A and B).

In young adult animals (day 4, post-hatching), expression of 257cAT3q14 resulted in a diffuse neuronal pattern, as observed for full-length AT3q14 and YFP-alone expressing animals. However, animals expressing 128 polyQs (257cAT3q128) formed discrete foci throughout different cells of the nervous system (Fig. 3A). These animals were smaller in size and more lethargic than AT3q130 expressing animals and WT controls, yet they developed to the adult stage and had progeny, delayed by 1 day when compared with 257cAT3q14 animals. We then examined transgenic lines expressing intermediate polyQ lengths of 257cAT3q75 and 257cAT3q80 and observed the appearance of some neurons with discrete puncta, whereas in other cells only diffuse protein was detected (Fig. 3A). Protein aggregates were detected in day 2 animals (Supplementary Material, Fig. S4B). The appearance of foci in 257cAT3q75, but not in full-length AT3q75, reveals that the C-terminal truncated protein is more aggregation-prone. Animals expressing 257cAT3q75/80 also exhibited similar rates of development to adulthood as animals expressing full-length AT3q14/75 and WT truncated ATXN3 (257cAT3q14) (data not shown).

The biophysical properties of 257cAT3q75 were compared with 257cAT3q14 using FRAP analysis and showed that 257cAT3q14 exhibited rapid recovery after photobleaching (Fig. 3B), whereas foci in 257cAT3q75 neurons did not recover [Fig. 3B, 257cAT3q75(A)]. We observed heterogeneity among 257cAT3q75 expressing neurons; FRAP analysis of multiple VNC neurons showed differences in 257cAT3q75 protein solubility, ranging from completely soluble [Fig. 3B, 257cAT3q75(S)] to completely insoluble [Fig. 3B, 257cAT3q75(A)]. Molecular heterogeneity was also observed in neurons of the head and tail ganglia of the same animals and from independent transgenic lines (data not shown). By comparison, 257cAT3q128 foci formed immobile aggregates in all neurons tested (Fig. 3B). These results demonstrate that the presence of soluble or aggregated C-terminal ATXN3 protein can vary among different neurons and that this aggregation phenotype is strongly influenced by polyQ length.

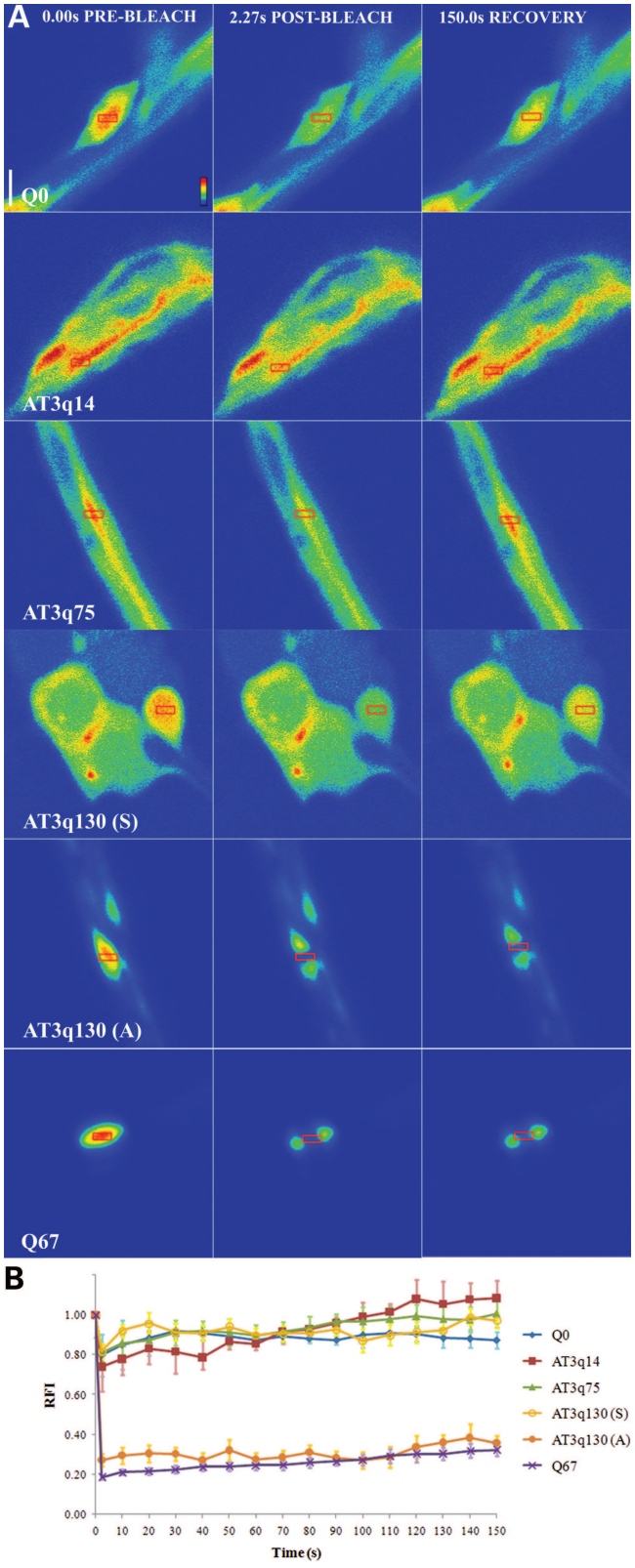

Figure 2. Expression of full-length ATXN3 in live neuronal cells causes polyQ length-dependent aggregation. For FRAP of neurons expressing Q0 proteins, the RFI of the photobleached area (red box), recovers rapidly (**A** and **B** 'Q0'). Similar results were obtained in neurons expressing WT AT3q14 and AT3q75 (A and B 'AT3q14' and 'AT3q75'), indicating the presence of soluble proteins, whereas bleached Q67 foci did not recover (A and B 'Q67'). Q67 proteins are insoluble and were used as an aggregated experimental control. FRAP experiments on AT3q130 animals revealed that some areas display fast FRAP [A and B 'AT3q130 (S)'], whereas others, containing protein foci, did not recover, indicating the presence of a highly immobile aggregated protein [A and B 'AT3q130 (A)']. Quantification (B) was performed in six or more experiments and is represented as the mean ± SEM. Scale bar, 5 μm. The images and FRAP measures were obtained using a Zeiss LSM 510 confocal microscope.

In summary, the aggregation profiles in *C. elegans* neurons for the C-terminal ATXN3 proteins were similar to that observed for the full-length ATXN3 model. The transition from soluble to aggregate states was observed only with the mutant polyQ expansion and exhibited neuron-to-neuron variation. Sequence context also has a role because the expression of 75Qs caused aggregation only in the context of C-terminal ataxin-3 and not of the full-length ATXN3 protein.

Aggregation of mutant ataxin-3 in specific neuronal cells is not stochastic

Previous studies on aggregation of Q40-alone proteins in the nervous system of *C. elegans* showed that aggregation is cell-type-specific and not stochastic, suggesting that polyQ solubility is modulated by the intrinsic properties of the neuronal cell environment (32).

We examined the properties of AT3q130 and 257cAT3q75 in specific neurons of at least two independent transgenic lines. Using the FRAP analysis, both mutant ATXN3 proteins were detected only in a soluble state in HSN neurons (Fig. 4A), whereas in the VNC and DNC neurons both soluble and immobile AT3q130 and 257cAT3q75 were detected (Figs 2 and 3B). Protein aggregates were also detected in certain neuronal processes in the head (Fig. 4B, square), but this occurred only in animals expressing mutant ATXN3-flanking sequences, and not in animals expressing polyQ-alone tracts (32). Many of these processes correspond to sensory neurons. To further examine the expression of mutant ATXN3 in sensory neurons, we co-expressed AT3q130 with mCherry under the regulation of the CHE-13 promoter ($P_{CHE\text{-}13}$::mCherry) that is expressed in nearly all ciliated sensory neurons. Aggregates were not detected in the cell bodies of ASJ, ASI, ADL, ASK, ASE and ASH neurons (data not shown). However, in 88% of the animals analyzed ($N = 50$), CHE-13-positive processes contained aggregated mutant ATXN3 proteins (Fig. 4C). Despite the occasional appearance of aggregates, all six dye-stainable chemosensory amphid neurons in the anterior region (as well as the phasmid tail neurons) exhibited normal DiD staining (data not shown), suggesting that they were functional and not undergoing degeneration.

To confirm that this aggregation pattern was specific rather than stochastic, we co-expressed Q40 (fused to CFP) (32) together with full-length ataxin-3 with polyQ75 (AT3q75) fused to YFP. Whereas AT3q75 does not aggregate in *C. elegans* neuronal cells, co-expression with Q40 resulted in aggregate formation in certain VNC neurons. Analysis of these double-transgenic animals revealed that AT3q75 and Q40 proteins had a synergistic effect in the *C. elegans* nervous

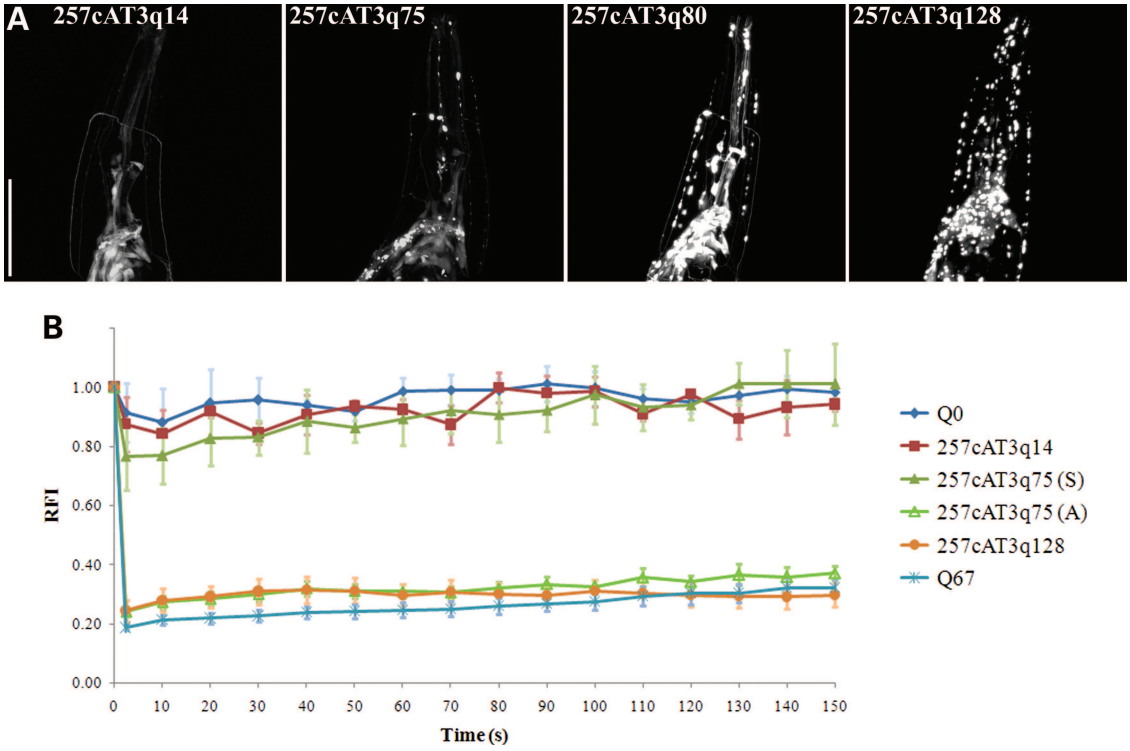

Figure 3. Expression of C-terminal ataxin-3 forms polyQ length-dependent aggregates in *C. elegans* neurons. Flattened z-stacks of *C. elegans* heads revealed that the expression of a range of polyQ lengths within the context of C-terminal ATXN3 flanking regions caused polyQ length-dependent aggregation (**A** and **B**). We observed that 257cAT3q14 proteins displayed a smooth and diffuse distribution pattern, whereas 257cAT3q128 proteins were distributed into discrete foci. The 257cAT3q75 and 257cAT3q80 animals contained protein foci in certain neurons and soluble protein in others (A). Neurons expressing Q0 and 257cAT3q14 proteins recovered rapidly after photobleaching (B, 'Q0' and '257cAT3q14'), indicating the presence of soluble proteins. Bleached Q67 and 257cAT3q128 foci did not recover (B, 'Q67' and '257cAT3q128'). FRAP experiments on 257cAT3q75 animals revealed that some neurons displayed fast FRAP [B, '257cAT3q75 (S)'] whereas others, containing protein foci, did not recover, indicating the presence of insoluble protein (B- '257cAT3q75 (A)'). Quantification (B) was performed in eight or more experiments and is represented as the mean ± SEM. All animals depicted are young adults (4 days post-hatching). Scale bar, 50 μm. The images and FRAP measures were obtained using a Zeiss LSM 510 confocal microscope.

system, as we observed the formation of protein foci in certain processes in the head (Fig. 4D, arrows), but not when either Q40 or AT3q75 proteins were expressed alone, nor when WT AT3q14 and Q40 (Supplementary Material, Fig. S6A) or Q40::CFP and Q40YFP proteins were co-expressed (Supplementary Material, Fig. S6B). Figure 4E shows the quantification of aggregates (42) of the processes of AT3q75;Q40 animals head ($^{*}P < 0.05$). Even in this example of polyQ synergy, aggregates were not detected in the HSN neurons. These data support a neuron-subtype-specific aggregation pattern in our ATXN3 pathogenesis model that reflects the consequences of ataxin-3 protein context and neuronal cell intrinsic factors.

Ataxin-3 aggregation is highly associated with motor dysfunction

To test whether ataxin-3 expression results in neuronal dysfunction, we performed a series of behavioral assays. Innervation of muscle cells requires more than 60 neurons in *C. elegans* and neuronal dysfunction often results in reduced motility due to a lack of coordination (31,43). In addition to the formation of protein aggregates, expression of mutant ATXN3 (AT3q130) resulted in reduced movement compared with age-matched WT ATXN3-expressing animals (Supplementary Material, Video S1). The motility of the ATXN3-expressing animals was quantified by scoring animals that remained within a 1 cm circle after being transferred into the centre of a freshly seeded plate (44). Animals expressing full-length WT AT3q14 and AT3q75 proteins did not exhibit any impairment at adulthood (day 4), whereas AT3q130 animals exhibited a significant reduction in motility ($^{*}P < 0.05$) (Fig. 5). In animals expressing the truncated ATXN3, 257cAT3, the effect on motility was even more severe, and we observed a polyQ length-dependent motor dysfunction that correlated with aggregation (Figs 3 and 5). For comparison, we also assessed animals expressing polyQ-alone, and in accordance with what was observed previously, animals expressing Q40 and Q67 had dramatic deficits in motility (32) (Fig. 5). Because protein aggregates were detected in sensory processes in the head, we tested for effects on chemosensation (45) in animals expressing full-length and truncated ATXN3. AT3q130 animals showed a slight reduction in chemotaxis index (Ci) to isoamyl alcohol (10^{-1} dilution) relative to WT animals (Supplementary Material, Fig. S7), and 257cAT3q75, but not Q40 animals showed a significant decrease in Ci (Supplementary Material, Fig. S7; $^{*}P < 0.05$).

Taken together, these results suggest that the presence of aggregates is associated with neuronal dysfunction in our *C. elegans* model of ATXN3 pathogenesis. Moreover, the

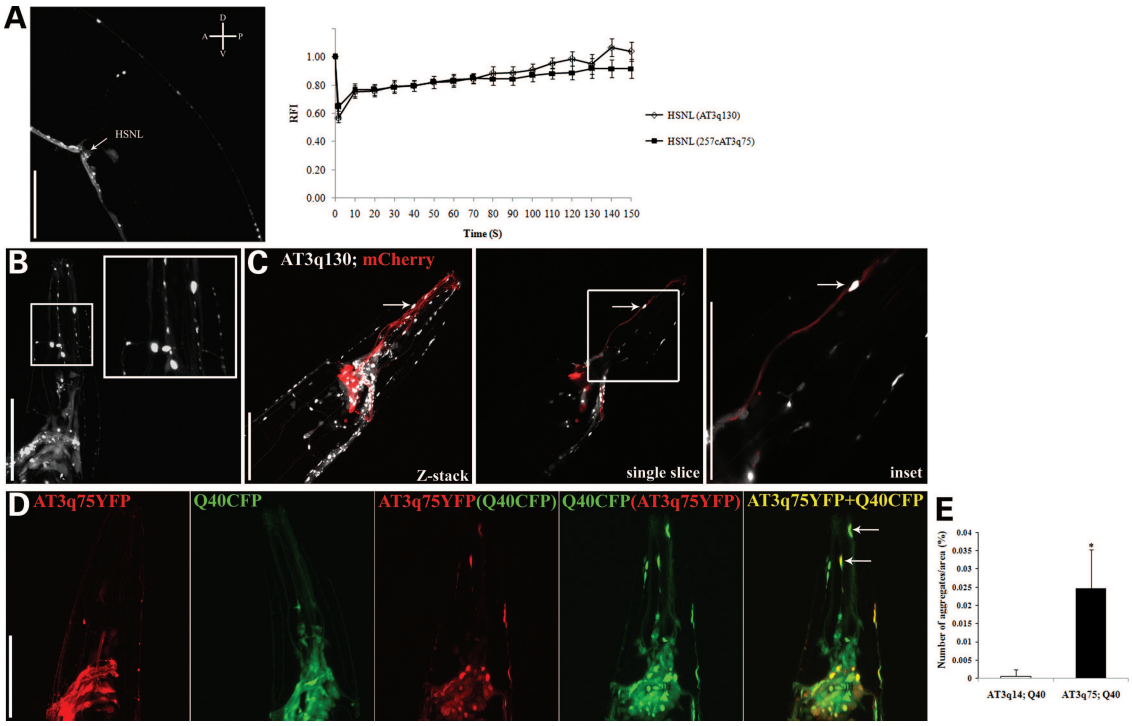

Figure 4. The aggregation pattern of mutant ATXN3 in specific neuronal cells is not stochastic. FRAP analysis of the HSN neuron on the left side (**A**) of AT3q130 and 257cAT3q75 animals revealed that both proteins were consistently soluble (at least 80% FRAP) in the two or three independent lines that were tested for each genotype. Quantification was performed in 10 or more experiments and is represented as the mean ± SEM. (A) Flattened z-series of *C. elegans* heads expressing mutant ataxin-3 proteins showed the presence of aggregates in certain neuronal processes [a 257cAT3q75 day 4 animal is shown as an example in (**B**)]. White box indicates the magnified region. The aggregates co-localized with mCherry proteins that were expressed under the regulation of the CHE-13 promoter (**C**). (C) depicts a z-stack (first panel) and a single slice (second panel), showing one aggregate co-localizing with the sensory neuron process (red) (C, arrows). Flattened z-stacks of day 4 animals co-expressing AT3q75::YFP with Q40::CFP proteins, showing protein aggregates in certain sensory processes of the head (**D**, arrows). The first panel shows the head of one animal expressing AT3q75 proteins; the second panel shows one animal expressing Q40 proteins; third and fourth panels show the expression of AT3q75 or Q40 proteins of a AT3q75; Q40 animal; fifth panel displays a merged image. (**E**) Quantification of the aggregates of the sensory processes of AT3q75;Q40 in comparison with AT3q14;Q40 animals (Supplementary Material, Fig. S6A). In all images, scale bar = 50 μm. The images were obtained using either an Olympus (A and C) or a Zeiss LSM 510 (B and D) confocal microscope. FRAP measurements (A) were performed using the Olympus FV100 confocal.

expression of full-length AT3q130, C-terminal 257cAT3q80 and Q40 proteins caused the same level of toxicity (Fig. 5, dashed line) highlighting the modulatory effects of flanking protein regions in polyQ-containing proteins on motor dysfunction.

Age-dependent changes in mutant ataxin-3 aggregation dynamics

The risk of developing a neurodegenerative disease increases with age. Previous work has shown that polyQ aggregation progresses in an age-dependent manner in muscle cells (36) and in specific neurons (23,33). Therefore, we analyzed the aggregation profile of ATXN3 transgenic animals during aging. In AT3q130 animals, aggregation (initially detected at day 1 post-hatching; Supplementary Material, Fig. S4) was observed to increase during aging. This was particularly clear in the anterior and ventral ganglia neurons in the nerve ring (Fig. 6A). Heterogeneity in protein solubility and aggregation persisted in the nerve cords during aging (data not shown). Of the C-terminal fragments, 257cAT3q75- and 257cAT3q80-expressing animals showed age-dependent aggregation (Fig. 6B). For both the full-length and C-terminal ATXN3 proteins, aggregates were not detected in HSN neurons of old animals. In comparison, AT3q75 did not form aggregates during aging; however in some animals, we observed large foci in day 10 of adulthood that corresponded to a soluble protein (Fig. 6A, arrows) by FRAP analysis (data not shown). Likewise, animals expressing WT (full-length and truncated) ATXN3 did not form aggregates during their lifespan. These results reveal that aging contributes to the onset and progression of ATXN3 polyQ aggregation, as has been reported for other model systems and humans. However, our ability to monitor the aggregation phenotypes across multiple subclasses of neurons reveals differential susceptibility, with certain neurons such as the HSN more resistant to aggregation compared with the VNC and DNC neurons that are more sensitive to aggregation during aging.

IIS and HSF-1 pathways modify mutant ataxin-3-mediated pathogenesis in *C. elegans*

Aggregation and toxicity of polyQ are strongly affected by the IIS pathway and the activities of transcription factors DAF-16 and HSF-1 (21,36). To test whether ataxin-3 proteotoxicity is influenced by these pathways, we examined the effects of

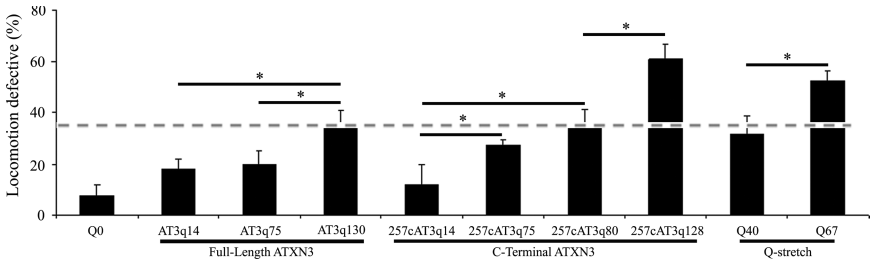

Figure 5. Increases in polyQ-length associated with neuronal dysfunction in ataxin-3 *C. elegans* model. Percentage of locomotion defective of age-synchronized young adult animals (day 4, post-hatching). There was a polyQ length-dependent increase in motor dysfunction in both full-length and C-terminal ATXN3-expressing animals. Q(n) lines were used as an experimental control. ATXN3 protein-flanking sequences modulate the animals' motor phenotype. Dashed line shows that the expression of AT3q130, 257cAT3q80 and Q40 proteins in all neurons caused similar percentages of defect in locomotion. Data are the mean ± SD, at least 150 animals per data point. Student's *t*-test, $^{*}P < 0.05$.

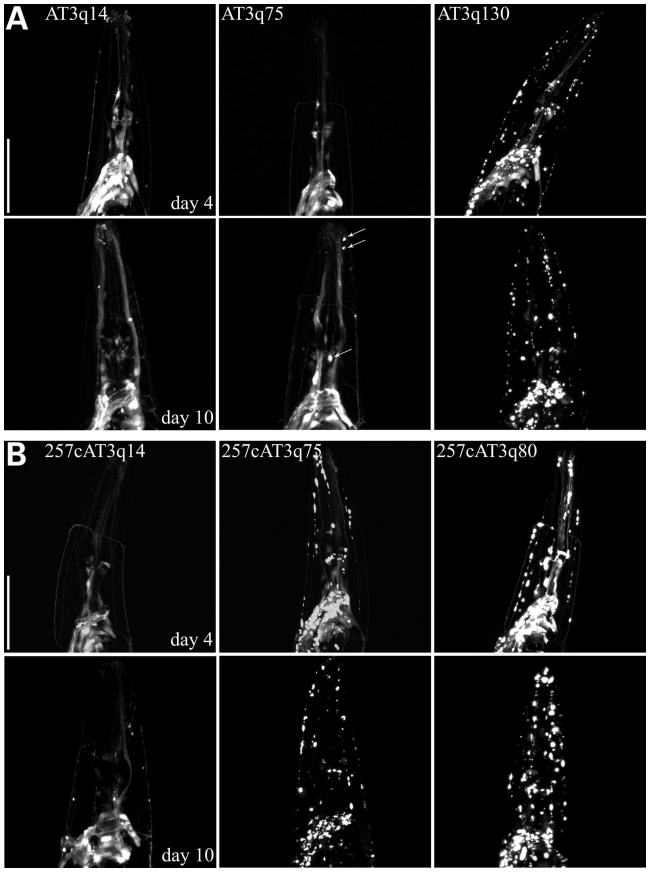

Figure 6. Influence of age on mutant ATXN3 aggregation dynamics. Flattened z-stacks of *C. elegans* heads of days 4 and 10 animals (post-hatching). The aggregation phenotype of AT3q130 (**A**) and 257cAT3q75/80 (**B**) animals was aggravated with age. The increase in aggregation was particularly evident in the circumpharyngeal nerve ring of the animals. Arrows in the AT3q75 panel indicate protein foci that did not correspond to aggregates, as assessed by FRAP (data not shown). Scale bar, 50 μm. All pictures were obtained using a Zeiss LSM 510 confocal microscope.

mutations in the insulin/IGF-1 receptor DAF-2 (46) on the properties of AT3q130. In the background of the *daf-2(e1370)* mutation, which confers a long-lived phenotype, animals expressing AT3q130 (*daf-2*; AT3q130) showed a tendency for decreased aggregation (Fig. 7A, squares, and F) with foci barely detected. Likewise, motor function improved 2-fold (from 46.8 to 25.6%) in *daf-2*; AT3q130 animals (Fig. 7G). Similar results were obtained with a loss-of-function allele (*hx546*) in *age-1* (47) that restored the motility of AT3q130 animals from 40% reduction to 14.7% (Fig. 7G). These results support the role of DAF-16 (48,49) in protection against proteotoxicity. Consistent with this, the *daf-16* null (*mu86*) allele had a major effect on motor dysfunction in *C. elegans daf-16*; AT3q130 animals (from 40.1 to 74.4%) (Fig. 7H). We further demonstrated a protective role for DAF-16 with valproic acid (VA) that stimulates the translocation of DAF-16 into the nucleus (50). VA partially rescued the motor dysfunction induced by AT3q130 expression, at day 10 of adulthood (a reduction in motility impairment from 71.8 to 37.9%), an effect that was suppressed in *daf-16(mu86)* mutants, suggesting that the mode of action for the rescue of mutant-ATXN3 toxicity was in part through the IIS pathway (Fig. 8A). Moreover, day 10 AT3q130 VA-treated animals showed the same locomotion defect as day 4 untreated animals. In contrast to the significant phenotype effect, and as for *daf-16(mu86)* mutation (Fig. 7D and F), VA treatment had only a mild effect on AT3q130 protein aggregation (Fig. 8B), which was not due to changes in AT3q130 protein levels (Supplementary Material, Fig. S8). In all cases, the effects of mutations in *DAF-2*, *AGE-1* and *DAF-16* genes in ATXN3 pathogenesis were not due to effects on AT3q130 expression (Supplementary Material, Fig. S9).

Recent studies have also implicated HSF-1 in lifespan extension caused by reduced DAF-2 activity, with cross-talk between the DAF-2 and HSF-1 pathways (20,21). Therefore, we tested the effect of the *hsf-1(sy441)* (51) mutation on ATXN3 pathogenesis. The loss of *hsf-1* was deleterious to transgenic animals, with mutant ataxin-3 proteins becoming fully aggregated in neuronal cells and detected in early embryos (Fig. 7E, arrow). Moreover, *hsf-1*; AT3q130 animals were completely paralyzed at day 4 (Fig. 7H). Consistent with these results, exposure of AT3q130 animals to the small-molecule Hsp90 inhibitor, 17-(dimethylaminoethylamino)-17-demethoxygeldanamycin (17-DMAG), that induces the heat shock response (HSR), improved motility when compared with untreated controls (Fig. 8C). The effect of 17-DMAG was dependent on *hsf-1* (Fig. 8C). Treatment with 17-DMAG also reduced the aggregation of AT3q130 animals (Fig. 8D), with no effect on ATXN3 steady-state

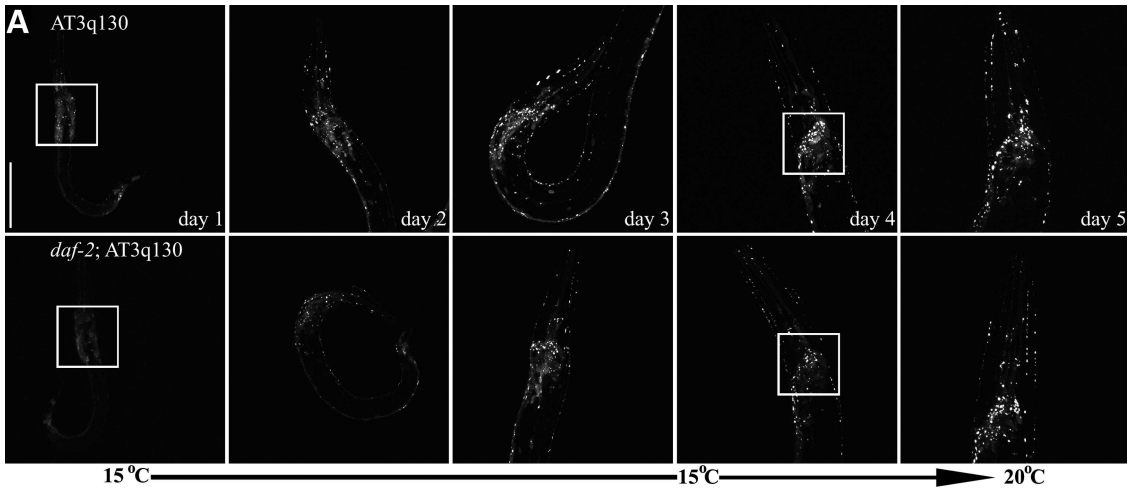
A
AT3q130
day 1
day 2
day 3
day 4
day 5
daf-2; AT3q130
15 °C
15°C
20°C

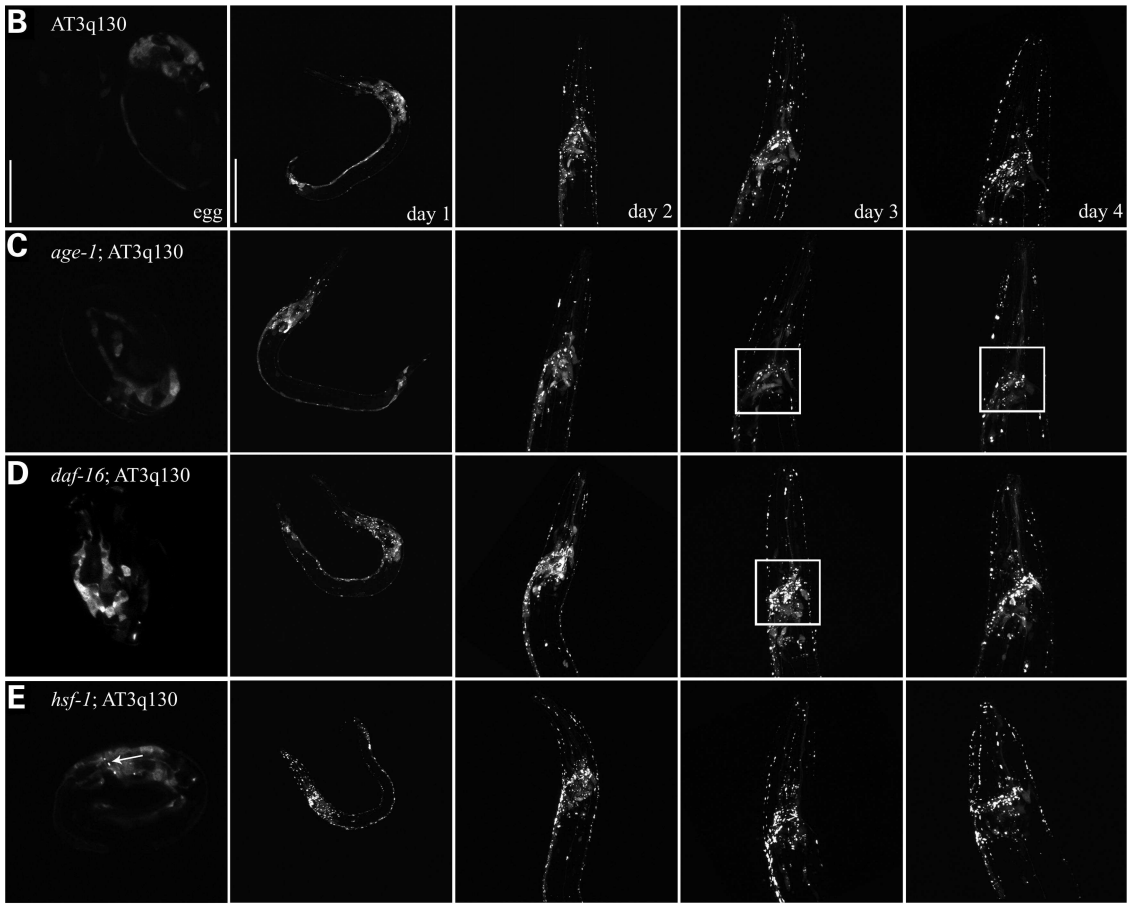
B
AT3q130
egg
day 1
day 2
day 3
day 4
C
age-1; AT3q130
D
daf-16; AT3q130
E
hsf-1; AT3q130

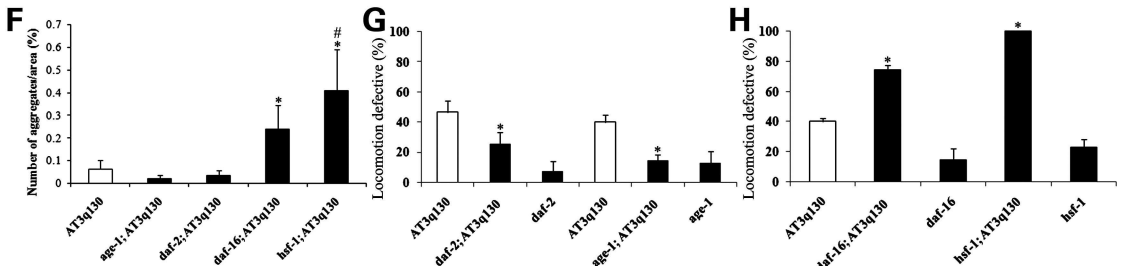
F
Number of aggregates/area (%)
AT3q130
age-1;AT3q130
daf-2;AT3q130
daf-16;AT3q130
hsf-1;AT3q130
G
Locomotion defective (%)
AT3q130
daf-2;AT3q130
daf-2
AT3q130
age-1;AT3q130
age-1
H
Locomotion defective (%)
AT3q130
daf-16;AT3q130
daf-16
hsf-1;AT3q130
hsf-1

protein levels (Supplementary Material, Fig. S8). 17-DMAG treatment still decreased the locomotion impairment of AT3q130 animals in the absence of DAF-16 (Supplemental Material, Fig. S10).

Interestingly, at early disease stages, mutation in *hsf-1* caused a more severe effect on AT3q130 aggregation, when compared with *daf-16*. Quantification of the aggregates (42) at day 1 revealed that the absence of HSF-1 significantly increased the percentage number of aggregates per total area when compared with *daf-16*; AT3q130 and AT3q130 animals ($^{\#}P < 0.05$, Fig. 7F). Moreover, quantification of the aggregates in specific areas of the nervous system revealed that total body aggregation correlates with aggregation in the animals head (nerve ring and head processes) and in the VNC (Supplemental Material, Fig. S11). Both total body aggregation (Fig. 7F) and neuron-specific aggregation (Supplemental Material, Fig. S12) are modified by IIS and HSF-1.

Taken together, these results demonstrate that ATXN3 proteotoxicity is strongly modulated by aging-related cellular changes, associated with the IIS pathway and the HSR.

DISCUSSION

We describe a new model system for human ATXN3 proteotoxicity in *C. elegans* neuronal cells, in which the use of tissue-specific promoters and the ability to monitor the fluorescence of reporter proteins in different neurons of live animals (by microscopy and dynamic imaging analysis) provides an effective means to continuously evaluate mutant ATXN3 aggregation and pathogenesis. We have taken advantage of the single-cell resolution of the FRAP analysis to scrutinize the solubility of ATXN3 in specific neuronal subtypes. In *C. elegans*, ATXN3-flanking sequences greatly modulate polyQ-mediated aggregation and neuronal dysfunction. The neuronal cell-type-specific susceptibility to expression of mutant ATXN3 proteins is not stochastic and differs significantly from that of polyQ-alone. We also show that mutant ATXN3 phenotypes are severely aggravated during aging and demonstrate the protective roles of the DAF-16 and HSF-1 pathways to suppress proteotoxicity.

Caenorhabditis elegans model for ATXN3 aggregation and neuronal dysfunction

In our *C. elegans* model, we observed the polyQ length-dependent aggregation of both full-length and C-terminal versions of mutant ATXN3 proteins expressed in *C. elegans*. Although ataxin-3 cleavage-fragment formation has not been unequivocally shown *in vivo*, many laboratories have proposed that smaller fragments containing the expanded polyQ sequence exhibit enhanced toxicity (25,38,40,41,52). Likewise, we show the importance of sequence context in that expression of 75 Qs leads to the formation of protein aggregates in the *C. elegans* nervous system within C-terminal ATXN3 flanking regions, but not in the full-length protein. This is likely due to the increased exposure of the polyQ tract in the truncated version of the protein, which eventually facilitates (i) misfolding and (ii) abnormal toxic interactions in the cellular environment of the affected neurons. There are several lines of evidence that support this hypothesis, namely that Q40 has been described as the Q-length threshold for aggregation and toxicity (32). Moreover, the majority of studies using cell lines, *Drosophila* and mouse models of MJD showed stronger phenotypes with truncated polyQ-containing versions of ATXN3 (24,41,53); in some cases, the full-length mutant ATXN3 did not cause pathogenesis (41,53). Regarding potential abnormal toxic interactions in the affected cellular environment, it has been reported that the presence of an expanded polyQ tract facilitates and strengthens the interaction between the C-terminal of ATXN3 and VCP (54), CBP and the transcriptional co-activators p300 and pCAF (55). These abnormal interactions may affect basic cellular maintenance mechanisms such as endoplasmic reticulum-associated protein degradation (56) and transcriptional regulation (55,57).

ATXN3-flanking sequences and cell-intrinsic factors may direct neuronal cell-type-specific susceptibility

Each of the polyQ disorders involves the loss of selected populations of neurons, leading to a characteristic clinical presentation, even though the mutant proteins are ubiquitously expressed (6). As in the human disease, we found that the neuronal cell-type susceptibility to mutant ATXN3 protein aggregation and toxicity in the *C. elegans* nervous system was not stochastic, but was rather neuron-type-specific and observed in multiple animals and transgenic lines.

A key finding here is that the aggregation pattern of ATXN3- and polyQ-expressing animals is quite distinct. Mutant ataxin-3 aggregates in several neuronal processes, including commissures, the DNC and sensory processes. In particular, the processes of certain CHE-13-positive sensory neurons contain protein foci only when the polyQ tract is expressed within ATXN3-flanking sequences and not when expressed alone (32). Although the cell bodies of lateral neurons contained soluble ataxin-3 proteins, even in very old animals, their processes often presented aggregates as

Figure 7. IIS and HSF-1 pathways regulated mutant ataxin-3-mediated proteotoxicity in *C. elegans* neurons. (**A**) Flattened z-series of AT3q130 and *daf-2*; AT3q130 animals that were grown at 15°C for 4 days and transferred to 20°C for 24 h. (**B**–**E**) Animals were grown at 20°C during their lifespan. White squares highlight the area where the decrease in aggregation is most clear. (A, B and **F**) *daf-2(e1370)* and *age-1(hx546)* mutations tend to reduce AT3q130-mediated aggregation. The absence of DAF-16 (D) and HSF-1 (E) increased aggregation of mutant ATXN3 (F). The *daf-16(mu86)* mutation caused a mild aggravation of the aggregation phenotype, visible at day 3 (post-hatching) (D, square). *hsf-1(sy441)* (E) mutation had a great impact on aggregation, with some aggregates visible already in embryos (arrow). Scale bar, 50 μm. All pictures were obtained using an Olympus FV1000 confocal microscope. (F) Quantification of the number of aggregates per area of animal of all strains. Data show the mean ± SD of eight or more animals. Asterisk indicates the significant mean difference between either *hsf-1*; AT3q130 or *daf-16*; AT3q130 and AT3q130 animals; hash symbol indicates the significant difference between *hsf-1*; AT3q130 and *daf-16*; AT3q130 (*ANOVA*, applying *Bonferroni* correction with 95% confidence intervals; $^{*,\#}P < 0.05$). (**G** and **H**) *daf-2* and *age-1* mutations reduced the percentage of motor dysfunction (from 46.8 to 25.6% and 40 to 14.7% reduction, respectively). *daf-16* and *hsf-1* mutations caused an increase in the % of locomotion defective animals (from 40.1 to 74.4% and 40.1 to 100%, respectively). Data are the mean ± SD, at least 102 animals per data point. Student's *t*-test, $^{*}P < 0.05$.

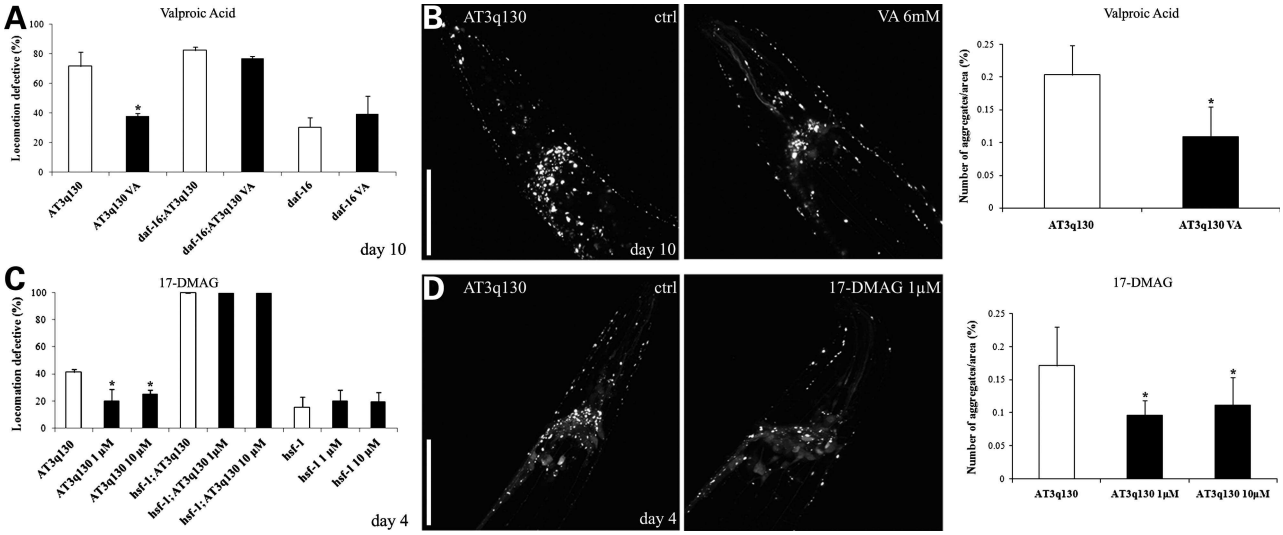

Figure 8. Pharmacological activation of DAF-16 and HSF-1 reduced mutant ataxin-3-mediated pathogenesis. VA-treated AT3q130 animals showed a reduction both in motor dysfunction (71.75% to 37.9% reduction in locomotion defective animals) (**A**) and in the aggregation phenotype at day 10 of adulthood (**B**). Despite the broad actions of VA, the effect on ATXN3 pathogenesis seemed to be highly dependent on DAF-16 (A). Day 4 animals treated with two concentrations of 17-DMAG also improved their motility performance. The effect of 17-DMAG on motor function was dependent on *hsf-1* (**C**). Animals also showed a reduction in aggregation (**D**). Motility data are the mean ± SD, at least 152 animals per data point. Student's *t*-test, $^{*}P < 0.05$. Quantification of number of aggregates per area is the mean ± SD of eight or more animals per group. ANOVA, $^{*}P < 0.05$.

determined by FRAP. By comparison, these processes were unaffected in Q40 animals (32). In agreement with these observations, a recent systematic immunohistochemical analysis of serial thick brain sections of MJD patients revealed the widespread presence of axonal aggregates in fiber tracts known to undergo neurodegeneration (58). This may be related to the protein cellular function since the josephin domain of ATXN3 was found to bind to alpha- and beta-tubulin in human cells and rat brain extracts (59,60) and that ATXN3 knock-down led to cytoskeletal disorganization (59). These results imply that ATXN3-flanking sequences, other than the polyQ stretch, in conjunction with cell-specific factors, may modulate neuronal vulnerability.

Recent studies have suggested that the specific symptoms of a given misfolding disorder, namely amyotrophic lateral sclerosis, may not be due solely to aggregation-mediated toxicity of SOD1 mutations, but also to their genetic interactions with mildly destabilizing missense temperature-sensitive alleles within a variety of cellular pathways (61). Studies in HD have also identified the small G protein Rhes, which is expressed and localized very selectively to the striatum, as an interactor of mutant huntingtin, contributing to cytotoxicity (62). These studies, together with our results, emphasize the importance of understanding the role of protein context in diseases characterized by protein aggregation.

Intriguingly, in both full-length and truncated ATXN3 models, the same neurons were affected, although at different ages or polyQ lengths. The fact that we have observed similar neuropathology in animals expressing the ATXN3 cleavage fragment lends support to the relevance of ataxin-3 fragment formation in MJD pathogenesis. However, additional experiments are required to determine the protein domain(s) of ATXN3 that determine the neuronal specificity of polyQ-mediated pathogenesis.

IIS- and HSF-1-mediated improved proteostasis protect against mutant ataxin-3 pathogenesis

Aging is a prominent determinant of the structural and functional changes that may contribute to the decline in brain function and susceptibility to neurodegenerative disease (63). The age-related IIS and HSF-1 pathway(s) are known to modulate many forms of toxic protein aggregation in *C. elegans* and other model organisms, including the aggregation of Aβ (22,64), α-synuclein (65,66), polyQ and huntingtin (20,36,67), suggesting that these pathways correspond to a common mechanism of detoxification. However, for MJD, the roles of the IIS and HSF-1 pathways had not been previously examined. In this study, we have shown that aging intensifies mutant ATXN3 aggregation and motor dysfunction. Moreover, neuronal toxicity was significantly affected by altering the aging/survival program. Specifically, DAF-16 and HSF-1 were found to be potent suppressors of mutant ataxin-3 aggregation and neuronal dysfunction in *C. elegans*. The absence of HSF-1 accelerated aggregation at early stages of development (embryos), whereas in a *daf-16* mutant, increased aggregation was more pronounced in adult animals. In agreement, VA-treated animals showed reduced aggregation and motor dysfunction later in life (day 10), which was dependent upon DAF-16. Aggregate quantification in day 1 animals further supported this finding, as we also showed that mutant ATXN3 aggregation was greatly enhanced by the *hsf-1* mutation compared with *daf-16*. This supports the proposal that HSF-1 and DAF-16 have different developmental requirements—early embryonic for HSF-1 versus adult for DAF-16—in protection against proteotoxicity as observed previously in a *C. elegans* model for Alzheimer's disease (68). In future studies, we aim to test whether the effects of DAF-16 and HSF-1 loss of function in mutant ATXN3-mediated pathogenesis are due to neuronal effects.

Transcriptomes regulated by DAF-16 and HSF-1 include mRNAs for many chaperones (20,21). In this sense, our results are in agreement with studies showing that, in the brain tissue of MJD patients, Hsp40 and Hsp70 localize to intranuclear aggregates (possibly causing a depletion of these chaperones) and that overexpression of the human DnaJ homolog (Hdj)-1 suppressed ATXN3 aggregation and toxicity in neuronal cell cultures (69). Moreover, knocking out the co-chaperone C-terminus of Hsp70-interacting protein enhanced ataxin-3 aggregation-mediated toxicity (70). Consistent with our results using a genetic approach, pharmacological treatment with 17-DMAG reduced mutant-ATXN3 proteotoxicity in *C. elegans*, probably by activating the disaggregation capacity of HSF-1 at early stages of the disease (22,68).

In conclusion, our study supports a link between lifespan determinants, integrity of protein folding and amelioration of aggregation-associated proteotoxicity in MJD. Our novel *C. elegans* ATXN3 pathogenesis model may constitute a useful tool for high-throughput testing of therapeutic strategies in age-related conformational disorders. Additionally, comparison of our system with the previously established polyQ protein-alone models and with *C. elegans* models for the pathogenesis of the different disease-associated proteins (huntingtin, androgen receptor or ataxin-1) could allow the clarification of both common and protein-specific mechanism(s) of aggregation, neuronal dysfunction and neurodegeneration.

MATERIALS AND METHODS

Plasmid constructs

Pan-neuronal ATXN3 expression was achieved by cloning AT3var1−1 cDNA into the $P_{F25B3.3}$Q0::YFP plasmid (32). F25B3.3::GFP is a post-mitotic pan-neuronal marker; its expression is observed after the terminal division of neurons and not in neuroblasts (37). Full-length ATXN3 cDNA with different polyQ lengths was generated by PCR using oligonucleotides containing restriction sites for *Bam*HI and pBluescriptIISK(+)::MJD1−1q14 or pGEM-7Zf(+)::MJD1−1q75 (kindly provided by Dr Jun Goto) as templates. ATXN3 amplicons were then digested and ligated into the *Bam*HI sites of $P_{F25B3.3}$Q0::YFP, generating $P_{F25B3.3}$AT3v1−1q(n)::YFP. Regarding the cloning of $P_{F25B3.3}$AT3v1−1q(130)::YFP, the first step was to subclone the tract of 130Qs from pPD95.77::Punc119::MJD1−130Q (kindly provided by Dr N. Nukina) into the *Bgl*II and *Eco*0109I restriction sites of pGEM-7Zf(+)::MJD1−1q75 vector. ATXN3 C-terminal YFP-tagged expression constructs were generated by PCR (using full-length constructs as a template) and cloned into the *Bam*HI sites of $P_{F25B3.3}$Q0::YFP, forming $P_{F25B3.3}$257cAT3q(n)::YFP. Sequencing confirmed the ATXN3 sequence (full-length and truncated forms), including the Q-length and YFP sequences, as well as the promoter region.

Nematode strains and general methods

For a list of strains used in this work and name abbreviations, see Supplementary Material, Table S1. Standard methods were used for culturing and observing *C. elegans*, unless otherwise noted (71). Nematodes were grown on NGM plates seeded with *Escherichia coli* OP50 strain at 20°C. All strains carrying the *daf-2* mutation (*e1370* allele) were grown at 15°C until the L4 stage and were then transferred to 20°C for 24 h. For the generation of transgenic neuronal animals, 50 ng/μl of DNA encoding $P_{F25B3.3}$AT3q(n)::YFP and $P_{F25B3.3}$257-cAT3q(n)::YFP was microinjected into the gonads of adult hermaphrodite N2 animals, as previously reported (32). Transgenic F1 progeny were selected on the basis of neuronal fluorescence. At least three independent stable lines for each transgene were isolated and analyzed, with similar results. Transgenic lines were frozen immediately after they were generated, as it has been previously reported that animals kept in continuous culture, particularly those expressing expanded polyQ tracts, eventually adapt to the transgene (72). Integrated lines were generated by gamma irradiation of transgenic animals expressing AT3q(n)::YFP and 257cAT3q(n)::YFP fusion proteins, allowing uniform expression of transgenes. Two or three independent lines were isolated and backcrossed at least five times with N2. P_{CHE-13}::mCherry DNA (PS431, kindly provided by Peter Swoboda, Karolinska Institute) was microinjected into adult hermaphrodite AT3q130 animals at 10 ng/μl. Populations were synchronized either by treating young adult animals with alkaline hypochlorite solution (0.5 M NaOH, ∼2.6% NaClO) for 7 min (73) or by collecting embryos laid by adult animals within a 3 h period. All animals were scored at the same chronological age, unless stated otherwise. During the reproductive period, animals were moved every day to avoid progeny contamination. Experiments were repeated at least three times. All assays were performed blind.

Confocal imaging

All images were captured either on a Zeiss LSM510 META (Oberkochen, Germany) or on an Olympus FV1000 (Japan) confocal microscope, under a 63× water or 60× oil objective, respectively. Animals were immobilized with 2 mM levamisole and mounted on a 3% agarose pad. Z-series imaging was taken of all the *C. elegans* lines generated, using 514/515 nm laser excitation for YFP, 458 nm for CFP and 593 nm for mCherry fusion proteins. The pinhole was adjusted to 1.0 Airy unit of optical slice, and a scan was taken every ∼0.5 μm along the *Z*-axis. Immobilized 4- or 10-day-old animals were subjected to FRAP as previously described (74) with the following modifications: imaging of full-length, C-terminal ATXN3 and ATXN3;Q40 animals was performed at 5% power of a 514 nm laser line with the bleaching power of 100% for 25 iterations. Relative fluorescence intensity (RFI) was determined using the following equation: RFI = (Tt/Ct)/(T0/C0), in which T0 is the total intensity of the region of interest (ROI) prior to photobleaching and Tt is the intensity of the same area at a given time after bleaching. The intensities were normalized against a non-bleached ROI within the same cell (C0, intensity of the control area prior to bleaching and Ct at any time after) as a control for general photobleaching and background fluorescence (74). FRAP analysis was consistently performed in all animals in at least six VNC (adjoining the vulva), DNC (opposing the

vulva) cells, head neurons and tail neurons (cell bodies and/or processes). FRAP of HSN neurons was performed on an Olympus FV1000 confocal microscope (1% power of a 515 nm laser line with bleaching power of 50%, using the Tornado scanning mode).

Quantification of the aggregates

Caenorhabditis elegans fluorescent images were acquired using the Olympus FV1000 confocal microscope. Confocal microscope parameters were set using Hi-Lo pallet, such that protein foci and not diffuse fluorescent areas of the animals nervous system presented pixel intensity higher than 255. The z-stack was collapsed and the aggregate load of each animal (per area unit) was calculated on an image-processing application using MeVisLab as a platform. Details on the application and on the segmentation algorithms were described elsewhere (42). At least eight images were analyzed per genotype and statistical assessment was performed using the Origin software (OriginLab) (ANOVA and Bonferroni mean correction tests for multiple comparisons).

Motility assay

All assays were performed at room temperature (~20°C) using synchronized animals grown at 15°C or 20°C. Five animals (4-, 5- or 10-day-old) were placed simultaneously in the middle of a freshly seeded plate, equilibrated at 20°C. Animals remaining inside a 1 cm circle after 1 min were scored as locomotion-defective. A total of 150 animals were scored in at least three independent assays for each strain, and the statistical significance was assessed by Student's *t*-test, as described previously (44).

VA treatment

VA treatment was performed according to the protocol described by Evason *et al.* (50). VA sodium salt was obtained from Sigma (St Louis, MO, USA). Animals were always grown in 6 mM VA plates at least one generation prior to the beginning of the assay and were kept in the dark. After 10 days (post-hatching), animals were scored for motility defects and alteration in the aggregation profile, using confocal imaging.

17-DMAG treatment

Drug assays were performed in 96-well plates in liquid culture, as previously described (43,75). Each well contained a final volume of 60 μl, including 20–25 animals in egg stage, drug at the appropriate concentration and OP50 bacteria to a final OD of 0.8 in the microtiter plate (Bio-Rad). Animals and bacteria were resuspended in S-medium supplemented with streptomycin, penicillin and nystatin (Sigma). Worms were grown with continuous shaking at 180 rpm at 20°C. Compound preparation: a stock solution of 16.2 mM 17-DMAG (NCS707545, InvivoGen) was prepared in water. On the indicated days, animals were imaged using a confocal microscope (Olympus FV1000) and tested for motility defects.

SUPPLEMENTARY MATERIAL

Supplementary Material is available at *HMG* online.

ACKNOWLEDGEMENTS

We are grateful to members of the Maciel and Morimoto laboratories for sharing reagents, for critical analysis of the data and for their helpful discussions on the manuscript. We thank Jun Goto (The University of Tokyo Hospital), David Pilgrim (University of Alberta), Nobuyuki Nukina (RIKEN Brain Science Institute) and Peter Swoboda (Karolinska Institute) for generously sharing reagents; we thank Thomas O'Halloran and Biological Imaging Facility (Northwestern University) for the use of microscopes. A special thanks to the *Caenorhabditis* Genetics Center (CGC), which is funded by the National Institutes of Health – National Center for Research Resources, for some of the nematode strains.

Conflict of Interest statement. None declared.

FUNDING

This work was supported by grants from Fundação Ciência e Tecnologia (FCT) to P.M. (PTDC/SAU-GMG/64076/2006, PTDC/SAU-GMG/112617/2009, SFRH/BD/27258/2006 to A.T.C., UMINHO/BI/052/2010 to A.J. and SFRH/BD/51059/2010 to A.N.C.), from the National Ataxia Foundation to PM and from the National Institutes of Health (NIGMS, NIA and NINDS) to R.M. This work was also granted by the Hospital San Rafael (Coruña) with the Rafael Hervada prize on Biomedical Research (2010).

REFERENCES

1. Schols, L., Amoiridis, G., Langkafel, M., Buttner, T., Przuntek, H., Riess, O., Vieira-Saecker, A.M. and Epplen, J.T. (1995) Machado–Joseph disease mutations as the genetic basis of most spinocerebellar ataxias in Germany. *J. Neurol. Neurosurg. Psychiatry*, **59**, 449–450.
2. Schols, L., Bauer, P., Schmidt, T., Schulte, T. and Riess, O. (2004) Autosomal dominant cerebellar ataxias: clinical features, genetics, and pathogenesis. *Lancet Neurol.*, **3**, 291–304.
3. Coutinho, P. and Andrade, C. (1978) Autosomal dominant system degeneration in Portuguese families of the Azores Islands. A new genetic disorder involving cerebellar, pyramidal, extrapyramidal and spinal cord motor functions. *Neurology*, **28**, 703–709.
4. Gatchel, J.R. and Zoghbi, H.Y. (2005) Diseases of unstable repeat expansion: mechanisms and common principles. *Nat. Rev. Genet.*, **6**, 743–755.
5. Perutz, M.F. (1999) Glutamine repeats and neurodegenerative diseases: molecular aspects. *Trends Biochem. Sci.*, **24**, 58–63.
6. Ross, C.A. (1995) When more is less: pathogenesis of glutamine repeat neurodegenerative diseases. *Neuron*, **15**, 493–496.
7. do Carmo Costa, M., Gomes-da-Silva, J., Miranda, C.J., Sequeiros, J., Santos, M.M. and Maciel, P. (2004) Genomic structure, promoter activity, and developmental expression of the mouse homologue of the Machado–Joseph disease (MJD) gene. *Genomics*, **84**, 361–373.
8. Rodrigues, A.J., Coppola, G., Santos, C., Costa Mdo, C., Ailion, M., Sequeiros, J., Geschwind, D.H. and Maciel, P. (2007) Functional genomics and biochemical characterization of the *C. elegans* orthologue of the Machado–Joseph disease protein ataxin-3. *FASEB J.*, **21**, 1126–1136.
9. Doss-Pepe, E.W., Stenroos, E.S., Johnson, W.G. and Madura, K. (2003) Ataxin-3 interactions with rad23 and valosin-containing protein and its

associations with ubiquitin chains and the proteasome are consistent with a role in ubiquitin-mediated proteolysis. *Mol. Cell. Biol.*, **23**, 6469–6483.
10. Burnett, B., Li, F. and Pittman, R.N. (2003) The polyglutamine neurodegenerative protein ataxin-3 binds polyubiquitylated proteins and has ubiquitin protease activity. *Hum. Mol. Genet.*, **12**, 3195–3205.
11. Donaldson, K.M., Li, W., Ching, K.A., Batalov, S., Tsai, C.C. and Joazeiro, C.A. (2003) Ubiquitin-mediated sequestration of normal cellular proteins into polyglutamine aggregates. *Proc. Natl Acad. Sci. USA*, **100**, 8892–8897.
12. Chow, M.K., Mackay, J.P., Whisstock, J.C., Scanlon, M.J. and Bottomley, S.P. (2004) Structural and functional analysis of the Josephin domain of the polyglutamine protein ataxin-3. *Biochem. Biophys. Res. Commun.*, **322**, 387–394.
13. Ferro, A., Carvalho, A.L., Teixeira-Castro, A., Almeida, C., Tome, R.J., Cortes, L., Rodrigues, A.J., Logarinho, E., Sequeiros, J., Macedo-Ribeiro, S. *et al.* (2007) NEDD8: a new ataxin-3 interactor. *Biochim. Biophys. Acta.*, **1773**, 1619–1627.
14. Sequeiros, J. and Coutinho, P. (1993) Epidemiology and clinical aspects of Machado–Joseph disease. *Adv. Neurol.*, **61**, 139–153.
15. Riess, O., Rub, U., Pastore, A., Bauer, P. and Schols, L. (2008) SCA3: neurological features, pathogenesis and animal models. *Cerebellum*, **7**, 125–137.
16. Lin, M.T. and Beal, M.F. (2006) Mitochondrial dysfunction and oxidative stress in neurodegenerative diseases. *Nature*, **443**, 787–795.
17. Amaducci, L. and Tesco, G. (1994) Aging as a major risk for degenerative diseases of the central nervous system. *Curr. Opin. Neurol.*, **7**, 283–286.
18. Cohen, E. and Dillin, A. (2008) The insulin paradox: aging, proteotoxicity and neurodegeneration. *Nat. Rev. Neurosci.*, **9**, 759–767.
19. Ben-Zvi, A., Miller, E.A. and Morimoto, R.I. (2009) Collapse of proteostasis represents an early molecular event in *Caenorhabditis elegans* aging. *Proc. Natl Acad. Sci. USA*, **106**, 14914–14919.
20. Hsu, A.L., Murphy, C.T. and Kenyon, C. (2003) Regulation of aging and age-related disease by DAF-16 and heat-shock factor. *Science*, **300**, 1142–1145.
21. Morley, J.F. and Morimoto, R.I. (2004) Regulation of longevity in *Caenorhabditis elegans* by heat shock factor and molecular chaperones. *Mol. Biol. Cell*, **15**, 657–664.
22. Cohen, E., Bieschke, J., Perciavalle, R.M., Kelly, J.W. and Dillin, A. (2006) Opposing activities protect against age-onset proteotoxicity. *Science*, **313**, 1604–1610.
23. Khan, L.A., Bauer, P.O., Miyazaki, H., Lindenberg, K.S., Landwehrmeyer, B.G. and Nukina, N. (2006) Expanded polyglutamines impair synaptic transmission and ubiquitin–proteasome system in *Caenorhabditis elegans*. *J. Neurochem.*, **98**, 576–587.
24. Warrick, J.M., Morabito, L.M., Bilen, J., Gordesky-Gold, B., Faust, L.Z., Paulson, H.L. and Bonini, N.M. (2005) Ataxin-3 suppresses polyglutamine neurodegeneration in *Drosophila* by a ubiquitin-associated mechanism. *Mol. Cell*, **18**, 37–48.
25. Goti, D., Katzen, S.M., Mez, J., Kurtis, N., Kiluk, J., Ben-Haiem, L., Jenkins, N.A., Copeland, N.G., Kakizuka, A., Sharp, A.H. *et al.* (2004) A mutant ataxin-3 putative-cleavage fragment in brains of Machado–Joseph disease patients and transgenic mice is cytotoxic above a critical concentration. *J. Neurosci.*, **24**, 10266–10279.
26. Bichelmeier, U., Schmidt, T., Hubener, J., Boy, J., Ruttiger, L., Habig, K., Poths, S., Bonin, M., Knipper, M., Schmidt, W.J. *et al.* (2007) Nuclear localization of ataxin-3 is required for the manifestation of symptoms in SCA3: *in vivo* evidence. *J. Neurosci.*, **27**, 7418–7428.
27. Boy, J., Schmidt, T., Wolburg, H., Mack, A., Nuber, S., Bottcher, M., Schmitt, I., Holzmann, C., Zimmermann, F., Servadio, A. *et al.* (2009) Reversibility of symptoms in a conditional mouse model of spinocerebellar ataxia type 3. *Hum. Mol. Genet.*, **18**, 4282–4295.
28. Silva-Fernandes, A., Costa, M.D., Duarte-Silva, S., Oliveira, P., Botelho, C.M., Martins, L., Mariz, J.A., Ferreira, T., Ribeiro, F., Correia-Neves, M. *et al.* (2010) Motor uncoordination and neuropathology in a transgenic mouse model of Machado–Joseph disease lacking intranuclear inclusions and ataxin-3 cleavage products. *Neurobiol. Dis.*, **40**, 163–167.
29. Alves, S., Regulier, E., Nascimento-Ferreira, I., Hassig, R., Dufour, N., Koeppen, A., Carvalho, A.L., Simoes, S., de Lima, M.C., Brouillet, E. *et al.* (2008) Striatal and nigral pathology in a lentiviral rat model of Machado–Joseph disease. *Hum. Mol. Genet.*, **17**, 2071–2083.
30. Albertson, D.G. and Thomson, J.N. (1976) The pharynx of *Caenorhabditis elegans*. *Phil. Trans. R. Soc. Lond .B. Biol. Sci.*, **275**, 299–325.
31. White, J.G., Southgate, E., Thomson, J.N. and Brenner, S. (1976) The structure of the ventral nerve cord of *Caenorhabditis elegans*. *Phil. Trans. R. Soc. Lond. B. Biol. Sci.*, **275**, 327–348.
32. Brignull, H.R., Moore, F.E., Tang, S.J. and Morimoto, R.I. (2006) Polyglutamine proteins at the pathogenic threshold display neuron-specific aggregation in a pan-neuronal *Caenorhabditis elegans* model. *J. Neurosci.*, **26**, 7597–7606.
33. Faber, P.W., Alter, J.R., MacDonald, M.E. and Hart, A.C. (1999) Polyglutamine-mediated dysfunction and apoptotic death of a *Caenorhabditis elegans* sensory neuron. *Proc. Natl Acad. Sci. USA*, **96**, 179–184.
34. Satyal, S.H., Schmidt, E., Kitagawa, K., Sondheimer, N., Lindquist, S., Kramer, J.M. and Morimoto, R.I. (2000) Polyglutamine aggregates alter protein folding homeostasis in *Caenorhabditis elegans*. *Proc. Natl Acad. Sci. USA*, **97**, 5750–5755.
35. Parker, J.A., Connolly, J.B., Wellington, C., Hayden, M., Dausset, J. and Neri, C. (2001) Expanded polyglutamines in *Caenorhabditis elegans* cause axonal abnormalities and severe dysfunction of PLM mechanosensory neurons without cell death. *Proc. Natl Acad. Sci. USA*, **98**, 13318–13323.
36. Morley, J.F., Brignull, H.R., Weyers, J.J. and Morimoto, R.I. (2002) The threshold for polyglutamine-expansion protein aggregation and cellular toxicity is dynamic and influenced by aging in *Caenorhabditis elegans*. *Proc. Natl Acad. Sci. USA*, **99**, 10417–10422.
37. Altun-Gultekin, Z., Andachi, Y., Tsalik, E.L., Pilgrim, D., Kohara, Y. and Hobert, O. (2001) A regulatory cascade of three homeobox genes, ceh-10, ttx-3 and ceh-23, controls cell fate specification of a defined interneuron class in *C. elegans*. *Development*, **128**, 1951–1969.
38. Berke, S.J., Schmied, F.A., Brunt, E.R., Ellerby, L.M. and Paulson, H.L. (2004) Caspase-mediated proteolysis of the polyglutamine disease protein ataxin-3. *J. Neurochem.*, **89**, 908–918.
39. Colomer Gould, V.F., Goti, D., Pearce, D., Gonzalez, G.A., Gao, H., Bermudez de Leon, M., Jenkins, N.A., Copeland, N.G., Ross, C.A. and Brown, D.R. (2007) A mutant ataxin-3 fragment results from processing at a site N-terminal to amino acid 190 in brain of Machado–Joseph disease-like transgenic mice. *Neurobiol. Dis.*, **27**, 362–369.
40. Haacke, A., Hartl, F.U. and Breuer, P. (2007) Calpain inhibition is sufficient to suppress aggregation of polyglutamine-expanded ataxin-3. *J. Biol. Chem.*, **282**, 18851–18856.
41. Haacke, A., Broadley, S.A., Boteva, R., Tzvetkov, N., Hartl, F.U. and Breuer, P. (2006) Proteolytic cleavage of polyglutamine-expanded ataxin-3 is critical for aggregation and sequestration of non-expanded ataxin-3. *Hum. Mol. Genet.*, **15**, 555–568.
42. Teixeira-Castro, A., Dias, N., Rodrigues, P., Oliveira, J.O., Rodrigues, N.F., Maciel, P. and Vilaça, J.L. (2011) An image processing application for quantification of protein aggregates in *Caenorhabditis elegans*. *In 5th International Conference on Practical Applications of Computational Biology & Bioinformatics. Advances in Soft Computing*. Springer, Vol. 93, pp. 31–38.
43. Garcia, S.M., Casanueva, M.O., Silva, M.C., Amaral, M.D. and Morimoto, R.I. (2007) Neuronal signaling modulates protein homeostasis in *Caenorhabditis elegans* post-synaptic muscle cells. *Genes Dev.*, **21**, 3006–3016.
44. Gidalevitz, T., Ben-Zvi, A., Ho, K.H., Brignull, H.R. and Morimoto, R.I. (2006) Progressive disruption of cellular protein folding in models of polyglutamine diseases. *Science*, **311**, 1471–1474.
45. Bargmann, C.I., Hartwieg, E. and Horvitz, H.R. (1993) Odorant-selective genes and neurons mediate olfaction in *C. elegans*. *Cell*, **74**, 515–527.
46. Kimura, K.D., Tissenbaum, H.A., Liu, Y. and Ruvkun, G. (1997) daf-2, an insulin receptor-like gene that regulates longevity and diapause in *Caenorhabditis elegans*. *Science*, **277**, 942–946.
47. Arantes-Oliveira, N., Berman, J.R. and Kenyon, C. (2003) Healthy animals with extreme longevity. *Science*, **302**, 611.
48. Lin, K., Dorman, J.B., Rodan, A. and Kenyon, C. (1997) daf-16: An HNF-3/forkhead family member that can function to double the life-span of *Caenorhabditis elegans*. *Science*, **278**, 1319–1322.
49. Ogg, S., Paradis, S., Gottlieb, S., Patterson, G.I., Lee, L., Tissenbaum, H.A. and Ruvkun, G. (1997) The Fork head transcription factor DAF-16 transduces insulin-like metabolic and longevity signals in *C. elegans*. *Nature*, **389**, 994–999.
50. Evason, K., Collins, J.J., Huang, C., Hughes, S. and Kornfeld, K. (2008) Valproic acid extends *Caenorhabditis elegans* lifespan. *Aging Cell*, **7**, 305–317.

51. Hajdu-Cronin, Y.M., Chen, W.J. and Sternberg, P.W. (2004) The L-type cyclin CYL-1 and the heat-shock-factor HSF-1 are required for heat-shock-induced protein expression in *Caenorhabditis elegans*. *Genetics*, **168**, 1937–1949.
52. Jung, J., Xu, K., Lessing, D. and Bonini, N.M. (2009) Preventing Ataxin-3 protein cleavage mitigates degeneration in a *Drosophila* model of SCA3. *Hum. Mol. Genet.*, **18**, 4843–4852.
53. Ikeda, H., Yamaguchi, M., Sugai, S., Aze, Y., Narumiya, S. and Kakizuka, A. (1996) Expanded polyglutamine in the Machado–Joseph disease protein induces cell death *in vitro* and *in vivo*. *Nat. Genet.*, **13**, 196–202.
54. Boeddrich, A., Gaumer, S., Haacke, A., Tzvetkov, N., Albrecht, M., Evert, B.O., Muller, E.C., Lurz, R., Breuer, P., Schugardt, N. *et al.* (2006) An arginine/lysine-rich motif is crucial for VCP/p97-mediated modulation of ataxin-3 fibrillogenesis. *EMBO J.*, **25**, 1547–1558.
55. Li, F., Macfarlan, T., Pittman, R.N. and Chakravarti, D. (2002) Ataxin-3 is a histone-binding protein with two independent transcriptional corepressor activities. *J. Biol. Chem.*, **277**, 45004–45012.
56. Zhong, X. and Pittman, R.N. (2006) Ataxin-3 binds VCP/p97 and regulates retrotranslocation of ERAD substrates. *Hum. Mol. Genet.*, **15**, 2409–2420.
57. Evert, B.O., Schelhaas, J., Fleischer, H., de Vos, R.A., Brunt, E.R., Stenzel, W., Klockgether, T. and Wullner, U. (2006) Neuronal intranuclear inclusions, dysregulation of cytokine expression and cell death in spinocerebellar ataxia type 3. *Clin. Neuropathol.*, **25**, 272–281.
58. Seidel, K., den Dunnen, W.F., Schultz, C., Paulson, H., Frank, S., de Vos, R.A., Brunt, E.R., Deller, T., Kampinga, H.H. and Rub, U. (2010) Axonal inclusions in spinocerebellar ataxia type 3. *Acta Neuropathol*, **120**, 449–460.
59. Rodrigues, A.J., do Carmo Costa, M., Silva, T.L., Ferreira, D., Bajanca, F., Logarinho, E. and Maciel, P. (2010) Absence of ataxin-3 leads to cytoskeletal disorganization and increased cell death. *Biochim. Biophys. Acta*, **1803**, 1154–1163.
60. Mazzucchelli, S., De Palma, A., Riva, M., D'Urzo, A., Pozzi, C., Pastori, V., Comelli, F., Fusi, P., Vanoni, M., Tortora, P. *et al.* (2009) Proteomic and biochemical analyses unveil tight interaction of ataxin-3 with tubulin. *Int. J. Biochem. Cell Biol.*, **41**, 2485–2492.
61. Gidalevitz, T., Krupinski, T., Garcia, S. and Morimoto, R.I. (2009) Destabilizing protein polymorphisms in the genetic background direct phenotypic expression of mutant SOD1 toxicity. *PLoS Genet.*, **5**, e1000399.
62. Subramaniam, S., Sixt, K.M., Barrow, R. and Snyder, S.H. (2009) Rhes, a striatal specific protein, mediates mutant-huntingtin cytotoxicity. *Science*, **324**, 1327–1330.
63. Dickstein, D.L., Kabaso, D., Rocher, A.B., Luebke, J.I., Wearne, S.L. and Hof, P.R. (2007) Changes in the structural complexity of the aged brain. *Aging Cell*, **6**, 275–284.
64. Cohen, E., Paulsson, J.F., Blinder, P., Burstyn-Cohen, T., Du, D., Estepa, G., Adame, A., Pham, H.M., Holzenberger, M., Kelly, J.W. *et al.* (2009) Reduced IGF-1 signaling delays age-associated proteotoxicity in mice. *Cell*, **139**, 1157–1169.
65. Outeiro, T.F., Kontopoulos, E., Altmann, S.M., Kufareva, I., Strathearn, K.E., Amore, A.M., Volk, C.B., Maxwell, M.M., Rochet, J.C., McLean, P.J. *et al.* (2007) Sirtuin 2 inhibitors rescue alpha-synuclein-mediated toxicity in models of Parkinson's disease. *Science*, **317**, 516–519.
66. van Ham, T.J., Thijssen, K.L., Breitling, R., Hofstra, R.M., Plasterk, R.H. and Nollen, E.A. (2008) *C. elegans* model identifies genetic modifiers of alpha-synuclein inclusion formation during aging. *PLoS Genet.*, **4**, e1000027.
67. Parker, J.A., Arango, M., Abderrahmane, S., Lambert, E., Tourette, C., Catoire, H. and Neri, C. (2005) Resveratrol rescues mutant polyglutamine cytotoxicity in nematode and mammalian neurons. *Nat. Genet.*, **37**, 349–350.
68. Cohen, E., Du, D., Joyce, D., Kapernick, E.A., Volovik, Y., Kelly, J.W. and Dillin, A. (2010) Temporal requirements of insulin/IGF-1 signaling for proteotoxicity protection. *Aging Cell*, **9**, 126–134.
69. Chai, Y., Koppenhafer, S.L., Bonini, N.M. and Paulson, H.L. (1999) Analysis of the role of heat shock protein (Hsp) molecular chaperones in polyglutamine disease. *J. Neurosci.*, **19**, 10338–10347.
70. Williams, A.J., Knutson, T.M., Colomer Gould, V.F. and Paulson, H.L. (2009) *In vivo* suppression of polyglutamine neurotoxicity by C-terminus of Hsp70-interacting protein (CHIP) supports an aggregation model of pathogenesis. *Neurobiol. Dis.*, **33**, 342–353.
71. Brenner, S. (1974) The genetics of *Caenorhabditis elegans*. *Genetics*, **77**, 71–94.
72. Brignull, H.R., Morley, J.F., Garcia, S.M. and Morimoto, R.I. (2006) Modeling polyglutamine pathogenesis in *C. elegans*. *Methods Enzymol.*, **412**, 256–282.
73. Lewis, J.A. and Fleming, J.T. (1995) Basic culture methods. *Methods Cell Biol.*, **48**, 3–29.
74. Phair, R.D. and Misteli, T. (2000) High mobility of proteins in the mammalian cell nucleus. *Nature*, **404**, 604–609.
75. Voisine, C., Varma, H., Walker, N., Bates, E.A., Stockwell, B.R. and Hart, A.C. (2007) Identification of potential therapeutic drugs for Huntington's disease using *Caenorhabditis elegans*. *PLoS One*, **2**, e504.

Supplemental material

Supplemental material to:

Neuron-specific proteotoxicity of mutant ataxin-3 in *C. elegans*: rescue by the DAF-16 and HSF-1 pathways.

Andreia Teixeira-Castro[1,2], Michael Ailion[3], Ana Jalles[1], Heather R. Brignull[2,#], João L. Vilaça[1,4], Nuno Dias[1,4], Pedro Rodrigues[1], João F. Oliveira[1], Andreia Neves-Carvalho[1], Richard I. Morimoto[2,+] and Patrícia Maciel[1,+,*]

[1] Life and Health Sciences Research Institute (ICVS), School of Health Sciences, Univ. of Minho, 4710-057 Braga, Portugal.

[2] Department of Biochemistry, Molecular Biology, and Cell Biology, Northwestern University Institute for Neuroscience, Rice Institute for Biomedical Research, Northwestern University Evanston, IL 60208.

[3] Department of Biology, University of Utah, Salt Lake City, Utah 84112, USA.

[4] DIGARC, Polytechnic Institute of Cávado and Ave, 4750-810 Barcelos, Portugal.

[#] Current address: Department of Biological Structure, University of Washington, Seattle, WA 98915, USA.

[+] Research was shared equally among the two laboratories.

* To whom correspondence should be addressed:

Patrícia Maciel, Life and Health Sciences Research Institute (ICVS), School of Health Sciences, University of Minho, Campus de Gualtar, 4710-057 Braga, Portugal, Tel: + 351 253 60 48 24, Fax: + 351 253 60 48 20, E-mail: **pmaciel@ecsaude.uminho.pt**.

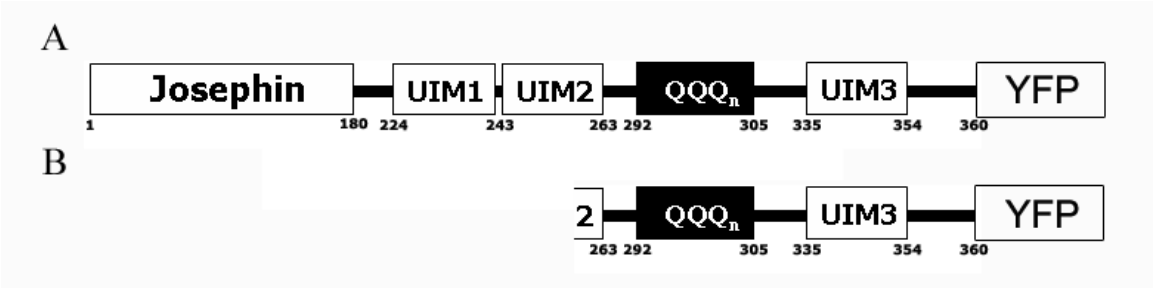

Figure S1: Scheme of the full-length and C-terminal ataxin-3::YFP fusion proteins expressed throughout the *C. elegans* nervous system. Graphic representation of the protein domains that constitute full-length ATXN3: the N-terminal Josephin domain, three ubiquitin interacting motifs (UIM) and the polyQ tract (QQQn), in which n represents the number of glutamine (Q) repeats. A value of n equal to 14 refers to wild-type (WT) ATXN3, whereas n equal to 75 or 130 corresponds to mutant ATXN3 forms (A). C-terminal ATXN3 proteins, containing the polyQ tract and the UIM3, were expressed in the *C. elegans* nervous system under the regulation of the F25B3.3 promoter. Here, too, n represents the number of Q: n equal to 14 represents WT C-terminal ATXN3, whereas n equal to 75, 80 or 128 refers to mutant 257cAT3 forms (B).

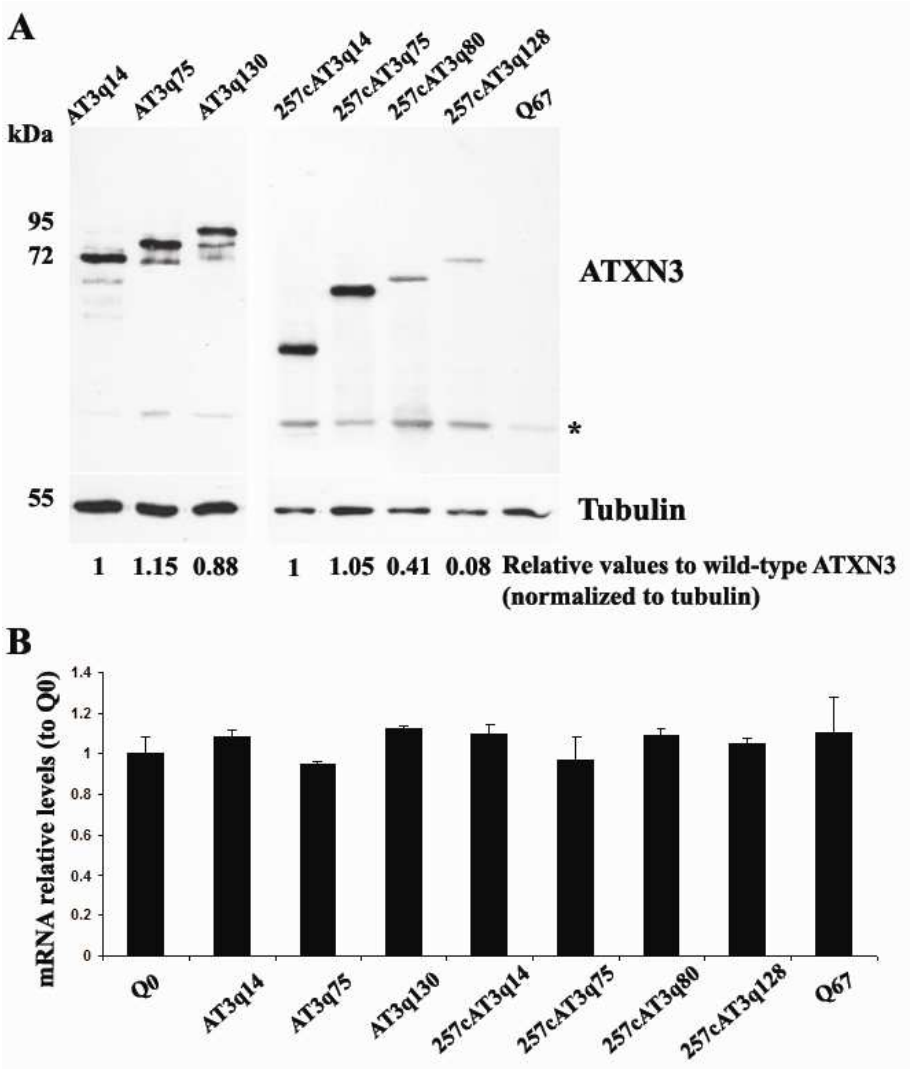

Figure S2: Steady-state protein levels and mRNA relative levels of ATXN3 transgenic lines. Representative Western-blot of ATXN3-expressing animals. AT3q75 and AT3q130 proteins are expressed at similar levels to WT full-length ATXN3. 257cAT3q75 is expressed at a level similar to 257cAT3q14 proteins, while 257cAT3q80 and 257cAT3q128 are expressed at lower levels (A). The upper panel shows an immunoblot with anti-ATXN3 antibody, the bottom panel with anti-tubulin antibody. Twenty-five individual young adult animals were picked from the indicated strains, boiled (15 min) in SDS sample buffer and resolved on 10% SDS gel. Immunoblots were scanned and quantified using Image J software. The numbers below the gel represent the quantification of ATXN3 signal normalized to tubulin. The symbol * may correspond to non-specific bands, present in animals expressing Q67 proteins. Amounts of mRNA were measured by quantitative real-time polymerase chain reaction (qRT-PCR) and normalized to Q0 values (B). Results show no significant differences among all ATXN3 transgenic lines. Each graph data point represents three independent biological replicates for each strain.

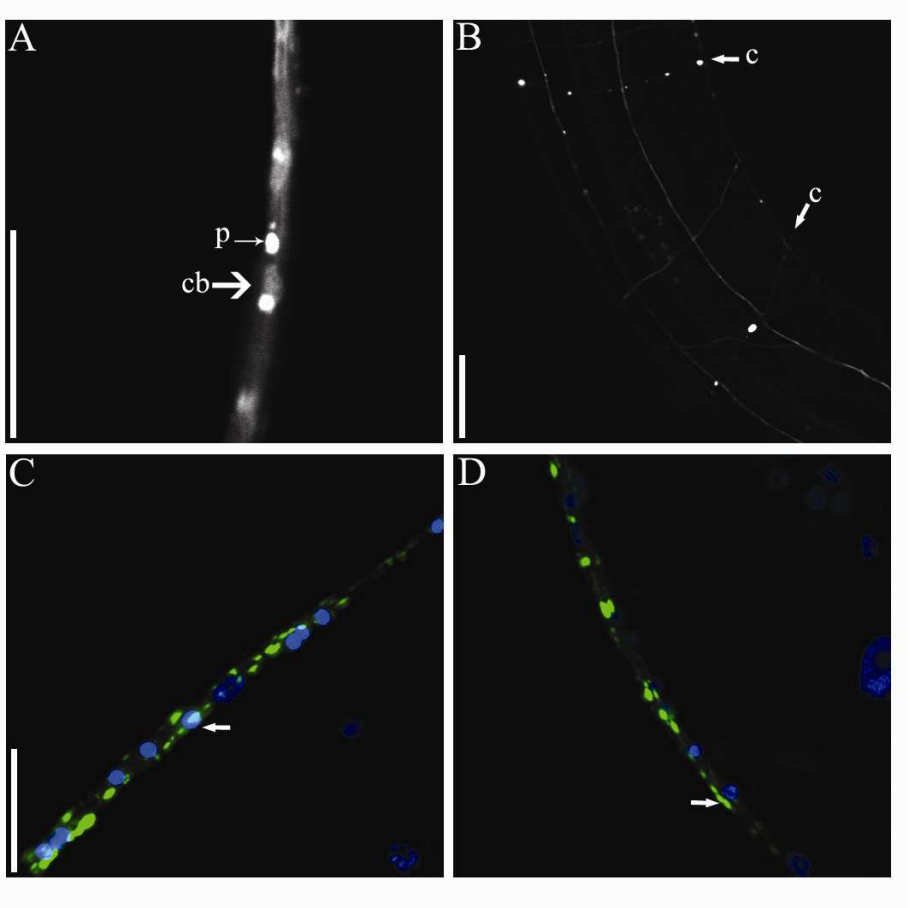

Figure S3: AT3q130 protein aggregates are found in cell bodies and neuronal processes, showing nuclear and cytoplasmic localisation as revealed by DAPI staining. Cells located in the VNC near the vulva show aggregates in the cell bodies (cb, thick arrow) and in neuronal processes (p, thin arrow) (A). Image from the posterior body shows aggregates in commissures (c, arrows) (B). AT3q130 proteins co-localise with DAPI in some neurons (C, arrow) and not in others (D, arrow), indicating both nuclear and cytoplasmic distribution within the neuronal cells. Animals imaged are young adults 4 days post-hatching, expressing AT3q130::YFP proteins (A-D); images C, D show AT3q130 animals fixed for DAPI staining. In all images, scale bar= 20 µm. The images were obtained using an Olympus FV1000 confocal microscope.

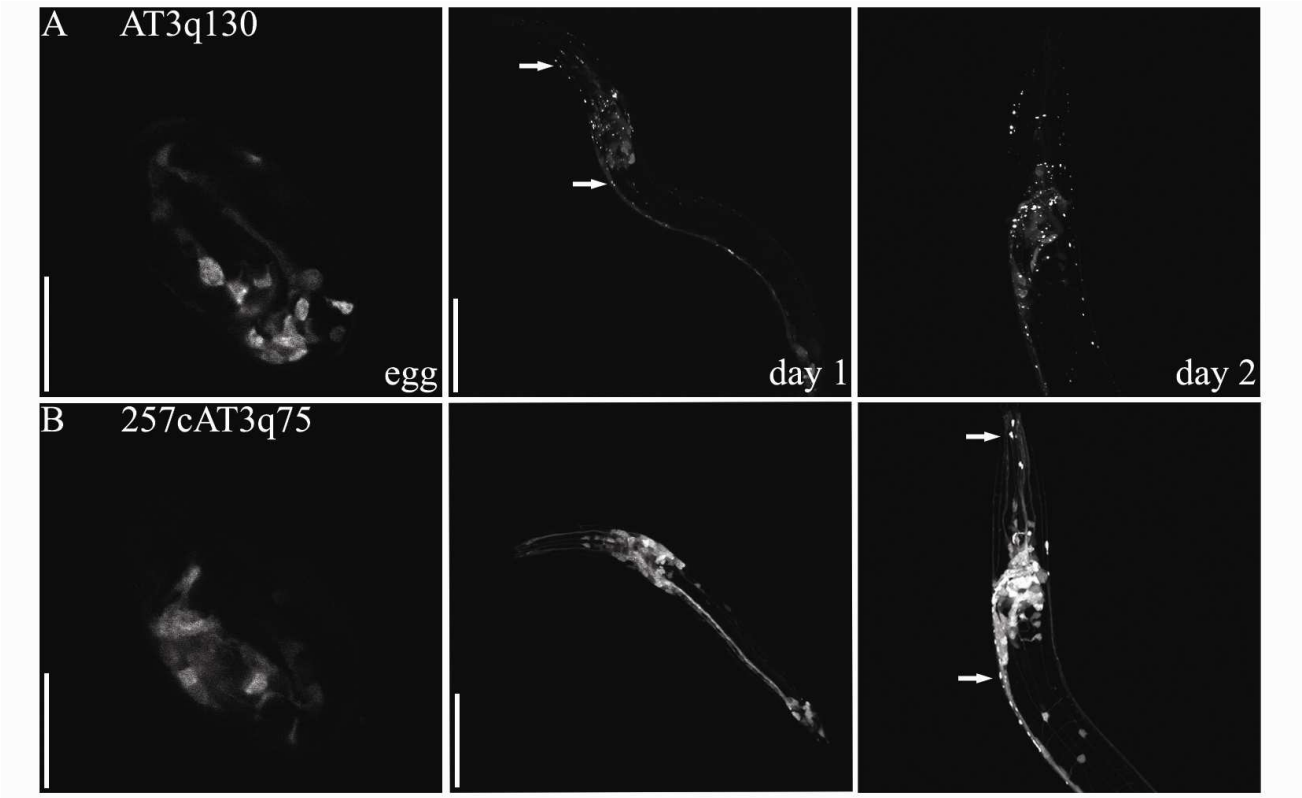

Figure S4: Protein foci are first detected at the initial stages of the animals' development in the full-length and C-terminal ATXN3 models. Flattened Z-stacks of animals expressing AT3q130 proteins show protein foci starting on day 1 (A) (post-hatching) (note the arrows). The punctate structures are first observed in animals expressing 257cAT3q75 proteins on day 2 (post-hatching) (arrows) (B). Scale bar= 20 μm, for the panels showing embryos; scale bar= 40 μm for all other panels. The images were obtained using an Olympus FV1000 confocal microscope.

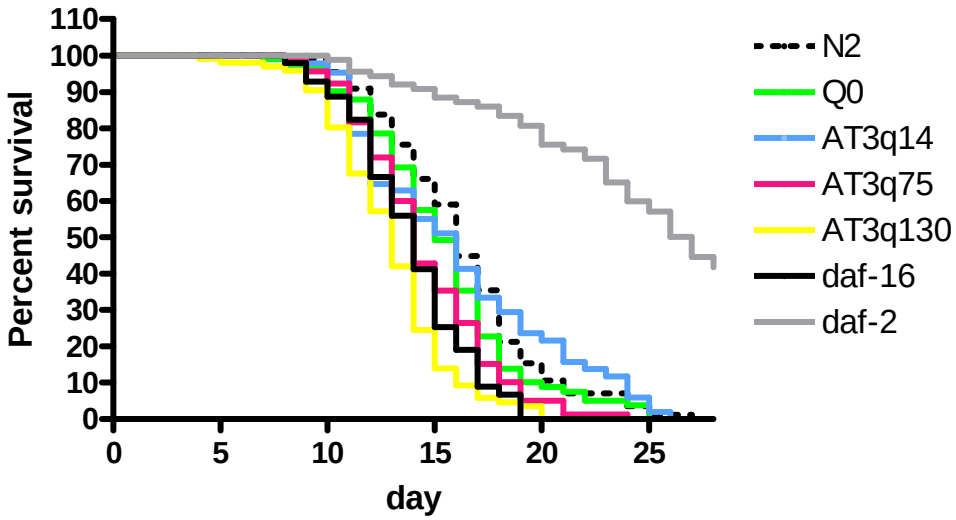

Figure S5: Mutant ATXN3- expressing animals have reduced lifespan. Lifespan measurements of WT N2 and transgenic animals that express YFP (Q0), WT AT3q14 and mutant ATXN3 (AT3q75 and AT3q130) proteins, in the *C. elegans* nervous system. Animals were grown on OP50 bacteria at 20^{0}C. The *daf-16(mu86)* and *daf-2(e1368)* animals were used as controls. AT3q130 animals show reduced survival when compared to N2 and AT3q14 animals ($p<0.0001$ and $p<0.0001$, respectively; Kaplan-Meyer analysis). Two independent trials gave similar results (N>86, per experiment).

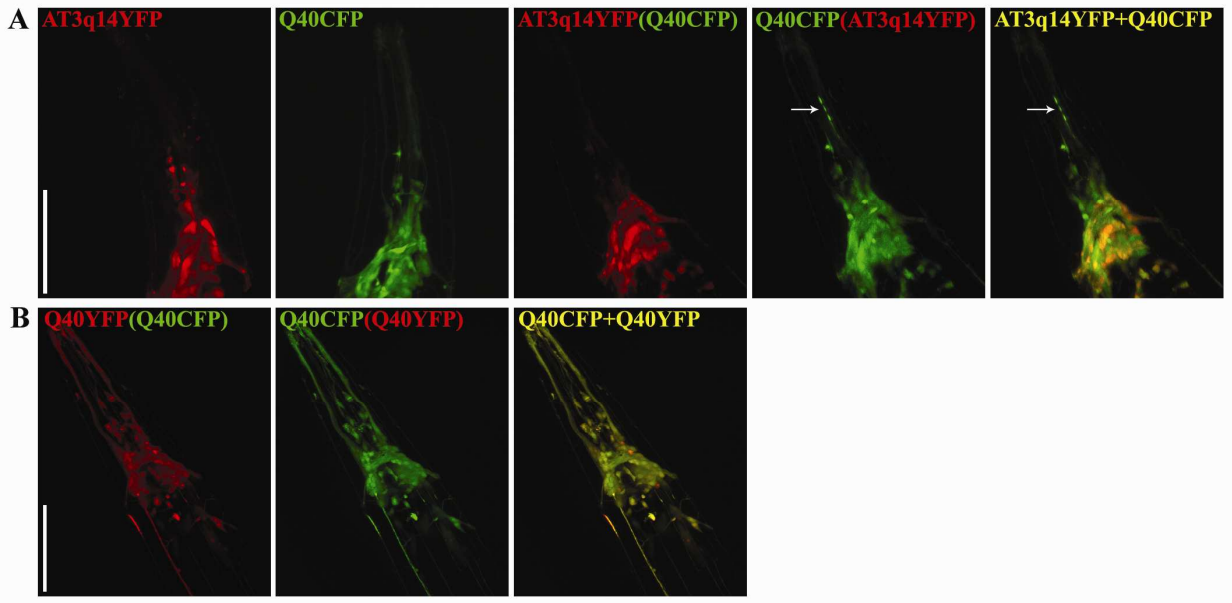

Figure S6: Co- expression of WT ATXN3::YFP with Q40::CFP or of Q40::YFP with Q40::CFP proteins did not cause overt foci formation in C. elegans processes of the head. Flattened Z-stacks of day-4 animals co-expressing AT3q14::YFP with Q40::CFP (A) or Q40::YFP with Q40::CFP (B) proteins did not contain protein aggregates in the sensory processes of the head. Q40 protein blobs (arrow) did not correspond to insoluble protein, as assessed by FRAP analysis (data not shown). Scale bars= 50 µm. The images were obtained using a Zeiss LSM 510 (A) or an Olympus FV1000 (B) confocal microscope.

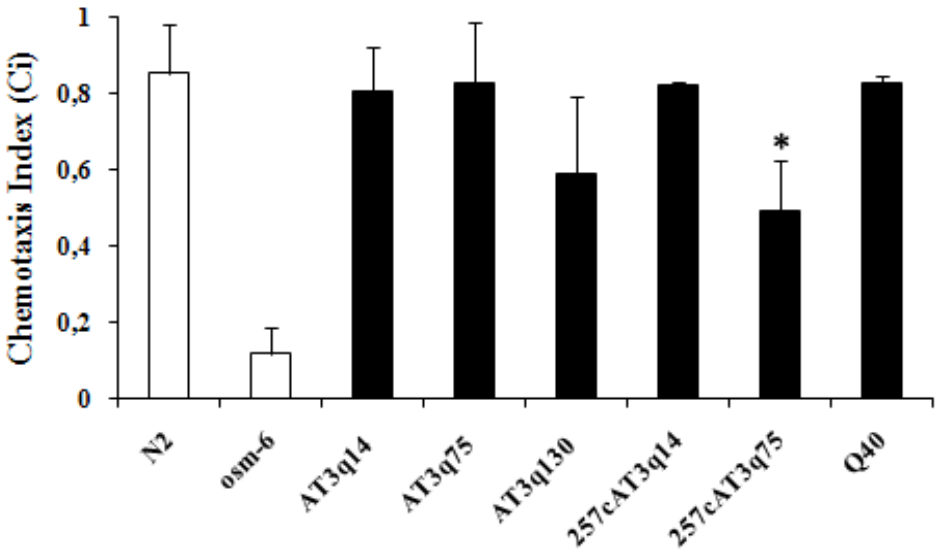

Figure S7: Mutant ATXN3 and not polyQ-alone expressing animals have slightly reduced chemotaxis index (Ci) to isoamyl alcohol (IAA). AT3q130-expressing animals show a tendency towards a reduction in chemosensation when exposed to a 10^{-1} dilution of the attractant IAA, compared to the WT controls (N2) and WT AT3q14 transgenics. Some AT3q130 animals failed to reach the attractant area, whereas others were attracted to it. 257cAT3q75 animals showed a significant reduction in Ci when compared to N2 ($p=0.0074$) and 257cAT3q14 animals ($p=0.0085$). Q40 animals are attracted to IAA. The *osm-6* (*p811*) mutants, which failed to show chemotactic behaviour to IAA, were used as a positive internal control. IAA stock was freshly diluted in ethanol, which was used as the counter-attractant. Each data point represents at least three independents trials, and error bars show standard deviation of the mean.

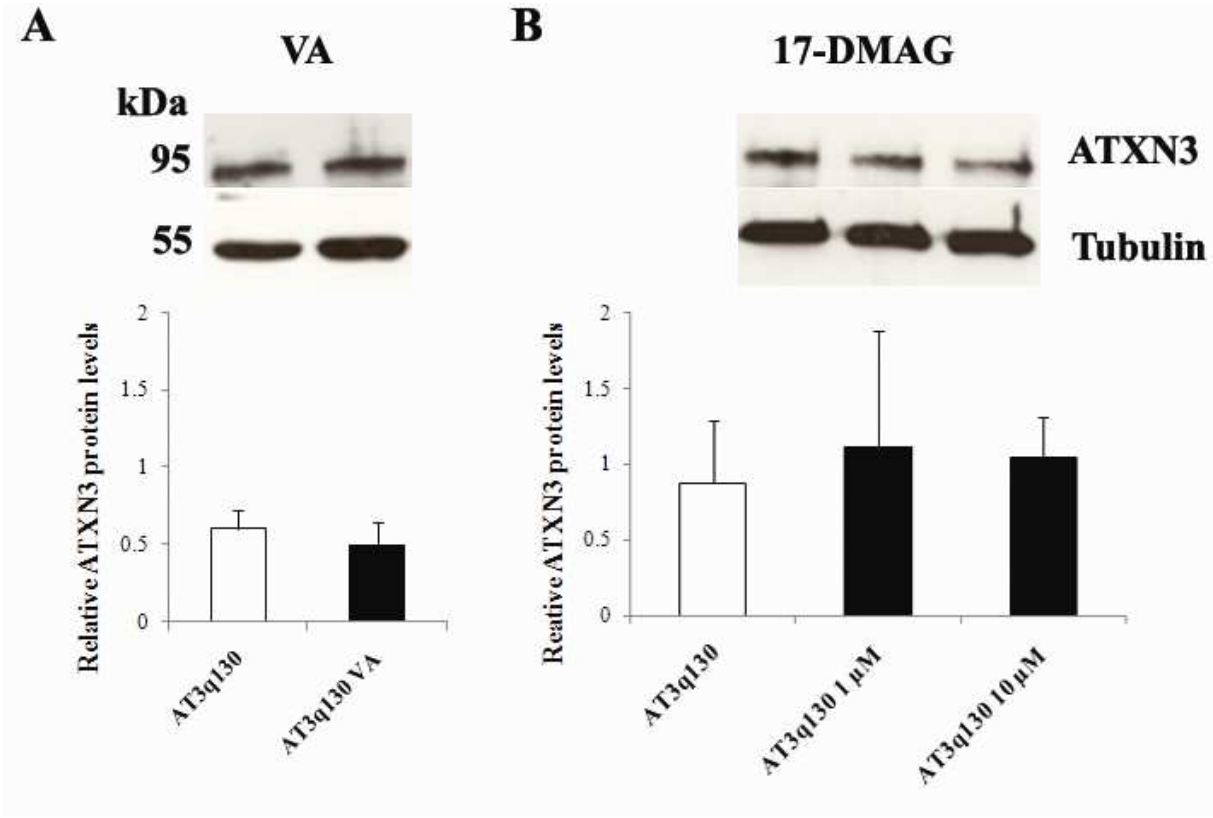

Figure S8: Mutant ATXN3 protein levels are not altered by VA or 17-DMAG treatment. Western-blot analysis indicates that VA (A) or 17-DMAG (B) treatment did not significantly change AT3q130 protein levels, compared to the AT3q130 animals. (A) Animals treated with VA were grown for 10 days on NGM plates containing 6 mM of the drug, whereas in (B) AT3q130 animals were treated for 4 days in liquid medium containing 1 µM or 10 µM of 17-DMAG. Upper panels show representative western-blots, and each graph data point represents three independent biological replicates per treatment. Error bars show standard deviation of the mean.

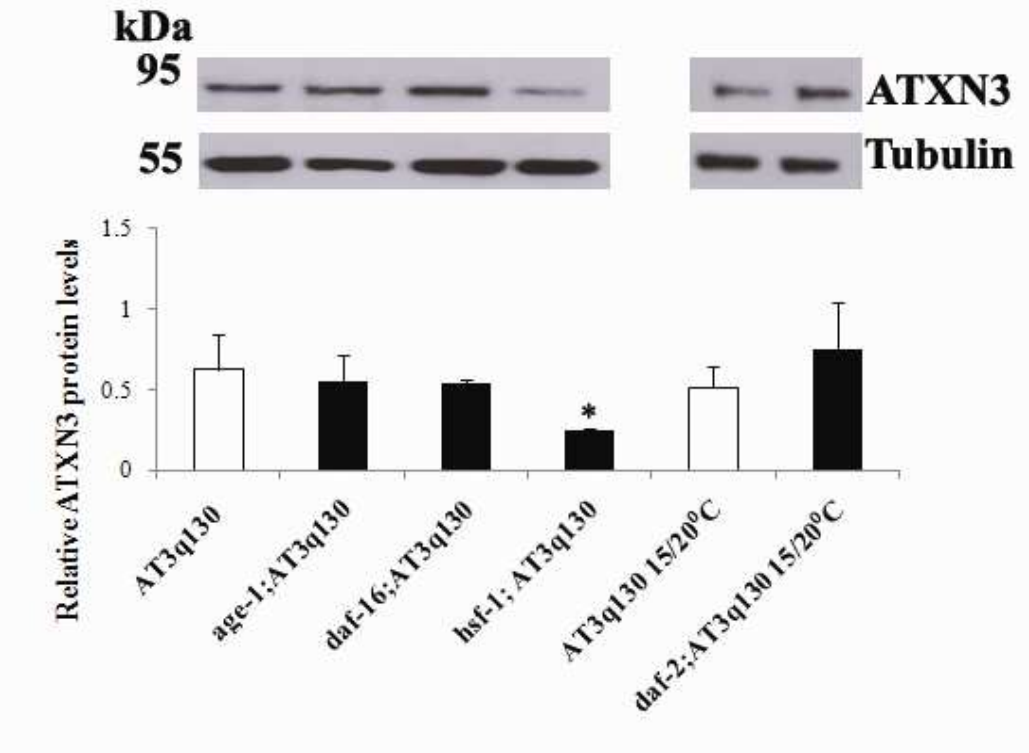

Figure S9: Mutant ATXN3 steady-state levels in the absence of IIS and HSF-1 genes. Western-blot analysis indicates that mutations in *age-1(hx546)*, *daf-16(mu86)* and *daf-2(e1370)* did not significantly change AT3q130 protein levels, compared to AT3q130 controls. Mutation in HSF-1 (*sy441* allele) increases protein aggregation and slightly decreases AT3q130 expression (*, p=0.042). Upper panel shows representative Western-blots, and each graph data point represents three independent biological replicates for each strain.

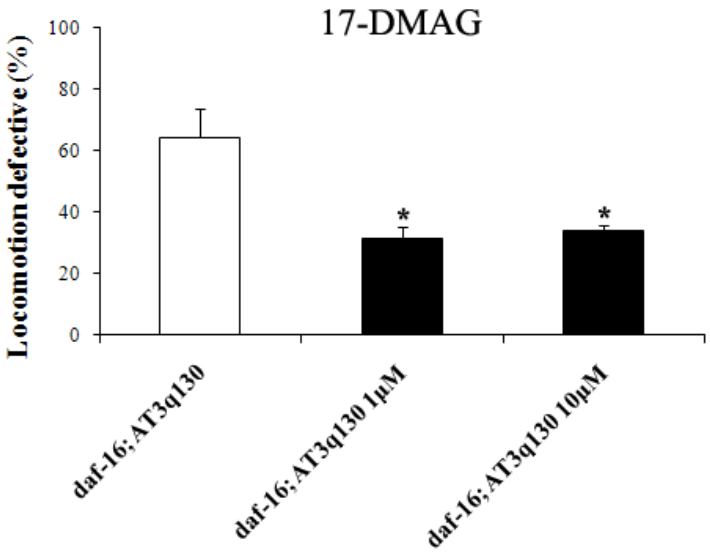

Figure S10: 17-DMAG treatment of mutant ataxin-3 animals reduced locomotion impairment in the absence of DAF-16. Day-4 *daf-16*; AT3q130 animals treated with two concentrations of 17-DMAG improved their motility performance. The effect of 17-DMAG on motor function was independent of DAF-16. Motility data are the mean ± SD, at least 147 animals per data point. Student's *t*-test, *, $p<0.05$.

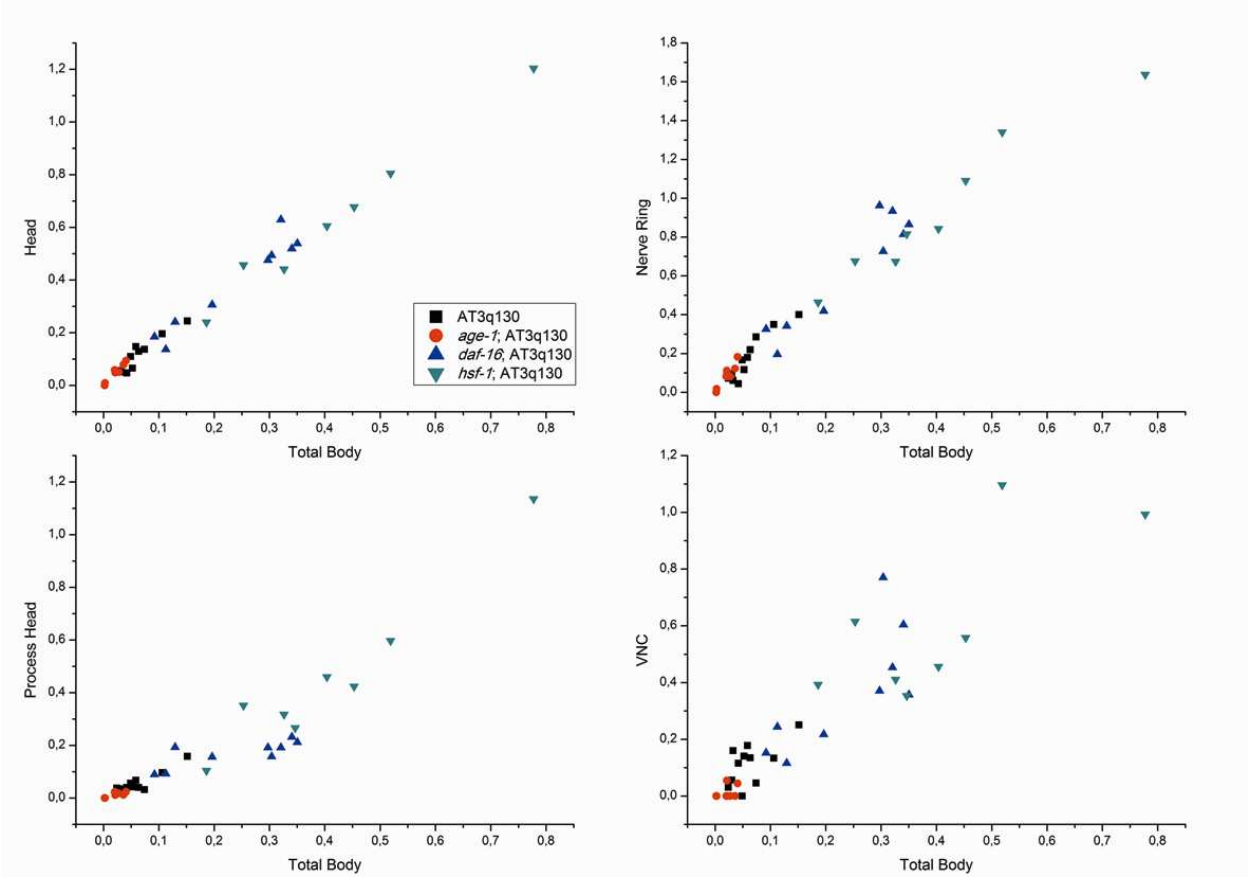

Figure S11. Quantification of the number of aggregates per area unit in specific regions of the nervous system revealed that total body aggregation is related to aggregation in specific regions. Neurons of the *C. elegans* head, nerve ring, processes of the head and VNC neurons show high correlation coefficient with total body aggregation (Pearson Correlation Coefficients of 0.99271, 0.98324, 0.93566 and 0.9207, respectively). Correlation graphs, coefficients and statistical assessment were performed using Origin software (OriginLab).

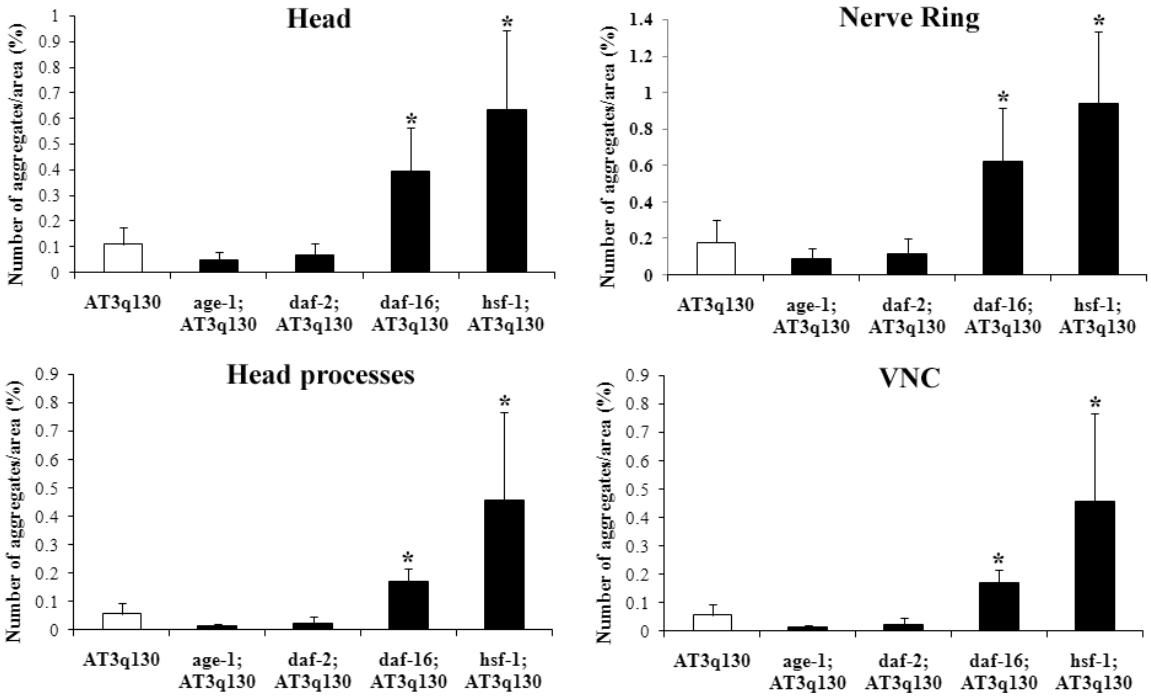

Figure S12. Quantification of the number of aggregates per area unit in specific regions of the nervous system revealed that IIS and HSF-1 pathways also modify aggregation. Similar to changes in the total body aggregation, in the neurons of the *C. elegans* head, nerve ring, processes of the head and VNC, *daf-2* and *age-1* mutations caused a tendency towards a reduction in aggregation, whereas the absence of DAF-16 and HSF-1significantly increased it (*, $p<0.05$).

Supplemental Methods:

Immunobloting analysis. For determination of the steady-state protein levels of ATXN3, 25 individual young adult animals were picked from indicated strains, boiled for 15 min in SDS sample buffer (in order to destroy all the aggregates) and resolved on a 10% SDS gel, as previously described (S1). Immunoblots were probed with anti-ATXN3 rabbit (S2) and anti-tubulin mouse antibodies (DSHB, USA); and detected with horseradish peroxidase-coupled secondary antibodies and chemiluminescence (ECL western-blotting detecting reagents, Amersham Pharmacia). Quantification of the ATXN3 signal, normalized to tubulin was performed using Image J software (NIH, USA).

mRNA levels. Total RNA was extracted from transgenic *C. elegans* using TRIzol reagent (Invitrogen) according to the manufacturer's instructions, with the following modifications: for extrachromosomal arrays, we selected at least 200 fluorescent worms, washed the worms with M9 buffer to remove bacteria and added 500 μL of TRIzol. We froze/thawed the samples 5x to break down the animals' cuticles. For integrated *C. elegans* lines, we washed off the animals from a 50-mm NGM-rich plate. The isolated RNA was treated with RQ1 RNase-free Dnase I (Promega): 0.5 μg of total RNA in a 20 μL reaction. Single-stranded cDNAs were synthesised using the iScript cDNA Synthesis Kit (Biorad). Primers were designed using Primer3 software (http://frodo.wi.mit.edu/cgi-bin/primer3/primer3_www.cgi), and the qRT-PCR reaction was performed using the SYBR green PCR kit (Applied Biosystems). We quantified YFP mRNA relative levels in all generated lines and used actin-1 (act-1) as an internal control, as previously described (S3).

Immunostaining. Fixed animals were incubated with 2 μg/mL DAPI in PBS for 30 min and rinsed 3x in PBS containing 0.1% of Tween 20, as previously described (S4).

Lifespan. Assays were performed at 20^0C as previously described (S5). Approximately 10 hermaphrodites were cultured on each Petri dish and were transferred to fresh plates every 1-2 days until the cessation of progeny production, and about every 3 days thereafter. Animals were scored as dead if they showed no spontaneous movement or response when prodded. Dead animals that displayed internally hatched progeny, extruded gonad or desiccation were excluded. Statistical analysis was performed using GraphPad Prism version 4 (Kaplan-Meyer analysis).

Population Chemotaxis Assays. Chemotaxis assays were performed as previously described (S6). Well-fed adult animals (day 4) were washed three times in S-Basal (S7) and once in water to remove bacteria and placed in the centre of a 10-cm Petri plate equidistant from the attractant (isoamyl alcohol 10^{-1}, Sigma) and the counterattractant (ethanol). The chemotaxis index (Ci) was calculated after 60 min as: (number of animals at attractant - number of animals at counterattractant)/total number of animals in the assay.

Table S1. List of strains, abbreviations and crosses used in this work

Strain (ref)	Abbreviation	Protein	Genotype
AM491	AT3q14	AT3q14::YFP	*rmEx228[P $_{F25B3.3}$ ::AT3v1-1q14::yfp]*
AM513	AT3q14	AT3q14::YFP	*rmIs231[P $_{F25B3.3}$ ::AT3v1-1q14::yfp]*
AM509	AT3q14	AT3q14::YFP	*rmIs227[P $_{F25B3.3}$ ::AT3v1-1q14::yfp]*
AM494	AT3q75	AT3q75::YFP	*rmEx230[P $_{F25B3.3}$ ::AT3v1-1q75::yfp]*
AM519	AT3q75	AT3q75::YFP	*rmIs237[P $_{F25B3.3}$ ::AT3v1-1q75::yfp]*
AM520	AT3q75	AT3q75::YFP	*rmIs238[P $_{F25B3.3}$ ::AT3v1-1q75::yfp]*
AM666	AT3q130	AT3q130::YFP	*rmEx298[P $_{F25B3.3}$ ::AT3v1-1q130::yfp]*
AM685	AT3q130	AT3q130::YFP	*rmIs263[p $_{F25B3.3}$ ::AT3v1-1q130::yfp]*
AM599	AT3q130	AT3q130::YFP	*rmIs261[P $_{F25B3.3}$ ::AT3v1-1q130::yfp]*
AM396	257cAT3q14	257cAT3q14::YFP	*rmEx204[P $_{F25B3.3}$ ::257cAT3v1-1q14::yfp]*
AM416	257cAT3q14	257cAT3q14::YFP	*rmIs210[P $_{F25B3.3}$ ::257cAT3v1-1q14::yfp]*
AM422	257cAT3q14	257cAT3q14::YFP	*rmIs211[P $_{F25B3.3}$ ::257cAT3v1-1q14::yfp]*
AM391	257cAT3q75	257cAT3q75::YFP	*rmEx199[P $_{F25B3.3}$ ::257cAT3v1-1q75::yfp]*
AM428	257cAT3q75	257cAT3q75::YFP	*rmIs217[P $_{F25B3.3}$ ::257cAT3v1-1q75::yfp]*
AM419	257cAT3q75	257cAT3q75::YFP	*rmIs210[P $_{F25B3.3}$ ::257cAT3v1-1q75::yfp]*
AM420	257cAT3q75	257cAT3q75::YFP	*rmIs214[P $_{F25B3.3}$ ::257cAT3v1-1q75::yfp]*
AM684	257cAT3q80	257cAT3q80::YFP	*rmEx259[P $_{F25B3.3}$ ::257cAT3v1-1q80::yfp]*
AM683	257cAT3q80	257cAT3q80::YFP	*rmEx251[P $_{F25B3.3}$ ::257cAT3v1-1q80::yfp]*
AM702	257cAT3q128	257cAT3q128::YFP	*rmEx260[P $_{F25B3.3}$ ::257cAT3v1-1q128::yfp]*
MAC69	AT3q130; mCherry	AT3q130::YFP and mCherry	*mnhEx1[P $_{CHE-13}$ ::mCherry]; rmIs263[P $_{F25B3.3}$ ::AT3v1-1q130::yfp]*
MAC70	257cAT3q75;mCherry	257cAT3q75::YFP and mCherry	*mnhEx2[P $_{CHE-13}$ ::mCherry]; rmIs214[P $_{F25B3.3}$ ::257cAT3v1-1q75::yfp]*
AM505	AT3q14; Q40	AT3q14::YFP and Q40::CFP	*rmEx228[P $_{F25B3.3}$ ::AT3v1-1q14::yfp];rmIs167[P $_{F25B3.3}$ ::q40::cfp]*
AM508	AT3q75; Q40	AT3q75::YFP and Q40::CFP	*rmEx227[P $_{F25B3.3}$ ::AT3v1-1q75::yfp];rmIs167[P $_{F25B3.3}$ ::q40::cfp]*
AM52 (S8)	Q0	Q0::YFP	*rmIs182[P $_{F25B3.3}$ ::q0::yfp]*
AM102 (S8)	Q40	Q40::YFP	*rmIs111[P $_{F25B3.3}$ ::q40::yfp]*
AM81 (S8)	Q67	Q67::YFP	*rmEx164[P $_{F25B3.3}$ ::q67::yfp]*
AM47 (S8)	Q40	Q40::CFP	*rmIs167[P $_{F25B3.3}$ ::q40::cfp]*
DR1572 (S9)	*daf-2*		*daf-2(e1368)III*
CB1370 (S10)	*daf-2*		*daf-2(e1370)III*
CF1038 (S11)	*daf-16*		*daf-16(mu86)I*
TJ1052 (S12)	*age-1*		*age-1(hx546)II*
PS3551 (S13)	*hsf-1*		*hsf-1(sy441)I*
MAC65	*age-1;* AT3q130	AT3q130::YFP	*age-1(hx546)II; rmIs261[P $_{F25B3.3}$ ::AT3v1-1q130::yfp]*
MAC66	*daf-2;* AT3q130	AT3q130::YFP	*daf-2(e1370)III;rmIs263[P $_{F25B3.3}$ ::AT3v1-1q130::yfp]*
MAC67	*daf-16;* AT3q130	AT3q130::YFP	*daf-16(mu86)I;rmIs263[P $_{F25B3.3}$::AT3v1-1q130::yfp]*
MAC68	*hsf-1;* AT3q130	AT3q130::YFP	*hsf-1(sy441)I;rmIs263[P $_{F25B3.3}$ ::AT3v1-1q130::yfp]*

References

S1. Gidalevitz, T., Krupinski, T., Garcia, S. and Morimoto, R.I. (2009) Destabilizing protein polymorphisms in the genetic background direct phenotypic expression of mutant SOD1 toxicity. *PLoS Genet.*, 5, e1000399.

S2. Ferro, A., Carvalho, A.L., Teixeira-Castro, A., Almeida, C., Tome, R.J., Cortes, L., Rodrigues, A.J., Logarinho, E., Sequeiros, J., Macedo-Ribeiro, S. et al. (2007) NEDD8: a new ataxin-3 interactor. *Biochim. Biophys. Acta*, 1773, 1619-1627.

S3. Prahlad, V., Cornelius, T. and Morimoto, R.I. (2008) Regulation of the cellular heat shock response in Caenorhabditis elegans by thermosensory neurons. *Science*, 320, 811-814.

S4. Gidalevitz, T., Ben-Zvi, A., Ho, K.H., Brignull, H.R. and Morimoto, R.I. (2006) Progressive disruption of cellular protein folding in models of polyglutamine diseases. Science, 311, 1471-1474.

S5. Morley, J.F. and Morimoto, R.I. (2004) Regulation of longevity in Caenorhabditis elegans by heat shock factor and molecular chaperones. *Mol Biol Cell*, 15, 657-664.

S6. Bargmann, C.I., Hartwieg, E. and Horvitz, H.R. (1993) Odorant-selective genes and neurons mediate olfaction in C. elegans. *Cell*, 74, 515-527.

S7. Brenner, S. (1974) The genetics of Caenorhabditis elegans. *Genetics*, 77, 71-94.

S8. Brignull, H.R., Moore, F.E., Tang, S.J. and Morimoto, R.I. (2006) Polyglutamine proteins at the pathogenic threshold display neuron-specific aggregation in a pan-neuronal Caenorhabditis elegans model. *J. Neurosci.*, 26, 7597-7606.

S9. Gems, D., Sutton, A.J., Sundermeyer, M.L., Albert, P.S., King, K.V., Edgley, M.L., Larsen, P.L. and Riddle, D.L. (1998) Two pleiotropic classes of daf-2 mutation affect larval arrest, adult behavior, reproduction and longevity in Caenorhabditis elegans. *Genetics*, 150, 129-155.

S10. Kenyon, C., Chang, J., Gensch, E., Rudner, A. and Tabtiang, R. (1993) A C. elegans mutant that lives twice as long as wild type. *Nature*, 366, 461-464.

S11. Lin, K., Dorman, J.B., Rodan, A. and Kenyon, C. (1997) daf-16: An HNF-3/forkhead family member that can function to double the life-span of Caenorhabditis elegans. Science, 278, 1319-1322.

S12. Arantes-Oliveira, N., Berman, J.R. and Kenyon, C. (2003) Healthy animals with extreme longevity. *Science*, 302, 611.

S13. Hajdu-Cronin, Y.M., Chen, W.J. and Sternberg, P.W. (2004) The L-type cyclin CYL-1 and the heat-shock-factor HSF-1 are required for heat-shock-induced protein expression in Caenorhabditis elegans. *Genetics*, 168, 1937-1949.

Chapter 2.1

An image processing application for quantification of protein aggregates in *Caenorhabditis elegans*

An image processing application for quantification of protein aggregates in *Caenorhabditis elegans*

Andreia Teixeira-Castro[1], Nuno Dias[1,2], Pedro Rodrigues[1], João Filipe Oliveira[1], Nuno F. Rodrigues[2,3], Patrícia Maciel[1], João L. Vilaça[1,2]

[1]Life and Health Sciences Research Institute - University of Minho 4710-057 Braga, Portugal

[2]DIGARC, Polytechnic Institute of Cávado and Ave, 4750-810 Barcelos, Portugal

[3]DI-CCTC University of Minho 4710-057 Braga, Portugal

e-mail: accastro@ecsaude.uminho.pt; nunodias@ecsaude.uminho.pt; pedrorodrigues@ecsaude.uminho.pt; joaooliveira@ecsaude.uminho.pt; nfr@di.uminho.pt; pmaciel@ecsaude.uminho.pt; joaovilaca@ecsaude.uminho.pt.

Abstract

Protein aggregation became a widely accepted marker of many polyQ disorders, including Machado-Joseph disease (MJD), and is often used as readout for disease progression and development of therapeutic strategies. The lack of good platforms to rapidly quantify protein aggregates in a wide range of disease animal models prompted us to generate a novel image processing application that automatically identifies and quantifies the aggregates in a standardized and operator-independent manner. We propose here a novel image processing tool to quantify the protein aggregates in a *Caenorhabditis elegans* (*C. elegans*) model of MJD. Confocal microscopy images were obtained from animals of different genetic conditions. The image processing application was developed using *MeVisLab* as a platform to process, analyse and visualize the images obtained from those animals. All segmentation algorithms were based on intensity pixel levels.The quantification of area or numbers of aggregates per total body area, as well as the number of aggregates per animal were shown to be reliable and reproducible measures of protein aggregation in *C. elegans*. The results obtained were consistent with the levels of aggregation observed in the images. In conclusion, this novel imaging processing application allows the non-biased, reliable and high throughput quantification of protein aggregates in a *C. elegans* model of MJD, which may contribute to a significant improvement on the prognosis of treatment effectiveness for this group of disorders.

Keywords— C. elegans, image processing, quantification of aggregates

Introduction

Machado-Joseph disease (MJD) is a neurodegenerative disorder caused by the expansion of a polyglutamine (polyQ) tract within the C-terminal of the ataxin-3 protein [1]. The leading hypothesis concerning the pathogenesis of polyQ diseases is that the expanded polyQ tract confers a toxic gain-of-function to the mutant proteins. These disease proteins acquire the ability to self associate and form aggregates, which ultimately constitute nuclear and cytoplasmic inclusion bodies. The presence of protein aggregates in specific affected regions of the patient's brain and of the majority of animal and cell disease models is a common feature of many polyQ disorders, including MJD. So, protein aggregation became a widely accepted disease marker and is often used as readout for the development of therapeutic strategies for this group of disorders.

Until now authors have been studying aggregation phenotypes based on qualitative observations [2], by counting aggregates manually on a limited cell sample or neuronal subtypes [3-5]; or recreating diseases through mutant proteins expression in non-neuronal tissues to simplify quantification [6, 7]. To improve productivity and diagnostic ability, from precise, fast, repeatable and objective measurements, image processing techniques could play an important role in the biological domain. There are several strategies for segmenting and quantifying images in literature. Ta et al. [8] presented a framework of graph-based tools for the segmentation of electron microscopic cellular images, which rely on a general formulation of discrete functional regularization on weighted graphs of arbitrary topology. Yu and Tan [9] used an object density-based image segmentation methodology, which incorporates segmentation techniques based on intensity, edge and texture. The object of interest was segmented by a watershed algorithm. A marker-controlled algorithm is used to avoid over segmentation results.

The lack of reliable platforms, to rapidly quantify aggregates in a wide range of disease animal models, prompted us to develop a novel image processing application (Fig. 1) that simultaneously identifies and quantifies the protein aggregates (number and total area). Recent data from our lab has shown that MJD can be properly modelled in *Caenorhabditis elegans* (*C. elegans*). In our animal model, expression of ataxin-3 in all 302 neuronal cells, with different Q-lengths, results in a consistent pattern of neuronal cell-type specific aggregation. Next, we have studied the impact of aging and of reprogramming animals' survival in our model. It was found that disrupting key genes of the insulin signalling (*daf-16*) and of the heat-shock response (*hsf-1*) pathways led to a significant aggravation in motor neuron dysfunction of these animals (Teixeira-Castro, *in preparation*). Here, we have developed a novel image processing application, using *MeVisLab* [10] as a platform to process, analyse and quantify the images obtained from those animals. All segmentation algorithms were based on intensity pixel levels. The quantification of the aggregates in the *C. elegans* model was shown to be reliable

and reproducible. Furthermore, using this application, we have found that the motor defect presented by the animals correlated with a significant aggravation of the aggregation phenotype.

In conclusion, we have generated a tool that permits a non-biased quantification of protein aggregates in many animal models of conformational disorders and that may facilitate high-throughput studies in the search for modifiers of protein aggregation.

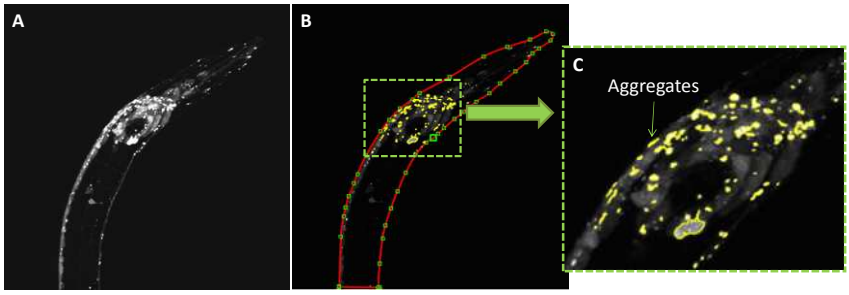

Figure 1 - Overview of the quantification of aggregates in *C. elegans*: (A) Image of the *C. elegans* acquired by confocal microscopy; (B) *C. elegans* outside perimeter (red) and segmented aggregates (yellow); and, (C) detail of the aggregates segmentation (yellow) area.

Methods

This section briefly presents how *MeVisLab* is being used as a platform for process, analysis and visualization of the described strategy.

The perimeter and area of *C. elegans* and its aggregates were determined by linking several *MeVisLab* modules (MM). An overview of the different method stages is given in Fig. 2: a) noise reduction and automatic selection of the region of interest (ROI); b) *C. elegans* outer perimeter determination; c) aggregates segmentation and delimitation; and, d) aggregates quantification.

Noise Reduction and Automatic Selection of ROI

The aims of this section were: reduction of the image noise contamination, image enhancement and automatic ROI selection for further processing. Due to the emission and detection of light in confocal microscopy image creation, noise is always present. The meaningful information of an image object can be lost if noise level is too high compared with object intensity.

All *C. elegans* images were acquired with an Olympus FV1000 confocal microscope (Japan) in RGB format. These input images were firstly converted to grayscale values using the *OrthoProjection*MM. The grayscale image was input to *ConstrainedConnectionCost* MM that calculates 2D connection cost of image pixels. This algorithm fills all the local valleys in grayscale input image,

producing uniformity in the output image intensity. Such output was used for ROI selection, by removing the existing noise around the *C. elegans*. The automatic ROI selection was achieved with the following steps:

a) Image enhancement with four image morphological transformations (two erosions followed by two dilations, using 3x3 and 5x5 kernel masks) through *Morphology* MM;
b) Estimation of neighbourhood relation between foreground (protein aggregates) and background using the *ConnectedComponents* MM;
c) Automatic calculation of a bounding box (using the *BoundingBox* MM) that groups all pixels within a given grey level interval. Therefore, it was created a bounding box around the *C. elegans* object;
d) ROI assessment, using the *DimensionSliceClone* and *MergeRegions*MMs, creates an output image with the same world coordinates as in the input image from the bounding box.

A Gaussian filter was implemented as a new MM to reduce the ROI noise [11].

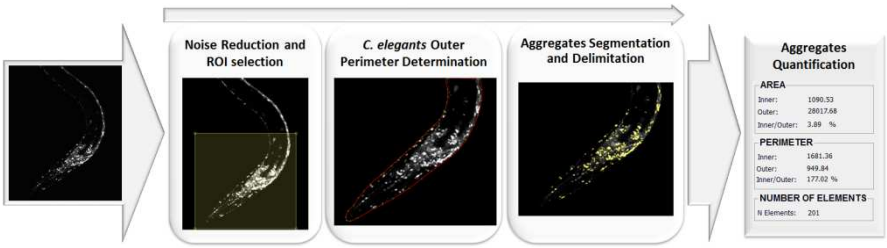

Figure 2 - Block diagram of the *C. elegans* image processing algorithm.

C. elegans Outer Perimeter Determination

Outcome of ROI is input to a threshold algorithm in order to determine the outer *C. elegans* perimeter and inner area. The output of these steps is a binary image, where the entire *C. elegans* object is represented at white and the remaining image as black.

Then, the external contour was performed through the application of a contour-based shape representation and description, using an 8-connectivity derivative Freeman Chain Code [12]. This method is based on the fact that an arbitrary curve is represented by a sequence of small unit length vectors and by a predefined set of possible directions. The chain code uses a numbered sequence that represents relative directions of boundary points selected in a counter-clockwise 45º direction changes. The application of Freeman Chain Code result is a two dimensional space organized boundary of the segmented image.

The developed application also allows manual sub-ROI delimitation. This option allows the user to select smaller portions of the *C. elegans* for more specific

analysis (see Fig. 2).This is optional, and is applied immediately before the steps of the algorithm described in this section.

Aggregates Segmentation and Delimitation

The aggregates have higher levels of intensity than soluble protein and of potential auto-fluorescence arising from the *C. elegans* gut. So the method chosen for its segmentation was based on intensity levels. Therefore, the ROI outcome is input to a *Morphology* and *Mask* MM. These modules allow a sub-region selection by applying a binary mask (fluorescent protein in the *C. elegans* nervous system is represented in white and the remaining image appears black). It avoids undesirable artefacts in the segmentation, caused by surrounding spot noise. This sub-region is input to a *CSOIsoGenerator* MM that determines all protein contours based on an iso value. This value is controlled in the user interface. The output of this module is an image with the aggregates in white, contours at yellow and the remaining image in black.

The *CSOIsoGenerator* MM was linked to *CSOManager* MM module, which stores the *CSOIsoGenerator* MM contours information. The numerical quantification of the contours, such as contours (aggregates) number, perimeter and area of each contour, is determined by *CSOInfo*MM that acquires all the information from the *CSOManager* MM output.

Aggregates Quantification

The quantification of protein aggregates in *C. elegans* is performed through the following indicators:

- Percentage of aggregates area on animal area- PAgAn_{area}:

$$\mathrm{PAgAn}_{area} = \frac{\sum_{i=1}^{n\_aggregates} Ag_{area}(i)}{An_{area}} x100 \quad (1)$$

  Where, $n\_aggregates$ is the number of aggregates, $Ag_{area}(i)$ is the area of aggregate and An_{area} is the animal area.

- Percentage of the number of aggregates on animal area - $\mathrm{PNAgAn}_{\mathrm{area}}$:

$$\mathrm{PNAgAn}_{\mathrm{area}} = \frac{n\_aggregates}{An_{\mathrm{area}}} x100 \quad (2)$$

User Interface

A user interface was developed to enable fast modification of computing parameters. This interface allows the user to:

- Navigate through a list of image files with different formats from the contents of a specified directory;
- Select a square subarea of interest from an input image;
- Control all computed parameters as the aggregates threshold level;
- Select the ROI of protein aggregates
- Edit contours of the object of interest by moving, copying, pasting and performing undo/redo operations;
- Visualize and save to a data file all the segmentation results.

Results

In order to evaluate genes with potential to modify protein aggregation, we have analysed at least six confocal input images of each genotype in our novel *C. elegans* image processing application. Analysis of day 1 animals, showed that the absence of *hsf-1* significantly increased (*i*) the area of aggregates divided by the total area of each animal, (*ii*) the number of aggregates per total area and also (*iii*) the absolute number of aggregates; whereas mutation in *daf-16* had a milder impact in the mutant ataxin-3 aggregation. A *Kolmogorov-Smirnov* normality test was applied on the three quantification variables and their results suggest non-significant differences to normality at 95% confidence (p=0,63; p=0,36; p=0,64).

Specifically, *hsf-1* mutation caused a statistical significant increase in the mean ratio of area of aggregates (*inner area* of the user interface) to the total area (*outer area* of the user interface) (*Bonferroni* mean comparison test, $p=2{,}02\times10^{-4}$) (Fig. 3a). Similarly, there was a significant increase in mean ratio of the number of aggregates to the total area and in the absolute number of aggregates (*number of elements* of the user interface) (*Bonferroni* test, $p=9{,}3\times10^{-5}$ and $p=3{,}14\times10^{-5}$, respectively) (Fig. 3b, c). The results were in agreement with our previous qualitative image observations (Teixeira-Castro, A. *in preparation*). Equally, knockout of *daf-16* gene caused a significant increase in the number of aggregates per unit area and in the absolute number of aggregates (*Bonferroni* test, p=0,03 and p=0,01, respectively), when compared with control AT3q130 animals (Fig. 3b, c). Although there is a tendency to an increase in the mean ratio of aggregates' area to the total area of the animal, this did not reach statistical significance. This result is in accordance with our previous qualitative observations that showed that *daf-16* has a mild impact in aggregation, especially in early stages of the disease. Additionally, the genotypes seem to be better differentiated by combining to aggregation measures: number of aggregates and the ratio of aggregates' area to the total animal area (Fig. 4). It is of great importance to highlight that, at day 1, number of aggregates and aggregates' area per unit area seem to present a linear

correlation (Fig. 4). We expect that further protein accumulation, as seen in older animals, will result in an increase of area of aggregates without significant further increase in the absolute number of aggregates.

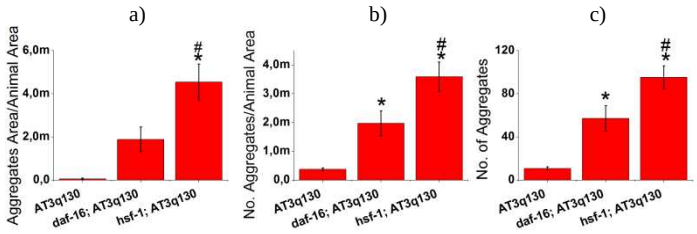

Figure 3 – Genotypes comparison according to a) the mean ratio of protein aggregates' area to the total animal area, b) the mean ratio of the number of protein aggregates to the total animal area, and c) the absolute number of protein aggregates. * indicates significant mean difference between either *hsf-1*;AT3q130 or *daf-16*;AT3q130 and AT3q130 genotype; # indicates significant difference between *hsf-1*;AT3q130 and *daf-16*;AT3q130 (applying *Bonferroni* correction with 95% confidence intervals).

hsf-1 mutation caused a major aggravation of the ataxin-3 aggregation profile, since this transcription factor is the main regulator of protein folding and proteotoxic stress in cells. *daf-16* is primarily involved in other stress types. Accordingly, quantification of the aggregates showed a statistical significant difference between the impact of the absence of *hsf-1* and *daf-16* on ataxin-3 aggregation profile, being the *hsf-1;* AT3q130 animals severely affected (*Boferroni* Test, #, p=0,017 (a), p=0.030 (b), p=0.032 (c)).

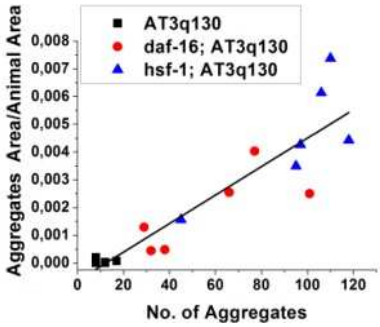

Figure 4 – Scatter plot of the number of aggregates and the mean ratio aggregates' area to the total animal area for all animals.

Conclusions

Whether protein aggregates are a cause or a result of cellular degeneration is still a controversial issue. In either case, quantification of these protein aggregates is used to evaluate the effect of gene and drug therapies for many conformational disorders, such as MJD. As so, this novel imaging processing application, which allows non-biased, reliable and high throughput quantification of protein aggregates, may contribute to a significant improvement on the prognosis of treatment effectiveness for these group of disorders.

The aggregates quantification was standardized by selecting a threshold level (the same value for all the animals analyzed) avoiding the manual counting of all aggregates. Moreover, it was also possible to select some image sub-regions to quantify the *C. elegans* outer contour.

The newly developed application proves to be a valuable tool by decreasing the total number of decisions, time-consumption and user dependence, while increasing the segmentation's efficiency and robustness.

Acknowledgements

The authors acknowledge to Foundation for Science and Technology (FCT) - Portugal for the fellowships with the references: SFRH/BD/27258/2006; SFRH/BPD/51058/2010; SFRH/BPD/66151/2009; and, SFRH/BPD/46851/2008. This work was also supported by FCT R&D project PTDC/SAU-BEB/103368/2008 and through a grant from National Ataxia Foundation (2010).

References

[1] O. Riess, U. Rüb, A. Pastore, P. Bauer, e L. Schöls, "SCA3: neurological features, pathogenesis and animal models," *Cerebellum (London, England)*, vol. 7, n. 2, pp. 125-137, 2008.

[2] L. A. Khan, P. O. Bauer, H. Miyazaki, K. S. Lindenberg, B. G. Landwehrmeyer, e N. Nukina, "Expanded polyglutamines impair synaptic transmission and ubiquitin-proteasome system in Caenorhabditis elegans," *Journal of Neurochemistry*, vol. 98, n. 2, pp. 576-587, Jul. 2006.

[3] L. J. Corcoran, T. J. Mitchison, e Q. Liu, "A novel action of histone deacetylase inhibitors in a protein aggresome disease model," *Current Biology: CB*, vol. 14, n. 6, pp. 488-492, Mar. 2004.

[4] M. Skogen, J. Roth, S. Yerkes, H. Parekh-Olmedo, e E. Kmiec, "Short G-rich oligonucleotides as a potential therapeutic for Huntington's Disease," *BMC Neuroscience*, vol. 7, p. 65, 2006.

[5] A. Kitamura et al., "Cytosolic chaperonin prevents polyglutamine toxicity with altering the aggregation state," *Nature Cell Biology*, vol. 8, n. 10, pp. 1163-1170, Out. 2006.

[6] J. F. Morley, H. R. Brignull, J. J. Weyers, e R. I. Morimoto, "The threshold for polyglutamine-expansion protein aggregation and cellular toxicity is dynamic and influenced by aging in Caenorhabditis elegans," *Proceedings of the National Academy of Sciences of the United States of America*, vol. 99, n. 16, pp. 10417-10422, Ago. 2002.

[7] S. M. Garcia, M. O. Casanueva, M. C. Silva, M. D. Amaral, e R. I. Morimoto, "Neuronal signaling modulates protein homeostasis in Caenorhabditis elegans post-synaptic muscle cells," *Genes & Development*, vol. 21, n. 22, pp. 3006-3016, Nov. 2007.

[8] V. Ta, O. Lézoray, A. Elmoataz, e S. Schüpp, "Graph-based tools for microscopic cellular image segmentation," *Pattern Recognition*, vol. 42, n. 6, pp. 1113-1125, Jun. 2009.

[9] J. Yu e J. Tan, "Object density-based image segmentation and its applications in biomedical image analysis," *Computer Methods and Programs in Biomedicine*, vol. 96, n. 3, pp. 193-204, Dez. 2009.

[10] "The ML Programming Guide - Programming Object-Oriented Image Processing with the MeVis Library," MeVis Medical Solutions, 2010.

[11] T. S. Yoo, *Insight into images: principles and practice for segmentation, registration, and image analysis*, 1.º ed. A K Peters, Ltd., 2004.

[12] H. Freeman, "Computer Processing of Line-Drawing Images," *ACM Comput. Surv.*, vol. 6, n. 1, pp. 57-97, 1974.

Chapter 3

Opposing effects of distinct aging-related pathways in mutant ataxin-3-mediated pathogenesis

Opposing effects of distinct aging-related pathways in mutant ataxin-3-mediated pathogenesis.

Andreia Teixeira-Castro[1,2,3], Ana Jalles[1,2], Andreia Neves-Carvalho[1,2], Richard I. Morimoto[3] and Patrícia Maciel[1,2]

[1]Life and Health Sciences Research Institute (ICVS), School of Health Sciences, University of Minho, 4710-057 Braga, Portugal; ; [2]ICVS/3B's - PT Government Associate Laboratory, Braga/Guimarães, Portugal; [3]Department of Molecular Biosciences, Northwestern University Institute for Neuroscience, Rice Institute for Biomedical Research, Northwestern University, Evanston, IL 60208.

Abstract

In *Caenorhabditis elegans* mutations reducing Insulin/IGF-1-like signaling ameliorate aberrant protein aggregation and neuronal dysfunction, associated with numerous neurodegenerative diseases, including Machado-Joseph disease. To understand how cellular mutations associated with increased longevity protect against disease, we employed *C. elegans* ataxin-3 aggregation models. Here, we found that distinct aging-related pathways exhibited opposing effects. Dietary restriction-induced longevity had no major effect against proteotoxicity in the neuronal cells. In turn, mutations leading to altered mitochondrial function showed heterogeneous effects: deletion of *clk-1*, which encodes a mitochondrial hydroxylase that is necessary for the biosynthesis of ubiquinone, aggravated the disease phenotype, whereas mutation in the mitochondrial complex III subunit gene *isp-1* led to a clear protection. Our data suggests that, although globally improving organism survival, manipulation of aging-related pathways may not always impact positively in the context of a neurodegenerative disease.

Introduction

Late onset human neurodegenerative diseases including Parkinson's, Alzheimer's and Huntington's disease and several spinocerebellar ataxias are associated with abnormal protein folding, aggregation and toxicity (1-3). In Spinocerebellar ataxia type 3 or Machado-Joseph disease (MJD), the formation of mutant ataxin-3 (ATXN3) aggregates is associated to disease through an unknown mechanism (reviewed in (3). In fact, the pathogenic mechanism(s) are not clear for any of afore mentioned conformational disorders. However, several commonalities have been identified. For example, all diseases cause cellular dysfunction and degeneration; all are associated with protein misfolding and aggregation. Most of the diseases have hereditary and sporadic forms and all show delayed onset, with symptoms appearing usually late in adulthood. Thus, aging has been suggested as a major risk factor for the development of these diseases and mitochondria were proposed to have a central contribution through the accumulation of mitochondrial DNA mutations and increased production of reactive oxygen species (ROS) (4, 5). Moreover, longevity genes appeared in several genetic screens as modulators of age-at-onset and disease progression (6-8).

Perhaps the most relevant pathway that controls longevity in worms, flies and mammals is the Insulin/insulin growth factor (IGF)-1-like signaling (IIS) pathway. In *C. elegans* the binding of an as yet unidentified ligand to DAF-2 (9), the sole IGF-1 receptor, activates IIS. DAF-2 dimerization and self-phosphorylation leads to AGE-1 recruitment and to the activation of the AKT family of kinases (10). This pathway culminates in DAF-16 (11-13) phosphorylation, preventing its translocation into the nucleus, where it would otherwise activate the expression of its target genes that regulate youthfulness, longevity and stress resistance (14). Mutation in *age-1* increases *C. elegans* lifespan in 65% and the animals show increased thermotolerance (15) and resistance to oxidative stress (16).

The transcription regulator heat shock factor-1 (HSF-1) is also critical for the longevity functions of IIS, and increased HSF-1 expression extends worms' lifespan in a *daf-16* dependent manner. HSF-1 regulates the expression of many molecular chaperones, which assist protein conformation and stability during synthesis, folding, translocation, protein complex assembly and degradation (17-19). Under stress conditions, such as heat shock, heat shock proteins (HSPs) become more abundant and counteract the deleterious effects of protein misfolding. Intriguingly, chronic expression of aggregation-prone proteins seems to not consistently activate the heat shock response in affected cells (20-22), even though modifications in the chaperone network were shown to be beneficial to disease progression (23-26).

Other gerontogenes were, however, identified that regulate lifespan (27). Interestingly, reduced dietary intake or altered mitochondrial function can also increase longevity via signaling mechanisms that are genetically regulated and autonomous (reviewed in (27). These pathways have been found to regulate longevity in *C. elegans* and in mice, suggesting an evolutionary conserved mechanism for lifespan determination.

Dietary restriction (DR) was the first metabolic treatment found to extend lifespan of an organism (28). When the available food is below the *ad libitum* amount (typically 40% less) lifespan increases. Recent studies

performed in *C. elegans* revealed that the transcription factors PHA-4 (29) and SKN-1 (30) have critical roles in enabling DR to mediate longevity. In addition, it was found that altering mitochondrial function and proper control of ROS production could substantially increase longevity. Decreasing the activity of the electron transporter chain (ETC) with RNA interference directed to the ETC complexes I, III, IV and V resulted in ~40% life extension (31-33).

Aggregation and toxicity of disease-associated misfolded prone proteins, such as huntingtin and Aβ peptide, is enhanced during aging. Downregulation of the IIS pathway and DR increase lifespan and suppress proteotoxicity of polyQ expansion proteins and Aβ peptides in the *C. elegans* body wall muscle cells and in mice (34-38). However, the molecular mechanisms underlying this protection remain unclear.

Our recent data reveals that the IIS and HSF-1 pathways suppress mutant ATXN3-mediated phenotypes in *C. elegans* neuronal cells (39). Here, we have studied the impact of other aging-related pathways in our model for ATXN3 pathogenesis. Our preliminary results show that genetically increasing lifespan in worms may have opposing effects in disease progression, depending on the aging-related pathway that is being targeted.

Results

Reduced dietary intake had limited effect in mutant ataxin-3-mediated neuronal toxicity

To gain further insight into how extended longevity reduces aberrant protein aggregation, we inquired whether other aging-related pathways, independent of the IIS pathway, would impact positively to retard or prevent neurodegenerative diseases. We tested the effects of dietary restriction (DR) by employing a genetic model. For that we crossed AT3q130 (39) expressing animals into a loss-of-function allele (*ad1113*) of *eat-2*. *eat-2* mutants have defects in pharyngeal pumping and an adult lifespan 29-57% longer than wild-type animals (40). However, we saw no major differences regarding AT3q130 aggregation (Fig. 1A) in live neuronal cells or in motor dysfunction (Fig. 1B), when food intake was reduced (*eat-2*; AT3q130). Thus, the pathogenesis caused by mutant ATXN3 expression in *C. elegans* is not rescued by DR-induced longevity, when the toxic ATXN3 proteins are expressed in neuronal cells.

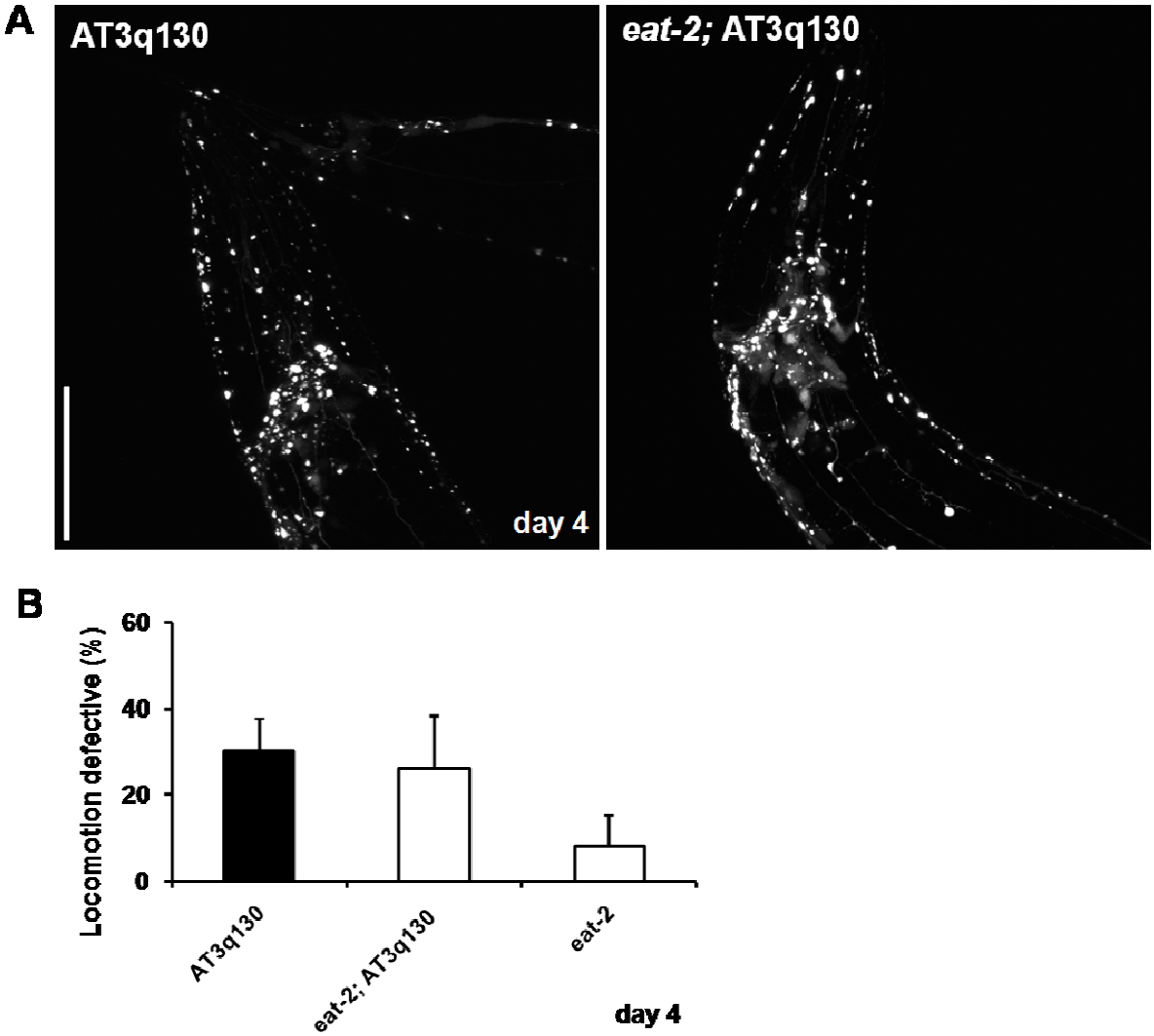

Figure 1. Genetic model of dietary restriction (*eat-2*) did not influence mutant ataxin-3-mediated pathogenesis in the *C. elegans* nervous system. *eat-2* mutation did not modulate aggregation (A) or locomotion defects (B) of AT3q130 animals at day 4 post-hatching. Flattened Z-stacks of AT3q130 and *eat-2*; AT3q130 animal heads.

Scale bar, 50 μm. Pictures were obtained using an Olympus FV1000 confocal microscope (A). Motility data (B) is the mean ± SD, at least 200 animals per data point. Student's *t*-test, p=0.59 (*eat-2*; AT3q130 vs. AT3q130).

Opposing effects of *isp-1* and *clk-1* –mediated increased longevity on ataxin-3 pathogenesis

Next, we tested whether mutations that alter mitochondrial function and increase *C. elegans* lifespan ameliorated ATXN3 pathogenesis. *isp-1(qm150)* mutants carry a missense mutation in the "Rieske" iron sulfur protein of complex III of the mitochondria ETC that leads to a large decrease in oxygen consumption and a significant increase in longevity (41). *isp-1* animals show slow development and behaviors, which precluded the assessment of neuronally regulated motility defects. However, mutation in the *ISP-1* gene highly suppressed AT3q130 aggregation in the *C. elegans* nervous system over a 4-day period (Fig. 2A, B). Since *isp-1* animals showed a clear developmental delay when compared to AT3q130 animals in a WT background, we have compared both day 4 post-hatching animals and young adult staged AT3q130 and *isp-1(qm150)*; AT3q130 animals. In the background of the *isp-1* mutation, AT3q130 animals took ~2.5 days longer to reach adulthood at 20ºC, and there was a clear suppression in the aggregation phenotype (data not shown).

clk-1 encodes an enzyme that is required for the biosynthesis of ubiquinone (UQ), a natural antioxidant that functions as a redox cofactor in the mitochondrial ETC and in the cytoplasm of cells (42-46). When *clk-1* is absent, worms become long lived probably due to a reduction in endogenous ROS production, mediated by the accumulation of demethoxyubiquinone (DMQ), a biosynthetic precursor and analog that functionally replaces UQ. Unexpectedly, the strong deletion *qm30* allele, which consists in a 590-base pair deletion encompassing the entire last exon of CLK-1 (47, 48), caused a great enhancement of mutant ATXN3 aggregation (Fig. 2A, C).

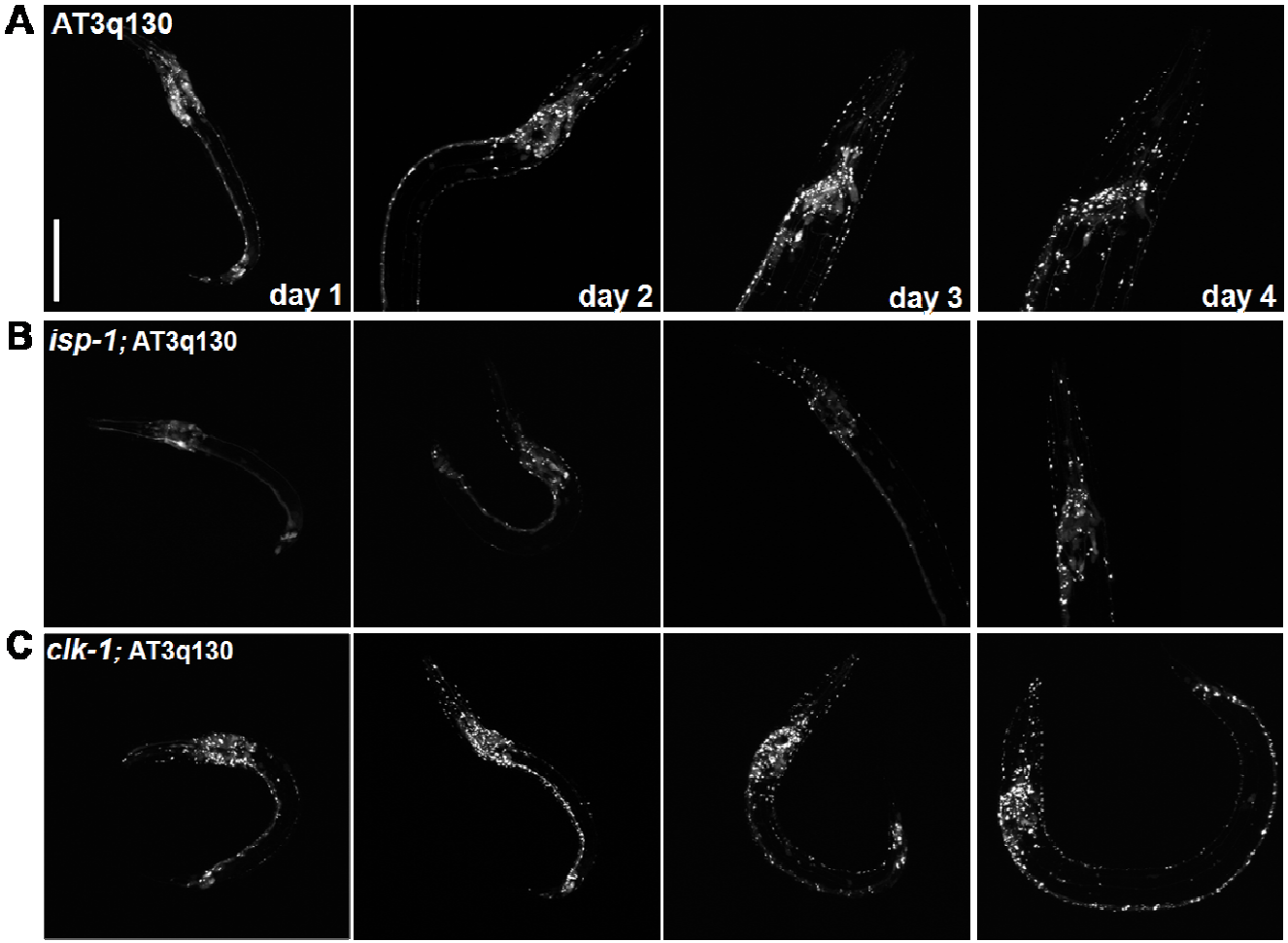

Figure 2. Mutations in *ISP-1* and *CLK-1* genes that increase life span modulated mutant ataxin-3-mediated proteotoxicity in *C. elegans*. Flattened z-stacks of AT3q130 (A), *isp-1*; AT3q130 (B) and *clk-1*; ATq130 animals were grown at 20°C for 4 days. The mutation *isp-1(qm150)* clearly reduced AT3q130-mediated aggregation, whereas in the background of *clk-1(qm130)* deletion there was an increase in aggregation of the AT3q130 animals. For both mutations, changes in aggregation were detected since early stages of development and occurred throughout the nervous system. Scale bar, 50 µm. All pictures were obtained using an Olympus FV1000 confocal microscope.

Next, we tested whether *isp-1* and *clk-1* mutations extended the life span of AT3q130 worms. *isp-1*; AT3q130 and *clk-1*; AT3q130 animals, grown at 20ºC, exhibited increased life spans compared with AT3q130 (Fig. 3), similar to previous results with WT *C. elegans* (41, 47) (Fig. S1).

These findings suggest that direct modulation of aging-related pathways, that increase organism survival, may not always impact positively in aging-associated neurodegenerative processes.

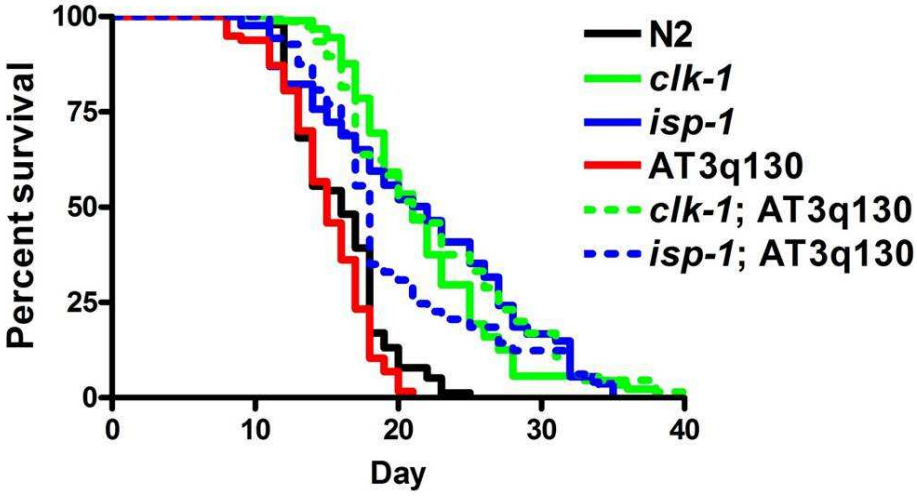

Figure 3. *isp-1* and *clk-1* mutations increased lifespan of AT3q130 animals. Lifespan measurements of wild-type (N2), mutant (*isp-1* and *clk-1*), transgenic (AT3q130) and double mutant (*isp-1*; AT3q130, *clk-1*; AT3q130) grown at 20°C. *isp-1*; AT3q130 and *clk-1*; AT3q130 animals showed increased survival when compared to AT3q130 ($p=0.0001$ and $p<0.0001$, respectively; Kaplan-Meyer analysis) and WT N2 worms ($p<0.0001$ for both comparisons, Kaplan-Meyer analysis). Two independent trials gave similar results (N>75, per experiment).

Discussion

Increased longevity has been associated with prevention of a wide array of diseases, aging-dependent deterioration and stress resistance. Here, we addressed the impact of aging as a major risk factor for neurodegenerative diseases, using a *C. elegans* model for ATXN3 pathogenesis. Our initial observations led us to the surprising finding that mutations that augment individual survival may have opposing effects on disease progression in *C. elegans*. This study provides the fist *in vivo* evidence for the fact that creating therapeutics that target aging-related pathways to circumvent the aging process, may not always impact positively in age-related conformational disorders.

The IIS pathway modulates many forms of toxic protein aggregation, such as the aggregation of Aβ peptides (35, 37), polyQ-alone, ataxin-3 and huntingtin proteins (34, 39, 49, 50), suggesting that this pathway may be a well conserved and non-specific detoxifying mechanism acting on the cell environment. *daf-2* and *age-1* adult animals exhibit extreme longevity phenotypes (10, 51), and resistance to stress. They are specifically resistant to hyperoxia and paraquat (52), as well as UV (53) and thermal stress (15). The increased thermotolerance of *age-1* animals is thought to be due to increased activation of the heat-sock response and higher accumulation of HSP16 (15). Additionally, it has been shown that a small disturbance in proper protein-folding homeostasis has a great impact on individual integrity (54), demonstrating that the protective mechanisms regulated by IIS pathway may link survival to proteostasis. A recent study added the fact that a general failure in protein homeostasis occurs at early stages of adulthood in *C. elegans*, and overlaps with a severe reduction on the ability of cells to activate the heat-shock and unfolded protein responses (55). This proteostasis collapse represents an early molecular event in aging that may potentiate the onset of many heritable age-dependent diseases (55).

Based in all these evidence and in our MJD studies in *C. elegans*, we propose a model for the effect of the distinct longevity pathways in neurodegenerative diseases: among the manipulations that improve general organism survival, only those that improve the folding capacity in cells may have a positive impact in age-associated conformational disorders (Fig. 4).

DAF-16 and HSF-1 regulated transcriptomes result in the expression of numerous chaperones (49, 56), and in fact we saw that both genes are potent suppressors of mutant ATXN3 aggregation and neuronal dysfunction (39).

According to the free radical theory of aging, macromolecules damage from ROS is the cause of aging and perhaps of many aging-related pathologies (57, 58). In MJD, it was proposed that increased oxidative stress, as a consequence of aging, increases mutant ataxin-3 nuclear localization and pathology (59). This theory of aging has been extensively tested in many organisms and because of that there have been many experiments that support it, but there are also data which challenge the notion that molecular damage leads to aging (reviewed in (60).

Proper control of ROS production, via modulation of mitochondrial activity, has also been shown to increase lifespan in *C. elegans*. In fact, *isp-1* and *clk-1* mutants show increased longevity through mechanism(s) that are still not well understood (61). Nevertheless, both mutants are characterized by slow development, slow defecation rate and decreased brood size (41, 47, 62), which is characteristic of altered mitochondrial function. Specifically, mutation in *ISP-1* was shown to lead to a decrease in oxygen consumption and severe reduction in electron transport (41), without affecting ATP levels (63). Several of the phenotypes that accompany increased longevity in *isp-1* (but not lifespan or electron transport) were shown to be significantly suppressed by a mutation in the cytochrome *b1* of complex III (*ctb-1(qm189)*). This compensatory effect suggests that increased longevity is a direct cause of slow electron transport and not a consequence of slow development or reduced fertility. *clk-1* mutants have also decreased complex I-dependent oxidative phosphorylation (64). Surprisingly, the abnormal pool of quinones in *clk-1* mutants did not affect complex II-dependent respiration. Regarding oxidative stress resistance, both mutants are more resistant to paraquat damage that wild-type animals (65), in spite of the reportedly variable levels of detoxifying enzymes (41, 66). In *isp-1* animals sod-3 levels are increased (41), whereas in *clk-1* mutants SOD activity is decreased, when compared to WT controls. Catalase levels are increased in *clk-1* mutants. Carbonylated groups, as a measure of protein damage, are decreased in *clk-1* and *isp-1* young adult animals (65). In fact, lower levels of endogenous ROS could explain the increased resistance to oxidative stress, since increased production of ROS induced by exogenous agents will be better tolerated if endogenous ROS production is low (61). However, recent studies suggest that damage from oxidative stress is not the cause of aging (62, 65). Increasing oxidative damage in *isp-1* mutants to the levels of wild-type animals did not shorten their lifespan (65). Moreover, relative protein damage of aged animals is not different between wild-type and *isp-1* (65).

In spite of this increased resistance to oxidative damage, it is not clear if there is also an increase in thermal stress resistance and increased cellular folding capacity in *isp-1* and *clk-1* mutants. The expression of genes enconding mitochondrial heat shock proteins and HSF-1 was found to be increased in *isp-1(RNAi)* but not in mutant animals (*isp-1(qm150)*) (63). However, it is still not known what happens in a condition of proteotoxic stress. Similarly, an increase in autophagy was only found in the *isp-1(RNAi)* condition (63).

Based on our data, we suggest that *isp-1* animals may have an increased capacity to activate the stress machinery, while *clk-1* mutants may not. In fact, it is known that silencing of the *C. elegans* homolog of mitochondrial Heat shock protein 70, Hsp-6, caused a reduction in the CLK-1 protein levels (67). The mechanism underlying this reduction is not known, however, it is possible that Hsp-6 levels are reduced in *clk-1* mutants as well.

Based on this, we propose that the increase in aggregation of mutant ATXN3 proteins, in the background of *clk-1* loss-of-function, may be due to a decrease in chaperone levels. Whereas the proteotoxic stress caused by chronic expression of mutant ATXN3 in *C. elegans* neurons may activate cellular detoxifying mechanisms in *isp-1* animals and confer protection against disease in our model, further experiments will be

required to clarify this hypothesis. RNAi of *sod-2* caused a decrease in longevity of *isp-1* in opposition to increased longevity of *clk-1* animals (62). This finding supports distinct mechanisms of longevity for these mutants that may reflect upon distinct effects on proteotoxicity.

Recently, links were found between autophagy, as a mechanism that helps to eliminate cellular and protein damaged components, and lifespan extension in worms (68) and aging in mice (69). At least part of the lifespan extension caused by DR requires activation of autophagy. Mutations in *eat-2* improve organism survival and potentiate SOD and catalase activities (70). Unlike other DR models, these mutants are as resistant to heat stress as wild-type animals (71). This data suggested that *eat-2* animals may cope with proteotoxicity similarly to wild-type animals, which could explain why we did see no effect in mutant ATXN3 pathogenesis in *C. elegans* neuronal cells in the background of *eat-2* loss-of-function. In this perspective, it may seem puzzling that in muscle cells *eat-2* dramatically suppresses age-associated paralysis in two nematode models of proteotoxicity (36); however, increased lifespan in a diet-restricted worm depends on a cell non-autonomous signaling (mediated by SKN-1) from central neuronal cells (the ASIs) to non-neuronal body tissues, including body wall muscle cells (30). Moreover, the effects of DR-mediated improved proteotoxicity were highly dependent on HSF-1 (36), sustaining our hypothesis of the importance of the folding capacity of long lived mutants in order to protect against proteotoxic stress.

Although extension of longevity by single genes mutation was first reported many years ago, the precise mechanism(s) underlying this effect remains unsolved. Here, we propose regulation of proteostasis as an important link between longevity and aging-related disorders, not only for the IIS pathway, but for other pathways.

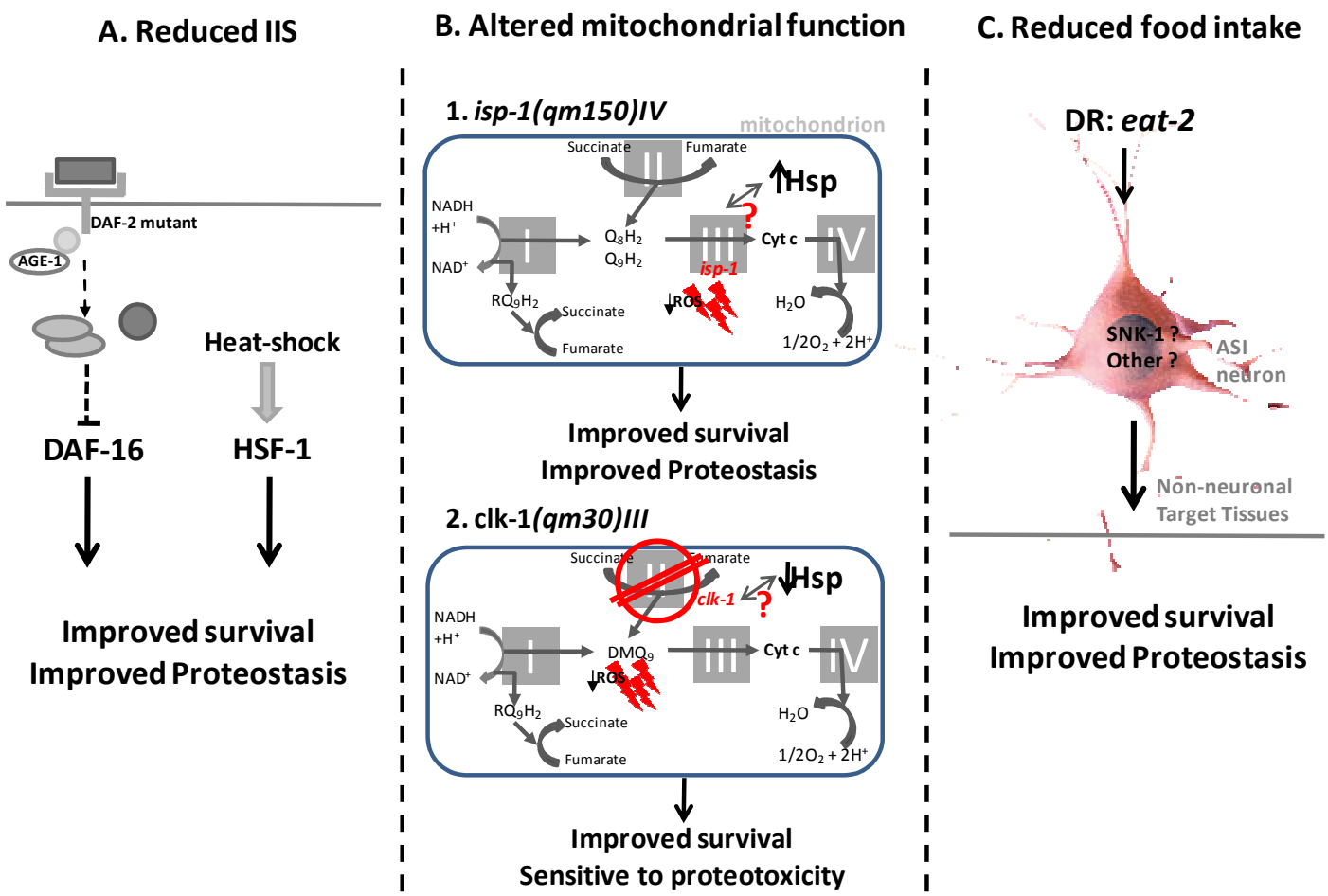

Figure 4. Proposed model relating longevity pathways and age-related conformational disorders. Mutants of the IIS pathway have improved survival and confer protection against proteotoxicity probably through the activation of DAF-16 and HSF-1 transcription factors that regulate proteostasis (A). Mutations that caused alterations in mitocondrial function show opposing effects: *isp-1* mutation improves aggregation of mutant ATXN3, whereas *clk-1* is sensitive to proteotoxic stress (B), possibly through differential activation of components of the proteostasis network. Dietary restriction-mediated improved survival also confers protection to conformational disorders in target non-neuronal tissues (C).

Final considerations

Further experiments are required to complete the initial observations described in this Chapter, that may confirm or reject our hypothesis. A list of future experiments follows:

- Quantify mutant ATXN3 protein levels in the background of *clk-1*, *isp-1* and *eat-2* mutations;
- Verify if the increase in aggregation of mutant ATXN3 is maintained in other *clk-1* deletion alleles;
- Perform clk-1 and isp-1 RNAi and measure ATXN3 aggregation;
- Rescue ATXN3 aggregation phenotype with the WT *CLK-1* gene;
- Determine the mitochondrial (and others) chaperone levels, catalase and SOD activities in all single and double mutants;
- Check activation of Hsp-6::GFP, Hsp-60::GFP, Hsp-4::GFP, Hsp-70::GFP and myo-3::GFPmit reporters in the *isp-1* and *clk-1* mutants/RNAi (always using IIS mutants to compare);
- Evaluate thermotolerance, resistance to paraquat and to tunicamycin of all strains;
- Evaluate levels of ROS in all strains;
- Test other DR protocols;
- Test effect of DR when mutant ATXN3 proteins are expressed in non-neuronal tissues;
- Make use of *ts* mutations to assess folding state in these animals;
- cross ctb-1(qm189); isp-1(q150) into mutant AT3q130 background to assess toxicity and aggregation;
- Test other gerontogenes: sod-2, nuo-6, mev-1, irs-2, etc.
- Perform *Hsf-1* RNAi in *isp-1*;AT3q130 animals
- Perform O/E of HSF-1 in *clk-1*;AT3q130
- Test *clk-1*, *isp-1* and *eat-2* in *C. elegans* models for A-β, tau, Htt, polyQ-alone, SOD1.

Materials and Methods

Nematode strains and general methods. For a list of stains used in this work see Table S1. Nematodes were grown on NGM plates seeded with *Escherichia coli* OP50 strain at 20ºC, according to standard methods (72). Populations were synchronized either by treating young adult animals with alkaline hypochlorite solution (0.5 M NaHO, ~2.6% NaClO) for 7 min (73) or by collecting embryos laid by adult animals within a 3-h period. All animals were scored at the same chronological age, unless stated otherwise. During the reproductive period, animals were moved every day to avoid progeny contamination. Experiments were repeated three to four times. All assays were performed blind.

Confocal imaging. All images were captured either on an Olympus FV1000 (Japan) confocal microscope, under 60x oil objective. One- to four-days-old animals were immobilized with 2 mM levamisole and mounted on a 3% agarose pad. Z-series imaging was taken of all the *C. elegans* lines generated using 514nm laser excitation for YFP fusion proteins. The pinhole was adjusted to 1.0 Airy unit of optical slice and a scan was taken every ~0.5 µm along the Z-axis.

Lifespan. Assays were performed at 20 ºC as previously described (56). Approximately 10 hermaphrodites were culture on each petri dish and were transferred to fresh plates every 1-2 days until the cessation of progeny production and about every 3 days thereafter. Animals were scored as dead if they showed no spontaneous movement or response when prodded. Dead animals that displayed internally hatched progeny, extruded gonad or desiccation were excluded. Statistical analysis was performed using GraphPad Prism version 4 (Kaplan-Meyer analysis).

Motility assay. All assays were performed at room temperature (~22 ºC) on synchronized animals grown at 20ºC. Five 4-days old animals were placed simultaneously in the middle of a freshly seeded plate, equilibrated at 20ºC. Animals remaining inside a one cm circle after 1 min were scored as locomotion defective. A total of 150 animals were scored in at least three independent assays for each strain, and the statistical significance was assessed by Student's *t-test*, as described previously (54).

Funding

This work was supported by grants from Fundação Ciência e Tecnologia (FCT) [PTDC/SAU-GMG/64076/2006, SFRH/BD/27258/2006 to A.T.C., UMINHO/BI/052/2010 to A.J. and SFRH/BD/51059/2010 to A.N.C.] and from Fundação Luso-Americana para o Desenvolvimento (FLAD) [Proj 271/2005]; from the National Ataxia Foundation and from the National Institutes of Health (National Institute of General Medical Sciences, National Institute on Aging) and the Huntington Disease Society of America Coalition for the Cure.

Acknowledgements

We are grateful to members of the Maciel and Morimoto laboratories for sharing reagents, for critical analysis of the data and for their helpful discussions on the manuscript. A special thanks to the Caenorhabditis Genetics Center (CGC), which is funded by the National Institutes of Health - National Center for Research Resources, for some of the nematode strains.

References

1 Selkoe, D.J. (2003) Folding proteins in fatal ways. *Nature*, **426**, 900-904.

2 Ross, C.A. and Tabrizi, S.J. Huntington's disease: from molecular pathogenesis to clinical treatment. *Lancet Neurol*, **10**, 83-98.

3 Riess, O., Rub, U., Pastore, A., Bauer, P. and Schols, L. (2008) SCA3: neurological features, pathogenesis and animal models. *Cerebellum*, **7**, 125-137.

4 Corral-Debrinski, M., Horton, T., Lott, M.T., Shoffner, J.M., Beal, M.F. and Wallace, D.C. (1992) Mitochondrial DNA deletions in human brain: regional variability and increase with advanced age. *Nat Genet*, **2**, 324-329.

5 Andreyev, A.Y., Kushnareva, Y.E. and Starkov, A.A. (2005) Mitochondrial metabolism of reactive oxygen species. *Biochemistry (Mosc)*, **70**, 200-214.

6 Nollen, E.A., Garcia, S.M., van Haaften, G., Kim, S., Chavez, A., Morimoto, R.I. and Plasterk, R.H. (2004) Genome-wide RNA interference screen identifies previously undescribed regulators of polyglutamine aggregation. *Proc Natl Acad Sci U S A*, **101**, 6403-6408.

7 Cohen, E. and Dillin, A. (2008) The insulin paradox: aging, proteotoxicity and neurodegeneration. *Nat Rev Neurosci*, **9**, 759-767.

8 van Ham, T.J., Thijssen, K.L., Breitling, R., Hofstra, R.M., Plasterk, R.H. and Nollen, E.A. (2008) C. elegans model identifies genetic modifiers of alpha-synuclein inclusion formation during aging. *PLoS Genet*, **4**, e1000027.

9 Kimura, K.D., Tissenbaum, H.A., Liu, Y. and Ruvkun, G. (1997) daf-2, an insulin receptor-like gene that regulates longevity and diapause in Caenorhabditis elegans. *Science*, **277**, 942-946.

10 Arantes-Oliveira, N., Berman, J.R. and Kenyon, C. (2003) Healthy animals with extreme longevity. *Science*, **302**, 611.

11 Lin, K., Dorman, J.B., Rodan, A. and Kenyon, C. (1997) daf-16: An HNF-3/forkhead family member that can function to double the life-span of Caenorhabditis elegans. *Science*, **278**, 1319-1322.

12 Ogg, S., Paradis, S., Gottlieb, S., Patterson, G.I., Lee, L., Tissenbaum, H.A. and Ruvkun, G. (1997) The Fork head transcription factor DAF-16 transduces insulin-like metabolic and longevity signals in C. elegans. *Nature*, **389**, 994-999.

13 Lin, K., Hsin, H., Libina, N. and Kenyon, C. (2001) Regulation of the Caenorhabditis elegans longevity protein DAF-16 by insulin/IGF-1 and germline signaling. *Nat Genet*, **28**, 139-145.

14 Murphy, C.T. (2006) The search for DAF-16/FOXO transcriptional targets: approaches and discoveries. *Exp Gerontol*, **41**, 910-921.

15 Lithgow, G.J., White, T.M., Melov, S. and Johnson, T.E. (1995) Thermotolerance and extended life-span conferred by single-gene mutations and induced by thermal stress. *Proc Natl Acad Sci U S A*, **92**, 7540-7544.

16 Larsen, P.L. (1993) Aging and resistance to oxidative damage in Caenorhabditis elegans. *Proc Natl Acad Sci U S A*, **90**, 8905-8909.

17 Hartl, F.U. (1996) Molecular chaperones in cellular protein folding. *Nature*, **381**, 571-579.

18 Morimoto, R.I., Kline, M.P., Bimston, D.N. and Cotto, J.J. (1997) The heat-shock response: regulation and function of heat-shock proteins and molecular chaperones. *Essays Biochem*, **32**, 17-29.

19 Bukau, B. and Horwich, A.L. (1998) The Hsp70 and Hsp60 chaperone machines. *Cell*, **92**, 351-366.

20 Zourlidou, A., Gidalevitz, T., Kristiansen, M., Landles, C., Woodman, B., Wells, D.J., Latchman, D.S., de Belleroche, J., Tabrizi, S.J., Morimoto, R.I. *et al.* (2007) Hsp27 overexpression in the R6/2 mouse model of Huntington's disease: chronic neurodegeneration does not induce Hsp27 activation. *Hum Mol Genet*, **16**, 1078-1090.

21 Satyal, S.H., Schmidt, E., Kitagawa, K., Sondheimer, N., Lindquist, S., Kramer, J.M. and Morimoto, R.I. (2000) Polyglutamine aggregates alter protein folding homeostasis in Caenorhabditis elegans. *Proc Natl Acad Sci U S A*, **97**, 5750-5755.

22 Batulan, Z., Shinder, G.A., Minotti, S., He, B.P., Doroudchi, M.M., Nalbantoglu, J., Strong, M.J. and Durham, H.D. (2003) High threshold for induction of the stress response in motor neurons is associated with failure to activate HSF1. *J Neurosci*, **23**, 5789-5798.
23 Auluck, P.K., Chan, H.Y., Trojanowski, J.Q., Lee, V.M. and Bonini, N.M. (2002) Chaperone suppression of alpha-synuclein toxicity in a Drosophila model for Parkinson's disease. *Science*, **295**, 865-868.
24 Westerheide, S.D., Bosman, J.D., Mbadugha, B.N., Kawahara, T.L., Matsumoto, G., Kim, S., Gu, W., Devlin, J.P., Silverman, R.B. and Morimoto, R.I. (2004) Celastrols as inducers of the heat shock response and cytoprotection. *J Biol Chem*, **279**, 56053-56060.
25 Kieran, D., Kalmar, B., Dick, J.R., Riddoch-Contreras, J., Burnstock, G. and Greensmith, L. (2004) Treatment with arimoclomol, a coinducer of heat shock proteins, delays disease progression in ALS mice. *Nat Med*, **10**, 402-405.
26 Tokui, K., Adachi, H., Waza, M., Katsuno, M., Minamiyama, M., Doi, H., Tanaka, K., Hamazaki, J., Murata, S., Tanaka, F. *et al.* (2009) 17-DMAG ameliorates polyglutamine-mediated motor neuron degeneration through well-preserved proteasome function in an SBMA model mouse. *Hum Mol Genet*, **18**, 898-910.
27 Wolff, S. and Dillin, A. (2006) The trifecta of aging in Caenorhabditis elegans. *Exp Gerontol*, **41**, 894-903.
28 McCay, C.M. (1935) Iodized Salt a Hundred Years Ago. *Science*, **82**, 350-351.
29 Panowski, S.H., Wolff, S., Aguilaniu, H., Durieux, J. and Dillin, A. (2007) PHA-4/Foxa mediates diet-restriction-induced longevity of C. elegans. *Nature*, **447**, 550-555.
30 Bishop, N.A. and Guarente, L. (2007) Two neurons mediate diet-restriction-induced longevity in C. elegans. *Nature*, **447**, 545-549.
31 Dillin, A., Hsu, A.L., Arantes-Oliveira, N., Lehrer-Graiwer, J., Hsin, H., Fraser, A.G., Kamath, R.S., Ahringer, J. and Kenyon, C. (2002) Rates of behavior and aging specified by mitochondrial function during development. *Science*, **298**, 2398-2401.
32 Lee, S.S., Lee, R.Y., Fraser, A.G., Kamath, R.S., Ahringer, J. and Ruvkun, G. (2003) A systematic RNAi screen identifies a critical role for mitochondria in C. elegans longevity. *Nat Genet*, **33**, 40-48.
33 Hamilton, B., Dong, Y., Shindo, M., Liu, W., Odell, I., Ruvkun, G. and Lee, S.S. (2005) A systematic RNAi screen for longevity genes in C. elegans. *Genes Dev*, **19**, 1544-1555.
34 Morley, J.F., Brignull, H.R., Weyers, J.J. and Morimoto, R.I. (2002) The threshold for polyglutamine-expansion protein aggregation and cellular toxicity is dynamic and influenced by aging in Caenorhabditis elegans. *Proc Natl Acad Sci U S A*, **99**, 10417-10422.
35 Cohen, E., Bieschke, J., Perciavalle, R.M., Kelly, J.W. and Dillin, A. (2006) Opposing activities protect against age-onset proteotoxicity. *Science*, **313**, 1604-1610.
36 Steinkraus, K.A., Smith, E.D., Davis, C., Carr, D., Pendergrass, W.R., Sutphin, G.L., Kennedy, B.K. and Kaeberlein, M. (2008) Dietary restriction suppresses proteotoxicity and enhances longevity by an hsf-1-dependent mechanism in Caenorhabditis elegans. *Aging Cell*, **7**, 394-404.
37 Cohen, E., Paulsson, J.F., Blinder, P., Burstyn-Cohen, T., Du, D., Estepa, G., Adame, A., Pham, H.M., Holzenberger, M., Kelly, J.W. *et al.* (2009) Reduced IGF-1 signaling delays age-associated proteotoxicity in mice. *Cell*, **139**, 1157-1169.
38 Duan, W. and Ross, C.A. Potential Therapeutic Targets for Neurodegenerative Diseases: Lessons Learned from Calorie Restriction. *Curr Drug Targets*.
39 Teixeira-Castro, A., Ailion, M., Jalles, A., Brignull, H.R., Vilaca, J.L., Dias, N., Rodrigues, P., Oliveira, J.F., Neves-Carvalho, A., Morimoto, R.I. *et al.* Neuron-specific proteotoxicity of mutant ataxin-3 in C. elegans: rescue by the DAF-16 and HSF-1 pathways. *Hum Mol Genet*.
40 Lakowski, B. and Hekimi, S. (1998) The genetics of caloric restriction in Caenorhabditis elegans. *Proc Natl Acad Sci U S A*, **95**, 13091-13096.
41 Feng, J., Bussiere, F. and Hekimi, S. (2001) Mitochondrial electron transport is a key determinant of life span in Caenorhabditis elegans. *Dev Cell*, **1**, 633-644.

42 Dallner, G. and Sindelar, P.J. (2000) Regulation of ubiquinone metabolism. *Free Radic Biol Med*, **29**, 285-294.
43 Miyadera, H., Amino, H., Hiraishi, A., Taka, H., Murayama, K., Miyoshi, H., Sakamoto, K., Ishii, N., Hekimi, S. and Kita, K. (2001) Altered quinone biosynthesis in the long-lived clk-1 mutants of Caenorhabditis elegans. *J Biol Chem*, **276**, 7713-7716.
44 Jonassen, T., Larsen, P.L. and Clarke, C.F. (2001) A dietary source of coenzyme Q is essential for growth of long-lived Caenorhabditis elegans clk-1 mutants. *Proc Natl Acad Sci U S A*, **98**, 421-426.
45 Hihi, A.K., Gao, Y. and Hekimi, S. (2002) Ubiquinone is necessary for Caenorhabditis elegans development at mitochondrial and non-mitochondrial sites. *J Biol Chem*, **277**, 2202-2206.
46 Levavasseur, F., Miyadera, H., Sirois, J., Tremblay, M.L., Kita, K., Shoubridge, E. and Hekimi, S. (2001) Ubiquinone is necessary for mouse embryonic development but is not essential for mitochondrial respiration. *J Biol Chem*, **276**, 46160-46164.
47 Ewbank, J.J., Barnes, T.M., Lakowski, B., Lussier, M., Bussey, H. and Hekimi, S. (1997) Structural and functional conservation of the Caenorhabditis elegans timing gene clk-1. *Science*, **275**, 980-983.
48 Felkai, S., Ewbank, J.J., Lemieux, J., Labbe, J.C., Brown, G.G. and Hekimi, S. (1999) CLK-1 controls respiration, behavior and aging in the nematode Caenorhabditis elegans. *EMBO J*, **18**, 1783-1792.
49 Hsu, A.L., Murphy, C.T. and Kenyon, C. (2003) Regulation of aging and age-related disease by DAF-16 and heat-shock factor. *Science*, **300**, 1142-1145.
50 Parker, J.A., Arango, M., Abderrahmane, S., Lambert, E., Tourette, C., Catoire, H. and Neri, C. (2005) Resveratrol rescues mutant polyglutamine cytotoxicity in nematode and mammalian neurons. *Nat Genet*, **37**, 349-350.
51 Kenyon, C., Chang, J., Gensch, E., Rudner, A. and Tabtiang, R. (1993) A C. elegans mutant that lives twice as long as wild type. *Nature*, **366**, 461-464.
52 Honda, Y. and Honda, S. (1999) The daf-2 gene network for longevity regulates oxidative stress resistance and Mn-superoxide dismutase gene expression in Caenorhabditis elegans. *FASEB J*, **13**, 1385-1393.
53 Murakami, S. and Johnson, T.E. (1996) A genetic pathway conferring life extension and resistance to UV stress in Caenorhabditis elegans. *Genetics*, **143**, 1207-1218.
54 Gidalevitz, T., Ben-Zvi, A., Ho, K.H., Brignull, H.R. and Morimoto, R.I. (2006) Progressive disruption of cellular protein folding in models of polyglutamine diseases. *Science*, **311**, 1471-1474.
55 Ben-Zvi, A., Miller, E.A. and Morimoto, R.I. (2009) Collapse of proteostasis represents an early molecular event in Caenorhabditis elegans aging. *Proc Natl Acad Sci U S A*, **106**, 14914-14919.
56 Morley, J.F. and Morimoto, R.I. (2004) Regulation of longevity in Caenorhabditis elegans by heat shock factor and molecular chaperones. *Mol Biol Cell*, **15**, 657-664.
57 Beckman, K.B. and Ames, B.N. (1998) The free radical theory of aging matures. *Physiol Rev*, **78**, 547-581.
58 Sohal, R.S., Mockett, R.J. and Orr, W.C. (2002) Mechanisms of aging: an appraisal of the oxidative stress hypothesis. *Free Radic Biol Med*, **33**, 575-586.
59 Reina, C.P., Zhong, X. and Pittman, R.N. Proteotoxic stress increases nuclear localization of ataxin-3. *Hum Mol Genet*, **19**, 235-249.
60 Muller, F.L., Lustgarten, M.S., Jang, Y., Richardson, A. and Van Remmen, H. (2007) Trends in oxidative aging theories. *Free Radic Biol Med*, **43**, 477-503.
61 Hekimi, S. and Guarente, L. (2003) Genetics and the specificity of the aging process. *Science*, **299**, 1351-1354.
62 Van Raamsdonk, J.M. and Hekimi, S. (2009) Deletion of the mitochondrial superoxide dismutase sod-2 extends lifespan in Caenorhabditis elegans. *PLoS Genet*, **5**, e1000361.
63 Yang, W. and Hekimi, S. Two modes of mitochondrial dysfunction lead independently to lifespan extension in Caenorhabditis elegans. *Aging Cell*, **9**, 433-447.

64 Kayser, E.B., Sedensky, M.M., Morgan, P.G. and Hoppel, C.L. (2004) Mitochondrial oxidative phosphorylation is defective in the long-lived mutant clk-1. *J Biol Chem*, **279**, 54479-54486.
65 Yang, W., Li, J. and Hekimi, S. (2007) A Measurable increase in oxidative damage due to reduction in superoxide detoxification fails to shorten the life span of long-lived mitochondrial mutants of Caenorhabditis elegans. *Genetics*, **177**, 2063-2074.
66 Braeckman, B.P., Houthoofd, K., Brys, K., Lenaerts, I., De Vreese, A., Van Eygen, S., Raes, H. and Vanfleteren, J.R. (2002) No reduction of energy metabolism in Clk mutants. *Mech Ageing Dev*, **123**, 1447-1456.
67 Kimura, K., Tanaka, N., Nakamura, N., Takano, S. and Ohkuma, S. (2007) Knockdown of mitochondrial heat shock protein 70 promotes progeria-like phenotypes in caenorhabditis elegans. *J Biol Chem*, **282**, 5910-5918.
68 Jia, K. and Levine, B. (2007) Autophagy is required for dietary restriction-mediated life span extension in C. elegans. *Autophagy*, **3**, 597-599.
69 Zhang, C. and Cuervo, A.M. (2008) Restoration of chaperone-mediated autophagy in aging liver improves cellular maintenance and hepatic function. *Nat Med*, **14**, 959-965.
70 Houthoofd, K., Braeckman, B.P., Lenaerts, I., Brys, K., De Vreese, A., Van Eygen, S. and Vanfleteren, J.R. (2002) No reduction of metabolic rate in food restricted Caenorhabditis elegans. *Exp Gerontol*, **37**, 1359-1369.
71 Houthoofd, K., Braeckman, B.P., Lenaerts, I., Brys, K., De Vreese, A., Van Eygen, S. and Vanfleteren, J.R. (2002) Axenic growth up-regulates mass-specific metabolic rate, stress resistance, and extends life span in Caenorhabditis elegans. *Exp Gerontol*, **37**, 1371-1378.
72 Brenner, S. (1974) The genetics of Caenorhabditis elegans. *Genetics*, **77**, 71-94.
73 Lewis, J.A. and Fleming, J.T. (1995) Basic culture methods. *Methods Cell Biol*, **48**, 3-29.

Supplemental material

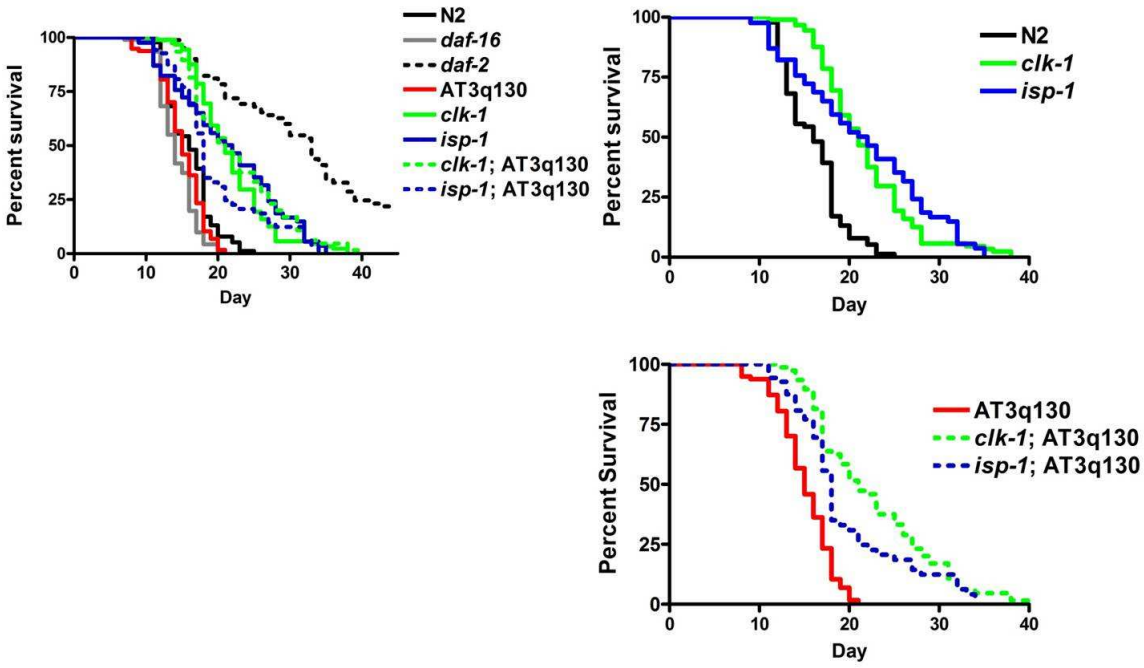

Figure S1. *isp-1* and *clk-1* mutations caused similar lifespan extension in AT3q130 and in WT N2 animals. Lifespan measurements of wild-type (N2), mutant (*isp-1* and *clk-1*), transgenic (AT3q130) and double mutant (*isp-1*; AT3q130, *clk-1*; AT3q130) animals grown at 20°C. Graph (A) shows all the strains: *daf-16* and *daf-2* strains were used as experimental controls. Graphs (B) and (C) highlight data subsets. *isp-1* and *clk-1* mutations increase life span of WT N2 animals (B) and of AT3q130 expressing animals (C) similarly.

Table S1. List of strains used in this work.

Strain (ref)	Abbreviation	Protein	Genotype
AM685 (S1)	AT3q130	AT3q130::YFP	*rmls263[p $_{F25B3.3}$::AT3v1-1q130::yfp]*
AM599 (S1)	AT3q130	AT3q130::YFP	*rmls261[P $_{F25B3.3}$::AT3v1-1q130::yfp]*
CB1370 (S2)	*daf-2*		*daf-2(e1370)III*
CF1038 (S3)	*daf-16*		*daf-16(mu86)I*
MQ887 (S4)	*isp-1*		*isp-1(qm150)IV*
MQ130 (S5)	*clk-1*		*clk-1(qm30)III*
DA1113 (S6)	*eat-2*		*eat-2(ad1113)II*
MAC69	*isp-1;* AT3q130	AT3q130::YFP	*isp-1(qm150)IV; rmls263[P $_{F25B3.3}$::AT3v1-1q130::yfp]*
MAC70	*clk-1;* AT3q130	AT3q130::YFP	*clk-1(qm30)III;rmls263[P $_{F25B3.3}$::AT3v1-1q130::yfp]*
MAC71	*eat-2;* AT3q130	AT3q130::YFP	*eat-2(ad1113)II;rmls261[P $_{F25B3.3}$::AT3v1-1q130::yfp]*

References

S1. Teixeira-Castro A, Ailion M, Jalles A, Brignull HR, Vilaca JL, Dias N, Rodrigues P, Oliveira JF, Neves-Carvalho A, Morimoto RI, Maciel P. Modulation of the Insulin-Signaling and HSF-1 pathways rescues mutant ataxin-3-mediated proteotoxicity in *C. elegans* neurons, *submitted*.

S2. Gems, D., Sutton, A.J., Sundermeyer, M.L., Albert, P.S., King, K.V., Edgley, M.L., Larsen, P.L. and Riddle, D.L. (1998) Two pleiotropic classes of daf-2 mutation affect larval arrest, adult behavior, reproduction and longevity in Caenorhabditis elegans. Genetics, 150, 129-155.

S3. Lin, K., Dorman, J.B., Rodan, A. and Kenyon, C. (1997) daf-16: An HNF-3/forkhead family member that can function to double the life-span of Caenorhabditis elegans. Science, 278, 1319-1322.

S4. Feng, J., Bussiere, F. and Hekimi, S. (2001) Mitochondrial electron transport is a key determinant of life span in Caenorhabditis elegans. Dev Cell, 1, 633-644.

S5. Ewbank, J.J., Barnes, T.M., Lakowski, B., Lussier, M., Bussey, H. and Hekimi, S. (1997) Structural and functional conservation of the Caenorhabditis elegans timing gene clk-1. Science, 275, 980-983.

S6. Lakowski, B. and Hekimi, S. (1998) The genetics of caloric restriction in Caenorhabditis elegans. Proc Natl Acad Sci U S A, 95, 13091-13096.

Chapter 4

Role of wild-type ataxin-3 in Machado-Joseph disease: a study in *C. elegans*.

Role of wild-type ataxin-3 in Machado-Joseph disease: a study in *C. elegans*.

Andreia Teixeira-Castro[1,2,3], Heather Brignull[3], Diogo Ribeiro[1,2], Richard I. Morimoto[3] and Patrícia Maciel[1,2]

[1]Life and Health Sciences Research Institute (ICVS), School of Health Sciences, University of Minho, 4710-057 Braga, Portugal; ; [2]ICVS/3B's - PT Government Associate Laboratory, Braga/Guimarães, Portugal; [3]Department of Molecular Biosciences, Northwestern University Institute for Neuroscience, Rice Institute for Biomedical Research, Northwestern University, Evanston, IL 60208.

Abstract

The role of the wild-type proteins in the pathology of polyglutamine diseases remains unclear. There are conflicting reports on whether the expression of the wild-type proteins should be increased, maintained or abolished in the disease context for therapeutic means. To gain insight into this issue, we have used novel *C. elegans* models that allowed us to simultaneously study the aggregation dynamics of both wild-type and pathological forms of ataxin-3 proteins *in vivo*, as well as its toxic outcomes at the behavioral level of the organism. We show that (i) recruitment of ataxin-3 into polyQ-containing cellular aggregates is polyQ length-dependent, (ii) that wild-type ataxin-3 sequestration worsens motor behavior of affected polyQ-expressing animals and that (iii) endogenous ataxin-3 knock-out did not aggravate aggregation or motor neuron dysfunction in a *C. elegans* model of ataxin-3 pathogenesis. Our findings support the idea that wild-type ataxin-3 is unlikely to play a neuroprotective role in MJD.

Introduction

At least nine human neurodegenerative diseases are caused by the expansion of CAG repeats within the coding region of otherwise unrelated genes. Among these diseases, Machado-Joseph disease (MJD), also known as Spinocerebellar ataxia type 3 (SCA3), is the most common dominantly inherited ataxia worldwide (1-8) and is caused by an expansion of a polyglutamine (polyQ) segment in the corresponding protein ataxin-3 (ATXN3). In healthy individuals, ATXN3 has 12 to 47 glutamine (Q) units in the protein repetitive segment; but when this segment expands beyond 55 Qs it becomes pathogenic (reviewed in (9). The physiological role of ATXN3 is still poorly understood, although its involvement in the ubiquitin-proteasome system (UPS), as a deubiquitylating enzyme (DUB) it has been strongly suggested (10-13). ATXN3 ortholog proteins in *C. elegans* and mice display conserved DUB activity at least *in vitro* (14, 15). Other ATXN3 functions are known but have been less explored (16-19).

The ambiguity regarding the normal function of polyQ proteins underlies a crucial question regarding the influence of the wild-type (WT) non-expanded allele to modulate polyQ pathology. Since the leading hypothesis concerning the pathogenesis of polyQ diseases is that the expanded polyQ tract confers a gain-of-function to the mutant proteins, less attention has been dedicated to the normal function of these proteins, particularly in the context of the nervous system. More recently, however, for proteins such as huntingtin (involved in Huntington disease, HD) and the androgen receptor (involved in Spinobulbar muscular atrophy, SBMA) evidence has been obtained suggesting that there is also partial loss-of-function in cells and animals expressing the mutant proteins, and that this loss-of-function may be of relevance for the disease. In the case of huntingtin, for instance, the excessive sequestration of huntingtin into inclusions may affect its normal neuroprotective role, thought to be linked to its ability to regulate BDNF expression (20). Cell culture studies also show that aggregation of mutant huntingtin promotes fibrillogenesis of the WT protein (21). In a mouse model of SBMA, loss of the endogenous androgen receptor was proven to significantly worsen the disease phenotype (22). For ataxin-1 (involved in SCA1) opposing effects of the polyQ expansion have been reported in regards to the formation of native protein complexes in cells (23). Apparently mutant ataxin-1 maintains the usual molecular partners, but the polyQ tract expansion strengthens interactions whithin some protein complexes (RBM17) and attenuates them in others (CIC), perhaps contributing to SCA1 through gain- and loss-of-function mechanisms, respectively. The finding that there are shared gene expression changes on cerebellar RNA from Atxn1$^{-/-}$ and Atxn1$^{154Q/+}$ mice further supports the hypothesis (24).

Studies using double-transgenic mice (25) and Drosophila models (26) suggested beneficial effects of the non-expanded ATXN3 allele in MJD. However, more recent works failed to support these findings (27, 28). These conflicting data urge for a model system that allows simultaneously monitoring of the fate of non-expanded and expanded ataxin-3 in neurons, in a progressive disease background, and evaluation of its toxic outcome at the organism level.

In the present study, we generated and characterized pan-neuronal *C. elegans* models in which we could follow WT and pathological forms of ataxin-3 being recruited into polyQ cellular aggregates. The dynamics of aggregation of normal ataxin-3 was followed *in vivo* (and through age), in parallel with its impact on motor neuron dysfunction of these animals. We show that wild-type ataxin-3 fails to display a neuroprotective role during disease progression and that loss-of-function of endogenous ataxin-3 has limited effect on polyQ pathogenesis.

Results

Full-length ATXN3 is recruited into polyQ aggregates in *C. elegans* neuronal cells in a polyQ length-dependent manner

To study the contribution of WT ATXN3 protein in MJD pathology, we used a recently developed *C. elegans* model (29). In this model, expression of WT ATXN3 in fusion with yellow fluorescent proteins (AT3q14::YFP) and of a pathological sub-threshold AT3q75::YFP protein did not cause aggregation or neuronal toxicity (29).

To assess the dynamics of WT ATXN3 recruitment process *in vivo*, we crossed *C. elegans* strains expressing human WT or mutant sub-threshold ATXN3 with animals expressing Q67::CFP proteins, which aggregate throughout the *C. elegans* nervous system (30). The two fluorochromes (YFP-tagged ATXN3 and CFP labeling polyQ aggregated "seeds") allowed monitoring of the different species *in vivo*.

Co-expression of AT3q75 with Q67 proteins (30) (Fig. 1A, panel 2), caused a dramatic alteration in ATXN3 cellular distribution, into the Q67 cellular inclusions (Fig. 1A, panel 3). At day 4, virtually all AT3q75 molecules, that were diffuse when expressed alone (Fig. 1A, panel 1), co-localized into Q67 aggregates (Fig. 1A, panel 5) forming punctated-looking structures (for a magnified image see panel 6). Strikingly, WT ATXN3 was also significantly recruited in *C. elegans* neuronal cells. However, AT3q14 proteins were only partially localized within cell aggregates, appearing both with a diffuse localization and within foci (Fig. 1B, panels 5 and 6). Conversely, when we co-expressed AT3q75 with Q40 proteins (Q40 is an intermediate polyQ-length, near threshold for aggregation and neurotoxicity) (30), co-aggregation appeared only in specific neuronal-subtypes (29). These data suggested that the efficiency of protein recruitment may be Q-length dependent.

The co-expression of mutant AT3q75 with Q19::CFP (Fig. S1, panels 1 and 3) showed a similar localization pattern to the one observed with the single expression of AT3q75 proteins. This indicates that ATXN3 co-aggregation may be caused not by the presence of a second over-expressed polyQ protein in neuronal cells, but only by the co-expression with misfolding- or aggregation-prone species capable of shifting the cell's protein homeostasis (proteostasis) through nucleation events or accumulation of polyQ ubiquitylated species that ATXN3 binds to.

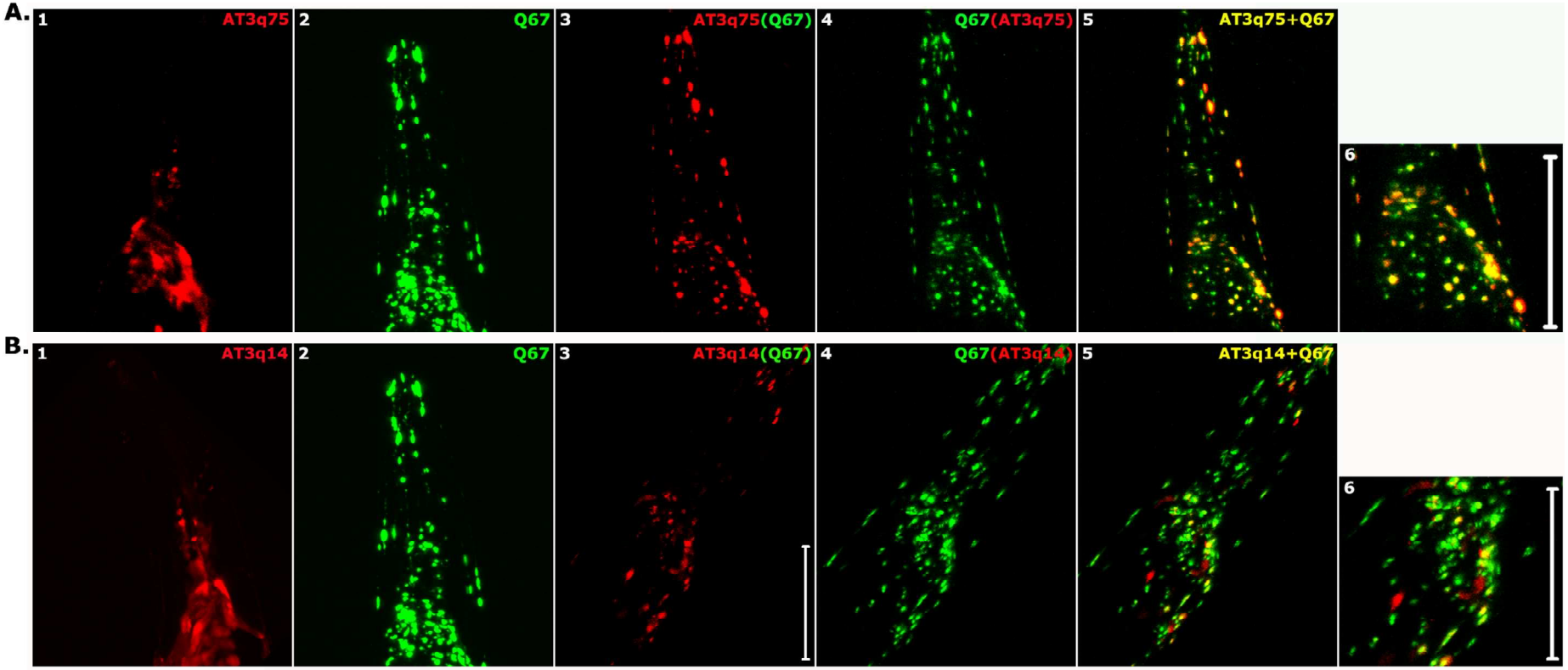

Figure 1. Ataxin-3 is recruited into polyQ cellular aggregates in a polyQ dependent manner. Flattened Z-stacks of the *C. elegans* head co-expressing Q67::CFP with either AT3q75::YFP (A) or AT3q14::YFP (B) proteins. (A) The diffuse expression of AT3q75 (panel 1) was altered when co-expressed with an expanded Q tract (panel 3) and mutant ATXN3 co-localized with Q67 inclusions (panel 5 and 6, for a magnified region). (B) When expressed alone, AT3q14 displayed a diffuse expression pattern (panel 1) that was altered in the presence of Q67 proteins (panel 3), forming foci-like structures; only a subset of AT3q14 co-localized with Q67::CFP aggregates (panel 5 and 6, for a magnified region). Co-expression with mutant (A, panels 2 and 4) and wild-type AT3 (B, panels 2 and 4) did not cause an alteration on Q67 protein distribution. Scale bar= 50 μm. White boxes are indicative of magnified regions, shown in panels 6.

In order to determine if the polyQ tract has a single dominant effect in the recruitment of ATXN3 into the polyQ aggregates or if the other ATXN3 domains influence it, we generated a *C. elegans* strain expressing an ATXN3 polyQ deletion mutant (AT3q1), containing only one glutamine at the place of the polyQ tract. Similar to WT ATXN3, AT3q1 proteins were diffusely expressed throughout the *C. elegans* nervous system (Figure 2A, panel 1). Interestingly, co-expression of AT3q1 and Q67 proteins resulted in AT3q1 sequestration and in the formation of foci-like structures in a limited number of neurons (Fig. 2A, panels 1 and 3 square), whereas YFP-alone (Q0) proteins were not significantly recruited into the polyQ aggregates (Fig. 2B, panel 3 square). In spite of AT3q1 being sequestrated to a lesser extent when compared to AT3q14 proteins, our data suggest that ATXN3 recruitment into cellular aggregates may not be exclusively mediated by the polyQ-tract of ataxin-3.

The co- expression of mutant ATXN3 (AT3q75, Fig. 1A, panels 2 and 4), WT ATXN3 (AT3q14, Figure 1B, panels 2 and 4) and AT3q1 (Figure 2A, panel2 and 4) with the Q67 proteins did not alter the cellular localization of the latter.

Our data suggests that ATXN3 sequestration into cellular aggregates is a dynamic process strongly, but not exclusively, dependent on the presence of a polyQ-tract in this protein.

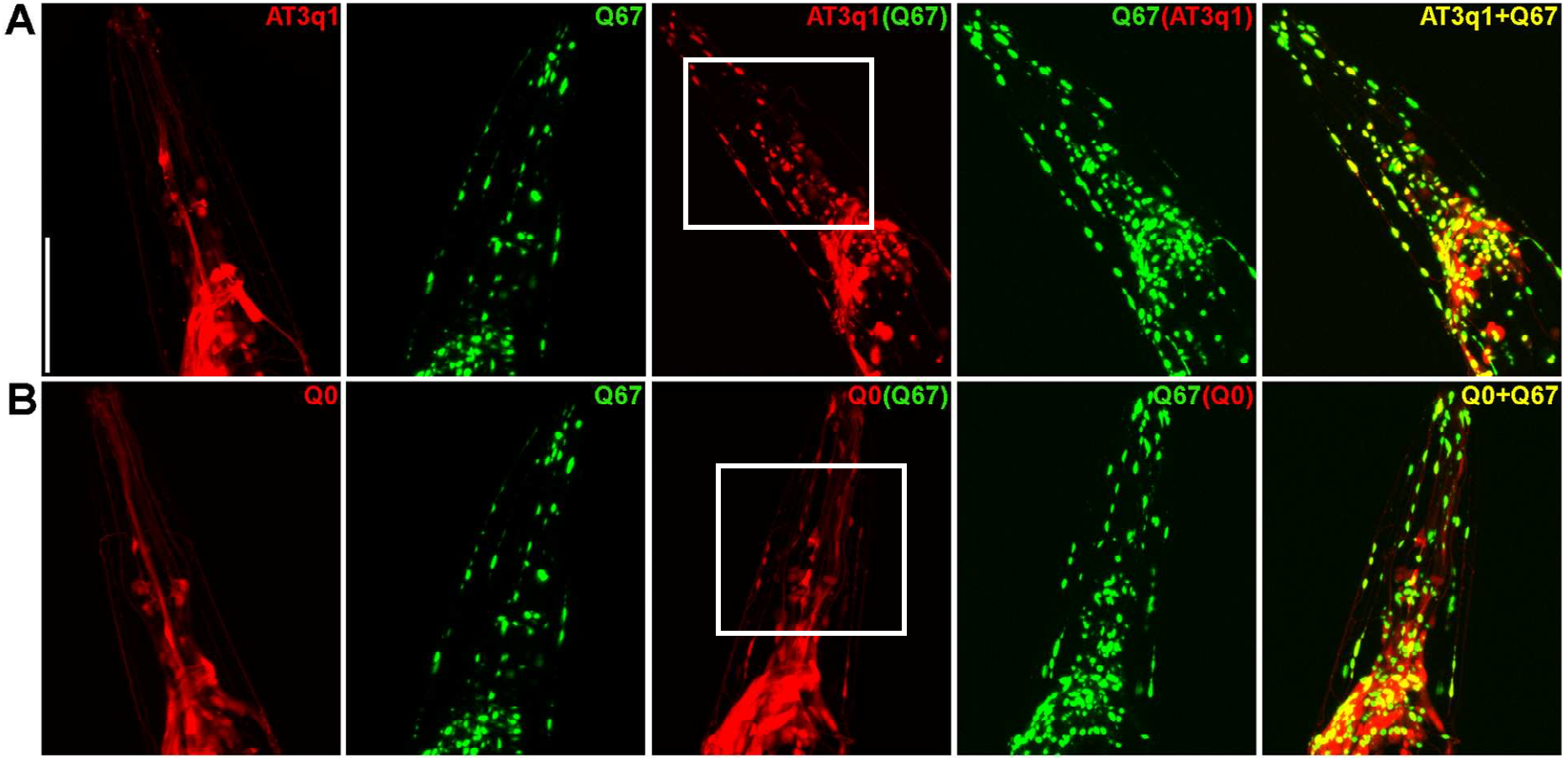

Figure 2. Q-less ATXN3 (AT3q1) proteins are recruited into the Q67 aggregates in a limited number of cells. (A) Flattened Z-stacks of *C. elegans* heads co- expressing At3q1 and Q67 proteins showed recruited in a subset of neuronal cells (A, panels 1 and 3), whereas YFP-alone protein distribution (Q0) was not significantly affected by the presence Q67 aggregates within the same cells (B, panels 1 and 3). Scale bar= 50μm. White squares of panels 3 show regions where levels of AT3q1and Q0 proteins should be compared.

ATXN3 recruitment into polyQ aggregates aggravates with age

We observed that the ATXN3 distribution pattern, in the background of the polyQ expressing lines, was variable as the animals aged. Animals expressing ATXN3 proteins showed clearly delineated cell bodies and processes, throughout their life span. This soluble distribution pattern could be observed even at day 8 (post-hatching), namely in the neurons of the head, where it was possible to identify the neuroanatomy of the sensory processes (Fig. 3B, panel 1 arrow) and the circumpharyngeal nerve ring (Fig. 3B, panel 1 arrowhead) (31). As shown before, at day 4 the co-expression of AT3q75 with threshold-length polyQ proteins (Q40) resulted in foci formation in specific affected neurons, namely in sensory processes of the head and in certain ventral and dorsal nerve cord (VNC and DNC) neurons (29). Interestingly, when we analyzed younger animals (day 2 post-hatching) no foci were yet formed (Fig. 3A). These animals were again observed at 8 days of age and we could observe an increase in the number of foci. These observations were consistent between all animals analyzed (Fig. 3B, panels 3 and 4). AT3q75 and Q40 proteins co-localized within these foci-like structures (Fig. 3B, panels 5 (thin arrows) and 6). In contrast, co-expression of AT3q14 with Q40-alone proteins did not cause the formation of punctated structures in the sensory processes of the animals head even at day 8 (Fig. S2). However, AT3q14 proteins were recruited into Q40 aggregates located at certain VNC neurons (data not shown).

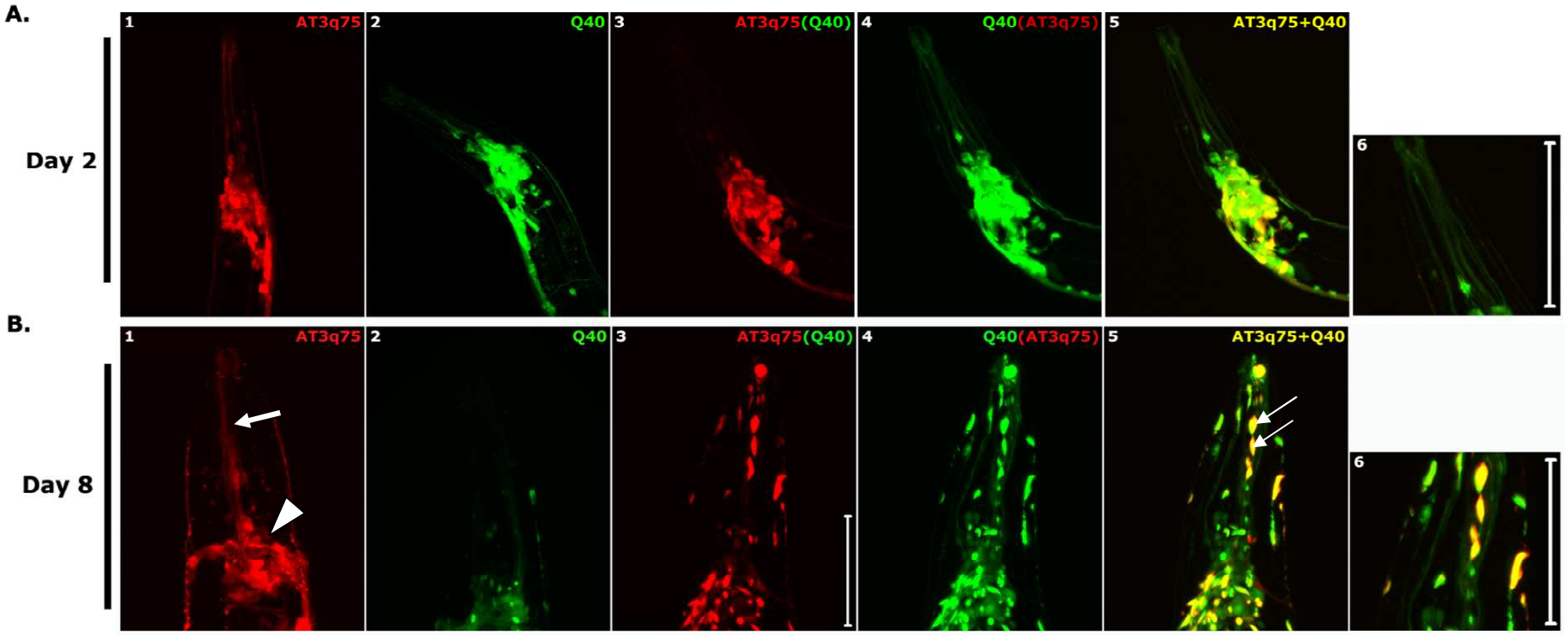

Figure 3. The formation of foci-like structures in AT3q75Q40 animals increased as the animals aged. Flattened Z-stacks of *C. elegans* head co-expressing Q40::CFP with AT3q75::YFP proteins. At day 2, animals expressing both mutant ATXN3 and Q40 proteins showed diffuse protein expression (A, panels 3 and 4); whereas at day 8, the formation of foci-looking structures was visible in the sensory processes of the head neurons (B, panels 3 and 4); no inclusions were observed in animals expressing AT3q75 and Q40 proteins alone (B, panels 1 and 2). Within these foci AT3q75 and Q40 proteins co-localized (B, panel 5, thin arrow). Scale bar= 50 μm. White boxes are indicative of magnified pictures, shown in panel 6.

Since the efficiency of ATXN3 recruitment into cellular aggregates is Q-length dependent, we anticipated that the sequestration of ATXN3, in a Q67 background, could occur at earlier stages of the worm development. In fact, at day 2 animals co-expressing WT ATXN3 and Q67 proteins displayed AT3q14 with a generally diffuse pattern, except for a few foci that were already visible in the sensory processes of the head (Fig. 4A, panel 3, arrow); whereas at day 8, WT AT3 appeared to be mostly recruited into the Q67 aggregates, the chemosensory processes being no longer visible in these animals (Fig. 4B, panel 5). Strikingly, AT3q75 was recruited into the Q67 aggregates already at early stages of the animal's development (Fig. S3). In summary, ATXN3 recruitment into cellular aggregates aggravates as the animals age in a Q length-dependent manner.

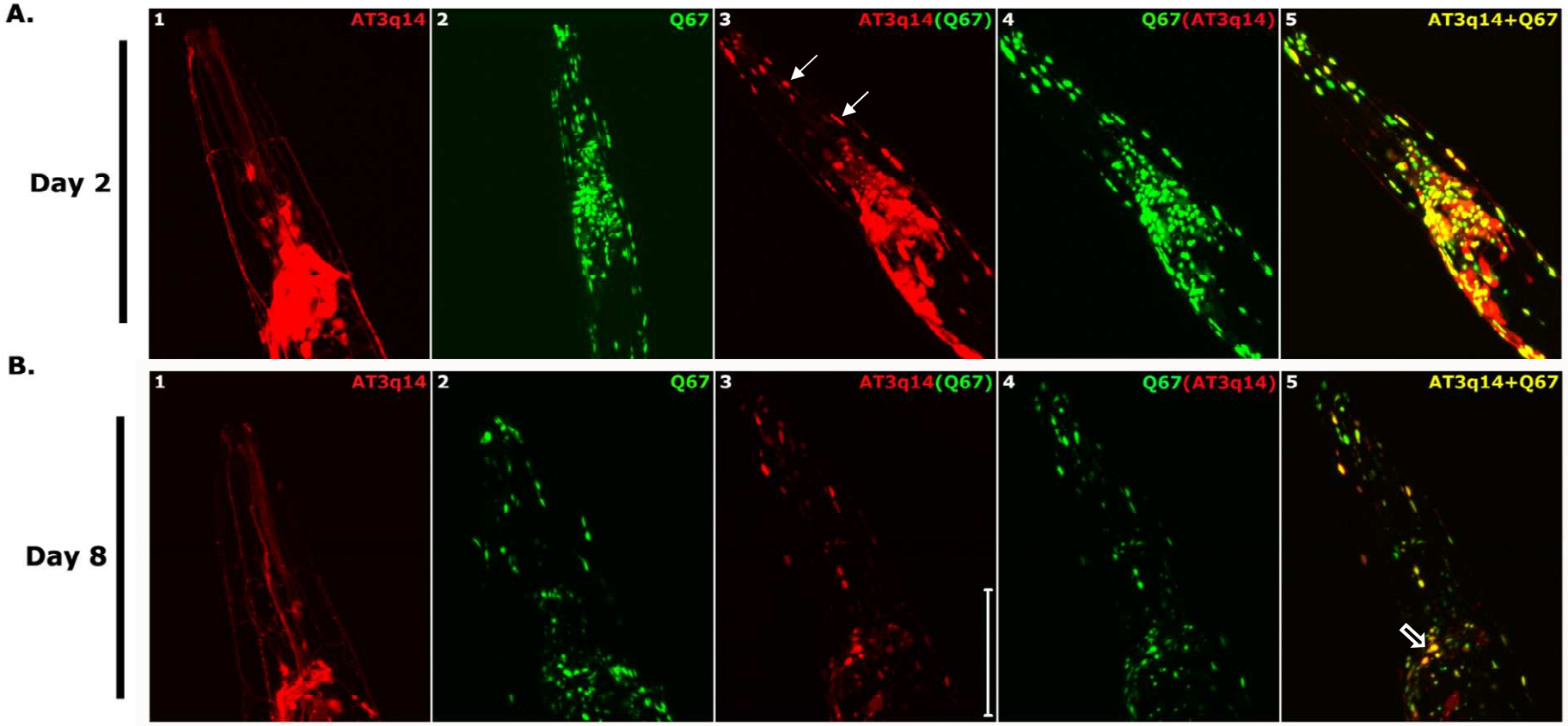

Figure 4. Wild-type ATXN3 sequestration into the Q67 aggregates increases as the animals age. Day 2 (A) and day 8 (B) flattened Z-stacks of *C. elegans* head co-expressing AT3q14::YFP and Q67::CFP proteins. At day 2 (A), AT3q14 was recruited into the Q67 aggregates mainly in the sensory processes of the head (panel 3, arrows), while in the neurons of the nerve ring ATXN3 showed a diffuse distribution. In contrast, at day 8 (B) wild-type ATXN3 was fully sequestered into the Q67 aggregates: AT3q14 formed inclusions in all neurons of the head, the shape of the neuronal chemosensory processes being no longer visible. In the neurons of the nerve ring (panel 6, open arrow) AT3q14 also showed a punctated-like shape co-localizing with Q67 proteins. Scale bar= 50 μm.

ATXN3 recruited into polyQ aggregates acquired properties of highly immobile protein

The cellular distribution pattern of ATXN3 in a polyQ aggregated background [AT3q(n);Q(n)] is visually distinct from the one observed when ATXN3 is expressed alone. To assess whether the visual changes in protein distribution and the formation of foci-like structures corresponded to changes in protein solubility, and to determine how dynamic the recruitment process is, we performed fluorescence recovery after photobleaching (FRAP) analysis. In agreement with previous reports (30) the FRAP analysis performed on polyQ, CFP-tagged proteins, showed that co- expression with ATXN3 proteins did not alter the polyQ-alone mobility pattern (data not shown).

FRAP analysis of AT3q75(;Q40) animals at day 4 showed that the foci-like structures, not detected in neurons of the head of Q40-alone expressing lines, corresponded to immobile, aggregated protein (Fig. 5A, AT3q75;Q40(a)). We could also find soluble mutant ATXN3 protein, namely in the lateral neurons (Fig. 5A, AT3q75;Q40(s)) of the same animals. Moreover, extensive FRAP testing within the VNC neurons revealed that AT3Q75 protein could exist either in a rapid recovery (soluble) state or completely immobile. A similar differential solubility pattern was found in 8 days old animals for ATXN3 (Fig. 5B).

In a Q40 background, WT ATXN3 did not lead to foci formation (Fig. 2B and S3). In fact, Q40 protein was found in an highly soluble state in the chemosensory processes of *C. elegans*, even at day 8 (Fig. 5A and B, AT3q14;Q40). These results point out that WT ATXN3 does not exacerbate the aggregation phenotype of Q40 animals by leading to the formation of new aggregates, being only recruited into the already formed Q40 aggregates.

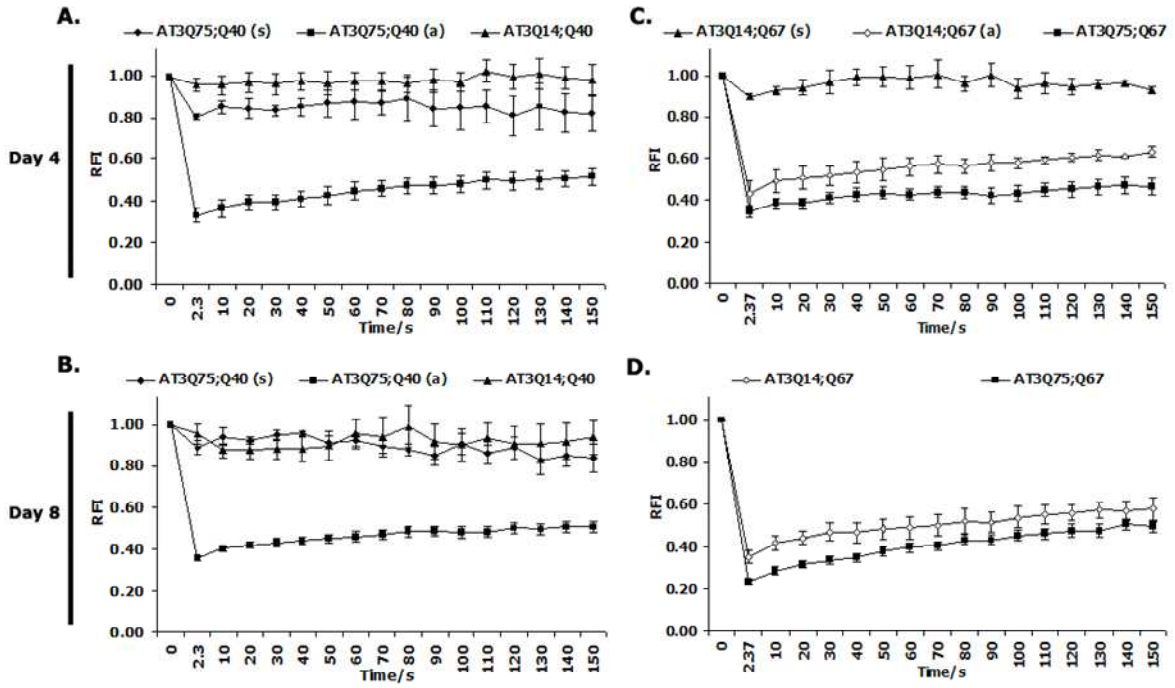

Figure 5. ATXN3 recruited into cellular aggregates acquired properties of immobile amd aggregated protein. Panels A and B show ATXN3 aggregation dynamics in the background of Q40 proteins. At day 4, FRAP of neurons expressing AT3q75;Q40 protein-containing foci-like structures, showed that protein within the foci was immobile, corresponding to aggregated protein (AT3Q74;Q75(a)) (A). Certain DNC and lateral neurons displayed highly mobile, soluble AT3q75 protein (AT3Q74;Q75(s)). (B) At day 8, the mobility rates of these proteins showed a similar pattern with aggregation of AT3q75 protein within the foci and soluble protein in the lateral neurons (AT3q75;Q40(s)). Wild-type ATXN3, in a Q40 background, had rapid recovery rates after photobleaching, corresponding to soluble protein, both in day 4 (A) and day 8 (B) animals (AT3q14;Q40). AT3q14 recruited into Q40 aggregates corresponded to aggregated protein, showing low recovery rates after photobleaching (data not shown). Panels C and D show ATXN3 aggregation dynamics in the background of Q67 proteins. (C) FRAP analysis on AT3q75, in the background of Q67 protein showed reduced recovery after photobleaching, indicating that mutant ATXN3 was co-aggregating with Q67 proteins, both at day 4 (A) and day 8 (B) (AT3q75;Q67). Wild-type ATNX3 was partially recruited into the Q67 aggregates and both (C) soluble (AT3q14;Q67(s)) and aggregated (AT3q14;Q67(a)) protein could be found at day 4. (D) At day 8, no highly soluble AT3q14 protein was found indicating that more wild-type protein became sequestered into the Q67 aggregates (AT3Q14;Q67). Quantification (A, B, C and D) was performed in eight or more experiments, and is represented as the mean ± SEM. Scale Bar, 5 μm. RFI, Relative fluorescence intensity.

FRAP analysis on AT3q75 in the background of Q67 protein (AT3q75(;Q67)) revealed almost no recovery after laser photobleaching, showing that the protein is mostly immobile. This is a strong indication that protein aggregates have formed (Fig. 5C, AT3q75;Q67(a)). As expected, when the solubility pattern of mutant ATXN3 was also assessed at day 8, no differences were found (Fig. 5D, AT3q75;Q67(a)). Immobile proteins were present in nearly all neurons FRAPed, suggesting that nascent AT3q75 is being sequestered into the Q67 aggregates, either co- or post-translationally. In fact, Western-blot analysis (Fig. 6) showed that when ATXN3 is recruited into cellular inclusions it is SDS resistant (2% SDS treatment), a know biochemical property of the

polyQ aggregates (32, 33). Likewise, extracts of AT3q75; Q67 day 4 animals contained SDS-resistant aggregates, whereas we were unable to detect SDS-resistant AT3q75(;Q40) proteins (Fig. 6).

At day 4, WT ATXN3 was also recruited, although only partially, into the Q67 aggregates. In some DNC and VNC neurons ATXN3 displayed fast recovery after photobleaching, indicating that soluble protein was also present in those neurons (Fig. 5C, AT3q14;Q67(s)). Interestingly, at day 8 no highly soluble AT3q14 was found in the neurons of these animals, despite the extensive FRAP testing (Fig. 5D). In accordance with our microscopy results (Fig. 4), FRAP analysis suggested that, as the animals age, more protein is being recruited into the Q67 aggregates, becoming less mobile. This aggravation of the aggregation profile may be a result of kinetics of the aggregation process or of a decline of the cells' quality control machinery.

As expected, both mutant and WT ATNX3 showed properties of mobile protein, i.e., they were highly soluble, when co-expressed with Q19::CFP (data not shown), showing solubility properties close to ATXN3-alone proteins (29). In summary, the visual changes in neuronal ATNX3 protein distribution into cellular aggregates correlated with the alterations in protein solubility detected by FRAP.

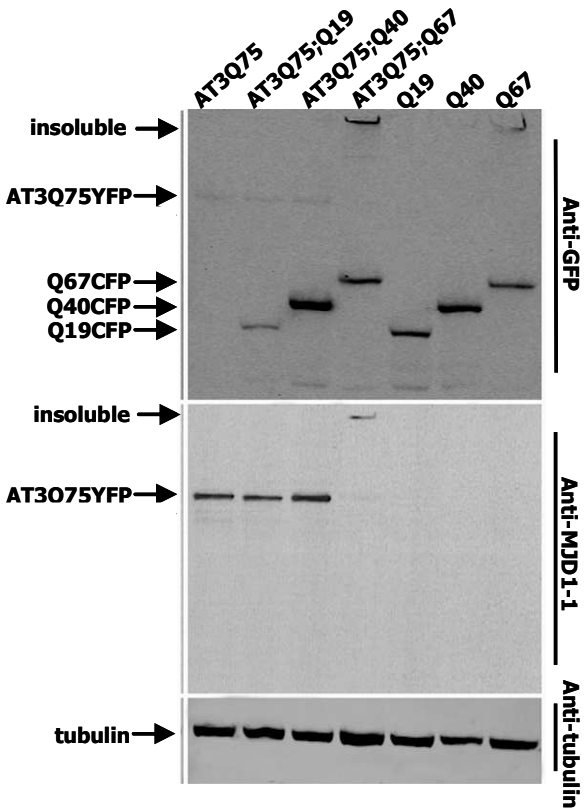

Figure 6. Biochemical analysis AT3q75;Q67 proteins revealed that when recruited into Q67 aggregates, AT3q75 proteins became insoluble and resistant to SDS-treatment. AT3q75;Q(n) *C. elegans* lines show the expression of the full-length AT3q75 proteins with normal and expanded Q-stretches (Q19; Q40 and Q67). Total protein extracts from animals expressing YFP/CFP fusion proteins were treated with 2% SDS, separated by SDS-PAGE and immunoblotted with anti-GFP, anti-MJDv1-1 and anti-tubulin antibodies. In accordance to our FRAP results, when co-expressed with Q67 proteins, mutant ATXN3 became insoluble.

Wild-type ATXN3 recruitment into cellular aggregates increased neuronal dysfunction

Several *C. elegans* neurons enervate muscle cells and dysfunction of these neurons may result in lack of coordination or even lack of ability to crawl (34). To determine the effect of WT and of mutant subthreshold ATXN3 recruitment into cellular aggregates on neurotoxicity of these animals, we have performed motility assays to assess potential alterations in locomotion. WT and AT3q75 protein expression did not cause overt neuronal toxicity when compared with animals expressing YFP alone (Q0) (Fig. 7A); whereas animals expressing expanded polyQ-alone proteins (Q40 and Q67) showed dramatic defects on motility (Fig. 7) when compared with animals expressing a non-pathogenic Q-stretch (Q19) ($p=0.0002$ and $p=8.7x10^{-6}$, respectively). This is consistent with what has been previously described using similar behavioral assays (30). Interestingly, WT ATXN3 co-expression significantly enhanced motor neuron dysfunction of Q67 animals (*, $p= 0.0061$), and the locomotion defect was even more striking when Q67 proteins were co-expressed with AT3q75 proteins (*, $p=0.0009$) (Fig. 7A). The data suggests that recruitment of the WT ATXN3 into aggregates can have deleterious effects to the neuronal cells. Moreover, the accelerated dynamics of sequestration shown by mutant ATXN3 (in comparison with WT ATXN3) correlate with increased neuronal dysfunction in our *C. elegans* model (*, $p=0.04$, AT3q14;Q67 vs. AT3q75;Q67). In the background of Q19 proteins, the phenotype displayed by AT3q(n);Q19 animals was mainly due to the expression of the human ATXN3 protein and it was not significantly different from animals expressing full-length ATXN3 alone (Fig. 7A).

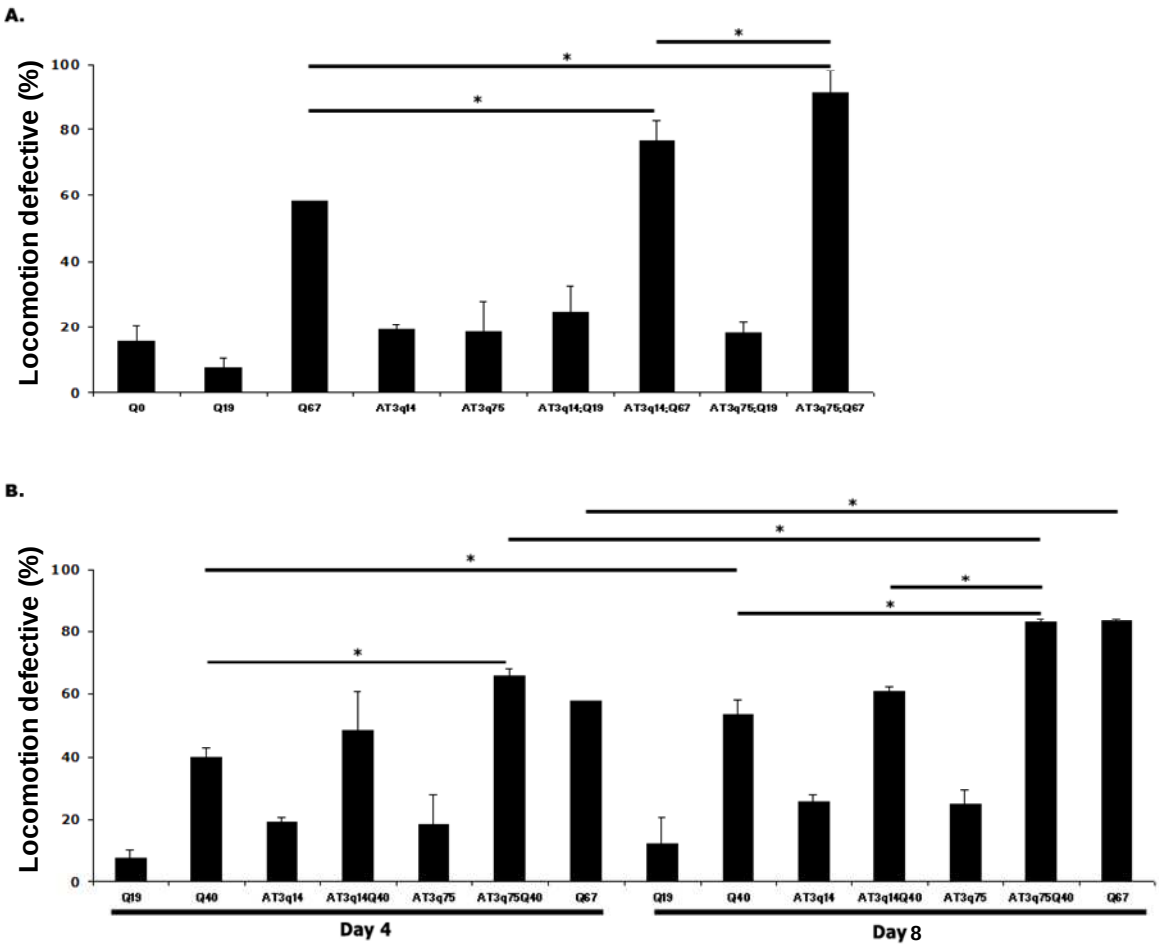

Figure 7. Wild-type ATXN3 recruitment into Q67 aggregates increases motor neuron-dysfunction. (A) The presence of ATXN3 increases the locomotion defects of Q67-alone expressing animals (*, ** $p<0.05$). More than 90% of the AT3q75; Q67 animals tested presented defects in motility (#, $p< 0.05$, compared with AT3q14; Q67), whereas the percentage of locomotion defective animals is identical in normal and expanded ATXN3-alone expressing animals. Behavior analysis was performed in 4 days-old animals. (B) At day 4, co-aggregation of Q40 with AT3q75 proteins (and not with AT3q14) significantly enhanced the animals' locomotion defects ($p<0.05$), whereas at day 8, expression of mutant ATXN3 significantly increased motor neuron dysfunction relatively to normal ATXN3. At least 150 animals were tested. Statistical significance was assessed by *t-Student* test.

At day 4, we observed that co-aggregation of Q40 with pathological sub-threshold AT3q75 proteins (and not with AT3q14) significantly enhanced motor neuron dysfunction (*, $p=0.0082$). At day 8, there was a general increase in the percentage of locomotion-defective animals (Fig. 7B) probably also due to the animals' normal aging process. However, when we compared WT and mutant ATXN3 expressing animals, there was a significant increase in toxicity ($p=0.004$) that was not seen at day 4. This result is in accordance with the aggregation profile, since at day 8 there is a clear increase in the number of foci in AT3q75;Q40 animals and not in AT3q14;Q40 (Fig. 3 and S2).

In summary, we found that AT3q14 overexpression aggravated motor neuron dysfunction of the animals, when recruited into the Q67 aggregates and not into the Q40 proteins.

Absence of endogenous ATX3 had no effect on mutant ATXN3-mediated pathogenesis

One of the important conclusions of our co-expression experiments was that overexpression of WT ATXN3 did not protect against aggregation-mediated toxicity in *C. elegans* neuronal cells. Next, we asked whether the absence of endogenous ataxin-3 in neuronal cells would suppress human ATXN3 pathogenesis in *C. elegans*. For that purpose, we crossed animals expressing full-length ataxin-3 proteins containing 130 Qs (AT3q130) and endogenous ATX-3 knock-out animals (*atx-3*), previously characterized by us (29). AT3q130 animals display, among other features, neuronal sub-type specific aggregation and motor neuron dysfunction (14, 29, 35). Of notice, *C. elegans* ATX-3 presents deubiquitylating activity *in vitro*, analogous to the human ortholog (14) and *atx-3* animals showed no overt phenotype at 20ºC. In our *atx-3*; AT3q130 model, loss of endogenous *atx-3* did not alter significantly the disease phenotype, both at the aggregation and motor neuron dysfunction levels (Fig. 8A). However, recent studies have shown that *atx-3* knock-out animals have an improved stress response and express increased levels of molecular chaperones when grown at 25ºC (35). Based on this, we grew *atx-3*; AT3q130 animals at higher temperature. Even at 25ºC, *atx-3* loss-of-function failed to modulate the disease phenotype (Fig. 8B). Our data suggests that loss-of-function of WT ataxin-3 may have limited effects on MJD pathogenesis.

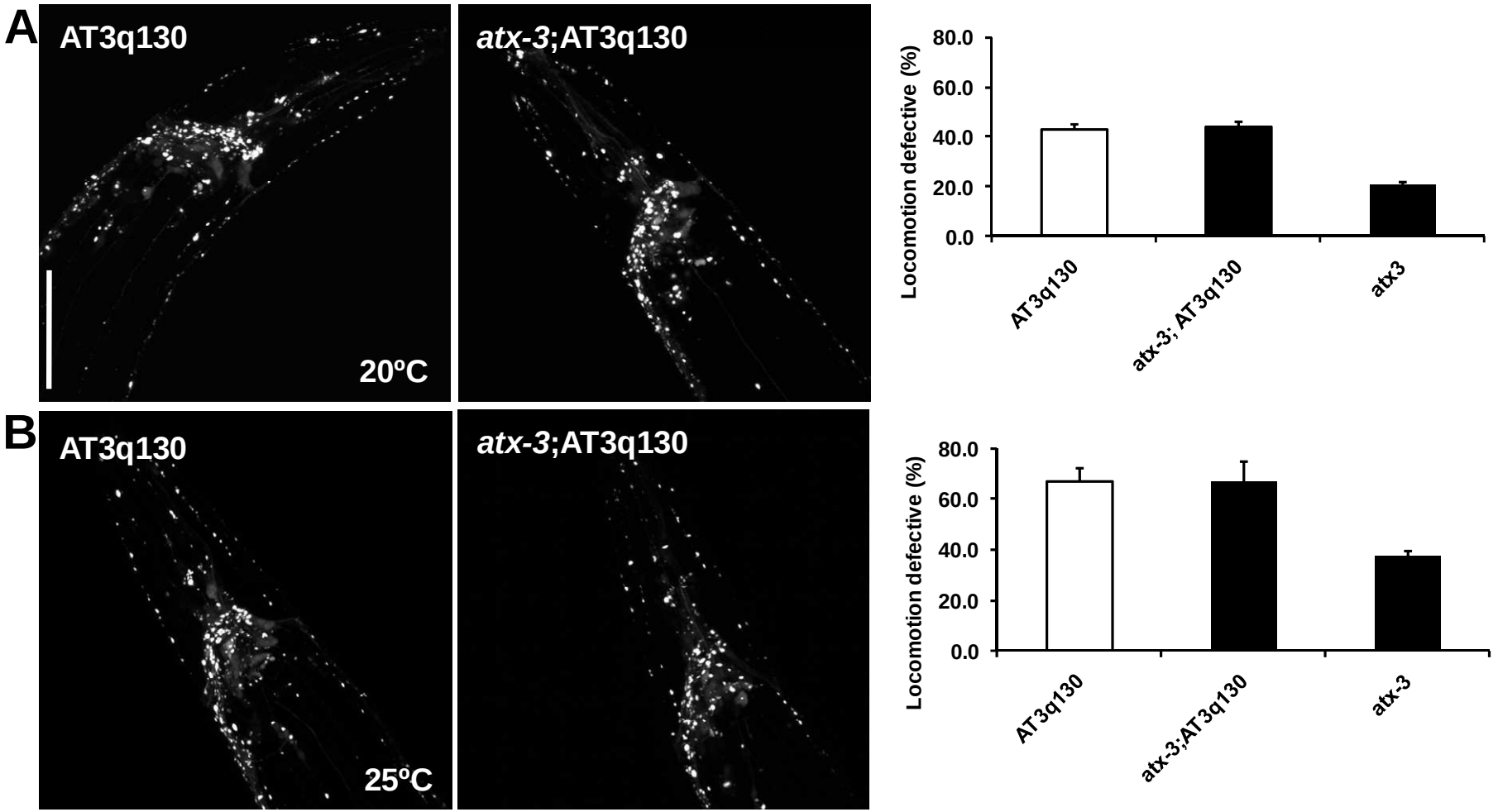

Figure 8. Absence of endogenous ATX-3 did not modulate pathological ATXN3-mediated proteotoxicity. The mutation *atx-3(gk193)* did not significantly change the AT3q130-mediated aggregation at day 4 (post-hatching) at 20°C (A). Motility analysis showed no differences in motor neuron dysfunction of *atx-3*; AT3q130 animals when compared to AT3q130 transgenics (A). At 25°C, adult *atx-3*; AT3q130 animals (2.5 days post-hatching) showed similar aggregation pattern and locomotion defects to the AT3q130 transgenics (B).

Discussion

The role of the WT ataxin-3 in MJD pathogenesis remains unclear, particularly, the cross-talk between the cellular fate of the normal protein in a disease context (i. e. recruitment into aggregated species), and its effect on the pathogenic cascade. The relevance of this question it is not only academic, since the decision of making use of gene therapy or pharmacologic strategies to manipulate levels of the mutant and WT protein in the clinic depends on further clarification of these aspects. In this work, we investigated the potential neuroprotective role of normal ataxin-3 by overexpressing or silencing it in a disease context. In our model, we analyzed (i) the sequestration profile of wild-type ataxin-3 into cellular aggregates (Q-length and age-dependency), and (ii) the impact of co-aggregation on motor neuron dysfunction of these animals. Finally, (iii) we addressed the effect of knocking-out endogenous ATX-3 in a *C. elegans* model of MJD pathogenesis.

Wild-type ATXN3 is recruited into cellular aggregates

MJD homozygous patients develop the disease at early ages and show a more severe and progressive neurological phenotype than heterozygous individuals (36-38). Is this due to the absence of a functional non-expanded ataxin-3 allele or from an increased load of the mutant ataxin-3? or from a combination of gain and loss-of-function?

It was known from previous work that WT ataxin-3 had the ability to interact and co-localize with cleaved C-terminal fragments or truncated forms of expanded ataxin-3 (39). We crossed *C. elegans* strains expressing wild-type and mutant subthreshold ATXN-3 proteins (YFP-fused) into animals expressing expanded polyQ-stretches (CFP-fused). This model recreates many features of MJD, since we have previously shown that, at the aggregation threshold (AT3q75; Q40), the neuronal cell type-specific susceptibility is comparable to that of animals expressing full-length AT3q130 proteins and C-terminal 257cAT3q75 (29). The use of different fluorophores allowed tracking the two species *in vivo* in the neuronal cells. One question that remained unanswered from previous studies was if the recruited ATXN3 molecules became immobile in the cell or if instead they were able to keep their solubility and, perhaps, intact function. Indeed, it has been described that molecular chaperones are recruited and interact with polyQ aggregates in a dynamic way, exhibiting rapid association and dissociation rates (40). In contrast, we show that wild-type ATXN3 molecules are sequestered into cellular aggregates and acquire properties of immobile proteins. Additional studies will be required to evaluate ATXN3 function *in vivo* in these cellular aggregates.

The efficiency of ATXN3 recruitment is polyQ-length dependent. Increased ATXN3 Q-length potentiates sequestration into pan-neuronal aggregates (Q67 model). At day 4, AT3q75 proteins completely co-localize with Q67 aggregates, whereas a proportion of WT AT3q14 proteins was still soluble. Interestingly, however, the deletion of the Q-tract (AT3q1) did not totally prevent ATXN3 recruitment, suggesting that ATXN3 protein domains other than the Q-stretch may contribute to this interaction. FRAP analysis further supported this finding, since we found that a proportion of AT3q1 proteins presented reduced mobility/solubility in the neuronal cells

(data not shown). In fact, WT ATXN3 was also found in non-polyQ intranuclear cellular aggregates in neuronal intranuclear hyaline inclusion disease (NIHID) (41). Co-localization of AT3 with cellular aggregates can be related with its DUB function. Cellular studies show that endogenous AT3 colocalizes with aggresomes and pre-aggresome particles of the misfolded cystic fibrosis transmembrane regulator (CFTR) mutant CFTRDeltaF508 and associates with histone deacetylase 6 and dynein, proteins required for aggresome formation and transport of misfolded protein (42).

One of the great advantages of using *C. elegans* as a model system is that one can add the dimension time/age to investigate several hypothesis at the level of the neuronal circuit. In our worm, WT ATXN3 recruitment was also shown to be modulated by age. As the animals grew older, more ATXN3 proteins became trapped into the Q67 and Q40 aggregates. Particularly, in the Q67 background, AT3q14 proteins passed from a more soluble condition to a totally aggregated state, as monitored by FRAP analysis. In agreement, previous studies in mouse and rat models showed a comparable tendency to an increase in the total number of aggregates when WT ATXN3 proteins were co-expressed with the expanded allele (27, 28).

Interestingly, AT3q75; Q40 animals also showed a clear increase in the number and size of aggregates through age, which was mainly due to the formation of new aggregates. In fact, in the Q40 model WT and mutant subthreshold ATq75 proteins showed differential effects in the aggregation pattern of the animals. AT3q14 proteins were recruited into Q40 aggregates of the VNC, whereas AT3q75, besides that, formed new aggregates in cells that weren't affected when Q40 species were expressed alone (29).

The aggravation of the ATXN3 recruitment phenotype as the animals got older could be due to the kinetics of the co-aggregation process or to a decline of proteostasis function in cells or both. We found no significant differences in the co-aggregation profile of AT3q(n); Q(n) in the background of the long lived strain *daf-2* (data not shown), suggesting that kinetics may have a major effect on recruitment.

Differential impact of wild-type ATXN3 recruitment on motor dysfunction

Importantly, Cemal et al. (2002) reported that the co-expression of ATXN3 with 84 CAG repeats and ATXN3 with 22 CAGs proteins in a mouse model resulted in a mild phenotype, comparable to that of a line expressing ATXN3 with 72Qs (25). The neuronal loss, number of inclusions and gliosis presented by the MJD22.1/84.1 line was considerable reduced when compared with MJD84.2 line. Studies in *Drosophila* reinforced the concept of a protective role of WT ATXN3 in MJD pathogenesis. Warrick and collaborators reported that wild-type and functionally active ATXN3 suppressed polyQ-induced neuropathology and behavioral defects (26). Recently, however, studies in rodents failed to support these findings (27, 28). Double transgenic mice did not show any behavioral rescue or death delay (27). In rats, a larger DARPP-32-depleted region was associated with co-expression of mutant and wild-type alleles of ataxin3, suggesting increased toxicity (28).

We observed a differential impact on *C. elegans* behavior depending on the length of the expanded allele, which was not dependent on the animals' age. Specifically, WT ATXN3 was recruited into high Q-length

polyQ aggregates (Q67), causing an aggravation on locomotion defects of the animals. In contrast, when AT3q14 was sequestered into polyQ-expanded, near aggregation threshold Q40 aggregates it had no phenotypic effect, even in older animals (day 8). Our data provides experimental evidence that for MJD, the effect of the WT protein may depend on level of disease severity and degree of progression, as well as on the type of aggregated structures formed.

Loss-of-function of ATXN3 has limited effect in the modulation of pathogenesis

Loss of endogenous function of several polyQ proteins was shown to have a negative impact on pathogenesis (22, 23). Particularly, in SCA1, pathogenesis involves changes in other regions of ataxin-1protein in addition to the polyQ tract (43, 44). In MJD, silencing of endogenous rat ATXN3 was found to have no effect on the total number of ubiquitin-positive cells as well as in the mutant ATXN3-induced brain lesion (DARRPP-32 staining) (28), suggesting that probably the behavior of the animals was also not affected. Here, we show that the absence of *C. elegans atx-3* had limited effect both on the aggregation pattern of pathogenic human ATXN3 and on the motor function of the animals.

Our data suggests that WT ATXN3 overexpression in a disease context may have differential effects depending on the Q-length of the disease causing allele. However, we failed to find a neuroprotective role for normal ATXN3 as well as beneficial effects on the animals' behavior resulting from its overexpression. The absence of normal ATXN3 function also did not modulate MJD pathogenesis. Thus, manipulation of WT ATXN3 levels as a therapeutic intervention to prevent neurological phenotypes in MJD is unlikely to lead to beneficial results.

Materials and methods

Plasmid construct. Pan-neuronal ATXN3 expression was achieved by cloning AT3var1-1 cDNA into the $P_{F25B3.3}$Q0::YFP plasmid (30), as previously described (29). Full-length AT3q1 cDNA with different polyQ- lengths was generated by PCR using oligonucleotides containing restriction sites for *BamH* I and pGEM-7Zf(+)::MJD1-1q1 as templates. AT3q1 amplicons were then digested and ligated into the *BamH* I sites of $P_{F25B3.3}$Q0::YFP generating $P_{F25B3.3}$AT3v1-1q1::YFP. Sequencing confirmed the AT3q1 sequence, YFP and the promoter region.

***C. elegans* methods.** Standard methods were used for culturing and observing *C. elegans* (45). For generation of transgenic neuronal animals, 50 ng.µL-1 of DNA encoding $P_{F25B3.3}$AT3q1 was microinjected into the gonads of adult hermaphrodite N2 animals. Transgenic F1 progeny were selected on the basis of neuronal fluorescence. At least three independent stable lines for each transgene were isolated and analyzed with similar results. Transgenic lines were frozen immediately after they were generated. Populations were synchronized either by treating young adult animals with alkaline hypochlorite solution (0.5 M NaHO, ~2.6% NaClO) for 7 min (46) or by collecting embryos laid by adult animals within a 3-h period.

***C. elegans* strains generated.** All strains used the F25B3.3 promoter with full-length AT3q(n) fused to YFP. ATXN3 full-length lines included the following: (AT3q1) AM649 *rmEx285*, AM650 *rmEx286*; (AT3q14) AM491 *rmEx*228, AM500 *rmEx*232; and (AT3q75) AM489 *rmEx*227, AM495 *rmEx*231. Dual-colored lines generated for imaging and FRAP included the following (AT3q75;Q(67)) AM502 *rmEx*227[$P_{F25B3.3}$::AT3v1-1q75::YFP];*rmIs*190[$P_{F25B3.3}$::Q67::CFP]; (AT3q75;Q(40)) AM508 *rmEx*227[$P_{F25B3.3}$::AT3v1-1q75::YFP];*rmIs*167[$P_{F25B3.3}$::Q40::CFP]; (AT3q75;Q(19)) AM502 *rmEx*227[$P_{F25B3.3}$::AT3v1-1q75::YFP];*rmIs*172[$P_{F25B3.3}$::Q19::CFP]; (AT3q14;Q(67)) AM504 *rmEx*232[$P_{F25B3.3}$::AT3v1-1q14::YFP];*rmIs*190[$P_{F25B3.3}$::Q67::CFP]; (AT3q14;Q(40)) AM505 *rmEx*228[$P_{F25B3.3}$::AT3v1-1q14::YFP];*rmIs*167[$P_{F25B3.3}$::Q40::CFP]; (AT3q14;Q(19)) AM507 *rmEx*228[$P_{F25B3.3}$::AT3v1-1q14::YFP];*rmIs*172[$P_{F25B3.3}$::Q19::CFP]; (AT3q1;Q(67)) AM672 *rmEx285*[$P_{F25B3.3}$::AT3v1-1q1::YFP];*rmIs*190[$P_{F25B3.3}$::Q67::CFP]; (Q0;Q67) AM655 *rmIs182*[$P_{F25B3.3}$::Q0::YFP];*rmIs*190[$P_{F25B3.3}$::Q67::CFP].
All strains expressing variable Q lengths were generated previously (30) and were either used as controls or to cross with ATXN3 full-length lines. CFP lines included: (Q19) AM282 *rmIs*172, (Q40) AM305 *rmIs*167, (Q67) AM308 *rmIs*190. YFP lines included: (Q0) AM52 *rmIs182*.

Immunobloting analysis. Nematodes were collected, washed with M9 buffer and frozen in liquid nitrogen. Worm pellets were sonicated for ~2 min in lysis buffer (20 mM Tris pH7.4, 10% glycerol, 5 mM MgCl2, 0.5% Triton X-100, 0.2 mM PMSF, 1 µg/ml leukopeptin, protease inhibitor cocktail (Roche)). Protein concentration was determined using the Bradford assay (Biorad). Ten micrograms of total protein, previously treated with 2% SDS, were separated by SDS-PAGE and analyzed by immunobloting with IRDye 800 Conjugated affinity purified

anti- GFP [goat IgG] (Rockland), anti-alpha-tubulin mouse (Sigma) and AlexaFluor 680 goat anti-mouse (Molecular Probes). Images were captured using Odyssey Infrared Imaging System. All membranes were re-probed with anti-MJD1-1 antibody (19) and detected with horseradish peroxidase-coupled secondary antibody and chemiluminescence (ECL western-blotting detecting reagents, Amersham Pharmacia).

Confocal imaging. All images were captured on a Zeiss LSM510 META confocal microscope (Oberkochen, Germany) under a 63x water objective. Animals were immobilized with 1.5 mM levamisole and mounted on a 3% agarose pad. Z-series imaging was taken of all the *C. elegans* lines generated using 514 nm laser excitation for YFP and 458 nm for CFP. The pinhole was adjusted to 1.0 μm of optical slice and a scan was taken every ~0.5 μm along the Z-axis. Immobilized 4- or 8-d-old animals were subjected to Fluorescence Recovery After Photobleaching (FRAP) as described (47) with the following modifications: imaging on full-length AT3 and AT3;Q(n) animals was performed at 5% power of a 514 nm laser line with bleaching power of 100 % and 25 iterations. Relative fluorescence intensity (RFI) was determined using the following equation: RFI=(Tt/Ct)/(T0/C0), in which T0 is the total intensity of the region of interest (ROI) prior to photobleaching and Ct is the intensity of the same area at a given time after bleaching. The intensities were normalized against a nonbleached ROI within the same cell (C0, intensity of the control area prior to bleaching and T0 at any time after) as a control for general photobleaching and background fluorescence (47).

Motility assay. All assays were performed at room temperature (~20°C) using synchronised animals grown at 20°C or 25°C. Five animals (2.5, 4- or 8-day-old) were placed simultaneously in the middle of a freshly seeded plate, equilibrated at 20°C. Animals remaining inside a 1-cm circle after one min were scored as locomotion defective. More than 101 animals were scored in at least three independent assays for each strain, and the statistical significance was assessed by Student's *t*-test, as described previously (48).

Acknowledgments

We are grateful to members of the Maciel and Morimoto laboratories for sharing reagents, for critical analysis of the data and for their helpful discussions on the manuscript. We thank David Pilgrim (University of Alberta) for generously sharing *C. elegans* plasmids; and we thank Thomas O'Halloran and Biological Imaging Facility (Northwestern University) for the use of microscopes. A special thanks to the Caenorhabditis Genetics Center (CGC), which is funded by the National Institutes of Health - National Center for Research Resources, for some of the nematode strains.

Funding

This work was supported by grants from Fundação Ciência e Tecnologia (FCT) [PTDC/SAU-GMG/64076/2006, SFRH/BD/27258/2006 to A.T.C.] and from Fundação Luso-Americana para o Desenvolvimento (FLAD); from the National Ataxia Foundation and from the National Institutes of Health (National Institute of General Medical Sciences, National Institute on Aging) and the Huntington Disease Society of America Coalition for the Cure.

References

1 Coutinho, P. (1992) Doenca de Machado-Joseph. *Grande Premio Bial de Medicina.*

2 Schols, L., Amoiridis, G., Langkafel, M., Buttner, T., Przuntek, H., Riess, O., Vieira-Saecker, A.M. and Epplen, J.T. (1995) Machado-Joseph disease mutations as the genetic basis of most spinocerebellar ataxias in Germany. *J Neurol Neurosurg Psychiatry*, **59**, 449-450.

3 Ranum, L.P., Lundgren, J.K., Schut, L.J., Ahrens, M.J., Perlman, S., Aita, J., Bird, T.D., Gomez, C. and Orr, H.T. (1995) Spinocerebellar ataxia type 1 and Machado-Joseph disease: incidence of CAG expansions among adult-onset ataxia patients from 311 families with dominant, recessive, or sporadic ataxia. *Am J Hum Genet*, **57**, 603-608.

4 Durr, A., Stevanin, G., Cancel, G., Duyckaerts, C., Abbas, N., Didierjean, O., Chneiweiss, H., Benomar, A., Lyon-Caen, O., Julien, J. *et al.* (1996) Spinocerebellar ataxia 3 and Machado-Joseph disease: clinical, molecular, and neuropathological features. *Ann Neurol*, **39**, 490-499.

5 Inoue, K., Hanihara, T., Yamada, Y., Kosaka, K., Katsuragi, T. and Iwabuchi, K. (1996) Clinical and genetic evaluation of Japanese autosomal dominant cerebellar ataxias; is Machado-Joseph disease common in the Japanese? *J Neurol Neurosurg Psychiatry*, **60**, 697-698.

6 Watanabe, H., Tanaka, F., Matsumoto, M., Doyu, M., Ando, T., Mitsuma, T. and Sobue, G. (1998) Frequency analysis of autosomal dominant cerebellar ataxias in Japanese patients and clinical characterization of spinocerebellar ataxia type 6. *Clin Genet*, **53**, 13-19.

7 Moseley, M.L., Benzow, K.A., Schut, L.J., Bird, T.D., Gomez, C.M., Barkhaus, P.E., Blindauer, K.A., Labuda, M., Pandolfo, M., Koob, M.D. *et al.* (1998) Incidence of dominant spinocerebellar and Friedreich triplet repeats among 361 ataxia families. *Neurology*, **51**, 1666-1671.

8 Soong, B.W., Lu, Y.C., Choo, K.B. and Lee, H.Y. (2001) Frequency analysis of autosomal dominant cerebellar ataxias in Taiwanese patients and clinical and molecular characterization of spinocerebellar ataxia type 6. *Arch Neurol*, **58**, 1105-1109.

9 Riess, O., Rub, U., Pastore, A., Bauer, P. and Schols, L. (2008) SCA3: neurological features, pathogenesis and animal models. *Cerebellum*, **7**, 125-137.

10 Doss-Pepe, E.W., Stenroos, E.S., Johnson, W.G. and Madura, K. (2003) Ataxin-3 interactions with rad23 and valosin-containing protein and its associations with ubiquitin chains and the proteasome are consistent with a role in ubiquitin-mediated proteolysis. *Mol Cell Biol*, **23**, 6469-6483.

11 Burnett, B., Li, F. and Pittman, R.N. (2003) The polyglutamine neurodegenerative protein ataxin-3 binds polyubiquitylated proteins and has ubiquitin protease activity. *Hum Mol Genet*, **12**, 3195-3205.

12 Donaldson, K.M., Li, W., Ching, K.A., Batalov, S., Tsai, C.C. and Joazeiro, C.A. (2003) Ubiquitin-mediated sequestration of normal cellular proteins into polyglutamine aggregates. *Proc Natl Acad Sci U S A*, **100**, 8892-8897.

13 Chow, M.K., Mackay, J.P., Whisstock, J.C., Scanlon, M.J. and Bottomley, S.P. (2004) Structural and functional analysis of the Josephin domain of the polyglutamine protein ataxin-3. *Biochem Biophys Res Commun*, **322**, 387-394.

14 Rodrigues, A.J., Coppola, G., Santos, C., Costa Mdo, C., Ailion, M., Sequeiros, J., Geschwind, D.H. and Maciel, P. (2007) Functional genomics and biochemical characterization of the C. elegans orthologue of the Machado-Joseph disease protein ataxin-3. *FASEB J*, **21**, 1126-1136.

15 do Carmo Costa, M., Bajanca, F., Rodrigues, A.J., Tome, R.J., Corthals, G., Macedo-Ribeiro, S., Paulson, H.L., Logarinho, E. and Maciel, P. Ataxin-3 plays a role in mouse myogenic differentiation through regulation of integrin subunit levels. *PLoS One*, **5**, e11728.

16 Wang, G., Sawai, N., Kotliarova, S., Kanazawa, I. and Nukina, N. (2000) Ataxin-3, the MJD1 gene product, interacts with the two human homologs of yeast DNA repair protein RAD23, HHR23A and HHR23B. *Hum Mol Genet*, **9**, 1795-1803.

17 Li, F., Macfarlan, T., Pittman, R.N. and Chakravarti, D. (2002) Ataxin-3 is a histone-binding protein with two independent transcriptional corepressor activities. *J Biol Chem*, **277**, 45004-45012.

18 Evert, B.O., Araujo, J., Vieira-Saecker, A.M., de Vos, R.A., Harendza, S., Klockgether, T. and Wullner, U. (2006) Ataxin-3 represses transcription via chromatin binding, interaction with histone deacetylase 3, and histone deacetylation. *J Neurosci*, **26**, 11474-11486.
19 Ferro, A., Carvalho, A.L., Teixeira-Castro, A., Almeida, C., Tome, R.J., Cortes, L., Rodrigues, A.J., Logarinho, E., Sequeiros, J., Macedo-Ribeiro, S. *et al.* (2007) NEDD8: a new ataxin-3 interactor. *Biochim Biophys Acta*, **1773**, 1619-1627.
20 Gauthier, L.R., Charrin, B.C., Borrell-Pages, M., Dompierre, J.P., Rangone, H., Cordelieres, F.P., De Mey, J., MacDonald, M.E., Lessmann, V., Humbert, S. *et al.* (2004) Huntingtin controls neurotrophic support and survival of neurons by enhancing BDNF vesicular transport along microtubules. *Cell*, **118**, 127-138.
21 Busch, A., Engemann, S., Lurz, R., Okazawa, H., Lehrach, H. and Wanker, E.E. (2003) Mutant huntingtin promotes the fibrillogenesis of wild-type huntingtin: a potential mechanism for loss of huntingtin function in Huntington's disease. *J Biol Chem*, **278**, 41452-41461.
22 Thomas, P.S., Jr., Fraley, G.S., Damian, V., Woodke, L.B., Zapata, F., Sopher, B.L., Plymate, S.R. and La Spada, A.R. (2006) Loss of endogenous androgen receptor protein accelerates motor neuron degeneration and accentuates androgen insensitivity in a mouse model of X-linked spinal and bulbar muscular atrophy. *Hum Mol Genet*, **15**, 2225-2238.
23 Lim, J., Crespo-Barreto, J., Jafar-Nejad, P., Bowman, A.B., Richman, R., Hill, D.E., Orr, H.T. and Zoghbi, H.Y. (2008) Opposing effects of polyglutamine expansion on native protein complexes contribute to SCA1. *Nature*, **452**, 713-718.
24 Crespo-Barreto, J., Fryer, J.D., Shaw, C.A., Orr, H.T. and Zoghbi, H.Y. Partial loss of ataxin-1 function contributes to transcriptional dysregulation in spinocerebellar ataxia type 1 pathogenesis. *PLoS Genet*, **6**, e1001021.
25 Cemal, C.K., Carroll, C.J., Lawrence, L., Lowrie, M.B., Ruddle, P., Al-Mahdawi, S., King, R.H., Pook, M.A., Huxley, C. and Chamberlain, S. (2002) YAC transgenic mice carrying pathological alleles of the MJD1 locus exhibit a mild and slowly progressive cerebellar deficit. *Hum Mol Genet*, **11**, 1075-1094.
26 Warrick, J.M., Morabito, L.M., Bilen, J., Gordesky-Gold, B., Faust, L.Z., Paulson, H.L. and Bonini, N.M. (2005) Ataxin-3 suppresses polyglutamine neurodegeneration in Drosophila by a ubiquitin-associated mechanism. *Mol Cell*, **18**, 37-48.
27 Hubener, J. and Riess, O. Polyglutamine-induced neurodegeneration in SCA3 is not mitigated by non-expanded ataxin-3: Conclusions from double-transgenic mouse models. *Neurobiol Dis*.
28 Alves, S., Nascimento-Ferreira, I., Dufour, N., Hassig, R., Auregan, G., Nobrega, C., Brouillet, E., Hantraye, P., Pedroso de Lima, M.C., Deglon, N. *et al.* Silencing ataxin-3 mitigates degeneration in a rat model of Machado-Joseph disease: no role for wild-type ataxin-3? *Hum Mol Genet*, **19**, 2380-2394.
29 Teixeira-Castro, A., Ailion, M., Jalles, A., Brignull, H.R., Vilaca, J.L., Dias, N., Rodrigues, P., Oliveira, J.F., Neves-Carvalho, A., Morimoto, R.I. *et al.* Neuron-specific proteotoxicity of mutant ataxin-3 in C. elegans: rescue by the DAF-16 and HSF-1 pathways. *Hum Mol Genet*.
30 Brignull, H.R., Moore, F.E., Tang, S.J. and Morimoto, R.I. (2006) Polyglutamine proteins at the pathogenic threshold display neuron-specific aggregation in a pan-neuronal Caenorhabditis elegans model. *J Neurosci*, **26**, 7597-7606.
31 Bargmann, C.I. and Kaplan, J.M. (1998) Signal transduction in the Caenorhabditis elegans nervous system. *Annu Rev Neurosci*, **21**, 279-308.
32 DiFiglia, M., Sapp, E., Chase, K.O., Davies, S.W., Bates, G.P., Vonsattel, J.P. and Aronin, N. (1997) Aggregation of huntingtin in neuronal intranuclear inclusions and dystrophic neurites in brain. *Science*, **277**, 1990-1993.
33 Scherzinger, E., Lurz, R., Turmaine, M., Mangiarini, L., Hollenbach, B., Hasenbank, R., Bates, G.P., Davies, S.W., Lehrach, H. and Wanker, E.E. (1997) Huntingtin-encoded polyglutamine expansions form amyloid-like protein aggregates in vitro and in vivo. *Cell*, **90**, 549-558.

34 White, J.G., Southgate, E., Thomson, J.N. and Brenner, S. (1976) The structure of the ventral nerve cord of Caenorhabditis elegans. *Philos Trans R Soc Lond B Biol Sci*, **275**, 327-348.
35 Rodrigues, A.J., Neves-Carvalho, A., Teixeira-Castro, A., Rokka, A., Corthals, G., Logarinho, E. and Maciel, P. Absence of Ataxin-3 Leads to Enhanced Stress Response in C. elegans. *PLoS One*, **6**, e18512.
36 Lang, A.E., Rogaeva, E.A., Tsuda, T., Hutterer, J. and St George-Hyslop, P. (1994) Homozygous inheritance of the Machado-Joseph disease gene. *Ann Neurol*, **36**, 443-447.
37 Lerer, I., Merims, D., Abeliovich, D., Zlotogora, J. and Gadoth, N. (1996) Machado-Joseph disease: correlation between the clinical features, the CAG repeat length and homozygosity for the mutation. *Eur J Hum Genet*, **4**, 3-7.
38 Fukutake, T., Shinotoh, H., Nishino, H., Ichikawa, Y., Goto, J., Kanazawa, I. and Hattori, T. (2002) Homozygous Machado-Joseph disease presenting as REM sleep behaviour disorder and prominent psychiatric symptoms. *Eur J Neurol*, **9**, 97-100.
39 Haacke, A., Broadley, S.A., Boteva, R., Tzvetkov, N., Hartl, F.U. and Breuer, P. (2006) Proteolytic cleavage of polyglutamine-expanded ataxin-3 is critical for aggregation and sequestration of non-expanded ataxin-3. *Hum Mol Genet*, **15**, 555-568.
40 Kim, S., Nollen, E.A., Kitagawa, K., Bindokas, V.P. and Morimoto, R.I. (2002) Polyglutamine protein aggregates are dynamic. *Nat Cell Biol*, **4**, 826-831.
41 Takahashi, J., Tanaka, J., Arai, K., Funata, N., Hattori, T., Fukuda, T., Fujigasaki, H. and Uchihara, T. (2001) Recruitment of nonexpanded polyglutamine proteins to intranuclear aggregates in neuronal intranuclear hyaline inclusion disease. *J Neuropathol Exp Neurol*, **60**, 369-376.
42 Burnett, B.G. and Pittman, R.N. (2005) The polyglutamine neurodegenerative protein ataxin 3 regulates aggresome formation. *Proc Natl Acad Sci U S A*, **102**, 4330-4335.
43 Tsuda, H., Jafar-Nejad, H., Patel, A.J., Sun, Y., Chen, H.K., Rose, M.F., Venken, K.J., Botas, J., Orr, H.T., Bellen, H.J. *et al.* (2005) The AXH domain of Ataxin-1 mediates neurodegeneration through its interaction with Gfi-1/Senseless proteins. *Cell*, **122**, 633-644.
44 Emamian, E.S., Kaytor, M.D., Duvick, L.A., Zu, T., Tousey, S.K., Zoghbi, H.Y., Clark, H.B. and Orr, H.T. (2003) Serine 776 of ataxin-1 is critical for polyglutamine-induced disease in SCA1 transgenic mice. *Neuron*, **38**, 375-387.
45 Brenner, S. (1974) The genetics of Caenorhabditis elegans. *Genetics*, **77**, 71-94.
46 Lewis, J.A. and Fleming, J.T. (1995) Basic culture methods. *Methods Cell Biol*, **48**, 3-29.
47 Phair, R.D. and Misteli, T. (2000) High mobility of proteins in the mammalian cell nucleus. *Nature*, **404**, 604-609.
48 Gidalevitz, T., Ben-Zvi, A., Ho, K.H., Brignull, H.R. and Morimoto, R.I. (2006) Progressive disruption of cellular protein folding in models of polyglutamine diseases. *Science*, **311**, 1471-1474.

Supplemental material

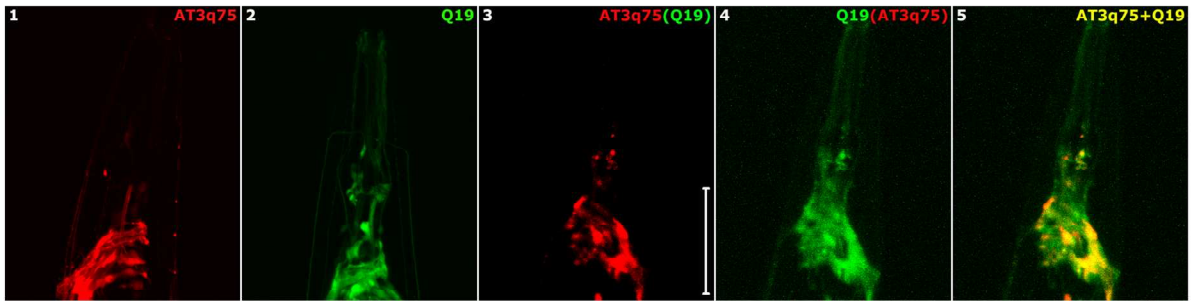

Figure S1. Flattened Z-stacks of *C. elegans* heads showed that co- expression of mutant subthreshold ATXN3 and Q19 proteins (panels 3 and 4) did not cause an alteration in protein distribution compared with animals expressing AT3q75 (panel 1) and Q19 (panel 2) proteins-alone even at day 8. Panel 5 shows the merged image. Scale bar= 50 μm.

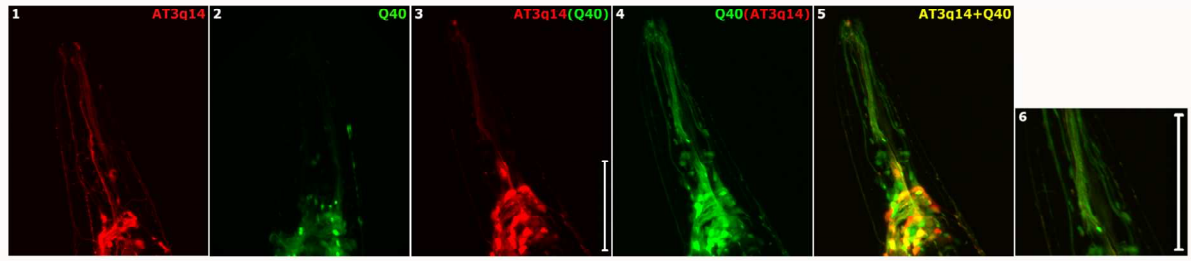

Figure S2. Flattened Z-stacks of *C. elegans* head co- expression of wild-type ATXN3 with Q40 proteins did not cause the formation of foci-like structures in the sensory processes even at day 8. Scale bar= 50 μm. White box is indicative of magnified picture, shown in panel 6.

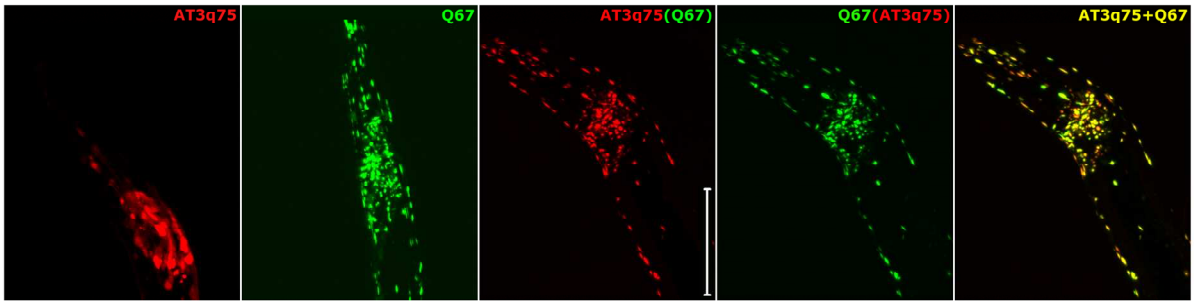

Figure S3. Flattened Z-stacks of *C. elegans* head expressing AT3q75::YFP with Q67::CFP proteins at day 2. AT3q75 was distributed into the Q67 aggregates and foci localization was visible along with the formation of the Q67 aggregates, indicating that mutant ATXN3 recruitment occurred earlier in the animals' development when compared with the recruitment dynamics of the wild-type protein. Panels one and two show expression of AT3q75 and of Q67 proteins, respectively. Panels three, four and five show an animal co-expressing AT3q75 and Q67 proteins. Scale bar= 50 μm.

Chapter 5

Searching for therapeutic strategies in a *C. elegans* model of MJD

Searching for therapeutic strategies in a *C. elegans* model for Machado-Joseph disease.

Andreia Teixeira-Castro, Adriana Miranda, Ana Jalles, Sara Carvalho, Carlos Bessa and Patrícia Maciel

[1]Life and Health Sciences Research Institute (ICVS), School of Health Sciences, University of Minho, 4710-057 Braga, Portugal; [2]ICVS/3B's - PT Government Associate Laboratory, Braga/Guimarães, Portugal.

Abstract

Machado-Joseph disease (MJD) is a late-onset neurodegenerative disorder, characterized by ataxia, ophthalmoplegia and spasticity. Its late-onset and slowly progressive nature increases both the time and cost of testing potential therapeutic compounds in mammalian models. An alternative is to initially assess the efficacy of compounds in invertebrate models, reducing the time of testing from months to days while still allowing the assessment of the compound's effectiveness at the organism level. We screened five candidate compounds previously identified as having therapeutic effect in cell culture/animal studies of several polyglutamine (polyQ) diseases in a *C. elegans* model of MJD and found that four drugs, lithium chloride, CCI-779 (an analog of rapamycin), SAHA and Resveratrol, reduced neuronal dysfunction. These compounds, however, had differential effects in mutant ATXN3 aggregation. The results suggest that the manipulation of distinct pathways thought to be involved in polyQ-induced degeneration could impact positively in MJD pathogenesis. The drug-testing assays presented here will be useful for rapid and inexpensive high-throughput testing of large number of small molecules with potential therapeutic significance for MJD, and for elucidating drug targets and pathogenic pathways associated with disease. Additionally, the neuroprotection conferred by the drugs, two of which are FDA-approved, suggests that they may be useful for MJD therapy, prompting us to test them in mouse models to validate these findings.

Introduction

Notwithstanding the prevalence of neurodegenerative diseases, effective therapies for protein misfolding disorders are lacking (1-3). Specifically for polyglutamine (polyQ) disorders, although in the majority of the cases the normal function of each disease-associated protein and its pathogenic effect when mutated are not clear, there seem to be common pathways that could be explored in the development of therapeutics. Also, since most of the polyQ proteins cannot be held as a tractable drug target it became common to look for downstream targets that might be involved in pathophysiology. Examples include the use of transglutaminase inhibitors, Hsp90 inhibitors and rapamycin to interfere with protein misfolding, aggregation and clearance (4-6); the application of creatine and ubiquinone to fight oxidative stress and restore mitochondrial electron transport chain activity (7, 8); the use of sodium butyrate (SB) and other histone deacetylase (HDAC) inhibitors to rescue transcriptional repression (9-11); the introduction of caspase inhibitors to prevent neuronal cell death and proteolysis of huntingtin (12); and administration of various compounds that restore neuronal excitability and neurotransmission alterations (13).

Importantly, the pathogenic mechanisms themselves have been used as assay readouts for the identification of novel, effective and disease-specific small molecules for drug discovery in Huntington's disease (HD) (14), Parkinson's (15), amyotrophic lateral sclerosis (ALS) (16), tauopathies (17) and in spinal bulbar muscular atrophy (SBMA) (18). Many of the primary screens for the identification of suitable small molecules have been based on *in vitro* aggregation assays (19, 20). Stable amyloid-like aggregates, formed when the glutathione S-transferase (GST) tag of a GST-Huntingtin (Htt) *E. coli* fusion protein was removed proteolytically, were used to screen for molecules that inhibited Htt aggregation (20). The authors developed a simple filter retardation assay and measured concentration-response values for several aggregation inhibitors like Congo red and thioflavine S (21). Cell-based aggregation assays have also been developed, using yeast cells (22), hippocampal brain slice cultures from transgenic mice (23) and Förster resonance energy transfer (FRET)-based mammalian cell assays (18, 24). Rapid advances are being made to develop automated high throughput image analysis algorithms that quantify protein aggregates in cell cultures, in order to identify potential aggregation inhibitors (25, 26). An alternative approach was the search for compounds that instead are able to increase the cellular degradation of soluble or aggregated forms of the mutated proteins, like autophagy-modulating molecules (27).

It is important to notice that the development of therapeutics has been less explored in MJD, an exception being the study by Chen and collaborators which relied on the administration of dantrolene, a known clinical relevant stabilizer of intracellular Ca^{2+} concentration, that improved motor performance and prevented neuronal cell loss in pontine nuclei and substantia nigra brain regions of the transgenic mouse model SCA3-YAC-84 (28). In another study, daily intraperitoneal administration of HDAC inhibitor SB significantly reversed ataxin-3-Q79-induced histone hypoacetylation and transcriptional downregulation in the cerebellum of SCA3 transgenic

mice. SB treatment also delayed the onset of ataxic symptoms, ameliorated neurological phenotypes and improved the mice survival rate (29). Induction of autophagy was also shown to reduce mutant ataxin-3 levels and toxicity in yet another mouse model of MJD, but this effect was less robust (30). In line with this finding, gene therapy studies in MJD, using a lentivirus-based rat model of MJD, suggested that overexpression of beclin-1, a crucial protein in the early nucleation step of autophagy, led to the stimulation of the autophagic flux and mutant ataxin-3 clearance (31). Moreover, it has been shown that shutting down the expression of the mutant protein (and of the wild-type allele) would have a positive impact on disease pathogenesis (32, 33). However, modulation of *ATXN3* gene expression is still hard to translate into the clinical practice.

The challenge of treating neurodegenerative disorders arises from an insufficient knowledge about the contribution of multiple pathways to disease pathogenesis. Furthermore, given the fact that the disease symptoms appear, in the majority of the cases, in aged populations, testing the therapeutic value of small molecules in vertebrate disease models requires time-consuming experimental designs. The development of rapid and inexpensive *in vivo* strategies is therefore of paramount importance. The usage of mammalian cell culture models is, as explained above, a good alternative, however, these systems lack non-cell-autonomous effect and the environment context of the organism. This is particularly relevant in the case of the nervous system, in which cells function in circuits that are continuously modulated by exposure to stimuli and result in outcomes such as behaviors, aspects that are absent in cell culture paradigms.

Recent data from our lab have shown that many aspects of MJD can be properly modeled in the round worm *Caenorhabditis elegans* (34), and others have shown that it can provide a suitable platform for both the discovery of new bioactive compounds and target identification (35). Furthermore, several years of neurobiological and anti-parasitic drug studies in *C. elegans* provide a strong foundation for the use of this organism in therapeutic compound identification (36-38). The present work was based on the idea that the finding of effective drugs can be accomplished by looking simultaneously at protein aggregation (conformational disorder) in the live neuronal cells, and on its impact on neuron-regulated behavior of the whole-animal (neurodegenerative disorder). Using a candidate drug approach, we tested compounds that have been previously shown to be effective in various model systems for other polyQ disorders. In addition to confirming the therapeutic effect of four of these compounds, we were able to validate our *C. elegans* model of MJD pathogenesis as a useful tool to be used in high-throughput testing of therapeutic small molecules and to identify promising drugs for treatment of MJD.

Results

Determination of compound concentration range for drug screening in *C. elegans*

We chose to test a collection of five compounds that have demonstrated therapeutic efficacy, in either cell culture and/or animal models of polyQ pathogenesis, in our *C. elegans* MJD model (34) (Fig. 1). These candidates represent compounds that may protect against mutant ATXN3-mediated pathogenesis by modulating a variety of cellular pathways, namely autophagy, mitochondrial function and transcription. We first employed a systematic method, previously described by Voisine and collaborators (39), for selecting optimal drug concentrations to be assessed in *C. elegans*. A drug dosage was considered non-toxic to wild-type (WT) animals, if did not affect growth, survival and fertility. All compounds were tested in a dose dilution series in the food clearance assay, starting with the highest soluble concentration. Compounds were monitored by measuring the rate at which the food (OP50 bacteria suspension) was consumed. Optical density was measured every day (from day 1 to day 8) at 595 nm (OD_{595}) (Fig. 1). At 20°C, after 4 days the OD of the wells without compound decreased significantly. Any drug concentration that was toxic to the animals resulted in a dose-dependent reduction of the rate at which food was cleared (Fig. 2). The highest concentration tolerated by *C. elegans* for each drug is depicted in Table 1. For all the compounds that showed decreased solubility in water, toxicity of the solvent (Ethanol for the Rapamycin analog, CCi-779 and DMSO for Suberoylanilide hydroxamic acid (SAHA) and Resveratrol) was previously determined in a similar manner (data not shown). Creatine showed very low solubility in any of the solvents tested (data not shown), so we supplemented the food source with Creatine powder and grew the animals on standard solid media. For this drug, we also assessed survival, fertility and growth to determine the highest non-toxic concentration (Table 1 and Fig. 3). In summary, we determined the concentration range to test in our *C. elegans* model for MJD pathogenesis for each of the candidate therapeutic compounds.

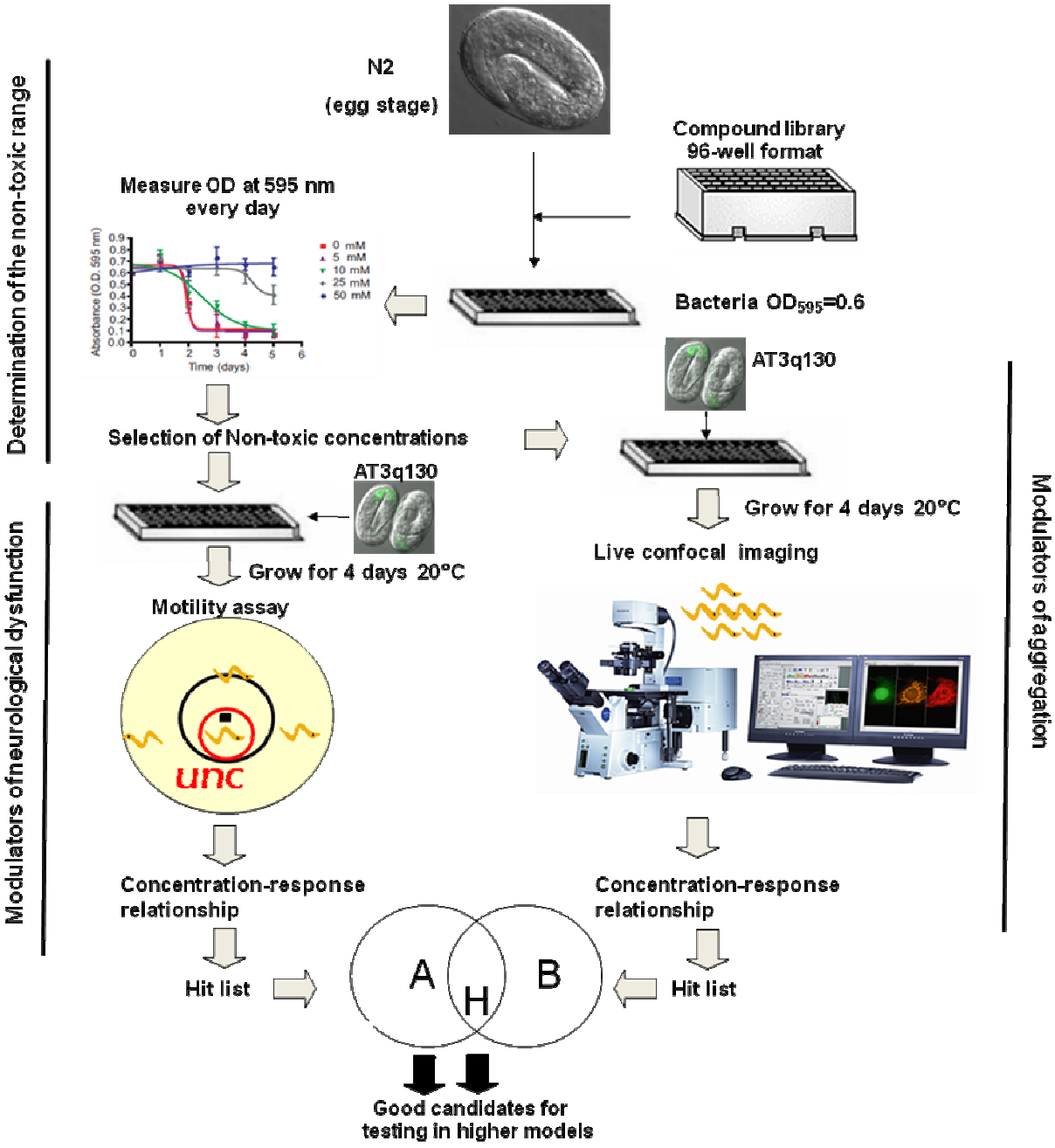

Figure 1. Experimental design for screening potential therapeutic compounds for MJD pathogenesis in *C. elegans*. The first step is to determine the range of safe concentrations for each compound, using the food clearance assay. The rate at which the food source is consumed by WT animals is a good indication of normal growth, survival and fecundity. Next, mutant ATXN3 animals are grown with different concentrations of each small molecule and assayed for locomotion defects and aggregation profile. Compounds that cause rescue of locomotion impairment and also a reduction of the aggregation load in AT3q130 animals, are considered good candidates for testing in higher model organisms.

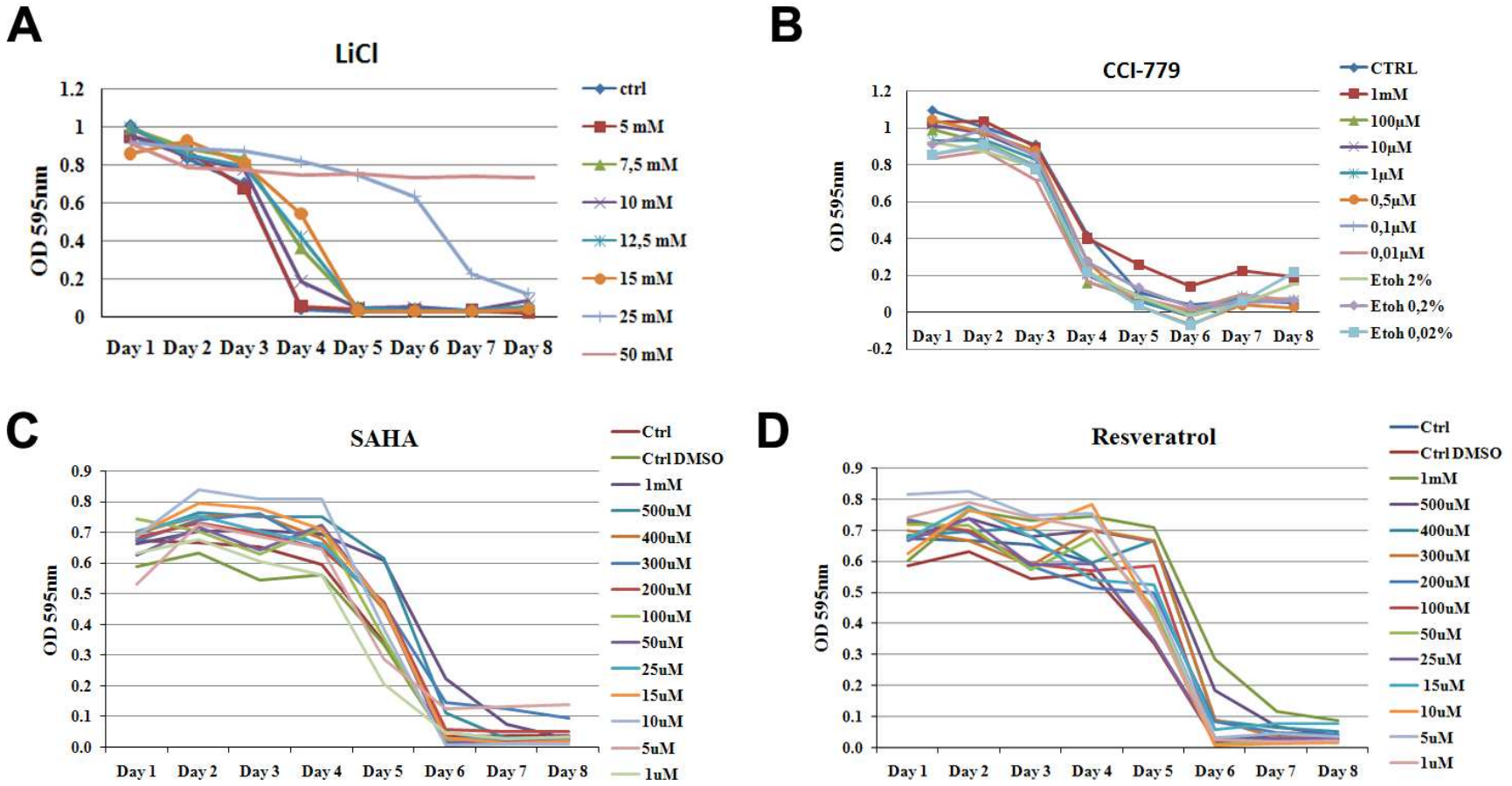

Figure 2. Concentration of compounds was assessed using a food clearance assay. The OD of *E. coli* is reported daily for each concentration of LiCl (A), CCI-779 (B), SAHA (C) and Resveratrol (D). The mean OD is calculated for each day from triplicate samples and plotted over time. Highest safe concentrations were established for each compound: <12.5mM for LiCl; ≤100µM for CCI-779;and < 100µM for SAHA and Resveratrol.

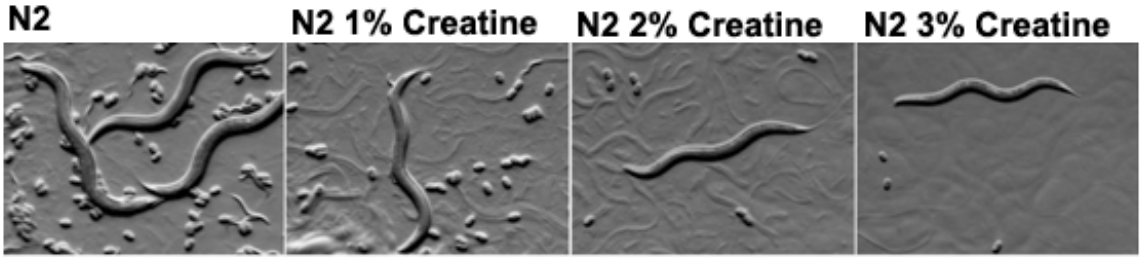

Figure 3. Wild-type animals were grown in NGM media seeded with OP50 supplemented with Creatine at the indicated concentrations. When treated with 3% creatine animals showed developmental delay and reduced brood size. Highest safe concentration was set as <2% for creatine-supplemented media. Pictures show day 4 (post-hatching) age-synchronized animals.

Table 1. Compounds screened in *C. elegans* MJD model for rescue of neuronal dysfunction and aggregation.

Compounds	Putative cell pathway	Conc. Tested	Effect in AT3q130
LICl	GSK-3β inhibitor ↑Autophagy	5- 10 mM	reduction of locomotion impairment mild reduction in the aggregation load
CCI-779	mTOR inhibitor ↑Autophagy	1- 100 μM	reduction of locomotion impairment mild reduction in the aggregation load
Creatine	Mitochondria stabilization ↓Oxidative stress	0.5- 2 %	no effect
SAHA	HDAC inhibitor ↑Transcription	1- 200 μM	reduction of locomotion impairment reduction in the aggregation load
Resveratrol	Sirtuin activator Anti-oxidant effect ↓Transcription; ↓Oxidative stress	1- 200 μM	reduction of locomotion impairment mild reduction in the aggregation load

Screening for compounds that rescued mutant ATXN3-mediated motor dysfunction

We evaluated compound efficacy to rescue neuronal dysfunction in our *C. elegans* model for MJD pathogenesis (Fig. 1) (34). Expression of mutant ATXN3 (AT3q130) in all *C. elegans* neuronal cells resulted in neuronal-cell type specific aggregation that correlated with toxicity. AT3q130 animals grown in liquid medium with or without drug for four days, and then tested for defects in locomotion, by employing a motility assay (40). Animals treated with lithium chloride (LiCl) and with CCi-779, treatments thought to activate autophagy in a mTOR-independent and dependent manner, respectively, resulted in a partial rescue of locomotion impairment (Fig. 4A, left and middle panels). Next, we evaluated the potential combinatorial effects of both compounds on motor dysfunction and found no further improvement in locomotion when the co-treatment was explored (Fig. 4A, right panel).

Creatine was shown to be neuroprotective in several *in vitro* and *in vivo* models of Alzheimer's, Huntigton's, Parkinson's disease and of amyotrophic lateral sclerosis (ALS) (41) and to target mitochondria and stabilize it. However, in our model creatine food supplementation had no effect in mutant ATXN3-mediated neuronal dysfunction (Fig. 4B) at all concentrations tested, not even after three generations (data not shown).

SAHA and Resveratrol modulate transcription in opposing directions through binding histone deacetylases (HDAC) targets in the cells. SAHA is a HDAC inhibitor (42), whereas Resveratrol is thought to be a sirtuin activator (43). AT3q130 animals treated with both drugs independently, showed a significant amelioration of motility defects in our *C. elegans* model (Fig. 4C).

Based on these results, we suggest autophagy and transcription modulation as promising therapeutic strategies also in MJD.

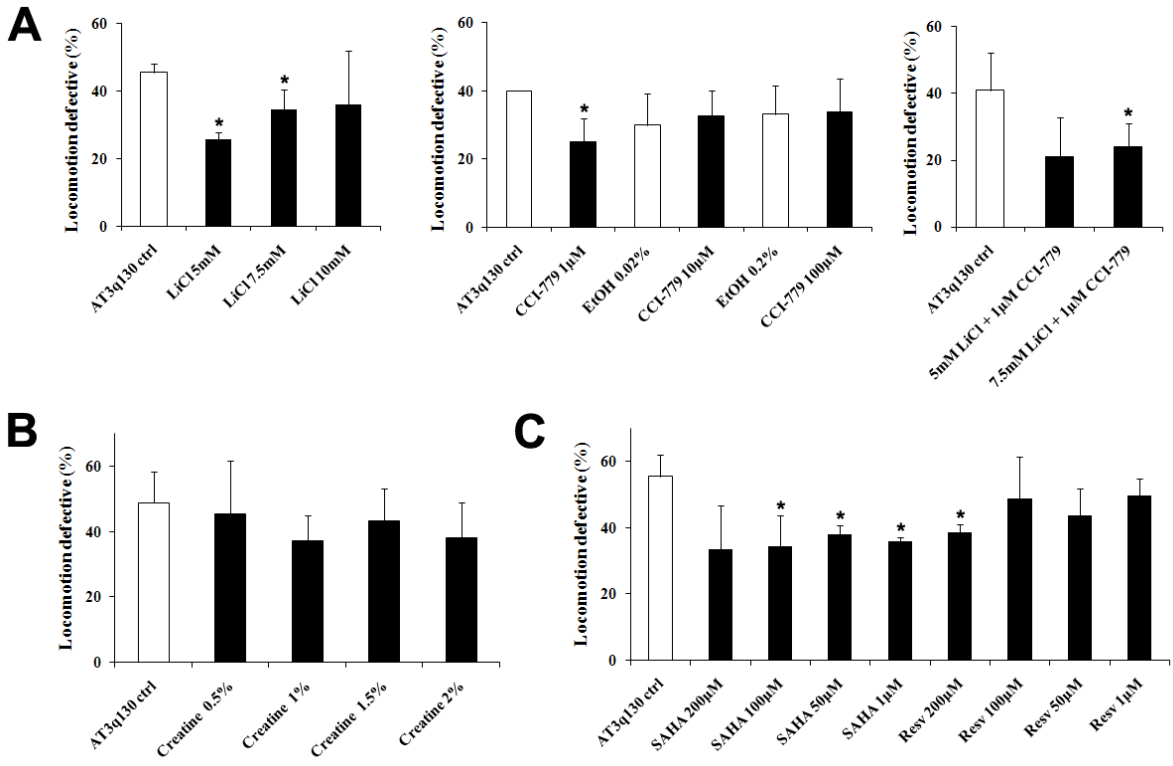

Figure 4. AT3q130 animals treatment with the small molecules targeting autophagy (A), mitochondrial toxicity (B) and transcription dysregulation (C). Animals treated with 5 and 7.5mM of LiCl showed a significant reduction in mutant AT3q130-mediated motility impairment (A, left panel). CCI-779 at 1 µM also caused a significant reduction in locomotion defects (A, middle panel). However, the combination of both drugs, which potentially would activate autophagy through independent cellular targets, did not further ameliorate motility defects of the transgenic animals. Creatine treatment showed no significant rescue of motor dysfunction (B). SAHA and resveratrol treated animals showed improvement in motor function. Data are the mean ± SD, at least 150 animals per data point. Student's t-test, ∗< P , 0.05.

Screening for compounds that rescued mutant ATXN3-mediated aggregation

To determine if the effects of the small molecules on motor dysfunction were coupled with potential alterations in mutant-ATXN3 aggregation profile in the animals, we performed live confocal imaging assays in day 4 treated and non-treated animals (Fig. 1 and 5). Aggregate quantification (44) of animals treated with LiCl and CCi779 revealed that both compounds caused a mild reduction of the aggregation load (Fig. 5A). As expected, AT3q130 animals fed with bacteria supplemented with creatine did not shown any significant differences in aggregation (Fig. 5B). SAHA treatment caused a significant reduction in aggregation, whereas resveratrol showed a milder effect (Fig. 5C).

Taken together, the results suggest that, like reduction in locomotion impairment, aggregation is also diminished upon drug treatment, with some drugs being more efficient than others. Ongoing experiments aim to determine the effect of the different compounds in total mutant ATXN3 protein levels.

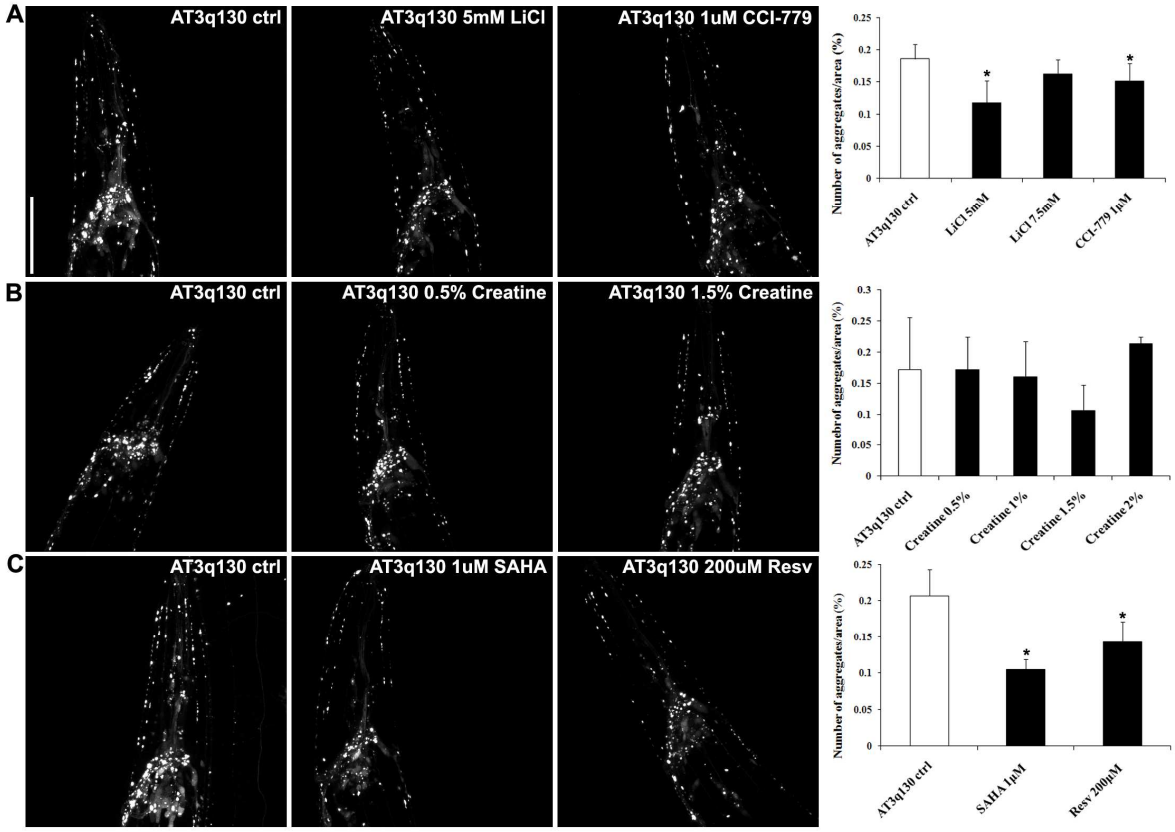

Figure 5. Pharmacologic treatment of mutant ATXN3 animals with LiCl, CCI-779, SAHA and resveratrol caused a significant reduction of the number of aggregates per area unit. LiCl-treated AT3q130 animals showed a reduction in the aggregation phenotype at day 4 of adulthood, more significant than the effect of CCI-779. Creatine at 1.5 % resulted in a tendency to a reduction in aggregation that did not reach statistical significance. SAHA and resveratrol also rescued mutant-ATXN3 aggregation, with SHA showing a stronger effect. Quantification of number of aggregates per area was performed using our novel imaging processing application for aggregates quantification in *C. elegans*, and values are the mean ± SD of six or more animals per group. ANOVA, * , $p<0.05$.

Discussion

In this study, we have started to develop strategies for efficiently assessing efficacy of compounds in our *C. elegans* MJD model (Fig. 1). The methods employed take advantage of the strengths of *C. elegans* for drug identification, namely (i) the small-scale liquid cultures that significantly reduce the amount of drug required, (ii) the visualization of fluorescently tagged proteins in live neuronal cells, and (iii) the ability to test drug impact on animals' behavior. With this work, we have validated our *C. elegans* model and approach for therapeutic value in MJD, using a candidate-drug strategy. In the near future, we aim to find new bioactive compounds using a hypothesis-free approach (see Appendix 2).

All cellular pathways and components are under continuous surveillance by intracellular quality control mechanisms. The major players involved in these quality control mechanisms are molecular chaperones, which detect abnormal proteins; and proteases, that eliminate them from the cells. Malfunctioning of cellular surveillance systems inevitably leads to cell toxicity and disease. As so, it is intuitive to think that these cell surveillance pathways and "escort" systems modulate the majority of diseases that highly rely on aggregation-prone proteins. Therefore, targeting the autophagic system may be a valuable strategy for the treatment of many neurodegenerative disorders. Since the first discovery of autophagic clearance of mutant huntingtin by rapamycin was reported (45), studies have identified novel autophagy-inducing pathways/drugs. Increased mutant ATXN3 clearance, due to rapamycin-analog CCI-779-treatment or overexpression of beclin-1, also ameliorated neurological symptoms and pathology in transgenic mice and rats, respectively (30, 31). In *C. elegans*, knockout of UNC-51, homolog of yeast ATG-1, enhanced polyQ aggregation (46). Here, we show that chronic treatment with CCI-779 in *C. elegans* reduced mutant ATXN3 mediated locomotion impairment and aggregation. However, it is important to notice that the treatment was only effective at very low dosages, which is consistent with the fact that mTOR controls several cellular processes besides autophagy, probably contributing to complications seen in long term usage of mTOR-dependent autophagy activators ((47) and Duarte-Silva, S., unpublished observations).

The usage of free Inositol-lowering agents (IMPase inhibitors), which in turn cause a depletion of inositol-1,4,5-trisphosphate levels, like lithium chloride, also reduced the proportion of cells with mutant huntingtin aggregates (48, 49).and in mutant huntingtin-mediated toxicity (39). The autophagy-inducing property of lithium has recently been suggested to contribute to its protective effects in ALS patients and mouse models, where the drug treatment increased survival and delayed disease progression (50). When treated with lithium, AT3q130 animals also show reduced pathogenesis. However, combination of lithium and CCI-779 showed no additive effect on mutant ATXN3-mediated neuronal dysfunction, which suggests that some level of toxicity in the dosages used may be occurring. Indeed, the combination of 5mM LiCl with 1μM of the rapamycin analog did not significantly reduce locomotion impairment of AT3q130 animals, in opposition to the results obtained when the compounds were used alone. This is a very surprising result since one would expect a triple protection

achieved by this co-treatment: activation of autophagy through two independent pathways and the neuroprotective effects caused by lithium-mediated glycogen synthase kinase-3β (GSK-3β) inhibition, due to activation of β-catenin-Tcf pathway, as has been suggested in HD (51). In fact, lithium may also be mediating its effects via autophagy-independent pathways. In *C. elegans*, lithium exposure at clinically relevant concentrations resulted in extended lifespan (52). Increased longevity is dependent on *gsk-3β* and results in reduced expression of a histone demethylase LSD-1, suggesting that Li^+ regulates survival by modulating histone methylation and chromatin structure (52). Pharmacogenetic approaches are ongoing in our study to implicate specific cellular pathways in each compound's mechanism of action.

The assumption that there are common pathophysiologic pathways that underlie many of these conformational disorders can, however, be misleading. There is a extensive body of literature, which has demonstrated that creatine has neuroprotective effects both *in vitro* and *in vivo* in Alzheimer's disease (AD), PD, HD and ALS (reviewed in (41), by improving overall cellular bioenergetics. Creatine was shown to protect against excitotoxic lesions produced by N-methyl-D-aspartate and to be neuroprotective against lesions produced by the toxins malonate and 3-nitropropionic acid (3-NP), which are reversible and irreversible inhibitors of succinate dehydrogenase, respectively. Creatine also produced dose-dependent neuroprotective effects against MPTP toxicity reducing the loss of dopamine within the striatum and the loss of dopaminergic neurons in the substantia nigra (53). In transgenic mice, creatine produced an extension of survival, improved motor performance, and a reduction in loss of motor neurons in a transgenic mouse model of ALS (54). Similar results were obtained in the R6/2 and the N-171-82Q transgenic mouse models of HD, even when its administration was delayed until the onset of disease symptoms (55). The neuroprotective effects of creatine in HD and PD were potentiated when in combination with coenzyme Q10 (CoQ10) (56). CoQ10 co-treatment produced additive neuroprotection against both MPTP and 3-NP toxicity, and reduced the appearance of alpha-synuclein aggregates (56). In the R6/2 transgenic mouse model of HD, the combination of CoQ and creatine produced additive effects in terms of improving survival. Creatine may stabilize mitochondrial creatine kinase, and prevent activation of the mitochondrial permeability transition. Administration of creatine increases the brain levels of creatine and phosphocreatine. Due to its neuroprotective effects, creatine is now in clinical trials for the treatment of PD and HD (41). However, we were not able to reproduce this neuroprotection in our *C. elegans* MJD model.

Despite differences in disease etiology and cellular properties of affected neurons in various types of neurodegenerative disorders, loss of acetylation homeostasis appears also to represent a critical mechanism commonly underlying neuronal dysfunction and degeneration. General loss of acetylating agents along with parallel gain of histone deacetylase (HDAC) activity may be the primary cause. The fine-tuning of the altered histone acetyl transferase (HAT)–HDAC balance can be achieved by using general HDAC inhibitors to reestablish the acetylation threshold in degenerating neurons (reviewed in (57)). Manipulative strategies aimed at restoring the acetylation homeostasis by rebating excess HDAC activity. Indeed, HDAC inhibitors like Trichostatin A (TSA),

SAHA and SB showed encouraging results from yeast to mouse models of expanded polyQ proteins (9, 10, 39, 58-60). TSA and SAHA treatment of a *C. elegans* model for Htt neurotoxicity caused a significant reduction in neurodegeneration (39, 60). Interestingly, the last study involving a preclinical application of HDAC inhibitor, SAHA showed encouraging results. SAHA increased acetylation globally in the brain and enhanced motor function significantly. Although SAHA does not appreciably penetrate brain barriers by itself, it does so when in complex with 2-hydroxypropyl-β-cyclodextrin in solution. Thus, a solution of this complex in drinking water can make SAHA a cost-effective pharmacological candidate that could be administered by unsophisticated means (57). Also in mutant ATXN3-expressing worms, SAHA treatment resulted in important improvements in motor function. There was also a significant reduction in aggregation, although at this point we still don't know what are the key protein effectors underlying this amelioration.

The usage of Sirtuin inhibitors was also found to have therapeutic value. Genetic inhibition of SIRT2 via small interfering RNA rescued α-synuclein toxicity. Furthermore, the inhibitors protected against dopaminergic cell death both *in vitro* and in a Drosophila model of Parkinson's disease (15).

The Sirtuin family of proteins is thought to play a role in aging. In *C. elegans*, overexpression of *sir2.1* extends lifespan (61) and chemical activation of SIR2.1 rescues mutant huntingtin-mediated neuronal toxicity in *C. elegans* and mouse (62). Although this result is conceptually in contrast with the usage of HDAC inhibitors, the effect of the sirtuin activators may be through other mechanisms that are associated with increased longevity and improving mitochondrial function (reviewed in (63). Resveratrol treatment had a mild effect in our MJD pathogenesis model and we will perform pharmacogenetic studies to determine if the effect is mediated by longevity determinating pathways.

Taken together, which of the small molecules tested will be promising candidates for rescuing neuronal dysfunction? Selection of a molecule for future drug development is based on detailed assessment of its biological potency, safety and pharmacotoxicity. Thorough determination of drug targets is also very important. So, *C. elegans* disease models should be valuable tools for rapid identification of potential therapeutic compounds for aging related human diseases and cellular pathway elucidation.

Finally, the strategy that we set up for these studies opens the door to higher-throughput approaches, to test thousands of compounds in the search for a suitable therapy for MJD.

Material and Methods

Nematode strains and general methods. *C. elegans* N2[wild-type] and *E. coli* food source OP50 were obtained from the *Caenorhabditis elegans* Genetics Center. AT3q130 expressing strains were previously described (34). Standard methods were used for culturing and observing *C. elegans*, unless otherwise noted (64). Nematodes were grown on NGM plates seeded with OP50 strain at 20°C. Populations were synchronised either by treating young adult animals with alkaline hypochlorite solution (0.5 M NaOH, ~2.6% NaClO) for 7 min (65) or by collecting embryos laid by adult animals within a 3-h period. All animals were scored at the same chronological age. Experiments were repeated at least three times. All assays were performed blind.

***C. elegans* treatment with small molecules.** Drug assays were performed in 96-well plates in liquid culture, as previously described (39, 66), with the following modifications: each well contained a final volume of 60 μL, including 20–25 animals in egg stage, drug at the appropriate concentration and OP50 bacteria to a final OD of 0.8 measured in the microplate reader (Bio-Rad microplate reader 680). Animals and bacteria were resuspended in S-medium supplemented with streptomycin, penicillin and nystatin (Sigma). Worms were grown with continuous shaking at 180 rpm at 20°C. Compound preparation: Stock solution of 200 mM LiCl (1.05679-0100, Merck) was prepared in water. CCi779 (T8040, LC-laboratories) 48.5 mM stock solution was prepared in EtOH. Stock solutions of 2.4 mM SAHA (Varinostat, V-8477, LC-laboratories) and Resveratrol (43007500, ACROS Organic) were prepared in DMSO. The effect of compounds on *C. elegans* physiology is monitored by the rate at which the *E. coli* food suspension was consumed, as a read out for *C. elegans* growth, survival or fecundity. The absorbance (OD 595nm) was measured daily in the microplate reader. We used N2 animals when determining compound concentration and AT3q130 animals for all the other assays. At day 4, AT3q130-drug treated and control animals were imaged using a confocal microscope (Olympus FV1000) and tested for motility defects.

Creatine treatment. Creatine treatment was performed in regular NGM plates (64). OP50 cultures were supplemented with Creatine powder obtained from Sigma (C0780, St. Louis, MO, USA), at the indicated percentages. Plates were seeded with 200 μL of OP50/Creatine and left at RT to dry. Animals were always grown on Creatine plates at least one generation prior to the beginning of the assays. For the toxicity screen, animals were observed every day and growth rates, fertility and survival parameters were evaluated. After determination of the safe toxicity range for Creatine, synchronized day 4 animals were scored for motility defects and alteration in the aggregation profile.

Motility assay. All assays were performed at room temperature (~20°C) using synchronised animals grown at 20°C. Five animals 4-day-old were placed simultaneously in the middle of a freshly seeded plate, equilibrated at

20°C. Animals remaining inside a 1-cm circle after one min were scored as locomotion defective. A total of 150 animals were scored in at least three independent assays for each condition, and the statistical significance was assessed by Student's *t*-test, as described previously (40).

Confocal imaging. All images were captured on an Olympus FV1000 (Japan) confocal microscope, under a 60x oil objective. Animals were immobilised with 2 mM levamisole and mounted on a 3% agarose pad. Z-series imaging was taken of all vehicle- and compound-treated animals, using a 515 nm laser excitation for YFP fusion proteins. The pinhole was adjusted to 1.0 Airy unit of optical slice, and a scan was taken every ~0.5 μm along the Z-axis.

Quantification of the aggregates. *C. elegans* fluorescent images were acquired using the Olympus FV1000 confocal microscope. Confocal microscope parameters were set using Hi-Lo pallet, such that protein foci and not diffuse fluorescent areas of the animals nervous system presented pixel intensity higher than 255. The z-stack was collapsed and the aggregate load of each animal (per area unit) was calculated on an imaging processing application using MeVisLab as a platform. Details on the application and on the segmentation algorithms were described elsewhere (44). At least six images were analyzed per genotype and statistical assessment was performed using Origin software (OriginLab) (*ANOVA* and *Bonferroni* mean correction test for multiple comparisons).

Acknowledgments

We are grateful to members of the Maciel laboratory for sharing reagents, for critical analysis of the data and for their helpful discussions on the manuscript. A special thanks to Susana Garcia and Cindy Voisine for helpful discussions regarding the food clearance assay. Also to the Caenorhabditis Genetics Center (CGC), which is funded by the National Institutes of Health – National Center for Research Resources, for nematode strains. This work was supported by grants from Fundacao para a Ciencia e Tecnologia (FCT) to P.M. (PTDC/SAU-GMG/64076/2006, PTDC/SAU-GMG/112617/2009, SFRH/BD/27258/2006 to A.T.C., UMINHO/BI/052/2010 to A.J.), and from the National Ataxia Foundation.

References:

1 Aguzzi, A. and O'Connor, T. Protein aggregation diseases: pathogenicity and therapeutic perspectives. *Nat Rev Drug Discov*, **9**, 237-248.

2 Bartolini, M. and Andrisano, V. Strategies for the inhibition of protein aggregation in human diseases. *Chembiochem*, **11**, 1018-1035.

3 Krainc, D. Clearance of mutant proteins as a therapeutic target in neurodegenerative diseases. *Arch Neurol*, **67**, 388-392.

4 Wilhelmus, M.M., van Dam, A.M. and Drukarch, B. (2008) Tissue transglutaminase: a novel pharmacological target in preventing toxic protein aggregation in neurodegenerative diseases. *Eur J Pharmacol*, **585**, 464-472.

5 Waza, M., Adachi, H., Katsuno, M., Minamiyama, M., Sang, C., Tanaka, F., Inukai, A., Doyu, M. and Sobue, G. (2005) 17-AAG, an Hsp90 inhibitor, ameliorates polyglutamine-mediated motor neuron degeneration. *Nat Med*, **11**, 1088-1095.

6 Wyttenbach, A., Hands, S., King, M.A., Lipkow, K. and Tolkovsky, A.M. (2008) Amelioration of protein misfolding disease by rapamycin: translation or autophagy? *Autophagy*, **4**, 542-545.

7 Ryu, H., Rosas, H.D., Hersch, S.M. and Ferrante, R.J. (2005) The therapeutic role of creatine in Huntington's disease. *Pharmacol Ther*, **108**, 193-207.

8 Matthews, R.T., Yang, L., Browne, S., Baik, M. and Beal, M.F. (1998) Coenzyme Q10 administration increases brain mitochondrial concentrations and exerts neuroprotective effects. *Proc Natl Acad Sci U S A*, **95**, 8892-8897.

9 Steffan, J.S., Bodai, L., Pallos, J., Poelman, M., McCampbell, A., Apostol, B.L., Kazantsev, A., Schmidt, E., Zhu, Y.Z., Greenwald, M. *et al.* (2001) Histone deacetylase inhibitors arrest polyglutamine-dependent neurodegeneration in Drosophila. *Nature*, **413**, 739-743.

10 Hockly, E., Richon, V.M., Woodman, B., Smith, D.L., Zhou, X., Rosa, E., Sathasivam, K., Ghazi-Noori, S., Mahal, A., Lowden, P.A. *et al.* (2003) Suberoylanilide hydroxamic acid, a histone deacetylase inhibitor, ameliorates motor deficits in a mouse model of Huntington's disease. *Proc Natl Acad Sci U S A*, **100**, 2041-2046.

11 Ferrante, R.J., Kubilus, J.K., Lee, J., Ryu, H., Beesen, A., Zucker, B., Smith, K., Kowall, N.W., Ratan, R.R., Luthi-Carter, R. *et al.* (2003) Histone deacetylase inhibition by sodium butyrate chemotherapy ameliorates the neurodegenerative phenotype in Huntington's disease mice. *J Neurosci*, **23**, 9418-9427.

12 Toulmond, S., Tang, K., Bureau, Y., Ashdown, H., Degen, S., O'Donnell, R., Tam, J., Han, Y., Colucci, J., Giroux, A. *et al.* (2004) Neuroprotective effects of M826, a reversible caspase-3 inhibitor, in the rat malonate model of Huntington's disease. *Br J Pharmacol*, **141**, 689-697.

13 Fan, M.M., Fernandes, H.B., Zhang, L.Y., Hayden, M.R. and Raymond, L.A. (2007) Altered NMDA receptor trafficking in a yeast artificial chromosome transgenic mouse model of Huntington's disease. *J Neurosci*, **27**, 3768-3779.

14 Fecke, W., Gianfriddo, M., Gaviraghi, G., Terstappen, G.C. and Heitz, F. (2009) Small molecule drug discovery for Huntington's Disease. *Drug Discov Today*, **14**, 453-464.

15 Outeiro, T.F., Kontopoulos, E., Altmann, S.M., Kufareva, I., Strathearn, K.E., Amore, A.M., Volk, C.B., Maxwell, M.M., Rochet, J.C., McLean, P.J. *et al.* (2007) Sirtuin 2 inhibitors rescue alpha-synuclein-mediated toxicity in models of Parkinson's disease. *Science*, **317**, 516-519.

16 Barber, S.C., Higginbottom, A., Mead, R.J., Barber, S. and Shaw, P.J. (2009) An in vitro screening cascade to identify neuroprotective antioxidants in ALS. *Free Radic Biol Med*, **46**, 1127-1138.

17 Crowe, A., Ballatore, C., Hyde, E., Trojanowski, J.Q. and Lee, V.M. (2007) High throughput screening for small molecule inhibitors of heparin-induced tau fibril formation. *Biochem Biophys Res Commun*, **358**, 1-6.

18 Desai, U.A., Pallos, J., Ma, A.A., Stockwell, B.R., Thompson, L.M., Marsh, J.L. and Diamond, M.I. (2006) Biologically active molecules that reduce polyglutamine aggregation and toxicity. *Hum Mol Genet*, **15**, 2114-2124.
19 Wanker, E.E., Scherzinger, E., Heiser, V., Sittler, A., Eickhoff, H. and Lehrach, H. (1999) Membrane filter assay for detection of amyloid-like polyglutamine-containing protein aggregates. *Methods Enzymol*, **309**, 375-386.
20 Heiser, V., Engemann, S., Brocker, W., Dunkel, I., Boeddrich, A., Waelter, S., Nordhoff, E., Lurz, R., Schugardt, N., Rautenberg, S. *et al.* (2002) Identification of benzothiazoles as potential polyglutamine aggregation inhibitors of Huntington's disease by using an automated filter retardation assay. *Proc Natl Acad Sci U S A*, **99 Suppl 4**, 16400-16406.
21 Frid, P., Anisimov, S.V. and Popovic, N. (2007) Congo red and protein aggregation in neurodegenerative diseases. *Brain Res Rev*, **53**, 135-160.
22 Krobitsch, S. and Lindquist, S. (2000) Aggregation of huntingtin in yeast varies with the length of the polyglutamine expansion and the expression of chaperone proteins. *Proc Natl Acad Sci U S A*, **97**, 1589-1594.
23 Smith, D.L., Portier, R., Woodman, B., Hockly, E., Mahal, A., Klunk, W.E., Li, X.J., Wanker, E., Murray, K.D. and Bates, G.P. (2001) Inhibition of polyglutamine aggregation in R6/2 HD brain slices-complex dose-response profiles. *Neurobiol Dis*, **8**, 1017-1026.
24 Pollitt, S.K., Pallos, J., Shao, J., Desai, U.A., Ma, A.A., Thompson, L.M., Marsh, J.L. and Diamond, M.I. (2003) A rapid cellular FRET assay of polyglutamine aggregation identifies a novel inhibitor. *Neuron*, **40**, 685-694.
25 Scotter, E.L., Narayan, P., Glass, M. and Dragunow, M. (2008) High throughput quantification of mutant huntingtin aggregates. *J Neurosci Methods*, **171**, 174-179.
26 Weiss, A., Klein, C., Woodman, B., Sathasivam, K., Bibel, M., Regulier, E., Bates, G.P. and Paganetti, P. (2008) Sensitive biochemical aggregate detection reveals aggregation onset before symptom development in cellular and murine models of Huntington's disease. *J Neurochem*, **104**, 846-858.
27 Sarkar, S., Perlstein, E.O., Imarisio, S., Pineau, S., Cordenier, A., Maglathlin, R.L., Webster, J.A., Lewis, T.A., O'Kane, C.J., Schreiber, S.L. *et al.* (2007) Small molecules enhance autophagy and reduce toxicity in Huntington's disease models. *Nat Chem Biol*, **3**, 331-338.
28 Chen, X., Tang, T.S., Tu, H., Nelson, O., Pook, M., Hammer, R., Nukina, N. and Bezprozvanny, I. (2008) Deranged calcium signaling and neurodegeneration in spinocerebellar ataxia type 3. *J Neurosci*, **28**, 12713-12724.
29 Chou, A.H., Chen, S.Y., Yeh, T.H., Weng, Y.H. and Wang, H.L. HDAC inhibitor sodium butyrate reverses transcriptional downregulation and ameliorates ataxic symptoms in a transgenic mouse model of SCA3. *Neurobiol Dis*, **41**, 481-488.
30 Menzies, F.M., Huebener, J., Renna, M., Bonin, M., Riess, O. and Rubinsztein, D.C. Autophagy induction reduces mutant ataxin-3 levels and toxicity in a mouse model of spinocerebellar ataxia type 3. *Brain*, **133**, 93-104.
31 Nascimento-Ferreira, I., Santos-Ferreira, T., Sousa-Ferreira, L., Auregan, G., Onofre, I., Alves, S., Dufour, N., Colomer Gould, V.F., Koeppen, A., Deglon, N. *et al.* Overexpression of the autophagic beclin-1 protein clears mutant ataxin-3 and alleviates Machado-Joseph disease. *Brain*.
32 Alves, S., Nascimento-Ferreira, I., Dufour, N., Hassig, R., Auregan, G., Nobrega, C., Brouillet, E., Hantraye, P., Pedroso de Lima, M.C., Deglon, N. *et al.* Silencing ataxin-3 mitigates degeneration in a rat model of Machado-Joseph disease: no role for wild-type ataxin-3? *Hum Mol Genet*, **19**, 2380-2394.
33 Alves, S., Regulier, E., Nascimento-Ferreira, I., Hassig, R., Dufour, N., Koeppen, A., Carvalho, A.L., Simoes, S., de Lima, M.C., Brouillet, E. *et al.* (2008) Striatal and nigral pathology in a lentiviral rat model of Machado-Joseph disease. *Hum Mol Genet*, **17**, 2071-2083.

34 Teixeira-Castro, A., Ailion, M., Jalles, A., Brignull, H.R., Vilaca, J.L., Dias, N., Rodrigues, P., Oliveira, J.F., Neves-Carvalho, A., Morimoto, R.I. *et al.* Neuron-specific proteotoxicity of mutant ataxin-3 in C. elegans: rescue by the DAF-16 and HSF-1 pathways. *Hum Mol Genet*.
35 Kwok, T.C., Ricker, N., Fraser, R., Chan, A.W., Burns, A., Stanley, E.F., McCourt, P., Cutler, S.R. and Roy, P.J. (2006) A small-molecule screen in C. elegans yields a new calcium channel antagonist. *Nature*, **441**, 91-95.
36 Bargmann, C.I. (1998) Neurobiology of the Caenorhabditis elegans genome. *Science*, **282**, 2028-2033.
37 Geary, T.G. and Thompson, D.P. (2001) Caenorhabditis elegans: how good a model for veterinary parasites? *Vet Parasitol*, **101**, 371-386.
38 Rand, J.B. and Johnson, C.D. (1995) Genetic pharmacology: interactions between drugs and gene products in Caenorhabditis elegans. *Methods Cell Biol*, **48**, 187-204.
39 Voisine, C., Varma, H., Walker, N., Bates, E.A., Stockwell, B.R. and Hart, A.C. (2007) Identification of potential therapeutic drugs for huntington's disease using Caenorhabditis elegans. *PLoS One*, **2**, e504.
40 Gidalevitz, T., Ben-Zvi, A., Ho, K.H., Brignull, H.R. and Morimoto, R.I. (2006) Progressive disruption of cellular protein folding in models of polyglutamine diseases. *Science*, **311**, 1471-1474.
41 Beal, M.F. Neuroprotective effects of creatine. *Amino Acids*, **40**, 1305-1313.
42 Kouraklis, G. and Theocharis, S. (2002) Histone deacetylase inhibitors and anticancer therapy. *Curr Med Chem Anticancer Agents*, **2**, 477-484.
43 Kelly, G. A review of the sirtuin system, its clinical implications, and the potential role of dietary activators like resveratrol: part 1. *Altern Med Rev*, **15**, 245-263.
44 Teixeira-Castro, A., Dias, N., Rodrigues, P., Oliveira, J.O., Rodrigues, N.F., Maciel, P. and Vilaça, J.L. (2011), In *5th International Conference on Practical Applications of Computational Biology & Bioinformatics. Advances in Soft Computing. Springer* Vol. 93, pp. 31-38.
45 Ravikumar, B., Duden, R. and Rubinsztein, D.C. (2002) Aggregate-prone proteins with polyglutamine and polyalanine expansions are degraded by autophagy. *Hum Mol Genet*, **11**, 1107-1117.
46 Khan, L.A., Yamanaka, T. and Nukina, N. (2008) Genetic impairment of autophagy intensifies expanded polyglutamine toxicity in Caenorhabditis elegans. *Biochem Biophys Res Commun*, **368**, 729-735.
47 Sarkar, S. and Rubinsztein, D.C. (2008) Huntington's disease: degradation of mutant huntingtin by autophagy. *FEBS J*, **275**, 4263-4270.
48 Sarkar, S., Floto, R.A., Berger, Z., Imarisio, S., Cordenier, A., Pasco, M., Cook, L.J. and Rubinsztein, D.C. (2005) Lithium induces autophagy by inhibiting inositol monophosphatase. *J Cell Biol*, **170**, 1101-1111.
49 Sarkar, S. and Rubinsztein, D.C. (2006) Inositol and IP3 levels regulate autophagy: biology and therapeutic speculations. *Autophagy*, **2**, 132-134.
50 Fornai, F., Longone, P., Cafaro, L., Kastsiuchenka, O., Ferrucci, M., Manca, M.L., Lazzeri, G., Spalloni, A., Bellio, N., Lenzi, P. *et al.* (2008) Lithium delays progression of amyotrophic lateral sclerosis. *Proc Natl Acad Sci U S A*, **105**, 2052-2057.
51 Sarkar, S., Krishna, G., Imarisio, S., Saiki, S., O'Kane, C.J. and Rubinsztein, D.C. (2008) A rational mechanism for combination treatment of Huntington's disease using lithium and rapamycin. *Hum Mol Genet*, **17**, 170-178.
52 McColl, G., Killilea, D.W., Hubbard, A.E., Vantipalli, M.C., Melov, S. and Lithgow, G.J. (2008) Pharmacogenetic analysis of lithium-induced delayed aging in Caenorhabditis elegans. *J Biol Chem*, **283**, 350-357.
53 Matthews, R.T., Ferrante, R.J., Klivenyi, P., Yang, L., Klein, A.M., Mueller, G., Kaddurah-Daouk, R. and Beal, M.F. (1999) Creatine and cyclocreatine attenuate MPTP neurotoxicity. *Exp Neurol*, **157**, 142-149.

54 Klivenyi, P., Ferrante, R.J., Matthews, R.T., Bogdanov, M.B., Klein, A.M., Andreassen, O.A., Mueller, G., Wermer, M., Kaddurah-Daouk, R. and Beal, M.F. (1999) Neuroprotective effects of creatine in a transgenic animal model of amyotrophic lateral sclerosis. *Nat Med*, **5**, 347-350.
55 Dedeoglu, A., Kubilus, J.K., Yang, L., Ferrante, K.L., Hersch, S.M., Beal, M.F. and Ferrante, R.J. (2003) Creatine therapy provides neuroprotection after onset of clinical symptoms in Huntington's disease transgenic mice. *J Neurochem*, **85**, 1359-1367.
56 Yang, L., Calingasan, N.Y., Wille, E.J., Cormier, K., Smith, K., Ferrante, R.J. and Beal, M.F. (2009) Combination therapy with coenzyme Q10 and creatine produces additive neuroprotective effects in models of Parkinson's and Huntington's diseases. *J Neurochem*, **109**, 1427-1439.
57 Saha, R.N. and Pahan, K. (2006) HATs and HDACs in neurodegeneration: a tale of disconcerted acetylation homeostasis. *Cell Death Differ*, **13**, 539-550.
58 Hughes, R.E., Lo, R.S., Davis, C., Strand, A.D., Neal, C.L., Olson, J.M. and Fields, S. (2001) Altered transcription in yeast expressing expanded polyglutamine. *Proc Natl Acad Sci U S A*, **98**, 13201-13206.
59 McCampbell, A., Taye, A.A., Whitty, L., Penney, E., Steffan, J.S. and Fischbeck, K.H. (2001) Histone deacetylase inhibitors reduce polyglutamine toxicity. *Proc Natl Acad Sci U S A*, **98**, 15179-15184.
60 Bates, E.A., Victor, M., Jones, A.K., Shi, Y. and Hart, A.C. (2006) Differential contributions of Caenorhabditis elegans histone deacetylases to huntingtin polyglutamine toxicity. *J Neurosci*, **26**, 2830-2838.
61 Tissenbaum, H.A. and Guarente, L. (2001) Increased dosage of a sir-2 gene extends lifespan in Caenorhabditis elegans. *Nature*, **410**, 227-230.
62 Parker, J.A., Arango, M., Abderrahmane, S., Lambert, E., Tourette, C., Catoire, H. and Neri, C. (2005) Resveratrol rescues mutant polyglutamine cytotoxicity in nematode and mammalian neurons. *Nat Genet*, **37**, 349-350.
63 Geldenhuys, W.J., Youdim, M.B., Carroll, R.T. and Van der Schyf, C.J. The emergence of designed multiple ligands for neurodegenerative disorders. *Prog Neurobiol*.
64 Brenner, S. (1974) The genetics of Caenorhabditis elegans. *Genetics*, **77**, 71-94.
65 Lewis, J.A. and Fleming, J.T. (1995) Basic culture methods. *Methods Cell Biol*, **48**, 3-29.
66 Garcia, S.M., Casanueva, M.O., Silva, M.C., Amaral, M.D. and Morimoto, R.I. (2007) Neuronal signaling modulates protein homeostasis in Caenorhabditis elegans post-synaptic muscle cells. *Genes Dev*, **21**, 3006-3016.

Chapter 6

Genetic reduction of *HSF-1* fails to aggravate MJD pathogenesis in mice

Genetic reduction of *HSF-1* fails to aggravate MJD pathogenesis in mice.

Andreia Teixeira-Castro[1,2], Sara Duarte-Silva[1,2], Ana Jalles[1,2], Anabela Silva-Fernandes[1,2], Teresa Cruto[1,2], Sofia D. Santos[3], Maria João Saraiva[3] and Patrícia Maciel[1,2,*]

[1] Life and Health Sciences Research Institute (ICVS), School of Health Sciences, Univ. of Minho, 4710-057 Braga, Portugal; [2]ICVS/3B's - PT Government Associate Laboratory, Braga/Guimarães, Portugal; [3]Molecular Neurobiology Unit, Institute of Molecular and Cell Biology, Porto, Portugal.

Abstract

Perturbations in neuronal protein homeostasis likely contribute to disease pathogenesis in polyglutamine (polyQ) neurodegenerative diseases. The heat shock factor 1 (HSF-1) is a major regulator of the heat shock response in cells and a central component to the maintenance of the homeostatic mechanisms counteracting the effect of toxic polyQ proteins in the brain. However, genetic reduction of *HSF-1* did not further aggravate disease in transgenic mice expressing polyQ-expanded ataxin-3, the pathogenic protein involved in Machado-Joseph disease (MJD). Half of *HSF-1* levels resulted in the appearance of neurological symptoms at the age of 2-3 months, which is comparable to the MJD transgenic mouse with normal levels of *HSF1* gene, and did not significantly change mutant ATXN3 subcellular localization, and aggregation pattern or brain pathology, in spite of an apparent increase in ATXN3 protein levels. Our results suggest that one copy of the *HSF-1* gene is sufficient to cope with mutant ATXN3-mediated proteotoxic stress in mice and open a discussion for a potential compensatory role of other cell factor(s) in a state of *HSF-1* reduction.

Introduction

Folding in the cell's crowded environment is highly challenging. Intermolecular interactions between the hydrophobic residues of non-native polypeptides become strongly favored due to the macromolecular crowding effect and can compete with the folding of proteins to a native state (1). An imbalance in protein homeostasis, whether caused by aging, cell stress or chronic expression of mutant aggregation-prone proteins, results in the appearance of alternative protein conformational states that can self-associate to form protein aggregates. The cell has developed a highly efficient protein misfolding quality control machinery to regulate proteostasis and to ensure that misfolded proteins do not accumulate (2-4). However, under several pathological conditions, the capacity of the protein quality control machinery is exceeded and misfolded proteins may accumulate to deleterious levels. In the brain, the importance of proteostasis is highlighted by various neurodegenerative diseases such as Parkinson's, Alzheimer's and the polyglutamine (polyQ) diseases (5-7). Particularly in Machado-Joseph disease (MJD) or Spinocerebellar Ataxia type 3 (SCA3), expansion of the polyQ domain in the ataxin-3 (ATXN3) protein promotes amyloid-like aggregate formation (8-10). Although protein aggregation occurs in all these diseases is uncertain how misfolding and aggregation damages the neuronal cells.

The heat shock response (HSR) and heat shock proteins (Hsps) have been implicated in many of these diseases mainly based on the association of chaperones with intracellular aggregates. Cell imaging experiments show that Hsp70 associates transiently with polyQ aggregates, with association-dissociation rates identical to chaperone interactions with unfolded subtracts (11). Moreover, overexpression of the Hsp70 chaperone network suppresses aggregate formation and cellular toxicity. Specifically in MJD, Hsp40 and (less frequently) Hsp70 proteins were found to co-localize into ATXN3 inclusions in the ventral pons of patients (12). In cellular and mice models for ATXN3 pathogenesis, a dynamic pattern of expression of several molecular chaperones (Hsp27, -40, -70 and -105), has been described, as the disease progresses (13-17). Overexpression of DNAJ-1 chaperone suppresses ATXN3-mediated aggregation and/or toxicity in cell culture and flies (12, 18, 19), whereas genetic reduction or absence of C-terminus Hsp70 interacting protein (CHIP) accelerates disease (20). Collectively, these observations have led to the hypothesis that the levels of heat shock proteins modulate aggregate formation and cellular degeneration.

The heat shock factor 1 (HSF-1) is the master stress-inducible regulator of molecular chaperones and proteostasis in cells (21). Expression of an active form of HSF1 significantly suppressed polyQ aggregate formation in cellular and mouse models (22). This suppression was found to be more significant than any combination of Hsps in cell lines (22). The lack of HSF1 expression in a Familial amyloidotic polyneuropathy (FAP) mouse model led to extensive transthyretin (TTR) deposition in the peripheral nervous system and at early ages (23). In *C. elegans*, genetic ablation of HSF-1 in a model of neuronal ATXN3 pathogenesis resulted in an aggravation of the aggregation pattern and motor neuron dysfunction, whereas pharmacological activation of the HSR partially rescued mutant ATXN3-mediated pathogenesis (24). Here, we used measures of chaperone analysis and genetic crossings of transgenic mice expressing full-length expanded ATXN3 (25) to define the role

of the HSR and of HSF-1 in ATXN3 pathogenesis in mice. We found that, although there was a decrease of Hsp60 and -70 in affected areas of the CMVMJD94 mice brain, half of the levels of *HSF-1* did not further aggravate motor coordination or aggregation of mutant ATXN3. This model suggests that half of the *HSF-1* levels are sufficient to maintain the cellular folding capacity, even in the context of the expression of an aggregation-prone protein like expanded ataxin-3.

Results

Decreased protein levels of Hsp60 and Hsp70 in affected brain regions of CMVMJD94 mice

Differential expression of specific molecular chaperones has been reported in animal models of polyQ pathogenesis during disease progression (reviewed in (26). Here, we determined the levels of the major classes of Hsps (Hsp105, Hsp70, Hsp60, Hsp40 and Hsp27) in the cerebellum and brainstem (two affected regions) of CMVMJD94$^{+/-}$ transgenic mice (25). These mice overexpress human expanded, full-length ATXN3 with 94 glutamine repeats, which is in the pathological range of Q-length for MJD patients (25). At early symptomatic ages (16-weeks) no differences were found in Hsp expression levels (data not shown) between hemizygous (CMVMJD94$^{+/-}$) and wild-type (WT) (CMVMJD94$^{-/-}$) mice, whereas 100-103 weeks old animals showed decreased expression of specific Hsps. Namely, Hsp60 levels were diminished in the cerebellum and brainstem, while Hsp70 was significantly decreased in the cerebellum of the CMVMJD$^{+/-}$ mice (Fig. 1). We also determined the levels of Hsps in the forebrain of these mice (including mostly regions not involved in the disease) and found no differences (data not shown).

These results imply the reduction of molecular chaperones and the HSR in the pathogenesis of ataxin-3 mice but only at late stages of the disease process.

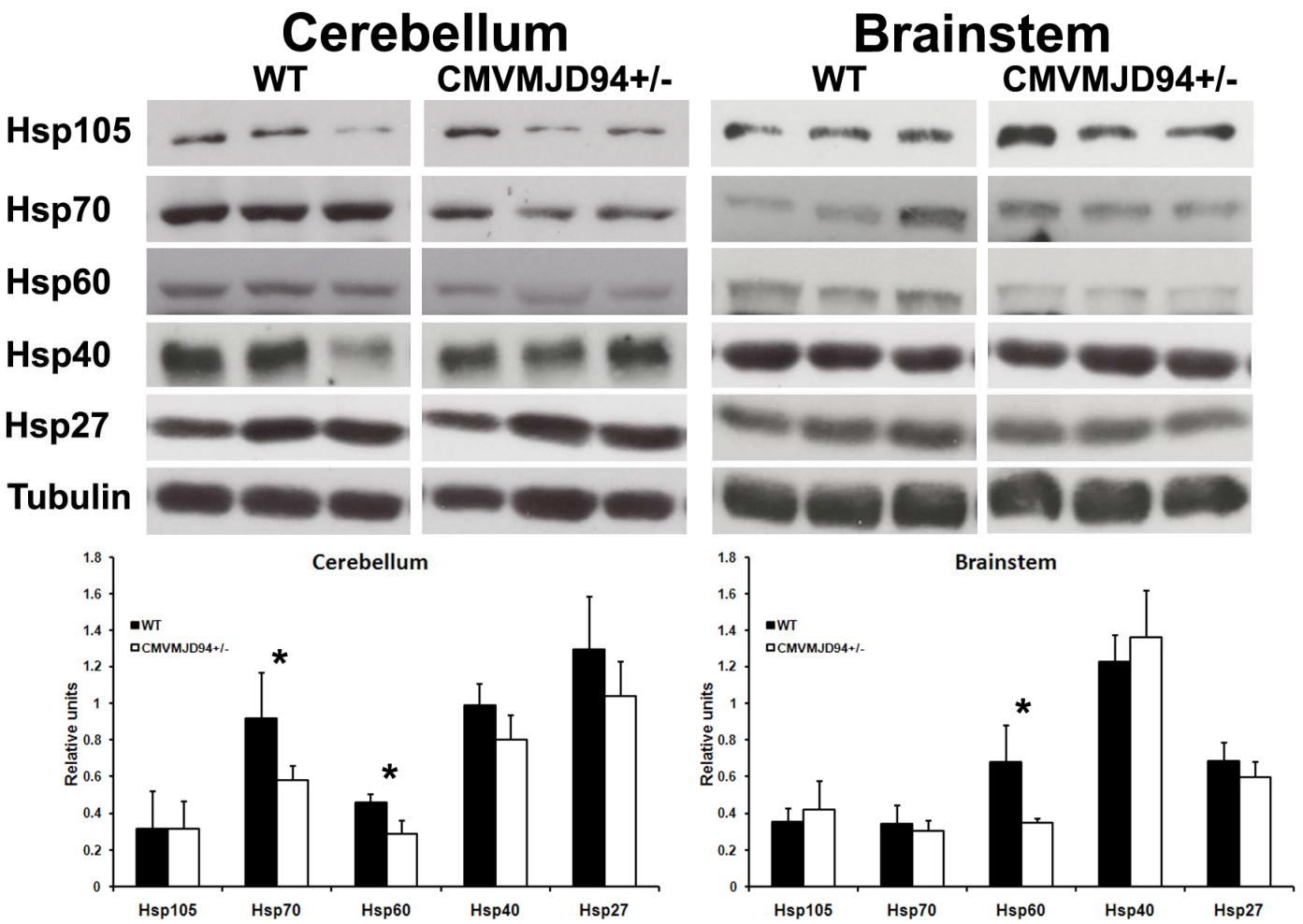

Figure 1. Reduced Hsp60 and Hsp70 protein levels in the cerebellum and brainstem of CMVMJD94$^{+/-}$. Representative Western-blots of heat shock proteins in the cerebellum and brainstem regions of CMVMJD94$^{+/-}$ mice brains (A). Comparable levels of Hsp105, Hsp40 and Hsp27 were found in both regions of the brain, whereas Hsp70 and Hsp60 were decreased in the cerebellum. In the brainstem Hsp60 was also decreased in CMVMJD94$^{+/-}$ animals when compared with WT littermates. Blot signals were quantified with ImageJ, the mean optical density for each genotype (n=6) was normalized to tubulin (B). *, $p<0.05$.

Absence of HSF-1 increased ATXN3 protein levels but did not alter its localization or aggregation pattern

Because HSF1 has been shown to regulate polyQ toxicity, we hypothesized that reducing *Hsf-1* would exacerbate the phenotype of CMVMJD94$^{+/-}$ mice. Hemizygous CMVMJD94 mice were crossed with *Hsf-1*-deficient mice (27) to generate CMVMJD94$^{+/-}$ animals with one (*Hsf1*$^{+/-}$) or two copies (*Hsf1*$^{+/+}$) of *Hsf-1* gene. All mice (CMVMJD94$^{+/-}$; *Hsf1*$^{+/-}$, CMVMJD94$^{+/-}$; *Hsf1*$^{+/+}$, CMVMJD94$^{+/-}$; *Hsf1*$^{-/-}$) were phenotypically indistinguishable from WT mice (CMVMJD94$^{-/-}$; *Hsf1*$^{+/+}$), which was consistent with previous reports of ATXN3 transgenic (25) and of *Hsf-1* heterozygous knock-out mice (27).

We first characterized CMVMJD94$^{+/-}$ and CMVMJD94$^{+/-}$; *Hsf1*$^{+/-}$ animals regarding the size of the CAG repeat and mutant ATXN3 protein levels. CAG repeat length was similar in both groups (mean of 94.64± 1.52 and 96.00± 1.16 for MJD transgenic and double mutant mice, respectively), whereas human ATXN3 protein levels were increased in the brainstem region of the CMVMJD94$^{+/-}$; *Hsf1*$^{+/-}$ mouse brains when compared with the CMVMJD94$^{+/-}$ mice (Fig. 2).

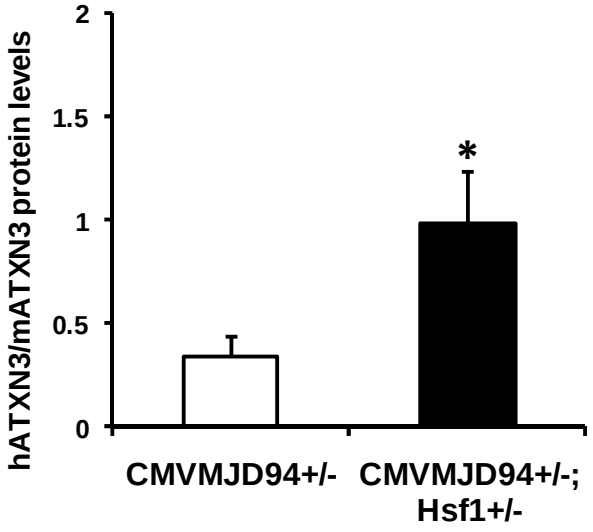

Figure 2. Half of the levels of *HSF1* caused an increase in mutant ATXN3 protein levels in the brainstem of transgenic mice. Western-blot analysis of human ATXN3 total protein levels in the brainstem region of hemi CMVMJD94 and CMVMJD94$^{+/-}$; *Hsf1*$^{+/-}$ mice with approximately 100 weeks of age. Genetic reduction of *HSF1* resulted in an increase in mutant ATXN3 protein levels without the appearance of insoluble protein in the stacking gel nor the presence of ATXN3 fragments.

HSF-1 is known to regulate the expression of several molecular chaperones in the cellular environment and to modulate misfolding and aggregation of polyQ proteins. Moreover, genetic reduction of *Hsf-1* caused an increase in mutant ATXN3 levels in MJD transgenic mice. Based on this, we determined if *Hsf-1* reduction would modify ATXN3 aggregation or subcellular localization. Anti- ataxin-3 IHC analysis revealed that mutant ATXN3 was detected in several brain regions of CMVMJD94$^{+/-}$; *Hsf1*$^{+/-}$ mice, including areas involved in MJD, namely in dentate nuclei of the cerebellum, pontine nuclei, locus coeruleus and in the substantia nigra (Fig. 3), as described for MJD transgenic mouse. Surprisingly, genetic reduction of *Hsf-1* did not cause any significant alteration regarding subcellular localization of ATXN3 and no intranuclear aggregates were detected in all the brain regions analyzed (Fig. 3). However, consistent with the Western-blot data, half of the *Hsf-1* levels resulted in an increase in ATXN3 staining in the dentate nuclei and pontine nuclei (Fig. 3).

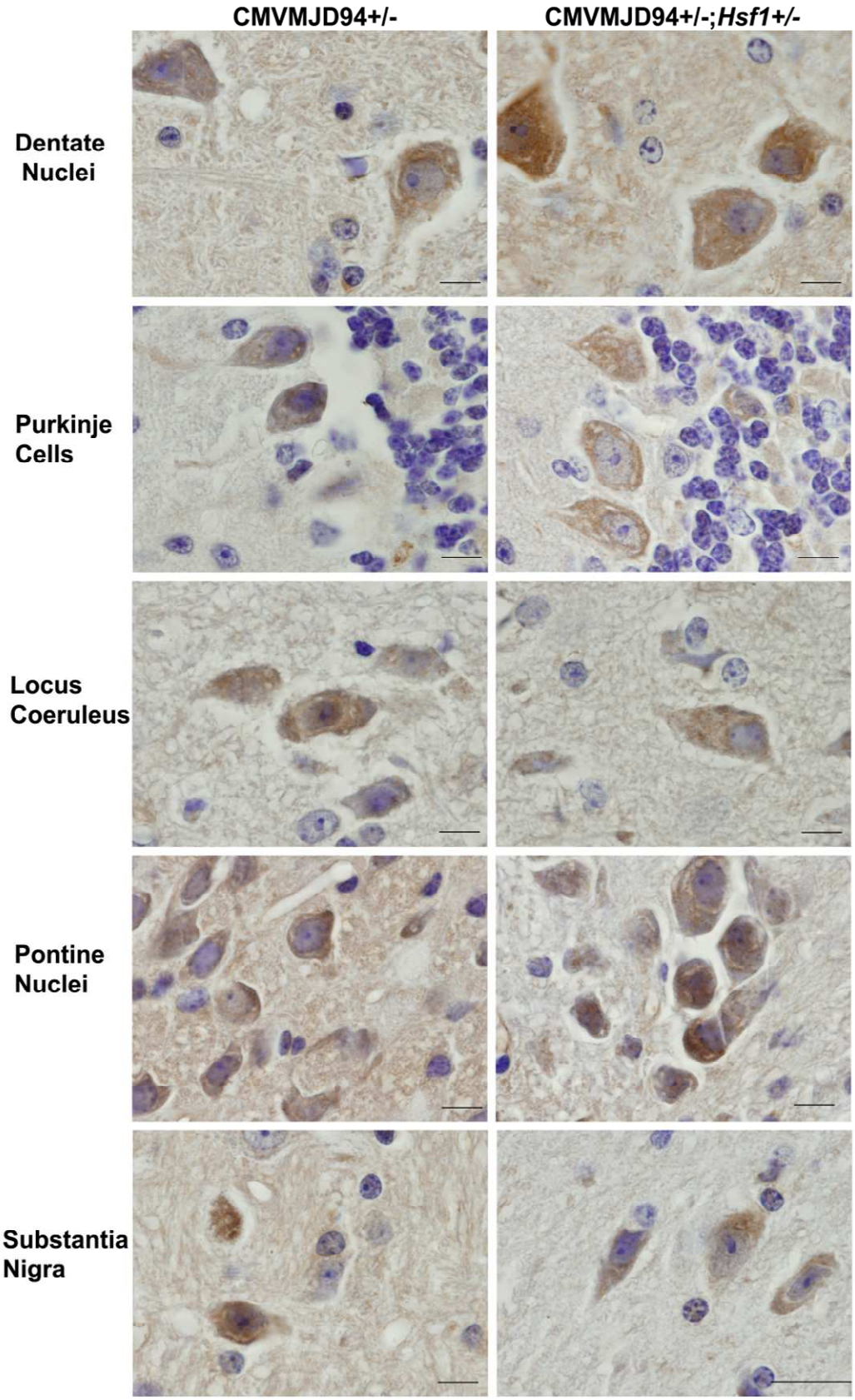

Figure 3. *HSF1* deficiency did not alter mutant ATXN3 subcellular localization in transgenic mice. Anti-ataxin-3 IHC analysis showed no differences in ATXN3 subcellular localization and distribution pattern in several brain regions of CMVMJD94$^{+/-}$; *Hsf1*$^{+/-}$ and CMVMJD94$^{+/-}$ mice at late disease stages (100 weeks). Scale bar: 10 μm.

Reduction of HSF1 did not alter motor behavior deficits of CMVMJD94 transgenic mice

Next, we searched for quantifiable motor deficits, using the rotarod apparatus. CMVMJD94$^{+/-}$ (CMVMJD94$^{+/-}$; *Hsf1*$^{+/+}$) mice showed a motor coordination impairment beginning at 8-16 weeks of age, as previously described (Fig. 4 and (25) and *Hsf1*$^{+/-}$ (CMVMJD94$^{+/-}$; *Hsf1*$^{+/-}$) animals displayed similar latency to fall when compared to WT littermates. CMVMJD94$^{+/-}$; *Hsf1*$^{+/-}$ double mutant mice did not significantly aggravate the motor uncoordination phenotype of ATXN3 transgenic mice, not even at 84-weeks of age (Fig. 4). Similarly to CMVMJD94$^{+/-}$ animals, CMVMJD94$^{+/-}$; *Hsf1*$^{+/-}$ double mutant mice maintained a slow progression disease rate with aging.

This data suggests that in mice (i) half of the levels of *HSF1* are sufficient for the animals to cope with the mutant ATXN3-mediated proteotoxicity in mice; and/or (ii) that compensatory mechanism(s) could balance proteostasis in the mouse brain, in spite of the reduced *Hsf-1* gene levels.

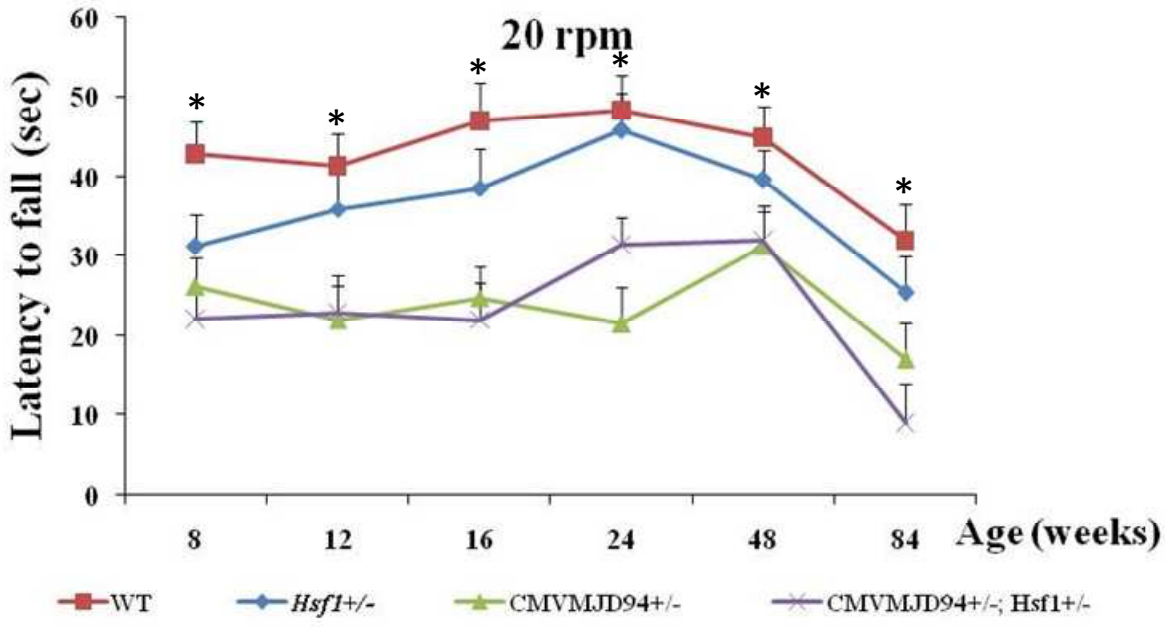

Figure 4. Half of the levels of *HSF-1* failed to aggravate motor coordination of CMVMJD94$^{+/-}$ mice. The rotarod test (n=10-11 for each tested group) demonstrated that hemi CMVMJD94 mice displayed a significant decrease in the latency to fall at 20 rpm (*Mann-Whitney U-test*; factor: genotype) in comparison with WT animals. *Hsf1+/-* mice behave similarly to WT animals and half of *HSF-1* levels did not worsen transgenic CMVMJD94 mice performance in the rotarod paradigm, until 84 weeks of age. Only WT versus CMVCMJD94$^{+/-}$ and CMVCMJD94$^{+/-}$;*Hsf1*$^{+/-}$comparisons are statistical significant and * is represented when $p<0.05$.

Histopathological observations of brain sections of CMVMJD94$^{+/-}$;*Hsf1*$^{+/-}$ and hemi CMVMJD94 mice revealed the presence of scattered dark and shrunken cells in several brain regions. Specifically, in dentate nuclei and purkinje cells of CMVMJD94$^{+/-}$;*Hsf1*$^{+/-}$ animals, there was an increase in cresil violet staining and more abnormally shapped cells were found. In contrast, in the pontine nuclei, hemi CMVMJD94 mice contained more

pyknotic nuclei and a basophilic cytoplasm in comparison with double mutant mice. Brain regions like the striatum, not affected in the human disease, are also spared in our model (Fig. 5).

In summary, reduction of *Hsf-1* levels had no major effect in mutant ATXN3 aggregation and subcellular localization, and had a mild impact in pathology among the two groups, with no consequences at the motor level.

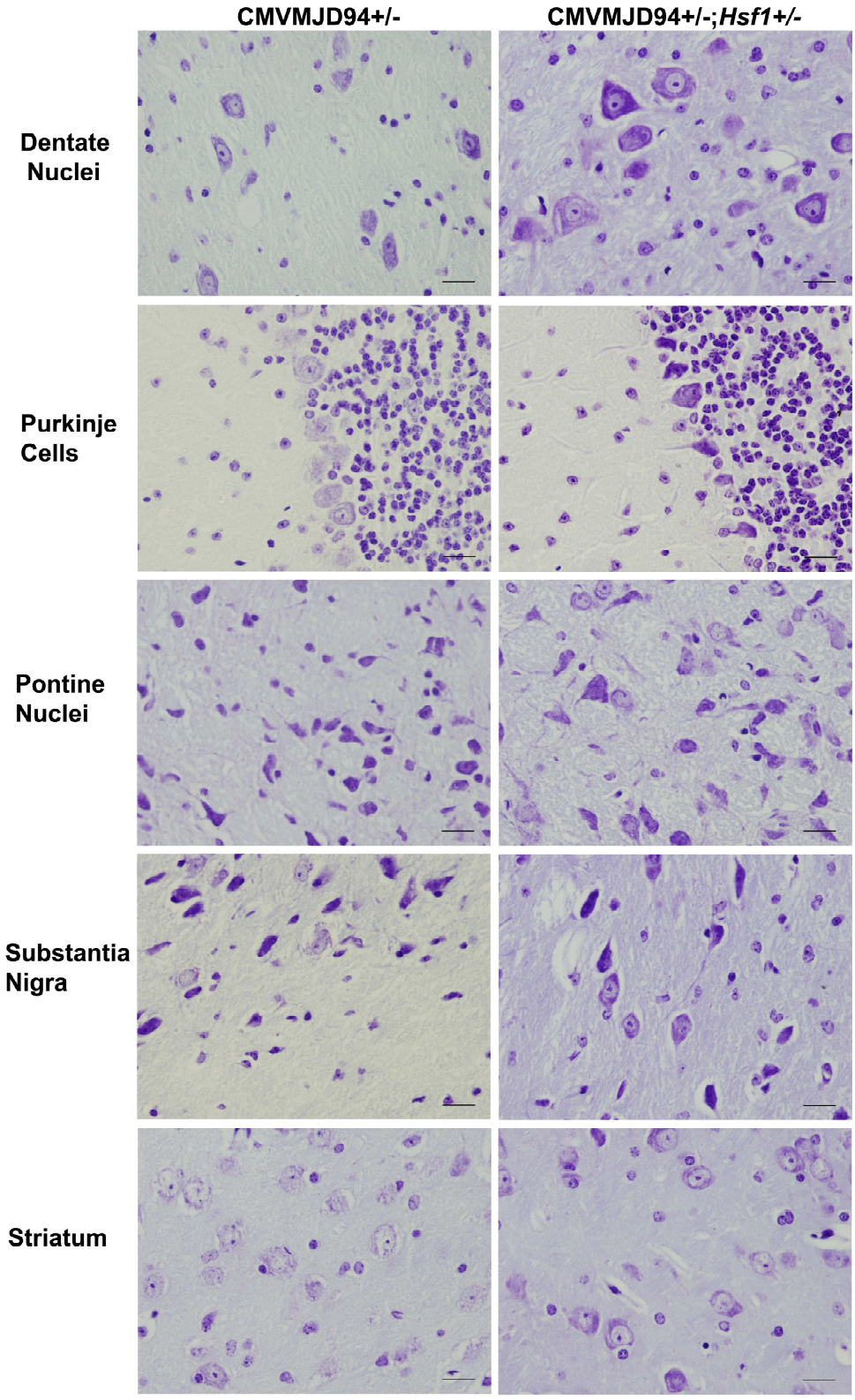

Figure 5. Neuropathology of CMVMJD94$^{+/-}$; *Hsf1*$^{+/-}$ mice. Comparative sections stained with Cresil violet of hemi CMVMJD94 and CMVMJD94$^{+/-}$; *Hsf1*$^{+/-}$ mice dentate nuclei, pukinje cells, pontine nuclei, substantia nigra and striatum at 100 weeks of age. CMVMJD94$^{+/-}$; *Hsf1*$^{+/-}$ and CMVMJD94$^{+/-}$ mouse neurons in the dentate nuclei, purkinje cells and pontine nuclei were observed by Cresil violet staining as scattered dark, shrunken cells with pyknotic nuclei and a basophilic cytoplasm (arrows). Dentate nuclei and purkinje cells were shown to be more affected in double mutant mice, whereas the pons of CMVMJD94$^{+/-}$ transgenics showed an increase in the presence of abnormal nuclei. Scale bar: 50 μm.

Discussion

Many studies have pointed towards an important role of HSF-1 and Hsps as protective protein effectors against neurodegeneration. HSF-1 has an indirect effect, regulating the expression of molecular chaperones that directly interact with misfolded proteins to prevent aggregate formation. If the refolding process is not efficient, proteins may be targeted for degradation. Expression of Hsp70 has been shown to suppress neurodegeneration in cell culture and animal models of Parkinson's disease (PD), Amyotrophic lateral sclerosis (ALS) and of several polyQ diseases (28-31). On the other hand, the expression of a dominant negative Hsp70 exacerbated neurodegeneration in a PD *Drosophila* model (28). In a TTR transgenic mouse model, there was upregulation of Hsp70 and of an endoplasmic reticulum resident Hsp70, BiP, in tissues with TTR deposition (23, 32). The fact that TTR aggregates are able to activate the HSR in peripheral neuronal and non-neuronal tissues, supports the globally protective role for the proteostasis network in conformational disorders. In line with this argument, genetic ablation of HSF-1 in the TTR mouse model significantly aggravated TTR deposition, and the aggregates appeared at earlier disease stages (23). In contrast with the TTR results, however, in several chronic neurodegenerative diseases, the HSR seems to be attenuated. There is a higher threshold for the induction of the stress response in ALS motor neurons of the spinal cord, which was found to be associated with a failure in HSF1 activation (33).

In general, HSF1 seems to be a key factor for the maintenance of a healthy proteome. HSF-1 knock-out mice exhibit a variety of phenotypes namely prenatal lethality, growth retardation, female infertility and aging-related motor coordination defects (27, 34). At the pathological level, *Hsf-1*$^{-/-}$ mouse exhibit enlarged ventricles, astrogliosis, neurodegeneration and demyelination (34, 35). All these phenotypes were present in a much attenuated form in heterozygous mice. The classical HSR is eliminated in *Hsf-1* homozygous and less robust in heterozygous animals. However, in basal conditions the expression of molecular chaperones is normal. *HSF-1* deficient mice also showed increased susceptibility to oxidative stress and increased accumulation of carbonylated and ubiquitylated proteins.

Here, we described a novel MJD transgenic mouse model in which the levels of the major regulator of the HSR, *HSF1* are reduced (CMVMJD94$^{+/-}$; *Hsf1*$^{+/-}$). We chose to reduce *HSF-1* levels and not to completely ablate it mainly because it would still allow us to test for potential aggravation of motor performance of the MJD transgenic mice and of brain pathology, maintaining the increased susceptibility to oxidative stress and increased levels of damaged protein. Surprisingly, CMVMJD94$^{+/-}$;*Hsf1*$^{+/-}$ animals developed neurological symptoms at the age of 2-3 months, comparable to the MJD transgenic mouse with normal levels of *HSF1* gene. Consistently, mutant ATXN3 subcellular localization and aggregation was also not altered, even in old animals. Based on this data, we propose that either (i) half of the *HSF-1* levels are sufficient to maintain proteostasis of MJD transgenic mice, and/or that (ii) other factors of the cellular environment may be compensating the lack of *HSF-1*, when the system is being challenged with chronic expression of an aggregation prone-protein. Additional experiments are required to elucidate the underlying mechanism(s).

In yeast, Drosophila and *C. elegans* there is a single *HSF* gene. Yeast *HSF* is an essential gene, whereas in *Drosophila*, *HSF* deficiency leads to defects during early development and lack of stress response (21, 36). Knockdown of *HSF-1* in *C. elegans* caused a reduction in lifespan and increased age-related phenotypes (37, 38). *HSF-1* was found in many genetic screens as a modifier gene of polyQ and alpha-synuclein invertebrate disease models (19, 24, 39, 40). We have recently shown that *HSF-1* is a potent suppressor of mutant ATXN3-mediated neuronal-specific aggregation and motor dysfunction in the worm (24). In this model, half of the levels of *HSF-1* also aggravated mutant ATXN3 aggregation, although into a lesser extent (our unpublished observations). Reduction of CHIP *in vivo* also aggravated neurological and aggregation symptoms of a different MJD transgenic mouse model, through a mechanism independent of heat shock protein levels (20). Therefore, it was surprising to observe no major effects of *HSF-1* deficiency in the MJD transgenic mouse model, in spite of an increase in ataxin-3 levels in affected brain regions, possibly due to reduced UPS degradation.

In mammalians, it is thought that there are four *HSF* (HSF-1, -2, -3 and -4) genes (21, 36, 41). As mentioned before, HSF-1 activation is dependent on environmental stresses, such as elevated temperature, oxidative stress, or conditions that increase protein misfolding in the cells. HSF2 and HSF4 participate in similar processes through activation of perhaps the same target genes, but the modes of their activation are less well defined. In fact, HSF-2 activity has been shown to be required during radial glial migration and development of reproductive organs (42-44). In addition, a part of HSF2 associates with HSF-1 in the nucleus and modulates expression of the classical heat-shock genes (45, 46) and of a nonclassical heat-shock gene, satellite III DNA (47). HSF2 also modulates HSF-1-mediated regulation of *Hsp* genes, such as Hsp110, Hsp70, Hsp40 and Hsp25, during heat shock and proteasome inhibition, clearly demonstrating a functional role of HSF2 in the proteotoxic stress response. The DNA binding ability of HSF2 is also modified by HSF-1, suggesting a close functional relationship for these two well conserved transcription factors. HSF-4 activity has been demonstrated during lens fiber cell differentiation (48, 49). Recently, a semicomprehensive analysis revealed that HSF4 binds to various genomic regions, and substantial numbers of genes (33%) in and near the HSF4- binding regions are nonclassical heat-shock genes (50). Remarkably, HSF4 is required for the expression of half of these genes, implying that not only HSF1, but also other HSF family members, play significant roles in the induction of nonclassical and classical genes in response to heat shock. Finally, HSF-3 that was recently identified in mice, restores the expression of specific non-classical heat shock genes in the absence of HSF-1 and in response to detrimental stresses (41). Thus, it is possible that in addition to HSF1, perhaps HSF2 and other factors may be important regulators in diseases such as cancer and neurodegeneration, where dysregulation of molecular chaperones are evident. We will test this hypothesis in MJD.

Materials and Methods

Generation of CMVMJD; HSF-1 mice, genotyping and molecular analysis of the (CAG)$_n$ repeat. HSF1 KO mice, which were kindly provided by Dr. Ivor Beijamin to M.J.S. (27), were backcrossed with C57Bl/6 mice (Harlan Iberican, Barcelona, Spain) for eight generations. We cross matted HSF-1 KO mice with transgenic mice for human ATXN3, expressing the cDNA ATXN3c variant containing 94 glutamine repeats, under the regulation of the cytomegalovirus promoter (pCMV) (25). CMVMJD94$^{-/-}$; *Hsf1*$^{-/-}$, CMVMJD94$^{-/-}$; *Hsf1*$^{+/+}$, CMVMJD94$^{-/-}$; *Hsf1*$^{+/-}$ CMVMJD94 animals and wild-type littermates (CMVMJD94$^{-/-}$; *Hsf1*$^{+/+}$) were obtained from colony inbreeding and mice genotyping was performed as previously described (25, 27). CAG repeat-length was also monitored in these mice (25).

Animals. All animals were housed and maintained under standard animal facility conditions as previously described (25). Mice health was monitored according to FELASA guidelines (51). All experimental protocols, people involved with animals handling and animal facilities were in accordance with European regulations (EU directive 86/609/EEC), with local Animal Ethics Committees (at ICVS, University of Minho and IBMC) and certified by the Direcção Geral de Veterinária (the Portuguese regulatory entity).

Molecular analysis of the (CAG)n repeat size. DNA extraction from tail biopsies of CMVMJD94$^{-/-}$ and CMVMJD94$^{+/-}$; *Hsf1*$^{+/-}$ animals was performed using the Puragene DNA isolation kit (Gentra systems). The relative (CAG)n size was determined by PCR amplification, using a 6-FAM fluorescently labeled primer, and products were sequenced in an ABI 310 automated DNA sequencer (Applied Biosystems, Foster City, CA), as previously described (25).

Phenotype analysis. Behavioral analysis was performed during diurnal period of CMVMJD94$^{-/-}$; *Hsf1*$^{+/-}$, CMVMJD94$^{+/-}$; *Hsf1*$^{+/+}$, CMVMJD94$^{+/-}$; *Hsf1*$^{+/-}$ animals and wild-type littermates (CMVMJD94$^{-/-}$; *Hsf1*$^{+/+}$) (n= 12 per genotype). In order to evaluate motor performance, animals were tested in the rotarod apparatus (TSA, Bad Homburg, Germany) according to the protocol previously described (25). Mice were evaluated at constant speeds (8, 15, 20, 24 and 31 rpm); and at 4, 8, 12, 16, 24, 48 and 84 weeks of age.

Immunoblotting analysis. Mice were anesthetized (misture of ketamine hydrochloride (150mg/kg) and medetomidine (0.3 mg/kg)) (n=6 per group) and sacrificed by transcardial perfusion with PBS, brain tissue was collected, regions of interest (cerebellum, brainstem and fore brain) were macrodissected, frozen in dry ice and stored at -80°C. For protein isolation, brain tissues were homogenized in 5 volumes of cold resuspension buffer (0.1 M Tris-HCl, pH7.5, 0.1 M EDTA pH 8,0.4 mM PMSF and protease inhibitors cocktail (Roche, Indianopolis, IN)). Preparation of total protein extracts, quantification and western-blot were performed as previously reported (25). Immunoblots were probed with the following antibodies: anti-ataxin-3 (kindly provided by Dr. H. Paulson)

(1:10, 000); anti-MJD1-1 (1: 2000) (52); anti- Hsp105 (1: 750) (58F12, Novocastra); anti- Hsp90 (1: 2000) (SPA-835; Stressgen); anti- Hsp70 (1: 2000) (SPA-810; Stressgen); anti- Hsp60 (1: 500) (SPA-828; Stressgen); anti- Hsp40 (1: 10, 000) (SPA-400; Stressgen); anti- Hsp27 (1: 500) (M20; Santa Cruz) and anti-tubulin (1:100) (DSBH, USA). Bond primary antibodies were detected with horseradish peroxidase-coupled secondary antibodies and chemiluminescence (ECL western-blotting detecting reagents, Amersham Pharmacia). Quantification of the ATXN3 and hsps signal was performed using Image J software (NIH, USA) and normalized to tubulin.

Immunohistochemistry. CMVMJD94$^{+/-}$; *Hsf1*$^{+/+}$, CMVMJD94$^{+/-}$; *Hsf1*$^{-/-}$ and control WT littermate mice (n=3 for each group) at different ages (16 and 100 weeks) were deeply anaesthetized and transcardially perfused with PBS followed by 4% paraformaldehyde (PFA) in PBS. Brains were post-fixed overnight in fixative solution and embedded in paraffin. Slides with 4-μm-thick paraffin sections were steamed for antigen retrieval and then incubated with rabbit anti-MJD1.1 (52) (1:40). A biotinylated secondary antibody was applied, followed by ABC coupled to horseradish peroxidase (DAKO) and DAB substrate (Vector Laboratories Inc., Burlingame, CA, USA). The slides were counterstained with hematoxylin according to standard procedures and analyzed with an optical microscope (Olympus, Hamburg, Germany). For morphological brain analysis, we performed cresyl violet staining.

Statistical Analysis. Rotarod data was analyzed using the non-parametric Mann-Whitney *U*-test when variables were non-continuous or did not present a normal distribution (Kolmodorov-Smirnov test $p< 0.05$). Continuous variables with normal distributions were analyzed through Student *t*-test or ANOVA. All statistical analyses were performed using SPSS 16.0 (SPSS Inc., Chicago, IL) or Excel. Results were considered statistical significant for $p<0.05$.

Acknowledgements

We are grateful to members of the Maciel and Saraiva laboratories for sharing reagents, for critical analysis of the data and for their helpful discussions on the manuscript. We would like to acknowledge Dr. Henry Paulson for providing anti-ataxin-3 serum. This work was supported by grants from Fundação Ciência e Tecnologia (FCT) [PTDC/SAU-GMG/64076/2006, SFRH/BD/27258/2006 to A.T-C., PTDC/SAU-GMG/64076/2006 to S.D-S. and T.C., SFRH/BD/15910/2005 to A. S-F. and UMINHO/BI/052/2010 to A.J.] and from Ataxia MJD Research Project.

References

1 Ellis, R.J. and Minton, A.P. (2006) Protein aggregation in crowded environments. *Biol Chem*, **387**, 485-497.

2 Horwich, A.L. and Weissman, J.S. (1997) Deadly conformations--protein misfolding in prion disease. *Cell*, **89**, 499-510.

3 Morimoto, R.I. (2002) Dynamic remodeling of transcription complexes by molecular chaperones. *Cell*, **110**, 281-284.

4 Nollen, E.A. and Morimoto, R.I. (2002) Chaperoning signaling pathways: molecular chaperones as stress-sensing 'heat shock' proteins. *J Cell Sci*, **115**, 2809-2816.

5 Taylor, J.P., Hardy, J. and Fischbeck, K.H. (2002) Toxic proteins in neurodegenerative disease. *Science*, **296**, 1991-1995.

6 Selkoe, D.J. (2004) Cell biology of protein misfolding: the examples of Alzheimer's and Parkinson's diseases. *Nat Cell Biol*, **6**, 1054-1061.

7 Walsh, D.M. and Selkoe, D.J. (2004) Oligomers on the brain: the emerging role of soluble protein aggregates in neurodegeneration. *Protein Pept Lett*, **11**, 213-228.

8 Kawaguchi, Y., Okamoto, T., Taniwaki, M., Aizawa, M., Inoue, M., Katayama, S., Kawakami, H., Nakamura, S., Nishimura, M., Akiguchi, I. *et al.* (1994) CAG expansions in a novel gene for Machado-Joseph disease at chromosome 14q32.1. *Nat Genet*, **8**, 221-228.

9 Chow, M.K., Mackay, J.P., Whisstock, J.C., Scanlon, M.J. and Bottomley, S.P. (2004) Structural and functional analysis of the Josephin domain of the polyglutamine protein ataxin-3. *Biochem Biophys Res Commun*, **322**, 387-394.

10 Ellisdon, A.M., Thomas, B. and Bottomley, S.P. (2006) The two-stage pathway of ataxin-3 fibrillogenesis involves a polyglutamine-independent step. *J Biol Chem*, **281**, 16888-16896.

11 Kim, S., Nollen, E.A., Kitagawa, K., Bindokas, V.P. and Morimoto, R.I. (2002) Polyglutamine protein aggregates are dynamic. *Nat Cell Biol*, **4**, 826-831.

12 Chai, Y., Koppenhafer, S.L., Bonini, N.M. and Paulson, H.L. (1999) Analysis of the role of heat shock protein (Hsp) molecular chaperones in polyglutamine disease. *J Neurosci*, **19**, 10338-10347.

13 Wen, F.C., Li, Y.H., Tsai, H.F., Lin, C.H., Li, C., Liu, C.S., Lii, C.K., Nukina, N. and Hsieh, M. (2003) Down-regulation of heat shock protein 27 in neuronal cells and non-neuronal cells expressing mutant ataxin-3. *FEBS Lett*, **546**, 307-314.

14 Chang, W.H., Cemal, C.K., Hsu, Y.H., Kuo, C.L., Nukina, N., Chang, M.H., Hu, H.T., Li, C. and Hsieh, M. (2005) Dynamic expression of Hsp27 in the presence of mutant ataxin-3. *Biochem Biophys Res Commun*, **336**, 258-267.

15 Chang, W.H., Tien, C.L., Chen, T.J., Nukina, N. and Hsieh, M. (2009) Decreased protein synthesis of Hsp27 associated with cellular toxicity in a cell model of Machado-Joseph disease. *Neurosci Lett*, **454**, 152-156.

16 Evert, B.O., Vogt, I.R., Vieira-Saecker, A.M., Ozimek, L., de Vos, R.A., Brunt, E.R., Klockgether, T. and Wullner, U. (2003) Gene expression profiling in ataxin-3 expressing cell lines reveals distinct effects of normal and mutant ataxin-3. *J Neuropathol Exp Neurol*, **62**, 1006-1018.

17 Chou, A.H., Yeh, T.H., Ouyang, P., Chen, Y.L., Chen, S.Y. and Wang, H.L. (2008) Polyglutamine-expanded ataxin-3 causes cerebellar dysfunction of SCA3 transgenic mice by inducing transcriptional dysregulation. *Neurobiol Dis*, **31**, 89-101.

18 Warrick, J.M., Chan, H.Y., Gray-Board, G.L., Chai, Y., Paulson, H.L. and Bonini, N.M. (1999) Suppression of polyglutamine-mediated neurodegeneration in Drosophila by the molecular chaperone HSP70. *Nat Genet*, **23**, 425-428.

19 Bilen, J. and Bonini, N.M. (2007) Genome-wide screen for modifiers of ataxin-3 neurodegeneration in Drosophila. *PLoS Genet*, **3**, 1950-1964.

20 Williams, A.J., Knutson, T.M., Colomer Gould, V.F. and Paulson, H.L. (2009) In vivo suppression of polyglutamine neurotoxicity by C-terminus of Hsp70-interacting protein (CHIP) supports an aggregation model of pathogenesis. *Neurobiol Dis*, **33**, 342-353.

21 Morimoto, R.I. (1998) Regulation of the heat shock transcriptional response: cross talk between a family of heat shock factors, molecular chaperones, and negative regulators. *Genes Dev*, **12**, 3788-3796.
22 Fujimoto, M., Takaki, E., Hayashi, T., Kitaura, Y., Tanaka, Y., Inouye, S. and Nakai, A. (2005) Active HSF1 significantly suppresses polyglutamine aggregate formation in cellular and mouse models. *J Biol Chem*, **280**, 34908-34916.
23 Santos, S.D., Fernandes, R. and Saraiva, M.J. The heat shock response modulates transthyretin deposition in the peripheral and autonomic nervous systems. *Neurobiol Aging*, **31**, 280-289.
24 Teixeira-Castro, A., Ailion, M., Jalles, A., Brignull, H.R., Vilaca, J.L., Dias, N., Rodrigues, P., Oliveira, J.F., Neves-Carvalho, A., Morimoto, R.I. *et al.* Neuron-specific proteotoxicity of mutant ataxin-3 in C. elegans: rescue by the DAF-16 and HSF-1 pathways. *Hum Mol Genet*.
25 Silva-Fernandes, A., Costa Mdo, C., Duarte-Silva, S., Oliveira, P., Botelho, C.M., Martins, L., Mariz, J.A., Ferreira, T., Ribeiro, F., Correia-Neves, M. *et al.* Motor uncoordination and neuropathology in a transgenic mouse model of Machado-Joseph disease lacking intranuclear inclusions and ataxin-3 cleavage products. *Neurobiol Dis*, **40**, 163-176.
26 Westerheide, S.D. and Morimoto, R.I. (2005) Heat shock response modulators as therapeutic tools for diseases of protein conformation. *J Biol Chem*, **280**, 33097-33100.
27 Xiao, X., Zuo, X., Davis, A.A., McMillan, D.R., Curry, B.B., Richardson, J.A. and Benjamin, I.J. (1999) HSF1 is required for extra-embryonic development, postnatal growth and protection during inflammatory responses in mice. *EMBO J*, **18**, 5943-5952.
28 Auluck, P.K., Chan, H.Y., Trojanowski, J.Q., Lee, V.M. and Bonini, N.M. (2002) Chaperone suppression of alpha-synuclein toxicity in a Drosophila model for Parkinson's disease. *Science*, **295**, 865-868.
29 Bruening, W., Roy, J., Giasson, B., Figlewicz, D.A., Mushynski, W.E. and Durham, H.D. (1999) Up-regulation of protein chaperones preserves viability of cells expressing toxic Cu/Zn-superoxide dismutase mutants associated with amyotrophic lateral sclerosis. *J Neurochem*, **72**, 693-699.
30 Cummings, C.J., Mancini, M.A., Antalffy, B., DeFranco, D.B., Orr, H.T. and Zoghbi, H.Y. (1998) Chaperone suppression of aggregation and altered subcellular proteasome localization imply protein misfolding in SCA1. *Nat Genet*, **19**, 148-154.
31 Cummings, C.J., Sun, Y., Opal, P., Antalffy, B., Mestril, R., Orr, H.T., Dillmann, W.H. and Zoghbi, H.Y. (2001) Over-expression of inducible HSP70 chaperone suppresses neuropathology and improves motor function in SCA1 mice. *Hum Mol Genet*, **10**, 1511-1518.
32 Teixeira, P.F., Cerca, F., Santos, S.D. and Saraiva, M.J. (2006) Endoplasmic reticulum stress associated with extracellular aggregates. Evidence from transthyretin deposition in familial amyloid polyneuropathy. *J Biol Chem*, **281**, 21998-22003.
33 Batulan, Z., Shinder, G.A., Minotti, S., He, B.P., Doroudchi, M.M., Nalbantoglu, J., Strong, M.J. and Durham, H.D. (2003) High threshold for induction of the stress response in motor neurons is associated with failure to activate HSF1. *J Neurosci*, **23**, 5789-5798.
34 Homma, S., Jin, X., Wang, G., Tu, N., Min, J., Yanasak, N. and Mivechi, N.F. (2007) Demyelination, astrogliosis, and accumulation of ubiquitinated proteins, hallmarks of CNS disease in hsf1-deficient mice. *J Neurosci*, **27**, 7974-7986.
35 Santos, S.D. and Saraiva, M.J. (2004) Enlarged ventricles, astrogliosis and neurodegeneration in heat shock factor 1 null mouse brain. *Neuroscience*, **126**, 657-663.
36 Wu, C. (1995) Heat shock transcription factors: structure and regulation. *Annu Rev Cell Dev Biol*, **11**, 441-469.
37 Hsu, A.L., Murphy, C.T. and Kenyon, C. (2003) Regulation of aging and age-related disease by DAF-16 and heat-shock factor. *Science*, **300**, 1142-1145.
38 Morley, J.F. and Morimoto, R.I. (2004) Regulation of longevity in Caenorhabditis elegans by heat shock factor and molecular chaperones. *Mol Biol Cell*, **15**, 657-664.

39 Nollen, E.A., Garcia, S.M., van Haaften, G., Kim, S., Chavez, A., Morimoto, R.I. and Plasterk, R.H. (2004) Genome-wide RNA interference screen identifies previously undescribed regulators of polyglutamine aggregation. *Proc Natl Acad Sci U S A*, **101**, 6403-6408.
40 van Ham, T.J., Thijssen, K.L., Breitling, R., Hofstra, R.M., Plasterk, R.H. and Nollen, E.A. (2008) C. elegans model identifies genetic modifiers of alpha-synuclein inclusion formation during aging. *PLoS Genet*, **4**, e1000027.
41 Fujimoto, M., Hayashida, N., Katoh, T., Oshima, K., Shinkawa, T., Prakasam, R., Tan, K., Inouye, S., Takii, R. and Nakai, A. A novel mouse HSF3 has the potential to activate nonclassical heat-shock genes during heat shock. *Mol Biol Cell*, **21**, 106-116.
42 Wang, G., Zhang, J., Moskophidis, D. and Mivechi, N.F. (2003) Targeted disruption of the heat shock transcription factor (hsf)-2 gene results in increased embryonic lethality, neuronal defects, and reduced spermatogenesis. *Genesis*, **36**, 48-61.
43 Wang, G., Ying, Z., Jin, X., Tu, N., Zhang, Y., Phillips, M., Moskophidis, D. and Mivechi, N.F. (2004) Essential requirement for both hsf1 and hsf2 transcriptional activity in spermatogenesis and male fertility. *Genesis*, **38**, 66-80.
44 Chang, Y., Ostling, P., Akerfelt, M., Trouillet, D., Rallu, M., Gitton, Y., El Fatimy, R., Fardeau, V., Le Crom, S., Morange, M. *et al.* (2006) Role of heat-shock factor 2 in cerebral cortex formation and as a regulator of p35 expression. *Genes Dev*, **20**, 836-847.
45 He, H., Soncin, F., Grammatikakis, N., Li, Y., Siganou, A., Gong, J., Brown, S.A., Kingston, R.E. and Calderwood, S.K. (2003) Elevated expression of heat shock factor (HSF) 2A stimulates HSF1-induced transcription during stress. *J Biol Chem*, **278**, 35465-35475.
46 Ostling, P., Bjork, J.K., Roos-Mattjus, P., Mezger, V. and Sistonen, L. (2007) Heat shock factor 2 (HSF2) contributes to inducible expression of hsp genes through interplay with HSF1. *J Biol Chem*, **282**, 7077-7086.
47 Sandqvist, A., Bjork, J.K., Akerfelt, M., Chitikova, Z., Grichine, A., Vourc'h, C., Jolly, C., Salminen, T.A., Nymalm, Y. and Sistonen, L. (2009) Heterotrimerization of heat-shock factors 1 and 2 provides a transcriptional switch in response to distinct stimuli. *Mol Biol Cell*, **20**, 1340-1347.
48 Fujimoto, M., Izu, H., Seki, K., Fukuda, K., Nishida, T., Yamada, S., Kato, K., Yonemura, S., Inouye, S. and Nakai, A. (2004) HSF4 is required for normal cell growth and differentiation during mouse lens development. *EMBO J*, **23**, 4297-4306.
49 Min, J.N., Zhang, Y., Moskophidis, D. and Mivechi, N.F. (2004) Unique contribution of heat shock transcription factor 4 in ocular lens development and fiber cell differentiation. *Genesis*, **40**, 205-217.
50 Fujimoto, M., Oshima, K., Shinkawa, T., Wang, B.B., Inouye, S., Hayashida, N., Takii, R. and Nakai, A. (2008) Analysis of HSF4 binding regions reveals its necessity for gene regulation during development and heat shock response in mouse lenses. *J Biol Chem*, **283**, 29961-29970.
51 Nicklas, W., Baneux, P., Boot, R., Decelle, T., Deeny, A.A., Fumanelli, M. and Illgen-Wilcke, B. (2002) Recommendations for the health monitoring of rodent and rabbit colonies in breeding and experimental units. *Lab Anim*, **36**, 20-42.
52 Ferro, A., Carvalho, A.L., Teixeira-Castro, A., Almeida, C., Tome, R.J., Cortes, L., Rodrigues, A.J., Logarinho, E., Sequeiros, J., Macedo-Ribeiro, S. *et al.* (2007) NEDD8: a new ataxin-3 interactor. *Biochim Biophys Acta*, **1773**, 1619-1627.

Chapter 7

General Discussion and Prospectus

General Discussion

Considerable effort has been employed in understanding how protein folding is regulated and in the identification of components involved in this process. Particular emphasis has been given to the role played by molecular chaperones and more recently, to the cellular degradation machinery, including the ubiquitin proteasome system and autophagy, in refolding and actively clearing misfolded proteins from the cell. Although there is now a considerable knowledge of these processes, it has also become clear that the full extent of proteins that constitute the network regulating protein homeostasis has not been uncovered.

Misfolding and the formation of protein aggregates are hallmarks of a broad and increasing number of diseases, most of which are age-dependent. These comprise Alzheimer's disease, Parkinson's disease, amyotrophic lateral sclerosis, polyglutamine expansion disorders, and many others (1). As human life expectancy increases, understanding the mechanism underlying misfolding and aggregation and the interaction of the misfolded species with the neuron cell-type-specific proteome represents a critical challenge for a continuously aging population.

In this work, we have developed a novel model system in *C. elegans*, which mimics many aspects of Machado-Joseph disease (MJD), namely neuron cell-type specific aggregation, which correlated with the appearance of neuronal dysfunction (Chapter 2). We also developed tools that allowed quantification of these phenotypes (Chapter 2.1). The fact that there was a great contribution of aging into the modulation of the phenotype of the mutant ATXN3-expressing animals, allowed for the first time the study of the influence of aging-related pathways in the pathogenesis of MJD (Chapters 2 and 3). We have also studied the impact of the wild-type (WT) ataxin-3 in pathogenesis (Chapter 4). Moreover, the validation of the model for the identification of therapeutic small molecules for MJD (Chapter 5) may be of great value for future treatment development in MJD.

Looking at the data gathered over these years, we certainly learned more about ATXN3 pathogenesis, although this work has also led to a number of questions that remained unanswered, which will be discussed in the following section.

A journey through the pathogenesis of MJD: the establishment of a new model in *Caenorhabditis elegans*

Since we started this work many model systems have become available that recapitulate many aspects of MJD. Expression of WT and expanded ATXN3 in **cell culture** allowed the visualization of the proteins *in vivo*, the evaluation of the subcellular localization and formation of aggregates, as well as addressing mutant ATXN3-mediated cytotoxicity (2-8). Microarray analysis of a cell culture model of ATXN3 pathogenesis gave a good

contribution for understanding both normal function and pathogenesis of ATXN3 (9). These models would be extremely useful platforms to perform genome-wide screens for modifiers of ATXN3 aggregation and toxicity and similar readouts could be employed in high-throughput drug testing. However, in these cell culture models, there is no integration of the cells behavior at the organism level, as happens in the human disease. In fact, although ATXN3 is ubiquitously expressed it seems that only specific neuronal subtypes are affected, suggesting that clonal cells may not mimic the disease context. Studies in ***Drosophila*** (10-12) also gave important insight into the further understanding of the disease, complementing the studies in cell culture by allowing behavioral testing. However, subcellular localization and aggregation states of mutant ATXN3 were, in this model, only possible to analyze in fixated tissue. Disease models in higher organisms like **mice** (4, 13-19) and **rat** (20-22) allow a greater variety of behavioral tests, with many aspects of behavior resembling that in humans; the basic cellular pathways are highly conserved, as well as the organization of the nervous system. However, when performing pharmacologic or gene therapy, the experimental designs can became very time-consuming and costly.

Based on this, we decided to generate a disease model in ***Caenorhabditis elegans***, because it would give us the opportunity to simultaneously: (i) follow the aggregation dynamics of ATXN3 *in vivo*; (ii) distinguish differential neuronal susceptibility to the expression of the disease protein; and (iii) determine the impact of toxic protein aggregation in the animals' behavior. Later on, this invertebrate model would allow fast and inexpensive testing of modifiers genes of ATXN3 aggregation and neuronal toxicity and also could constitute good platforms for drug testing (23).

With this in mind, we have generated and extensively characterized a novel *C. elegans* model for MD pathogenesis, regarding protein expression levels, biophysical properties of the mutant proteins in the live animals and performed behavioral characterization of the animals (Chapter 2). Expression of full-length and C-terminal truncated ATXN3 proteins in all *C. elegans* neuronal cells caused polyQ length-dependent aggregation in specific neurons, suggesting differential neuronal susceptibility to the presence of mutant ataxin-3. This aggregation correlated with locomotion defects in these animals. Neuronal-specific aggregation and neuronal dysfunction were used as readouts for determination of genetic modifiers of the disease and for the identification of potential therapeutic agents.

One way of studying genetic modifiers of the disease is to employ reverse genetics and choose candidate genes and pathways to test. Aging is a major risk factor of the majority of the neurodegenerative diseases and here we found that longevity pathway genes as specific modifiers of MJD pathogenesis in *C. elegans* (Chapters 2 and 3). One of the major limitations in finding modifiers of protein aggregation in *C. elegans* was the lack of good platforms to quantify protein aggregates. Many studies would qualitatively describe modifiers of protein aggregation (24, 25) or would perform manual counting of the aggregates (26). In our case counting aggregates in small neuronal cells would be very time-consuming and extremely dependent on the

operator. Thus, we developed an imaging processing application that allowed us to automatically quantify the number and area of aggregates in the animals' neuronal cells per total area of the animal (Chaper 2.1). We were also able to quantify aggregates in specific areas of the *C. elegans* nervous system and establish correlations between changes in aggregation (due to a particular modifier gene or drug treatment) in the entire nervous system versus specific regions. We are currently customizing our imaging processing application in order to be able to start quantifying aggregates in 3 dimensions. Quantification of volume of the aggregates through a 3D reconstruction of confocal microscopy images will give better and more reliable information of the aggregation phenotype in animal models for diseases of protein aggregation.

We have also quantified defects in locomotion in these animals, although using a low-throughput approach. Automation of motor function evaluation is being performed by using a video-based assay. The *Tracker* software (Goodman Laboratory, Stanford school of Medicine) analyzes videos of the animals crawling in NGM plates and measures locomotion speed, quantifies the number of tracks (paralyzed and normal), and determines the fraction of paralyzed animals. We are also collaborating with *Noldus Information Technology* to develop a system that will allow tracking of the animals, when grown in liquid 96-well plate cultures.

In summary, we were able to develop a new animal model of MJD and important tools to pursue our goals.

The mystery of the neuronal-specificity in polyQ diseases

Each of the polyQ disorders shows a characteristic pathological signature, even though the mutant proteins are ubiquitously expressed (27). The neuronal-specific susceptibility derived from the expression of aggregation-prone proteins is possibly determined by: (i) the protein context in which the polyQ-segment is expressed and by (ii) specific factors of the neuronal cellular environment. In fact, the interaction between the misfolded proteins and the neuron cell-specific proteome may direct neuronal vulnerability to aggregation, toxicity and ultimately death.

As discussed in Chapter 2, mutant ATXN3 aggregation in *C. elegans* neuronal cells was not stochastic, but there was a specific aggregation pattern, observed in multiple animals of independent transgenic lines. Moreover, the aggregation and toxicity profiles found were very consistent when comparing full-length and C-terminal ATXN3 models. This was a very intriguing result mainly because the C-terminal fragment of the protein does not contain the N-terminal Josephin domain (JD) of ATXN3, and one would expect that many protein interactions between ATXN3 and cellular components would be JD-dependent. ATXN3 being a deubiquitylating (DUB) enzyme, whose catalytic domain is located in the N-terminus of ATXN3, many ATXN3 protein interactions with the substrates may not be occurring in the C-terminus protein. The outcome(s) can be either a loss-of-function due to an inexistent interaction; or a gain of toxic function caused by accumulation of a DUB substrate, or an increased tendency to aggregate, leading to aggregation at a lower threshold of Q-length.

As an example, ATXN3 was shown to interact and to have hydrolase activity towards the neural precursor cell expressed developmentally downregulated 8 (NeDD8) proteins. This interaction is solely dependent on the JD of ATXN3, at least *in vitro*, and when the catalytic cysteine is mutated the two proteins are still able to bind but the mutation averts cleavage of a fluorogenic NEDD8 substrate (28).

Valosin-containing protein (VCP/p97) is a known molecular partner of ATXN3. VCP is not a substrate of ATXN3, but associates with ATXN3 and Rad23 to translocate ubiquitylated proteins into the proteasome (29). When ATXN3 shows no catalytic activity, by mutation of the cysteine-14, the interaction VCP-ATXN3C14A becomes weaker (30). In contrast, VCP and ATXN3 co-immunoprecipitation was found to be potentiated (increased affinity) when ATXN3 contained an expanded Q-tract (31). The physiological impact of this differential interaction with the WT versus expanded ATXN3 needs to be further explored. However, it is known that ATXN3 binding to VCP regulates translocation of endoplasmic reticulum-associated degradation (ERAD) substrates (32). For instance, ATXN3 increases the level of CD3delta by decreasing its degradation; pathogenic ATXN3 decreases degradation to a greater extent than the normal protein. Knock-down of endogenous ATXN3 decreases levels of CD3delta, suggesting that a normal function of ATXN3 is to regulate levels of ERAD substrates, which become altered in the presence of the expanded Q-tract. VCP is a very abundant protein in the brain and reduction of VCP levels stimulates ATXN3 fibrillogenesis *in vitro* and in *Drosophila* models of MJD pathogenesis (32). Indeed, also in *C. elegans* we found that absence of the VCP homolog CDC-48.2 aggravated mutant ATXN3-mediated pathogenesis (data not shown). Importantly, VCP and C-terminal ATXN3 are still able to interact, since the Arg/Lys rich motif of ATXN3 is maintained in our C-terminal ATXN3 animals. The usage of more neuron subtype-specific markers in our model (similar to CHE-13 promoter but for other types of neurons) would allow further definition of potential differences between the full-length and C-terminal ATXN3 pathogenesis model.

Taken together, these results suggest that differential affinity between WT and mutant ATXN3 and the molecular partners/substrates may have an impact in their levels and/or cause changes in ATXN3 aggregation. These effects can differ among distinct neurons according to their proteome, which might underlie the specificity.

One good example is the work by Subramaniam and collaborators that shows that the small guanine nucleotide-binding protein Rhes, which is localized very selectively to the striatum, binds physiologically to mutant Htt (mHtt). In the presence of purified Rhes and Htt proteins, Rhes bound much more to mHtt than to WT Htt. Rhes induces sumoylation of mHtt, which leads to cytotoxicity (33). Thus, Rhes-mHtt interactions could account for the localized neuropathology of HD. One possible explanation for the problem of the neuron-specific susceptibility seen in each of the polyQ disorders can arise from novel/aberrant interactions between the mutant protein and certain cell constituents that do not occur in the normal situation.

A variety of methods can be used for determining molecular partners of expanded ATXN3 in affected brain regions in mice, one of which is the use of a combination of pull-down and mass spectrometry assays.

Finding differentially interacting proteins whose expression was localized (or considerably more abundant) in the specific areas of MJD pathology could give new insight into the question: *why is pathology restricted to specific brain regions in each disease?* Resolving the neuron cell-type-specific proteome in the healthy brains versus disease brains would also be of great importance to clarify this aspect.

The protein flanking sequences in which the polyQ-segment is inserted direct protein function that may or may not be altered in the presence of the expanded Q-tract, but the degree of exposure of the Q-tract to the cellular environment also determines toxicity. When a polyQ stretch of 75 glutamines is expressed within full-length ATXN3 flanking sequences in *C. elegans* neurons it does not cause neuronal toxicity or the formation of aggregates. In contrast, C-terminal ATXN3 proteins of similar polyQ length result in protein aggregation in certain neuronal cells, that correlated with the appearance of locomotion defects and decreased chemotaxis function (Chapter 2). Expression of Q67 proteins with no additional flanking sequence (under the regulation of the same promoter and comparable protein levels) resulted in aggregation in all *C. elegans* neurons and the animals showed a high degree of motor dysfunction, defects in pharyngeal pumping and reduced defecation rates (34). As discussed in Chapter 2, polyQ-alone and ATXN3 proteins caused distinct neuronal vulnerability in *C. elegans* at the threshold-length for aggregation. Mutant ATXN3 aggregates in several neuronal processes, including commissures, the DNC and sensory processes. In particular, the processes of certain CHE-13-positive sensory neurons contain protein foci only when the polyQ tract is expressed within ATXN3-flanking sequences and not when expressed alone (34). Although the cell bodies of certain lateral neurons contained soluble ATXN3 proteins, even in very old animals, their processes often presented aggregates. By comparison, these processes were spared in Q40 animals. This neuronal specific pathogenesis validates both models as tools to find both common and protein-specific mechanism(s) of aggregation, neuronal dysfunction and neurodegeneration. Moreover, other disease models, for HD and SBMA, are currently being developed using the same promoter that will increase the power of comparative studies.

We predict that finding the molecular basis for neuronal cell-specific susceptibility to mutant ATXN3 proteotoxicity can be challenging. However, determining the transcriptional profile of specific neuronal-subtypes can be achieved in *C. elegans* by employing a mRNA-tagging method (35, 36) in sub-types of neurons. The idea is to determine the transcriptomic signature of sensory and motor neurons (among others) and compare the profiles among the different neuron-subtypes in WT N2 animals. After having an idea about differentially expressed genes among distinct neurons, we could employ the same techniques in WT and mutant ATXN3-expressing animals. This approach could give us good insight regarding the differentially expressed genes in affected and spared MJD neurons in *C. elegans*.

Gain and loss-of-function in MJD: role of the wild-type protein

The aberrant or novel protein-protein interactions due to the polyQ expansion (37-42) and the aggregation of mutated polyQ proteins with consequent sequestration of cellular components, suggest a toxic gain of function as the pathogenic mechanism underlying the polyQ disorders (43-47). However, more recently, it has been proposed that a combination of gain of novel properties and partial loss of the normal function modulates disease progression (39, 48).

If loss-of-function of ATXN3 were to be the primary mechanism underlying disease, knock-out models would phenocopy mutant ATXN3 overexpression phenotype, which does not seem to be the case (49, 50), although both models in *C. elegans* show temperature-sensitive locomotion defects (51). In mice, ubiquitous expression of ATXN3 with 94Qs caused motor uncoordination, astrogliosis and neuronal atrophy (19), whereas inactivation of the mouse *Atxn3* gene caused no gross morphological deficits or uncoordination, as assessed on the accelerating rotarod (50). However, these findings do not exclude a contribution of the (lack of) WT protein to disease. *atx-3* knock-out models in *C. elegans* showed improved thermotolerance, when submitted to a noxious heat stress (52). This phenotype is fully dependent on DAF-16 and is rescued by silencing the expression of small heat shock proteins and by knocking-down inducible Hsp70 proteins. Interestingly, a recent study by Kuhlbrodt *et al* reported a synergistic cooperation between CDC-48 and ATX-3 in ubiquitin-mediated proteolysis and aging regulation (53). Double mutant *cdc48; atx-3* animals demonstrated a significant increase in lifespan, via the IIS pathway. This phenotype was specifically dependent on the DUB activity of ATXN3 and suggests the involvement of *C. elegans* ATX-3 in proteostasis. Based on this, we evaluated the influence of the loss of endogenous ATX-3 in MJD pathogenesis in *C. elegans* and somehow surprisingly we found no major effect in mutant ATXN3 aggregation or motor dysfunction (Chapter 4). The influence of the double absence of ATX-3 and of CDC48 in disease remains unknown, although the *cdc48* mutation by itself aggravates MJD pathogenesis in *C. elegans* (our own unpublished observations).

Overexpression of WT ATXN3 in a *C. elegans* model of polyQ protein aggregation aggravated neuronal dysfunction, lacking the neuroprotective effect showed before in *Drosophila* and mice (11, 13) but supporting more recent observations in rats and in a distinct mouse model (21, 54). These controversial results lead us to conclude that beneficial, neutral or harmful effects of the normal ATXN3 in pathogenesis may depend on the cellular proteome and on the severity of the disease symptoms. Thus, caution needs to be taken when manipulation of the WT ATXN3 levels is considered as a therapeutic strategy in MJD.

The therapy challenge: knowing the multiple targets

As discussed before, neurodegenerative diseases tend to have a growing impact on society as a larger percentage of the population is reaching older ages. What emerges from the examination of the literature is that the etiopathology of these diseases is extremely complex and heterogeneous. Moreover, many of the key

reactions in living organisms are essentially based on interactions of moderate affinities and selectivities. This principle is responsible for the enormous redundancy of cellular circuits (55) and increases the difficulty of drug design. The most striking evidence pointing to the complexity of these diseases is that to date no single drug has been developed that can prevent the degenerative process or restore viability of neurons that are dying. Pharmaceutical research has only been able to bring drugs to the market that can, at best, modulate symptoms in patients suffering from the diseases, which in many cases only feel beneficial effects for limited time periods. The lack of good neuroprotective/neurorestorative compounds can at least in part be attributed to a "one-disease, one-target" paradigm that has been followed by most drug discovery laboratories (reviewed in (56, 57). The choice to develop selective compounds is driven by the observation that there likely exists an inverse relationship between drug target selectivity and side effects. Thus, by designing a highly selective compound which targets only one receptor or enzyme, the likelihood of side-effects resulting from cross-reactivity at other biological pathways is mitigated.

During the past few decades, however, a multi-drug approach to therapy has gained recognition. Two examples of diseases that have been treated with a combination of drugs with divergent therapeutic targets include high blood pressure and asthma (58). More recently, a new paradigm that addresses disease etiological complexity by a multi-target approach has gained increasing acceptance (59). In this type of approach, the agent has more than one mechanism of action and the compounds should be named, as suggested by Morphy and Rankovic, "designed multiple ligands" (DMLs)-compounds that are specifically designed to target the multiple mechanisms underlying the etiology of a specific disease or group of diseases (56, 57). Fig. 1 shows the change in drug design strategy over the past years.

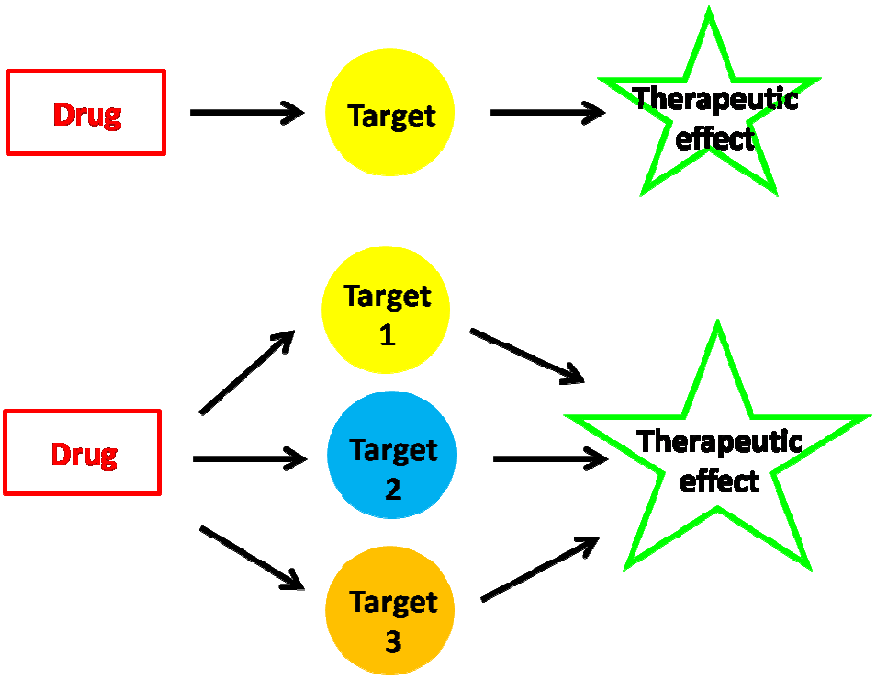

Figure 1. The drug discovery process for neurodegenerative disease and other complex pathologies have seen a significant change in the past few years. Traditional drug discovery focused on a specific target toward which the drug was designed to interact very potently. The rationale for this approach was primarily driven by the desire to minimize cross-reactivity with other cellular pathways, thereby resulting in fewer side-effects. Recently, more data show that multifunctional drugs targeting more than one disease pathway seemed to have better success at modulating complex diseases, with no demonstrable increase in side-effects reported in many cases. Adapted from (60, 61).

Neurodegenerative diseases appear to be particularly amenable to drug therapy strategies in which multiple drug targets are affected, rather than focusing on a single target (reviewed in (62). As a general example, L-3-n-butylphthalide is an extract from the seed of *Apiumgraveolens* Linn (Chinese celery) and has been employed in the treatment of AD transgenic mice (3xTg-AD). These animals developed both plaques and tangles with aging, as well as cognitive deficits. In all measures, L- butylphthalide treated animals showed significantly improved outcomes (63). Of interest in the context of multi-target drugs is the fact that L-3-n-butylphthalide markedly enhanced secretion of soluble amyloid precursor protein (α-APPs), alpha-secretase, and PKCα expression, but reportedly had no effect on steady-state full-length APP. L-3-n-butylphthalide also reduced glial activation and oxidative stress in these animals. It is therefore speculated that L-3-n-butylphthalide may direct APP processing toward a non-amyloidogenic pathway and in doing so, preclude Aβ formation in the 3xTg-AD mouse (64).

In fact, many of the small molecules are initially described to be targeting specific pathways in cells and years later other factors are implicated in the mode of action of the drugs. The geldanamycin analog, 17-AAG, is one such example. 17-AAG and derivatives are currently in clinical trials as anticancer drugs (65), that specifically bind to and inhibit Hsp90 and trigger the activation of a heat shock response in many model systems

(66-69). Recently, 17-AAG was also shown not only to cause upregulation of Hsps, but also to be an effective inducer of the autophagic pathway and thereby promoting the removal of prefibrillary α-synuclein aggregates (70) and of androgen receptor (71). Parallel to its role as an HDAC inhibitor, SAHA was also suggested to induce caspase-independent autophagic cell death by influencing mTOR pathway (72). Valproic acid acts primarily as an HDAC inhibitor, used in the clinics to treat bipolar disorders and epilepsy (73) but was found to increase longevity in *C. elegans* in a DAF-16-dependent manner (74).

These data suggest, as has been discussed also in Chapter 5, that one single compound can act in several pathways, being crucial to apply pharmacogenetics to determine all the targets and predict eventual side effects. A multiple-target drug approach can indeed be promising in finding treatments for neurodegenerative diseases, including MJD.

Longevity pathways and proteotoxicity

The discovery that the aging process can be slowed by reducing the activity of the insulin/insulin growth factor-(IGF)-1-signaling (IIS) opened the way for researchers to address the question of whether aging-related changes play a role in enabling protein aggregation to become toxic late in life. In *C. elegans* expressing a polyQ35-YFP chimera, aggregates were detectable by day 4 of adulthood. RNAi-mediated reduction of *age-1* (a central IIS component whose reduction leads to extended lifespan) protected worm embryos from polyQ82-YFP aggregation in a DAF-16-dependent manner. Furthermore, *age-1* RNAi treatment partially rescued the worms from motility impairments associated with the expression and aggregation of polyQ-YFP of different lengths (75). This seminal study indicated that slowing aging by reducing the activity of the IIS alleviates toxicity associated with polyQ aggregation and suggested that aging plays an active role in the temporal regulation of toxic protein aggregation. HSF-1 was also found to be required to enable IIS reduction to mediate protection from toxicity associated with polyQ-YFP aggregation (76). Expression and subsequent aggregation of the human Amyloid-β peptide in the body wall muscle cells of *C. elegans* caused progressive paralysis (77). In this model, *daf-2* RNAi also protected worms from this toxic effect in DAF-16 and HSF-1 dependent manners (78). Here, we found that DAF-16 and HSF-1 are also potent suppressors of mutant ATXN3 proteotoxicity (79).

It is known that HSF-1 activity is required for IIS-mediated increased lifespan in *C. elegans*, but *daf-16* mutation does not further decrease *hsf-1*-mediated decrease in lifespan. This result suggests that likely HSF-1 and DAF-16 may function in a common pathway to regulate longevity. How about their action in proteotoxicity? We found that in the absence of *daf-16*, 17-DMAG is still able to rescue mutant-ATXN3-mediated neuronal dysfunction (79). Moreover, late-life IIS reduction protects the worms from Aβ toxicity (80), when it can no longer affect lifespan (81). Taken together, these studies suggest that the counter-proteotoxic functions of IIS reduction can be uncoupled from its (more global) longevity effects, and that HSF-1 can be acting downstream of DAF-16 in protecting against proteotoxic stress.

Next, we asked if other aging-related pathways would also show this protective effect, like reduction of IIS. As discussed in Chapter 3, a genetic model of dietary restriction (DR) failed to rescue mutant ATXN3 pathogenesis in neuronal cells, probably because diet-restricted animals depend on an endocrine signal from the ASI neurons (which are not affected in our ATXN3 model) to non-neuronal tissues (82). However, when polyQ or Aβ proteins were expressed in *C. elegans* body wall muscle cells, DR reduced aggregation and toxicity of the mutant proteins (83). Also in this model, the effects of DR-mediated improved proteotoxicity were fully dependent on HSF-1 activity (83). Effect of HSF-1 in ISP-1-mediated reduced ATXN3 aggregation still remains to be determined.

Based on this, we propose a working model in which component(s) of the proteostasis network (e.g. HSF-1) are required for the protection against proteotoxicity provided by longevity-related pathways (Fig. 2).

Future studies aim to complete this model.

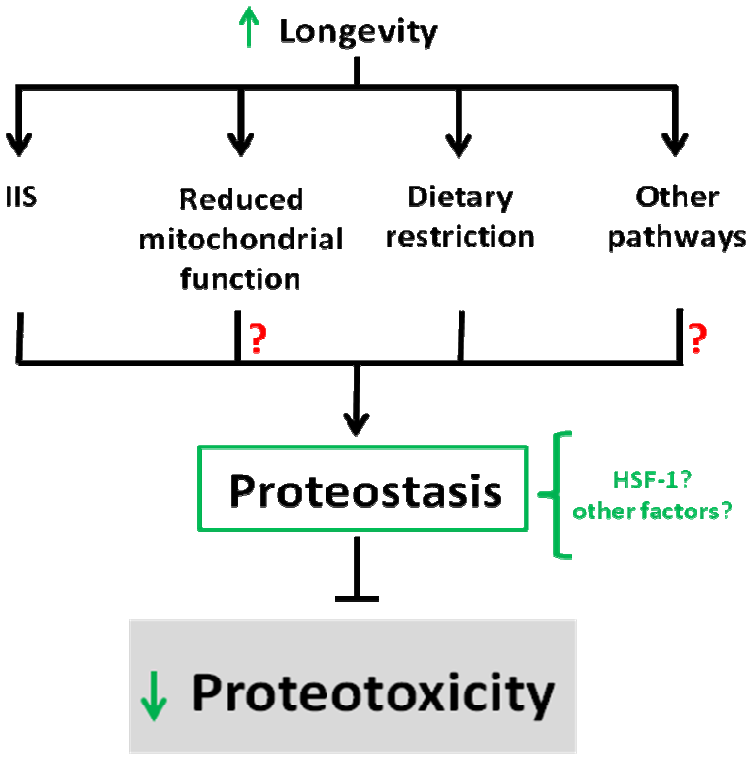

Figure 2. A working model for the role of component(s) of the proteostasis network in mediating the protective role of longevity-related pathways in proteotoxicity. Three independent mechanisms have been found to be aging and lifespan regulators; the Insulin/IGF signaling (IIS) pathway; dietary restriction (DR) and altered mitochondrial function. Other pathways were less explored. Based on the work gathered by many laboratories, we suggest that HSF-1 and/or other components of the proteostasis network are required for aging/longevity-related pathways-mediated improved proteotoxicity.

From *C. elegans* to the human disease: limitations and advantages

Although *C. elegans* has undoubtedly provided many insights into the underlying mechanisms of human diseases, many researchers still question whether *C. elegans* can really be used as a disease model and, if so, how relevant such a model can be. Does *C. elegans* demonstrate behaviors that could be linked to symptoms of MJD patients? The cerebellar ataxia is the most frequent clinical manifestation in patients and can be linked to alterations in locomotion in worms. However, other symptoms like limitations in ocular movement, which is very important in clinical differentiation from other polyQ diseases, are obviously difficult to model in *C. elegans*. Given that even mammalian models do not often reliably mimic disease in humans, it is, from a pre-clinical model perspective, improbable that an invertebrate model can, for instance, predict drug targets and safety in humans. Non-mammalian model organisms will be typically used in early steps of research to give fast answers to problems such as the discovery of a gene function *in vivo*, or pioneer medical research to identify novel therapeutic entry points, as we found in our work. Of such models, *C. elegans* is for sure the fastest and most amenable to cost-effective medium-/high-throughput technologies.

Although many neuronal subtypes are conserved, it is unrealistic to identify structures of the human brain in an invertebrate nervous system. Moreover, there are no descriptions of classical barriers between neurons and the fluid in the *C. elegans* body, which does not mimic the human condition. In spite of many differences, *C. elegans* neurons do interact with glial cells and besides their direct role in controlling neuronal activity, glia contribute to neuron function by ensuring that neurons attain their proper denditric shapes (reviewed in (84).

In spite of the difficult correlation between the human brain and the *C. elegans* pan-neuronal system, which limits the efforts to understand neuron-cell type specific susceptibility in MJD, we believe that *C. elegans* can be a valuable disease model. If we consider that it is the molecular basis of a cell that defines morphological and functional diversity of cell types in the nervous system, previously described as “gene batteries” (85), and *C. elegans* can be instrumental in defining the (molecular) pathogenesis underlying a disease.

Main conclusions

1. Pan-neuronal expression of mutant ATXN3 in *C. elegans* causes neuron-cell-type specific aggregation;
2. Pathological ATXN3 aggregation correlates with neuronal dysfunction;
3. Aging worsens ATXN3 aggregation and neuronal dysfunction in *C. elegans*;
4. *DAF-16* and *HSF-1* are suppressors of mutant ATXN3 pathogenesis in *C. elegans*;
5. Genetic reduction of *HSF-1* in mouse had limited impact in MJD pathogenesis.
6. Not all longevity-associated mutations impact positively in mutant ATXN3 aggregation and toxicity in *C. elegans*;
7. Wild-type ATXN3 does not play a neuroprotective role in MJD pathogenesis in *C. elegans*;
8. The novel *C. elegans* model we established is a useful tool for identification of potential therapeutic compounds for MJD;
9. Activators of autophagy, activators of transcription, and inhibitors of IIS pathway/activators of the heat shock response are good candidates for testing in MJD model in higher organisms, such as mice.

Future Perspectives

One of the advantages of establishing new model systems is related to the many exciting directions for future research. The disadvantage of developing and characterizing a new model is that not nearly enough time remains afterward to do all the exciting experiments envisioned at the outset of the project. Fortunately, our *C. elegans* model for ATXN3-mediated pathogenesis has attracted the interest of other researchers in the field. Parts of the work suggested in this prospectus will be and are currently being pursued in collaboration with other members of the Maciel lab.

This work opened several questions that we aim to answer in the near future.

Regarding the further understanding of the neuron cell-type-specific susceptibility to mutant ATXN3 in *C. elegans*, we intend to make use of neuronal fluorescent markers to label specific types of neurons, namely GABBAergic and dopaminergc neurons or neurons that express glutamate. This should allow us to map neuronal susceotibility to further detail. In order to continue studies began in Chapter 2, we also want to determine, in future studies, if HSF-1 and DAF-16 suppressor effects in mutant ATXN3 pathogenesis are cell-autonomous (i.e. neuron-regulated). For that purpose, we will overexpress HSF-1 and DAF-16 in neuronal cells only (motor neurons) and determine if there is rescue of the motility phenotype of *hsf-1*; AT3q130 and *daf-16*; AT3q130 animals, respectively.

In Chapter 2.1, we intend to further improve our image-processing application in order to be able to start the quantification of volume of the aggregates, which we believe will be a more reliable measure of the aggregation state of the animals.

The major challenge that remains from this work, which we will pursue in the future, is to understand what are the underlying mechanisms of the opposing effects of distinct longevity/aging-related pathways in protection against disease-associated proteotoxicity. For that, we intend to: (i) measure expression levels of key components of the proteostasis network; (ii) determine if similar effects occur in models for other neurodegenerative diseases in *C. elegans*; and (iii) perform epistasis studies that will allow us to understand the role of the several components of the same pathway in modulating proteotoxicity, i.e. to further dissect the protective pathways; and (iv) evaluate resistance of transgenic animals to a variety of stresses.

Regarding the limited effects in MJD pathogenesis caused by genetic reduction of HSF-1 in mice, we will investigate potential compensatory roles of other heat shock factor(s) in cells, namely HSF-2. We will measure the levels and activation state of HSF-2 and of downstream Hsp targets, in the *Hsf-1* knockdown.

Finally, regarding the identification of potential therapeutic compounds for testing in animal models of MJD, we are currently performing pharmacogenetic studies to determine drug target(s) and to anticipate potential side effects that may happen. Moreover, we are currently running a screen of 1120 FDA-approved compounds for rescuing mutant ATXN3-mediated pathogenesis (Appendix 3). So far, we have found three promising drugs for testing in a mouse model of MJD, previously generated in our laboratory (19).

References:

1 Gatchel, J.R. and Zoghbi, H.Y. (2005) Diseases of unstable repeat expansion: mechanisms and common principles. *Nat Rev Genet*, **6**, 743-755.

2 Paulson, H.L., Das, S.S., Crino, P.B., Perez, M.K., Patel, S.C., Gotsdiner, D., Fischbeck, K.H. and Pittman, R.N. (1997) Machado-Joseph disease gene product is a cytoplasmic protein widely expressed in brain. *Ann Neurol*, **41**, 453-462.

3 Perez, M.K., Paulson, H.L., Pendse, S.J., Saionz, S.J., Bonini, N.M. and Pittman, R.N. (1998) Recruitment and the role of nuclear localization in polyglutamine-mediated aggregation. *J Cell Biol*, **143**, 1457-1470.

4 Ikeda, H., Yamaguchi, M., Sugai, S., Aze, Y., Narumiya, S. and Kakizuka, A. (1996) Expanded polyglutamine in the Machado-Joseph disease protein induces cell death in vitro and in vivo. *Nat Genet*, **13**, 196-202.

5 Evert, B.O., Wullner, U., Schulz, J.B., Weller, M., Groscurth, P., Trottier, Y., Brice, A. and Klockgether, T. (1999) High level expression of expanded full-length ataxin-3 in vitro causes cell death and formation of intranuclear inclusions in neuronal cells. *Hum Mol Genet*, **8**, 1169-1176.

6 McCampbell, A., Taylor, J.P., Taye, A.A., Robitschek, J., Li, M., Walcott, J., Merry, D., Chai, Y., Paulson, H., Sobue, G. *et al.* (2000) CREB-binding protein sequestration by expanded polyglutamine. *Hum Mol Genet*, **9**, 2197-2202.

7 Chai, Y., Koppenhafer, S.L., Bonini, N.M. and Paulson, H.L. (1999) Analysis of the role of heat shock protein (Hsp) molecular chaperones in polyglutamine disease. *J Neurosci*, **19**, 10338-10347.

8 Haacke, A., Broadley, S.A., Boteva, R., Tzvetkov, N., Hartl, F.U. and Breuer, P. (2006) Proteolytic cleavage of polyglutamine-expanded ataxin-3 is critical for aggregation and sequestration of non-expanded ataxin-3. *Hum Mol Genet*, **15**, 555-568.

9 Evert, B.O., Vogt, I.R., Vieira-Saecker, A.M., Ozimek, L., de Vos, R.A., Brunt, E.R., Klockgether, T. and Wullner, U. (2003) Gene expression profiling in ataxin-3 expressing cell lines reveals distinct effects of normal and mutant ataxin-3. *J Neuropathol Exp Neurol*, **62**, 1006-1018.

10 Warrick, J.M., Chan, H.Y., Gray-Board, G.L., Chai, Y., Paulson, H.L. and Bonini, N.M. (1999) Suppression of polyglutamine-mediated neurodegeneration in Drosophila by the molecular chaperone HSP70. *Nat Genet*, **23**, 425-428.

11 Warrick, J.M., Morabito, L.M., Bilen, J., Gordesky-Gold, B., Faust, L.Z., Paulson, H.L. and Bonini, N.M. (2005) Ataxin-3 suppresses polyglutamine neurodegeneration in Drosophila by a ubiquitin-associated mechanism. *Mol Cell*, **18**, 37-48.

12 Warrick, J.M., Paulson, H.L., Gray-Board, G.L., Bui, Q.T., Fischbeck, K.H., Pittman, R.N. and Bonini, N.M. (1998) Expanded polyglutamine protein forms nuclear inclusions and causes neural degeneration in Drosophila. *Cell*, **93**, 939-949.

13 Cemal, C.K., Carroll, C.J., Lawrence, L., Lowrie, M.B., Ruddle, P., Al-Mahdawi, S., King, R.H., Pook, M.A., Huxley, C. and Chamberlain, S. (2002) YAC transgenic mice carrying pathological alleles of the MJD1 locus exhibit a mild and slowly progressive cerebellar deficit. *Hum Mol Genet*, **11**, 1075-1094.

14 Goti, D., Katzen, S.M., Mez, J., Kurtis, N., Kiluk, J., Ben-Haiem, L., Jenkins, N.A., Copeland, N.G., Kakizuka, A., Sharp, A.H. *et al.* (2004) A mutant ataxin-3 putative-cleavage fragment in brains of Machado-Joseph disease patients and transgenic mice is cytotoxic above a critical concentration. *J Neurosci*, **24**, 10266-10279.

15 Bichelmeier, U., Schmidt, T., Hubener, J., Boy, J., Ruttiger, L., Habig, K., Poths, S., Bonin, M., Knipper, M., Schmidt, W.J. *et al.* (2007) Nuclear localization of ataxin-3 is required for the manifestation of symptoms in SCA3: in vivo evidence. *J Neurosci*, **27**, 7418-7428.

16 Chou, A.H., Yeh, T.H., Ouyang, P., Chen, Y.L., Chen, S.Y. and Wang, H.L. (2008) Polyglutamine-expanded ataxin-3 causes cerebellar dysfunction of SCA3 transgenic mice by inducing transcriptional dysregulation. *Neurobiol Dis*, **31**, 89-101.

17 Boy, J., Schmidt, T., Schumann, U., Grasshoff, U., Unser, S., Holzmann, C., Schmitt, I., Karl, T., Laccone, F., Wolburg, H. *et al.* A transgenic mouse model of spinocerebellar ataxia type 3 resembling late disease onset and gender-specific instability of CAG repeats. *Neurobiol Dis*, **37**, 284-293.
18 Boy, J., Schmidt, T., Wolburg, H., Mack, A., Nuber, S., Bottcher, M., Schmitt, I., Holzmann, C., Zimmermann, F., Servadio, A. *et al.* (2009) Reversibility of symptoms in a conditional mouse model of spinocerebellar ataxia type 3. *Hum Mol Genet*, **18**, 4282-4295.
19 Silva-Fernandes, A., Costa Mdo, C., Duarte-Silva, S., Oliveira, P., Botelho, C.M., Martins, L., Mariz, J.A., Ferreira, T., Ribeiro, F., Correia-Neves, M. *et al.* Motor uncoordination and neuropathology in a transgenic mouse model of Machado-Joseph disease lacking intranuclear inclusions and ataxin-3 cleavage products. *Neurobiol Dis*, **40**, 163-176.
20 Alves, S., Nascimento-Ferreira, I., Auregan, G., Hassig, R., Dufour, N., Brouillet, E., Pedroso de Lima, M.C., Hantraye, P., Pereira de Almeida, L. and Deglon, N. (2008) Allele-specific RNA silencing of mutant ataxin-3 mediates neuroprotection in a rat model of Machado-Joseph disease. *PLoS One*, **3**, e3341.
21 Alves, S., Nascimento-Ferreira, I., Dufour, N., Hassig, R., Auregan, G., Nobrega, C., Brouillet, E., Hantraye, P., Pedroso de Lima, M.C., Deglon, N. *et al.* Silencing ataxin-3 mitigates degeneration in a rat model of Machado-Joseph disease: no role for wild-type ataxin-3? *Hum Mol Genet*, **19**, 2380-2394.
22 Alves, S., Regulier, E., Nascimento-Ferreira, I., Hassig, R., Dufour, N., Koeppen, A., Carvalho, A.L., Simoes, S., de Lima, M.C., Brouillet, E. *et al.* (2008) Striatal and nigral pathology in a lentiviral rat model of Machado-Joseph disease. *Hum Mol Genet*, **17**, 2071-2083.
23 Kaletta, T. and Hengartner, M.O. (2006) Finding function in novel targets: C. elegans as a model organism. *Nat Rev Drug Discov*, **5**, 387-398.
24 Khan, L.A., Bauer, P.O., Miyazaki, H., Lindenberg, K.S., Landwehrmeyer, B.G. and Nukina, N. (2006) Expanded polyglutamines impair synaptic transmission and ubiquitin-proteasome system in Caenorhabditis elegans. *J Neurochem*, **98**, 576-587.
25 Khan, L.A., Yamanaka, T. and Nukina, N. (2008) Genetic impairment of autophagy intensifies expanded polyglutamine toxicity in Caenorhabditis elegans. *Biochem Biophys Res Commun*, **368**, 729-735.
26 Garcia, S.M., Casanueva, M.O., Silva, M.C., Amaral, M.D. and Morimoto, R.I. (2007) Neuronal signaling modulates protein homeostasis in Caenorhabditis elegans post-synaptic muscle cells. *Genes Dev*, **21**, 3006-3016.
27 Ross, C.A. (1995) When more is less: pathogenesis of glutamine repeat neurodegenerative diseases. *Neuron*, **15**, 493-496.
28 Ferro, A., Carvalho, A.L., Teixeira-Castro, A., Almeida, C., Tome, R.J., Cortes, L., Rodrigues, A.J., Logarinho, E., Sequeiros, J., Macedo-Ribeiro, S. *et al.* (2007) NEDD8: a new ataxin-3 interactor. *Biochim Biophys Acta*, **1773**, 1619-1627.
29 Doss-Pepe, E.W., Stenroos, E.S., Johnson, W.G. and Madura, K. (2003) Ataxin-3 interactions with rad23 and valosin-containing protein and its associations with ubiquitin chains and the proteasome are consistent with a role in ubiquitin-mediated proteolysis. *Mol Cell Biol*, **23**, 6469-6483.
30 Todi, S.V., Laco, M.N., Winborn, B.J., Travis, S.M., Wen, H.M. and Paulson, H.L. (2007) Cellular turnover of the polyglutamine disease protein ataxin-3 is regulated by its catalytic activity. *J Biol Chem*, **282**, 29348-29358.
31 Boeddrich, A., Gaumer, S., Haacke, A., Tzvetkov, N., Albrecht, M., Evert, B.O., Muller, E.C., Lurz, R., Breuer, P., Schugardt, N. *et al.* (2006) An arginine/lysine-rich motif is crucial for VCP/p97-mediated modulation of ataxin-3 fibrillogenesis. *EMBO J*, **25**, 1547-1558.
32 Zhong, X. and Pittman, R.N. (2006) Ataxin-3 binds VCP/p97 and regulates retrotranslocation of ERAD substrates. *Hum Mol Genet*, **15**, 2409-2420.

33 Subramaniam, S., Sixt, K.M., Barrow, R. and Snyder, S.H. (2009) Rhes, a striatal specific protein, mediates mutant-huntingtin cytotoxicity. *Science*, **324**, 1327-1330.
34 Brignull, H.R., Moore, F.E., Tang, S.J. and Morimoto, R.I. (2006) Polyglutamine proteins at the pathogenic threshold display neuron-specific aggregation in a pan-neuronal Caenorhabditis elegans model. *J Neurosci*, **26**, 7597-7606.
35 Roy, P.J., Stuart, J.M., Lund, J. and Kim, S.K. (2002) Chromosomal clustering of muscle-expressed genes in Caenorhabditis elegans. *Nature*, **418**, 975-979.
36 Kunitomo, H., Uesugi, H., Kohara, Y. and Iino, Y. (2005) Identification of ciliated sensory neuron-expressed genes in Caenorhabditis elegans using targeted pull-down of poly(A) tails. *Genome Biol*, **6**, R17.
37 Shimohata, T., Nakajima, T., Yamada, M., Uchida, C., Onodera, O., Naruse, S., Kimura, T., Koide, R., Nozaki, K., Sano, Y. *et al.* (2000) Expanded polyglutamine stretches interact with TAFII130, interfering with CREB-dependent transcription. *Nat Genet*, **26**, 29-36.
38 Shimohata, T., Onodera, O. and Tsuji, S. (2001) Expanded polyglutamine stretches lead to aberrant transcriptional regulation in polyglutamine diseases. *Hum Cell*, **14**, 17-25.
39 Lim, J., Crespo-Barreto, J., Jafar-Nejad, P., Bowman, A.B., Richman, R., Hill, D.E., Orr, H.T. and Zoghbi, H.Y. (2008) Opposing effects of polyglutamine expansion on native protein complexes contribute to SCA1. *Nature*, **452**, 713-718.
40 Boutell, J.M., Thomas, P., Neal, J.W., Weston, V.J., Duce, J., Harper, P.S. and Jones, A.L. (1999) Aberrant interactions of transcriptional repressor proteins with the Huntington's disease gene product, huntingtin. *Hum Mol Genet*, **8**, 1647-1655.
41 Bao, J., Sharp, A.H., Wagster, M.V., Becher, M., Schilling, G., Ross, C.A., Dawson, V.L. and Dawson, T.M. (1996) Expansion of polyglutamine repeat in huntingtin leads to abnormal protein interactions involving calmodulin. *Proc Natl Acad Sci U S A*, **93**, 5037-5042.
42 Harjes, P. and Wanker, E.E. (2003) The hunt for huntingtin function: interaction partners tell many different stories. *Trends Biochem Sci*, **28**, 425-433.
43 Ross, C.A., Wood, J.D., Schilling, G., Peters, M.F., Nucifora, F.C., Jr., Cooper, J.K., Sharp, A.H., Margolis, R.L. and Borchelt, D.R. (1999) Polyglutamine pathogenesis. *Philos Trans R Soc Lond B Biol Sci*, **354**, 1005-1011.
44 Ross, C.A., Margolis, R.L., Becher, M.W., Wood, J.D., Engelender, S., Cooper, J.K. and Sharp, A.H. (1998) Pathogenesis of neurodegenerative diseases associated with expanded glutamine repeats: new answers, new questions. *Prog Brain Res*, **117**, 397-419.
45 Michalik, A. and Van Broeckhoven, C. (2003) Pathogenesis of polyglutamine disorders: aggregation revisited. *Hum Mol Genet*, **12 Spec No 2**, R173-186.
46 Zoghbi, H.Y. and Orr, H.T. (1999) Polyglutamine diseases: protein cleavage and aggregation. *Curr Opin Neurobiol*, **9**, 566-570.
47 Ross, C.A. (1997) Intranuclear neuronal inclusions: a common pathogenic mechanism for glutamine-repeat neurodegenerative diseases? *Neuron*, **19**, 1147-1150.
48 La Spada, A.R. and Taylor, J.P. (2003) Polyglutamines placed into context. *Neuron*, **38**, 681-684.
49 Rodrigues, A.J., Coppola, G., Santos, C., Costa Mdo, C., Ailion, M., Sequeiros, J., Geschwind, D.H. and Maciel, P. (2007) Functional genomics and biochemical characterization of the C. elegans orthologue of the Machado-Joseph disease protein ataxin-3. *FASEB J*, **21**, 1126-1136.
50 Schmitt, I., Linden, M., Khazneh, H., Evert, B.O., Breuer, P., Klockgether, T. and Wuellner, U. (2007) Inactivation of the mouse Atxn3 (ataxin-3) gene increases protein ubiquitination. *Biochem Biophys Res Commun*, **362**, 734-739.
51 Rodrigues, A.J., Neves-Carvalho, A., Ferro, A., Rokka, A., Corthals, G., Logarinho, E. and Maciel, P. (2009) ATX-3, CDC-48 and UBXN-5: a new trimolecular complex in Caenorhabditis elegans. *Biochem Biophys Res Commun*, **386**, 575-581.

52 Rodrigues, A.J., Neves-Carvalho, A., Teixeira-Castro, A., Rokka, A., Corthals, G., Logarinho, E. and Maciel, P. Absence of Ataxin-3 Leads to Enhanced Stress Response in C. elegans. *PLoS One*, **6**, e18512.
53 Kuhlbrodt, K., Janiesch, P.C., Kevei, E., Segref, A., Barikbin, R. and Hoppe, T. The Machado-Joseph disease deubiquitylase ATX-3 couples longevity and proteostasis. *Nat Cell Biol*, **13**, 273-281.
54 Hubener, J. and Riess, O. Polyglutamine-induced neurodegeneration in SCA3 is not mitigated by non-expanded ataxin-3: Conclusions from double-transgenic mouse models. *Neurobiol Dis*.
55 Schrattenholz, A., Groebe, K. and Soskic, V. Systems biology approaches and tools for analysis of interactomes and multi-target drugs. *Methods Mol Biol*, **662**, 29-58.
56 Morphy, R., Kay, C. and Rankovic, Z. (2004) From magic bullets to designed multiple ligands. *Drug Discov Today*, **9**, 641-651.
57 Morphy, R. and Rankovic, Z. (2005) Designed multiple ligands. An emerging drug discovery paradigm. *J Med Chem*, **48**, 6523-6543.
58 Ankerst, J. (2005) Combination inhalers containing inhaled corticosteroids and long-acting beta2-agonists: improved clinical efficacy and dosing options in patients with asthma. *J Asthma*, **42**, 715-724.
59 Zimmermann, G.R., Lehar, J. and Keith, C.T. (2007) Multi-target therapeutics: when the whole is greater than the sum of the parts. *Drug Discov Today*, **12**, 34-42.
60 Bolognesi, M.L., Matera, R., Minarini, A., Rosini, M. and Melchiorre, C. (2009) Alzheimer's disease: new approaches to drug discovery. *Curr Opin Chem Biol*, **13**, 303-308.
61 Cavalli, A., Bolognesi, M.L., Minarini, A., Rosini, M., Tumiatti, V., Recanatini, M. and Melchiorre, C. (2008) Multi-target-directed ligands to combat neurodegenerative diseases. *J Med Chem*, **51**, 347-372.
62 Geldenhuys, W.J., Youdim, M.B., Carroll, R.T. and Van der Schyf, C.J. The emergence of designed multiple ligands for neurodegenerative disorders. *Prog Neurobiol*.
63 Peng, Y., Sun, J., Hon, S., Nylander, A.N., Xia, W., Feng, Y., Wang, X. and Lemere, C.A. L-3-n-butylphthalide improves cognitive impairment and reduces amyloid-beta in a transgenic model of Alzheimer's disease. *J Neurosci*, **30**, 8180-8189.
64 Peng, Y., Hu, Y., Xu, S., Feng, N., Wang, L. and Wang, X. L-3-n-Butylphthalide regulates amyloid precursor protein processing by PKC and MAPK pathways in SK-N-SH cells over-expressing wild type human APP695. *Neurosci Lett*, **487**, 211-216.
65 Biamonte, M.A., Van de Water, R., Arndt, J.W., Scannevin, R.H., Perret, D. and Lee, W.C. Heat shock protein 90: inhibitors in clinical trials. *J Med Chem*, **53**, 3-17.
66 Sittler, A., Lurz, R., Lueder, G., Priller, J., Lehrach, H., Hayer-Hartl, M.K., Hartl, F.U. and Wanker, E.E. (2001) Geldanamycin activates a heat shock response and inhibits huntingtin aggregation in a cell culture model of Huntington's disease. *Hum Mol Genet*, **10**, 1307-1315.
67 McLean, P.J., Klucken, J., Shin, Y. and Hyman, B.T. (2004) Geldanamycin induces Hsp70 and prevents alpha-synuclein aggregation and toxicity in vitro. *Biochem Biophys Res Commun*, **321**, 665-669.
68 Waza, M., Adachi, H., Katsuno, M., Minamiyama, M., Sang, C., Tanaka, F., Inukai, A., Doyu, M. and Sobue, G. (2005) 17-AAG, an Hsp90 inhibitor, ameliorates polyglutamine-mediated motor neuron degeneration. *Nat Med*, **11**, 1088-1095.
69 Neef, D.W., Turski, M.L. and Thiele, D.J. Modulation of heat shock transcription factor 1 as a therapeutic target for small molecule intervention in neurodegenerative disease. *PLoS Biol*, **8**, e1000291.
70 Riedel, M., Goldbaum, O., Schwarz, L., Schmitt, S. and Richter-Landsberg, C. 17-AAG induces cytoplasmic alpha-synuclein aggregate clearance by induction of autophagy. *PLoS One*, **5**, e8753.
71 Rusmini, P., Simonini, F., Crippa, V., Bolzoni, E., Onesto, E., Cagnin, M., Sau, D., Ferri, N. and Poletti, A. 17-AAG increases autophagic removal of mutant androgen receptor in spinal and bulbar muscular atrophy. *Neurobiol Dis*, **41**, 83-95.

72 Hrzenjak, A., Kremser, M.L., Strohmeier, B., Moinfar, F., Zatloukal, K. and Denk, H. (2008) SAHA induces caspase-independent, autophagic cell death of endometrial stromal sarcoma cells by influencing the mTOR pathway. *J Pathol*, **216**, 495-504.
73 Isoherranen, N., Yagen, B. and Bialer, M. (2003) New CNS-active drugs which are second-generation valproic acid: can they lead to the development of a magic bullet? *Curr Opin Neurol*, **16**, 203-211.
74 Evason, K., Collins, J.J., Huang, C., Hughes, S. and Kornfeld, K. (2008) Valproic acid extends Caenorhabditis elegans lifespan. *Aging Cell*, **7**, 305-317.
75 Morley, J.F., Brignull, H.R., Weyers, J.J. and Morimoto, R.I. (2002) The threshold for polyglutamine-expansion protein aggregation and cellular toxicity is dynamic and influenced by aging in Caenorhabditis elegans. *Proc Natl Acad Sci U S A*, **99**, 10417-10422.
76 Hsu, A.L., Murphy, C.T. and Kenyon, C. (2003) Regulation of aging and age-related disease by DAF-16 and heat-shock factor. *Science*, **300**, 1142-1145.
77 Link, C.D. (1995) Expression of human beta-amyloid peptide in transgenic Caenorhabditis elegans. *Proc Natl Acad Sci U S A*, **92**, 9368-9372.
78 Cohen, E., Bieschke, J., Perciavalle, R.M., Kelly, J.W. and Dillin, A. (2006) Opposing activities protect against age-onset proteotoxicity. *Science*, **313**, 1604-1610.
79 Teixeira-Castro, A., Ailion, M., Jalles, A., Brignull, H.R., Vilaca, J.L., Dias, N., Rodrigues, P., Oliveira, J.F., Neves-Carvalho, A., Morimoto, R.I. *et al.* Neuron-specific proteotoxicity of mutant ataxin-3 in C. elegans: rescue by the DAF-16 and HSF-1 pathways. *Hum Mol Genet*.
80 Cohen, E., Du, D., Joyce, D., Kapernick, E.A., Volovik, Y., Kelly, J.W. and Dillin, A. Temporal requirements of insulin/IGF-1 signaling for proteotoxicity protection. *Aging Cell*, **9**, 126-134.
81 Dillin, A., Crawford, D.K. and Kenyon, C. (2002) Timing requirements for insulin/IGF-1 signaling in C. elegans. *Science*, **298**, 830-834.
82 Bishop, N.A. and Guarente, L. (2007) Two neurons mediate diet-restriction-induced longevity in C. elegans. *Nature*, **447**, 545-549.
83 Steinkraus, K.A., Smith, E.D., Davis, C., Carr, D., Pendergrass, W.R., Sutphin, G.L., Kennedy, B.K. and Kaeberlein, M. (2008) Dietary restriction suppresses proteotoxicity and enhances longevity by an hsf-1-dependent mechanism in Caenorhabditis elegans. *Aging Cell*, **7**, 394-404.
84 Procko, C. and Shaham, S. Assisted morphogenesis: glial control of dendrite shapes. *Curr Opin Cell Biol*, **22**, 560-565.
85 Hobert, O., Carrera, I. and Stefanakis, N. The molecular and gene regulatory signature of a neuron. *Trends Neurosci*, **33**, 435-445.

Appendices

Appendix 1

Capítulo 32

Doenças de expansão de poliglutaminas – o paradigma das doenças de Huntington e de Machado-Joseph

Ana Cristina Rego[1], Andreia Teixeira-Castro[2] e Patrícia Maciel[2]

[1]Faculdade de Medicina e Centro de Neurociências e Biologia Celular, Universidade de Coimbra, 3004-504 Coimbra; [2]Escola de Ciências da Saúde, Instituto de Investigação em Ciências da Vida e da Saúde, Campus de Gualtar, Universidade do Minho, 4710-057 Braga.

Palavras chave: agregação proteica; ataxina-3; doença de Huntington; doença de Machado-Joseph; huntingtina; poliglutaminas

Sumário

As doenças de expansão de poliglutaminas são patologias neurodegenerativas hereditárias causadas pela expansão do trinucleótido citosina-adenina-guanina (CAG) na região codificante de diferentes genes, que codificam proteínas específicas. São conhecidas nove doenças de poliglutaminas que afectam diferentes áreas cerebrais. Neste capítulo resumem-se as principais características da doença de Huntington (DH) e da doença de Machado-Joseph (DMJ), as duas doenças poliglutamínicas mais comuns. Estas doenças incuráveis afectam, respectivamente, as proteínas huntingtina (Htt) e ataxina-3 (ATXN3), conduzindo ambas à formação de agregados proteicos intracelulares. Diferentes mecanismos celulares parecem contribuir para a patogénese destas doenças, o que tem permitido a identificação de alvos terapêuticos e o desenvolvimento de terapias neuroprotectoras.

1. Introdução

A expansão de sequências repetitivas do trinucleótido citosina-adenina-guanina (CAG)[1] na região codificante de genes, que codificam proteínas específicas, é uma característica comum das doenças de expansão de poliglutaminas. Foram até hoje identificadas nove doenças de poliglutaminas que incluem a doença de Huntington (DH), a DRPLA (do inglês *dentatorubral-pallidoluysian atrophy*), a doença de Kennedy ou SBMA (do inglês *spinal bulbar muscular atrophy*), e as ataxias espinocerebelosas (SCA, do inglês *spinocerebellar ataxia*) 1, 2, 3, 6, 7 e 17. A SCA3 é também designada doença de Machado-Joseph (DMJ) (Macedo-Ribeiro et al., 2007, para revisão). A primeira expansão de CAGs a ser identificada foi a mutação associada à SBMA, que afecta o receptor do androgénio; esta é uma doença recessiva ligada ao cromossoma X, e por esta razão afecta predominantemente indivíduos do sexo masculino. Com excepção da SBMA, todas as outras patologias de poliglutaminas são autossómicas dominantes.

A mutação génica que ocorre nestas nove patologias afecta proteínas distintas, em termos de estrutura, sequência de aminoácidos e função biológica (de referir que a função da maior parte das proteínas é ainda desconhecida); por outro lado, para cada proteína, a expansão de poliglutaminas (poliQ) ocorre em diferentes locais da mesma, i.e., perto do terminal amínico, do terminal carboxílico ou a meio da sequência de aminoácidos. Em todas as doenças existe um limiar de repetições CAG a partir do qual os indivíduos apresentam sintomatologia, tal como exemplificado na **Tabela I**. Em geral, e considerando a amplitude das repetições CAG, existe uma correlação inversa entre o número de repetições CAG e a idade de início das patologias. Contudo, para determinadas repetições, a idade de início varia bastante, sugerindo que outros factores poderão contribuir para o aparecimento e progressão destas patologias. Um número de repetições CAG mais elevado está geralmente associado a formas raras, de aparecimento precoce (formas juvenis ou mesmo infantis), caracterizadas por uma maior

(1) O codão CAG codifica para o aminoácido glutamina (Q).

gravidade e/ou o aparecimento de sintomas adicionais. Estes incluem, por exemplo, o aparecimento de retinite pigmentosa, tal como observado num caso infantil de SCA2 com mais de 200 repetições CAG, ou o aparecimento de epilepsia mioclónica progressiva num caso juvenil de DH (Bates e Benn, 2002, para revisão).

Apesar da expressão ubíqua das proteínas afectadas, cada doença lesa de modo mais ou menos selectivo uma determinada região do sistema nervoso central (SNC) (**Tabela I**), e os padrões de lesão das regiões afectadas variam nas diferentes patologias. As nove doenças apresentam uma grande variedade de sintomas clínicos. Porém, a perda neuronal progressiva e um declínio das funções motoras e cognitivas são características comuns. Para além disso, nas formas mais frequentes, a sintomatologia surge na idade adulta, conduzindo à morte dos pacientes 10 a 30 anos após o aparecimento dos primeiros sintomas (Sequeiros e Coutinho, 1993).

Uma outra característica interessante destas doenças é o processo de "antecipação". Todas as expansões patogénicas ou que se situam no limite dos valores normais podem apresentar instabilidade na transmissão de uma geração para a seguinte. Esta instabilidade é mais pronunciada na transmissão paterna, traduzindo-se por um aumento das expansões de poliQ e pelo aparecimento mais precoce da sintomatologia em gerações sucessivas. Esta alteração do número de repetições parece ser devido a uma maior instabilidade genética da sequência nos espermatozóides; contudo, também pode ocorrer instabilidade nos gâmetas femininos. A mutação associada à SCA7 exibe o maior grau de instabilidade (aumento até 18,5 repetições CAG, através da linha masculina) e desta forma o maior grau de antecipação. Por outro lado, também podem ocorrer reduções no número de repetições CAG, de uma geração para outra, mais frequentes na transmissão materna (Bates e Benn, 2002). A instabilidade das repetições CAG traduz-se ainda na forma de mosaicismo somático, particularmente entre diferentes

regiões cerebrais e/ou entre diferentes tipos de células do SNC (*e.g.* entre neurónios e células da glia) (Bates e Benn, 2002).

A formação de agregados proteicos e inclusões ubiquitinados, presentes particularmente nos neurónios, e mais frequentes a nível nuclear (**Tabela I**), são outra característica das doenças de poliQ. A patogénese associada à expansão de poliQ tem sido associada a um ganho de função da proteína mutante e/ou a uma perda de função da proteína normal (*wild-type*). Um exemplo típico do ganho de função é a mutação do receptor do androgénio, que ocorre na SBMA. Nesta patologia, a mutação causa a degenerescência de neurónios motores, enquanto a perda de função daquele receptor causa efeitos feminizantes (Rego e de Almeida, 2005, para revisão).

Apesar dos múltiplos estudos de investigação, não existe actualmente cura para estas doenças devastadoras. Contudo, várias terapias neuroprotectoras têm sido desenvolvidas nos últimos anos. Assim, neste capítulo resumem-se as principais características clínicas e patológicas da DH e da DMJ ou SCA3, os conceitos actuais sobre a patogénese, e as novas perspectivas terapêuticas para estas doenças.

2. A Doença de Huntington e a Doença de Machado-Joseph

2.1 Prevalência clínica

A DH apresenta uma prevalência de 3 a 10 indivíduos afectados por cada 100.000 no oeste Europeu e América do Norte (Ho et al., 2001, para revisão), e uma prevalência idêntica em Portugal, entre 2 e 5 indivíduos por cada 100.000 (Costa et al., 2003). A DH foi inicialmente descrita em 1872 por George Huntington, que identificou não só as características clínicas da doença, mas também o seu padrão de transmissão familiar.

Por sua vez, a DMJ é, em muitas populações, a ataxia dominante mais comum, variando de cerca de 20% das famílias, na maioria das séries de doentes norte-americanos, até cerca de 50% em famílias no Japão, Alemanha e China (Paulson e Subramony 2003). Em Portugal, a prevalência da DMJ foi estabelecida em 3.1: 100.000, tendo sido identificadas cerca de 108 famílias com DMJ, oriundas das ilhas dos Açores e de Portugal continental (Coutinho, 1972;). Num estudo em que foram analisados 92 doentes com ataxia espinocerebelosa (não relacionados; 38% de origem portuguesa), verificou-se que 41% desses doentes tinham a mutação causadora da DMJ.

2.2. Principais manifestações clínicas

Cinicamente, existem alguns factores comuns a nível da sintomatologia descrita para as várias doenças de poliglutaminas, nomeadamente a perda de coordenação motora e de equilíbrio. Contudo, outros aspectos tornam cada uma destas doenças única.

Classicamente, a DH era descrita como Coreia de Huntington (‘*khorea*’ é a palavra grega para dança). De facto, clinicamente, a DH caracteriza-se por coreia progressiva, declínio cognitivo e perturbações psiquiátricas. Numa fase precoce podem ser observadas alterações moderadas na execução dos movimentos, movimentos involuntários *minor*, dificuldades na resolução de problemas, irritabilidade e depressão. Os movimentos involuntários tornam-se mais graves e os doentes perdem gradualmente a capacidade de se mover e, eventualmente, de comunicar. Desenvolvem-se sintomas como a coreia, disartria, disfagia e defeitos cognitivos. As características cognitivas deterioram-se ao longo do tempo, pelo que os doentes de Huntington em fase tardia apresentam demência severa. Por outro lado, um comportamento maníaco-depressivo e alterações de personalidade (irritabilidade, apatia e distúrbios sexuais) fazem parte dos sintomas psiquiátricos que caracterizam a DH (Gil e Rego, 2008).

Nas formas mais avançadas da DH surge também bradicinésia, rigidez severa e demência. A morte dos doentes ocorre geralmente devido a doença cardiovascular ou complicação infecciosa respiratória. Nos doentes com formas juvenis da DH, a sintomatologia é diferente relativamente às formas adultas da doença, sendo caracterizada por bradicinésia, tremor, rigidez e distonia, e a coreia pode mesmo estar ausente. As crianças afectadas pela DH podem também apresentar epilepsia (Gil e Rego, 2008; Bates e Benn, 2002, para revisão).

A maioria dos doentes sofre também de caquexia, com emaciação muscular e perda de peso, que surgem apesar de um consumo calórico constante. Alterações endócrinas têm sido também descritas em doentes de DH, incluindo um aumento dos níveis de corticosteróides e uma diminuição dos níveis de testosterona. Para além disso, cerca de 10-15% dos doentes de DH exibem diabetes mellitus (Gil e Rego, 2008, para revisão). A doença progride ao longo do tempo e torna-se fatal 15 a 20 anos após o aparecimento dos primeiros sintomas (Ho et al., 2001).

Foi em 1972 que apareceram as primeiras publicações clínicas sobre a DMJ, descrevendo duas das famílias "fundadoras", invariavelmente citadas em todos os trabalhos sobre a doença e que irão dar o nome à mesma. A primeira publicação é de Nakano e colaboradores, que descrevem a "*Doença de Machado, uma ataxia hereditária em emigrantes portugueses no Massachusetts*". No mesmo ano, Woods e Schaumburg publicam outra família, também açoriana e igualmente estabelecida no estado de Massachusetts. O membro mais antigo desta família conhecido como doente é José Tomás, e o seu nome americaniza-se entretanto dando origem ao nome da família: "A família Thomas". Finalmente, em 1976, Rosenberg e colaboradores descreveram uma terceira família açoriana, a família Joseph, originaria da ilha das Flores e emigrada para a Califórnia. Em 1980 Coutinho e Sequeiros sugeriram pela primeira vez que os diferentes quadros clínicos descritos para estas doenças constituíam uma

mesma entidade genética com expressão fenotípica variável- a unificação da DMJ (Sequeiros & Coutinho, 1993, para revisão).

No caso da DMJ, um factor muito importante no diagnóstico clínico no que diz respeito à exclusão de outras ataxias espinocerebelosas hereditárias cuja apresentação clínica é semelhante, é o facto da função cognitiva ser preservada nestes doentes. Os poucos casos descritos com declínio cognitivo são de natureza moderada. No que diz respeito a outros aspectos, o espectro clínico da DMJ é muito pleomórfico pelo que quatro subfenótipos foram sugeridos (Coutinho, 1992; Burk et al., 2003):

i) Tipo I: deficits extrapiramidais (maioritariamente distonia) e piramidais; início precoce da doença (entre os 5-30 anos);

ii) Tipo II: deficits piramidais e cerebelosos; início da doença em idades intermédias (20-50 anos);

iii) Tipo III: deficits cerebelosos e neuropatia periférica; início tardio (40-75 anos);

iv) Tipo IV (muito raro): neuropatia e parkinsonismo; o início da doença é variável.

Outras características que não estão restritas a nenhum subtipo específico da DMJ incluem oftalmoplegia, visão dupla, fasciculação facial e da língua, perda de peso mas com preservação do apetite (tal como na DH), incontinência, e a síndrome de pernas inquietas (do inglês "*restless legs*") (Coutinho e Andrade 1978; Sequeiros e Coutinho, 1993).

Os doentes têm uma sobrevida média de 21 anos e normalmente a morte ocorre devido a incapacidade motora e a imobilidade prolongadas que originam, entre outras, complicações pulmonares graves (Coutinho, 1992).

2.3. Neuropatologia

Neuropatologicamente, a DH caracteriza-se por atrofia gradual do estriado (núcleo caudado e *putamen*) e do córtex cerebral nos casos mais avançados da patologia; contudo, o

globo pálido, o tálamo, os núcleos subtalâmicos, a *substantia nigra*, a substância branca e o cerebelo também poderão estar afectados (**Tabela I e Figura 1**). Estudos mais recentes também apoiam a hipótese que o hipotálamo possa estar afectado em doentes de Huntington. Paralelamente, e de forma semelhante ao que acontece noutras patologias neurodegenerativas, a morte neuronal é acompanhada por gliose, i.e., pela proliferação de células da glia. Devido a uma atrofia cerebral generalizada, o peso cerebral pode diminuir até 40% nos casos mais graves da DH (*e.g.* Rego e de Almeida, 2005).

Os neurónios mais afectados no estriado são os neurónios espinhosos médios, que correspondem a cerca de 95% do número total de neurónios estriatais. Estes neurónios são regulados por neurónios dopaminérgicos que partem da *substantia nigra pars compacta* e por neurónios glutamatérgicos do córtex cerebral. Por sua vez, os neurónios estriatais projectam para os segmentos interno e externo do *globus pallidus* e *substantia nigra pars reticulata* através das vias directa e indirecta; a última atravessa o segmento externo do *globus pallidus* e o núcleo subtalâmico.

Os neurónios espinhosos médios do estriado utilizam o neurotransmissor inibitório ácido γ-aminobutírico (GABA) e dinorfina, encefalina ou substância P como co-transmissores. Os neurónios da via directa contêm substância P e expressam receptores da dopamina (DA) do tipo D1 (estimulam a enzima adenilciclase), enquanto os neurónios da via indirecta contêm encefalina e expressam receptores do tipo D2 (inibem a enzima adenilciclase) (Gil e Rego, 2008, para revisão). Uma vez que os neurónios estriatais exercem acção inibitória mediada por GABA, pensa-se que a perda desta esteja na base dos movimentos incontrolados característicos da DH. De facto, ambas as vias indirecta (GABA/encefalina) e directa (GABA/substância P) parecem ser precocemente afectadas durante o desenvolvimento da doença. Por outro lado, os interneurónios estriatais médios não-espinhosos (que marcam para somatostatina, neuropeptídeo Y ou NADPH-diaforase (ou sintetase do óxido nítrico (NOS)),

os interneurónios colinérgicos e os neurónios GABAérgicos que contêm parvalbumina são relativamente poupados nos cérebros dos doentes de Huntington (Gil e Rego, 2008).

Anatomopatologicamente, a DMJ é caracterizada por uma degenerescência dos núcleos espinocerebelosos, denteados, pônticos e vestibulares, da *substantia nigra*, do *locus coeruleus* e do complexo palidoluisiano; por uma redução neuronal nos núcleos e atrofia dos nervos cranianos motores e dos cornos anteriores da medula, nos gânglios raquidianos e cordões posteriores (**Tabela I e Figura 1**). Apesar da forte degeneração e despigmentação observada na *substantia nigra*, muitos doentes nunca apresentam características de parkinsonismo. Em geral, estruturas como o córtex cerebral, o córtex cerebeloso e as olivas bulbares são preservadas (Coutinho e Andrade, 1978). Na maioria dos doentes com DMJ, tal como na DH, o peso do cérebro é inferior ao de indivíduos sem história clínica de doenças neurológicas (Riess et al., 2008, para revisão).

2.4. Genética

A expansão instável de repetições CAG na região codificante (exão 1) do gene *DH* (anteriormente designado por gene *IT15*, do inglês '*Interesting Transcript 15*'), que codifica para a proteína huntingtina (Htt, uma proteína com aproximadamente 350 kDa), foi descoberta em 1993 pelo *The Huntington's Disease Collaborative Research Group*. O gene *DH* contém 67 exões e está localizado no braço curto do cromossoma 4 (4p16.3) (Rego e de Almeida, 2005). A mutação resulta numa expansão de resíduos de glutamina localizados no terminal amínico da Htt, 17 aminoácidos após a metionina iniciadora (**Figura 2A**). Tal como referido anteriormente, o alelo mutante é instável durante a meiose, alterando o seu comprimento na maioria das transmissões intergeracionais. Tal como referido anteriormente, as expansões maiores ocorrem nas transmissões paternas, reflectindo uma maior taxa de

mutação durante a espermatogénese (*The Huntington's Disease Collaborative Research Group*, 1993).

Normalmente, indivíduos assintomáticos possuem menos de 35 repetições CAG no gene DH (**Figura 2A**). A DH manifesta-se quando o número de repetições excede este limite. Alelos com 35 a 39 repetições CAG estão associados com as formas mais tardias da doença; porém, uma penetrância incompleta tem sido observada nalguns indivíduos que não apresentam sintomas ou sinais neuropatológicos. Alelos com 40 a 50 unidades dão origem à forma adulta, mais comum, da DH, enquanto repetições mais longas são responsáveis pelos casos juvenis e infantis (*The Huntington's Disease Collaborative Research Group*, 1993) (**Figura 2A**). O número de repetições CAG parece afectar a progressão da doença, particularmente se considerarmos repetições superiores a cerca de 60 CAGs. De facto, um número elevado de repetições CAG conduz ao aparecimento dos primeiros sintomas muito precocemente, contudo estes casos são raros.

Os estudos pioneiros demonstraram que a Htt é uma proteína essencial para o desenvolvimento embrionário normal. De forma interessante, a Htt mutante humana pode compensar a ausência de Htt endógena durante o desenvolvimento (Leavitt et al., 2001), sugerindo que a função da Htt durante o desenvolvimento embrionário é independente do comprimento da cauda de poliQ. De facto, apesar da Htt mutante ser expressa em todo o organismo ao longo de toda a vida de um indivíduo, na maioria dos casos, o aparecimento dos primeiros sintomas surge apenas na meia-idade, entre os 35 e os 50 anos.

A mutação génica responsável pela DMJ foi identificada cerca de um ano mais tarde, em 1994, por investigadores Japoneses (Kawaguchi et al., 1994). O gene *ATXN3/MJD1* foi mapeado no braço longo do cromossoma 14, mais concretamente, na região 14q32.1 (Kawaguchi et al., 1994), estando a expansão da repetição trinucleotídica $(CAG)_n$ localizada no exão 10 dos 11 exões que constituem o gene (**Figura 2B**). Um grande número de estudos

genéticos ao longo dos últimos anos estabeleceu aspectos importantes para uma melhor compreensão da DMJ: (i) um individuo normal pode ter até 47 repetições CAG. No entanto, (ii) foram identificados casos sintomáticos em que o tamanho do segmento de CAG variava entre 44 e 86 repetições. Esta sobreposição parcial entre os tamanhos normal e expandido do segmento de CAG tinha já sido mostrada para outras doenças (incluindo a DH), correspondendo na maioria das vezes a casos de penetrância reduzida. Outros estudos indicaram, como referido anteriormente para a DH, que (iii) o alelo expandido é muito instável, principalmente em casos de transmissão paterna; evidências apontam para a (iv) existência de mosaicismo somático em termos do tamanho da expansão $(CAG)_n$ e, finalmente, foi sugerido que, (v) para além do tamanho do segmento repetitivo CAG, outros factores genéticos poderão estar a determinar a idade de início da doença.

A proteína ataxina-3 (ATXN3) apresenta um peso molecular de aproximadamente 42 kDa em indivíduos normais, que se torna significativamente maior em pacientes com DMJ- confirmando que a repetição CAG é traduzida numa expansão de poliQ. Foram identificadas várias isoformas da proteína que diferem no seu terminal carboxílico. A procura de motivos/domínios na proteína sugeriu que a ATXN3 é uma proteína de ligação à ubiquitina. Ensaios funcionais subsequentes mostraram que a ATXN3 tem maior afinidade para cadeias de tetra-ubiquitina do tipo Lisina-48 (K48), e que esta ligação é mediada por motivos de interacção com a ubiquitina (UIMs, do inglês *ubiquitin interacting motifs*), situados no C-terminal da ATXN3, perto do domínio de poliQ (**Figura 2B**) (Riess et al., 2007, para revisão). O potencial envolvimento da ATXN3 em mecanismos de degradação proteica da célula via proteossoma foi reforçado pela identificação de vários parceiros moleculares, nomeadamente a Rad23 e a VCP (do inglês *valosin-containing protein*). As proteínas Rad23 por sua vez interactuam com a subunidade S5a do proteossoma, o que sugere um papel importante deste complexo na translocação de proteínas para degradação via proteossoma (Riess et al., 2007,

para revisão). Esta função é particularmente importante na degradação de proteínas do lúmen e membranares pela via de degradação proteica associada ao retículo endoplasmático (do inglês *endoplasmic reticulum associated protein degradation*, ERAD), processo este que depende grandemente da VCP. Assim, células transfectadas com ATXN3 apresentam especificamente níveis elevados de substratos dependentes de ERAD (CD3δ e TCRα), diminuindo a sua degradação. Os níveis de CD3δ são dependentes da interacção ATXN3-VCP, pelo que a mutação do domínio de interacção da ATXN3 com a VCP reduz a acumulação de CD3δ .

O mapeamento e clonagem dos genes associados a estas doenças, juntamente com o desenvolvimento de tecnologias genéticas, possibilitaram a criação de modelos celulares e animais que recriam a doença humana, mesmo quando estas doenças não ocorrem naturalmente nestes organismos. Estas tecnologias podem ser aplicadas em qualquer modelo animal, mas modelos em murganho (M*us musculus*), peixe zebra (*Danio rerio*), mosca da fruta (*Drosophila melanogaster*) e nemátodes (*Caenorhabditis elegans*) são os mais usados. Em geral, são aplicadas duas abordagens principais que visam a alteração da constituição genética dos animais: a (i) primeira envolve a inserção de um gene mutado na linha germinativa; enquanto que a (ii) segunda envolve a alteração da expressão de gene(s) endógeno(s) por mutagénese (dirigida ou aleatória) ou silenciamento do gene por RNA de interferência. Na **Tabela II e III**, encontram-se sumariados alguns modelos animais da DH e da DMJ que têm contribuído grandemente para o conhecimento destas patologias.

2.5. Agregados proteicos

Outra consequência positiva da clonagem dos genes *HTT* e *ATXN3* foi permitir a expressão de proteínas recombinantes, em sistemas heterólogos, o que possibilitou a criação

de anticorpos específicos que foram de extrema importância para o estudo da patologia destas doenças. De facto, sabe-se que a expansão da sequência de poliQ altera a estrutura das proteínas e o desenvolvimento de anticorpos que reconhecem especificamente a forma mutante da Htt, ATXN1, 2 e 3 sugeriu que a conformação das proteínas mutantes é distinta da conformação *wild-type*. Esta alteração na conformação nativa das proteínas resulta na capacidade anómala destas proteínas se associarem, formando espécies de maior peso molecular (oligómeros) que, finalmente, dão origem a agregados proteicos ou inclusões que acumulam de forma estável na célula, e que são reconhecidos quer por anticorpos contra a proteína específica quer por anticorpos contra a ubiquitina.

A DH é caracterizada pela presença de inclusões neuronais intranucleares e por agregados proteicos em neurites distróficas de neurónios estriatais e corticais. Na DMJ as inclusões nucleares foram encontradas com maior frequência nos núcleos pônticos (ventrais) e também, embora em menor número, na *substantia nigra*, globo pálido, medula dorsal e núcleos denteados (Paulson e Subramony 2003). Adicionalmente, foram encontrados múltiplos agregados em axónios, localizados em fibras afectadas na DMJ (Seidel et al., 2010).

Dois mecanismos principais têm sido sugeridos para explicar a formação dos agregados de Htt mutante e que são geralmente aceites para outras doenças de poliglutaminas: (i) O modelo 'Polar Zipper' (*e.g.* Perutz et al., 1994), que pressupõe a formação de estruturas em folha beta, em resultado da destabilização da conformação terciária da proteína, conduzindo ao estabelecimento de ligações de hidrogénio com outras proteínas; e (ii) O modelo da transglutaminase, pelo qual a enzima estabelece ligações cruzadas entre resíduos de glutamina. De acordo com este modelo, verificou-se um aumento da actividade das transglutaminases em cérebros de doentes de Huntington (*e.g.* Karpuj et al., 1999).

Contudo, nestas doenças neurodegenerativas parece haver uma dissociação entre a agregação e a neurodegenerescência. De facto, no cérebro humano, os neurónios que possuem

inclusões não são os mais vulneráveis. Alguns interneurónios que são poupados durante a progressão da DH, por exemplo, também apresentam agregados, o que sugere que os agregados proteicos não sejam tóxicos. Assim, as inclusões poderão representar apenas um efeito secundário da disfunção celular ou mesmo exercer um efeito protector durante as fases iniciais da doença. É possível que as inclusões representem um meio da célula sequestrar fragmentos e oligómeros tóxicos formados por clivagem da Htt, da ATXN3 ou de outras proteínas cuja conformação normal esteja alterada. De acordo com esta hipótese, estudos *in vitro* têm demonstrado que a presença de inclusões nucleares não se correlaciona com a morte celular induzida pela proteína mutante.

2.6. Mecanismos de neurodegenerescência

A expansão de poliQ parece conferir um ganho de função tóxica às proteínas mutantes e/ou uma perda parcial da função normal, quer da Htt quer da ATXN3. Vários mecanismos celulares e moleculares parecem contribuir para a alteração da homeostase intracelular (**Figura 3 e 4**). De entre estes destacam-se: (i) O défice de mecanismos intracelulares que promovem a aquisição e manutenção da conformação nativa das proteínas e a diminuição da sua degradação, contribuindo para a formação de agregados proteicos e para a activação da autofagia; (ii) A disfunção da transcrição; (iii) A disfunção sináptica (e.g. sinapses cortico-estriatais) e o processo de excitotoxicidade (mais relevante na DH), que conduz à alteração da homeostase intracelular do ião cálcio; (iv) A disfunção mitocondrial e a desregulação metabólica; (v) O stresse oxidativo; e (vi) A activação de caspases (que promove a apoptose) e de calpaínas, culminando na disfunção e morte neuronal. Estes mecanismos podem ocorrer paralelamente, de forma ‘silenciosa’, ao longo da vida de um indivíduo portador de uma mutação para as diferentes doenças de poliglutaminas, conduzindo inevitavelmente à

sintomatologia descrita na secção *2.2*. Os mecanismos celulares e moleculares de neurodegenerescência na DH e na DMJ são detalhados seguidamente.

2.6.1. Alteração da conformação e da degradação proteíca

A expansão de poliQ altera a conformação normal das proteínas. Esta alteração conformacional está na base da interacção das proteínas mutantes com as proteínas de choque térmico (*chaperones*), envolvidas na aquisição e manutenção de uma conformação proteica normal. Contudo, ao serem sequestradas pelos agregados proteicos que contêm Htt ou ATXN3 mutantes, as proteínas de choque térmico deixam de exercer a sua função normal protectora, resultando numa alteração da proteostase celular (Ho et al., 2001, para revisão).

O envolvimento do sistema ubiquitina-proteossoma (UPS) é uma das características das doenças de poliglutaminas, em que se verifica uma acumulação de cadeias poliubiquitina K48 em extractos proteicos de cérebros de doentes e em modelos animais para a patogénese da doença. Particularmente, na DH foi sugerido que a proteína mutada com a expansão de poliQ pode bloquear fisicamente o proteossoma (**Figura 3**), prevenindo a entrada e consequente degradação no proteossoma da Htt ou de outras proteínas alvo de degradação por esta via. Apesar de na DMJ e noutras doenças de poliglutaminas ainda não ter sido claramente estabelecida uma disrupção global do UPS, a presença de ubiquitina nos agregados proteicos parece ser o resultado de uma tentativa mal sucedida da célula em marcar a proteína mutada (ou os fragmentos proteicos) e desta forma dirigi-la para o proteossoma.

O processo autofágico representa também uma tentativa das células eliminarem a proteína mutada e removerem os agregados proteicos que se acumulam ao longo da progressão da doença (**Figura 3**). Cérebros de doentes com DH apresentam organelos endossomais/lisossomais, corpos multivesiculares, e a acumulação de lipofuscina, reminiscentes do processo autofágico, existindo uma correlação positiva entre o número de

vacúolos autofágicos e a expansão de poliQ em linfoblastos de DH (Gil e Rego, 2008). Vários estudos demonstraram também que a expressão de Htt mutante induz a actividade endossomal/lisossomal e o sequestro da proteína mTOR (do inglês *mammalian target of rapamycin*, uma proteína cinase envolvida na regulação do processo autofágico) nos agregados de Htt mutante, com a subsequente activação da autofagia (*e.g.* Ravikumar et al., 2004). Resultados semelhantes foram obtidos na presença de rapamicina, um inibidor da via dependente de mTOR (que induz autofagia), promovendo a remoção dos fragmentos de Htt mutante e atenuando a sua toxicidade. Na DMJ, genes envolvidos na autofagia foram identificados como supressores de agregação mediada por fragmentos de ATXN3 mutada em *C. elegans* e o tratamento com análogos de rapamicina reverteu o fenótipo de descoordenação motora de murganhos transgénicos para a DMJ (Menzies et al., 2010).

2.6.2. Disfunção da transcrição

A Htt mutante interage directamente com vários factores de transcrição, recrutando-os nos agregados e inibindo a sua actividade transcricional (**Figura 3**). Estes incluem a TBP (do inglês *thymine-adenine-thymine-adenine (TATA)-binding protein*), a CBP [do inglês *CREB (cyclic-adenosine monophosphate (cAMP) response element (CRE) binding protein)-binding protein]*, a Sp1 (do inglês *specific protein-1*), a $TAF_{II}130$ (do inglês *TBP associated factor*) e o factor de transcrição pró-apoptótico p53 (Gil e Rego, 2008, para revisão).

Na presença de Htt mutante, a CBP é recrutada para os agregados de Htt, levando a uma hipoacetilação das histonas e à inibição da transcrição mediada por CBP. Por outro lado, verificou-se, em modelos animais da DH e em doentes de Huntington, que a expressão da Htt mutante conduz a uma diminuição da expressão do PGC-1α (do inglês '*peroxisome proliferator-activated receptor-γ coactivator-1α*') (*e.g.* Cui et al., 2006), um co-activador

transcricional que regula vários processos metabólicos, incluindo a biogénese mitocondrial e a respiração, em modelos animais para a DH ou nos doentes de Huntington.

A Htt mutante perde também a capacidade de interagir com factores de transcrição que ligam ao elemento NRSE (do inglês *neuron restrictive silencer element*), regulados pela Htt *wild-type*, entre os quais se inclui o gene *Bdnf*, que codifica para o factor neurotrófico derivado do cérebro (BDNF, do inglês *brain-derived neurotrophic factor*) (Gil e Rego, 2008, para revisão) (**Figura 3**). Este é um dos exemplos em que a perda de função da Htt normal pode ter efeitos nocivos, conduzindo ao decréscimo dos níveis de BDNF, um importante factor de sobrevivência para os neurónios estriatais.

Um cenário semelhante foi descrito para a ATXN3. Esta interage com a CBP e outras acetiltransferases, nomeadamente a p300 e o Factor Associado a p300/CBP (pCAF) e inibe a transcrição mediada por estes co-activadores. A ATXN3 contendo uma expansão de glutaminas liga-se aos referidos factores de transcrição com maior afinidade relativamente à proteína normal, pelo que a repressão transcricional foi sugerida como um possível mecanismo de patogénese também na DMJ. Por outro lado, foi demonstrado que a ATXN3 normal se liga a locais específicos da cromatina, nomeadamente na região do promotor do gene da metaloproteinase-2 da matriz (MMP-2) e reprime a sua transcrição através do recrutamento da desacetilase das histonas 3 (HDAC3), do receptor nuclear co-repressor (NCoR), e através da desacetilação de histonas ligadas ao referido promotor. Neste caso, foi sugerido que a ATXN3 mutante activa a transcrição de forma aberrante através do seu domínio catalítico uma vez que perde a capacidade de formar um complexo repressor nestas regiões especificas da cromatina (Riess et al., 2008, para revisão).

Em suma, estes resultados sugerem que a expansão de poliQ nas proteínas poderá causar uma disfunção dos mecanismos de regulação dos processos transcricionais (**Figuras 3 e 4**), o

que está de acordo com os vários estudos de expressão de genes (análise de *microarrays*) no contexto destas doenças.

2.6.3. Disfunção sináptica e excitotoxicidade

A observação neuroimagiológica do cérebro de doentes de Huntington revelou uma degenerescência cortical sensorial e motora numa fase precoce da doença (Gil e Rego, 2008, para revisão), sugerindo que a disfunção cortico-estriatal contribui para a DH.

A disfunção sináptica nesta via pode ser uma consequência directa da desregulação do transporte axonal e/ou de uma diminuição nos níveis das proteínas sinápticas devido à sua sequestração em inclusões de Htt mutante e/ou à alteração da transcrição. Alterações do transporte axonal de BDNF foram também observadas na DH, contribuindo para uma diminuição do suporte neurotrófico no estriado (Gil e Rego, 2008, para revisão).

A Htt mutante também parece causar disfunção sináptica através da alteração da reciclagem, expressão e actividade de receptores pré- e pós-sinápticos para os neurotransmissores. De facto, os níveis do receptor metabotrópico do glutamato (mGluR)2 (um receptor pré-sináptico que regula a libertação de glutamato) encontram-se diminuídos nos murganhos R6/2 (que expressam apenas o exão-1 da proteína humana, que contém a expansão de poliQ), contribuindo para um aumento da libertação de glutamato e, consequentemente, para o processo de excitotoxicidade. Um outro factor que poderá contribuir para aumentar os níveis extracelulares de glutamato é a diminuição da capacidade de remoção do glutamato da fenda sináptica pelas células da glia. De acordo com este pressuposto, foi observado um decréscimo da expressão do principal transportador de glutamato dos astrócitos no estriado e no córtex de murganhos R6/1 e R6/2, que poderá resultar da acumulação de Htt mutante nas células da glia (Gil e Rego, 2008, para revisão).

Neste contexto, é interessante referir que o ácido quinolínico [QA (do inglês *quinolinic acid*), um agonista dos receptores *N*-metil-D-aspartato (NMDA) do glutamato e um produto endógeno resultante da degradação do triptofano] foi inicialmente utilizado na criação de um dos modelos de DH, pois induzia a morte localizada de neurónios em ratos e em primatas.

Uma vez que o estriado recebe *input* excitatório glutamatérgico de todo o córtex cerebral, uma maior vulnerabilidade dos neurónios estriatais na DH poderá também ser consequência dos subtipos de receptores glutamatérgicos presentes nos neurónios estriatais. A maioria dos neurónios estriatais GABAérgicos apresenta uma expressão elevada da subunidade NR2B do receptor NMDA e de mGluR5 (**Figura 3**). O envolvimento dos receptores mGluR5 e NR2B no processo excitotóxico associado à expressão de Htt mutante foi anteriormente descrito em neurónios do estriado derivados de murganhos YAC (do inglês *yeast artificial chromosome*), que expressam a Htt humana *full-length* ou completa (Gil e Rego, 2008, para revisão). Por outro lado, a Htt mutante aumenta a sensibilidade do receptor do inositol-(1,4,5)-trifosfato (InsP3R), do retículo endoplasmático, promovendo o aumento dos níveis de cálcio intracelular (**Figura 3**). Este aumento de sensibilidade do InsP3R1 parece não ser específico para a Htt uma vez que também a ATXN3 mutante se liga a este receptor, activando-o. A ATXN3 expandida facilita assim a libertação de cálcio intracelular mediada por InsP3R1, pelo que foi proposto que a disfunção da sinalização mediada por cálcio nas células neuronais poderá contribuir para a patogénese destas doenças (**Figura 4**).

A expansão de poliQ também interfere com a capacidade da Htt (mutada e normal) em interagir com a proteína PSD-95 (do inglês *postsynaptic density 9*5) (**Figura 3**), resultando numa maior sensibilização dos receptores NMDA e na promoção do processo excitotóxico. Em condições em que ocorre a activação crónica dos receptores NMDA, a concentração intracelular de cálcio aumenta, conduzindo à disfunção mitocondrial, à activação da isoforma neuronal da NOS (nNOS), à formação de espécies reactivas de oxigénio (ROS, do inglês

reactive oxygen species) (**Figura 3**) e de nitrogénio, à activação de proteases dependentes de cálcio como as calpaínas (**Figura 3**), e consequentemente, à morte neuronal (Rego e Oliveira, 2003, para revisão).

2.6.4. Disfunção metabólica e mitocondrial

Estudos realizados em modelos celulares e animais da DH, em doentes de Huntington e em tecido *post-mortem* destes doentes permitiram observar várias alterações mitocondriais e metabólicas: (1) Uma diminuição da captação de glucose no córtex e no estriado de indivíduos assintomáticos e sintomáticos para a DH; (2) Uma diminuição da actividade da aconitase no estriado e no córtex cerebral; (3) Um decréscimo das actividades dos complexos II-III e IV no estriado; (4) Um aumento da concentração de lactato no estriado e córtex cerebral e no líquido cefalorraquidiano de doentes de Huntington; (5) Um decréscimo do rácio fosfocreatina/fosfato inorgânico no sistema músculo-esquelético; (6) Um decréscimo da formação de ATP mitocondrial; (7) Um decréscimo do potencial membranar mitocondrial em linfoblastos derivados de doentes de Huntington heterozigóticos e homozigóticos, ou em células estriatais derivadas de murganhos *knock-in* para a DH; e (8) Uma diminuição do contéudo e a presença de mutações no DNA mitocondrial em amostras de doentes com DH (*e.g.* Gil e Rego, 2008).

A injecção sistémica do ácido 3-nitropropiónico (3-NP, um inibidor irreversível da succinato desidrogenase, que faz parte do complexo II mitocondrial) causa neurodegenerescência estriatal em ratos e primatas, corroborando a importância anteriormente descrita da disfunção mitocondrial e metabólica na DH. A neurodegenerescência estriatal induzida por 3-NP em modelos animais também parece estar relacionada com a alteração da permeabilidade da barreira hemato-encefálica, conduzindo à lesão aparentemente selectiva do estriado (*e.g.* Gil e Rego, 2008).

Na DMJ, os potenciais mecanismos de disfunção metabólica e mitocondrial têm sido menos explorados. Estudos em doentes descrevem que apesar de se verificarem níveis elevados de lactato e diminuição dos níveis de piruvato (com consequente aumento do rácio lactato/piruvato), esta alteração poderá não estar associada a alterações no metabolismo mitocondrial (Matsuishi et al., 1996). Contudo, estes estudos foram realizados num número reduzido de doentes pelo que serão necessários estudos adicionais. Outros estudos revelaram que doentes com DMJ apresentam hipometabolismo (redução no consumo de um derivado marcado de glucose) no córtex occipital, nos hemisférios cerebelosos, no *vermis* cerebeloso e no tronco cerebral (Soong et al., 1997). Estudos de espectroscopia magnética de protões, que permite a determinação de valores de metabolitos *in vivo* em tecidos humanos, revelaram uma diminuição do metabolito N-acetilaspartato na substância branca profunda de cérebros de doentes de DMJ (D'Abreu et al., 2009).

2.6.5. Stresse oxidativo

A disfunção mitocondrial contribui para a formação de radicais livres (**Figura 3**). Estes, associados à activação da nNOS mediada por estímulos excitotóxicos e ao metabolismo da DA, conduzem ao stresse oxidativo (e nitrativo) através da oxidação (e nitração) de proteínas, lípidos e/ou DNA. Estudos anteriores demonstraram a alteração da expressão e actividade da NOS, assim como da enzima antioxidante superóxido dismutase (SOD) em murganhos R6/1 e R6/2. Por outro lado, existem evidências de lesão oxidativa em tecido periférico de doentes de Huntington, nomeadamente um aumento dos níveis de 8-hidroxideoxiguanosina em leucócitos, um aumento de malonildialdeído, um decréscimo da actividade das enzimas antioxidantes Cu/Zn-SOD (SOD1) e glutatião peroxidase em eritrócitos, e um decréscimo de actividade da catalase em fibroblastos. Para além disso, a produção de ROS aumenta no estriado dos murganhos R6/1. A formação mitocondrial de ROS na DH pode estar relacionada

com a supressão de PGC-1α mediada pela Htt mutante, uma vez que este co-activador transcricional é requerido para a indução de Mn-SOD (SOD2) e de glutatião peroxidase (Gil e Rego, 2008).

Na DMJ, modelos celulares mostraram igualmente um decréscimo significativo do rácio GSH/GSSH e de glutationa total quer em condições normais de crescimento quer quando as células foram sujeitas a um stresse oxidativo ligeiro. Adicionalmente, células que expressam ATXN3 mutante apresentam níveis diminuídos de varias enzimas antioxidantes nomeadamente a catalase, glutationa reductase e SOD quando comparadas com células com expressão da ATXN3 *wild-type* (Yu et al., 2009). Células de pacientes com DMJ apresentaram ainda um decréscimo no número de cópias e aumento de uma delecção (4,977bp) do DNA mitocondrial, factores indicativos de stresse oxidativo.

Por outro lado, foi também descrito que a exposição a stresse oxidativo (peróxido de hidrogénio e 3-NP) induz a translocação da ataxin-3 do citoplasma para o núcleo (Reina et al., 2009), pelo que estudos recentes têm vindo a sugerir o núcleo como um factor chave na patologia da DMJ.

No caso específico da DH, e uma vez que o estriado recebe sinapses dopaminérgicas da *substantia nigra pars compacta*, a lesão do estriado compromete também a via nigro-estriatal (Gil e Rego, 2008, para revisão). Vários estudos demonstraram a degenerescência de projecções nigro-estriatais e uma atrofia dos neurónios dopaminérgicos na *substantia nigra*. Agregados de Htt mutante também foram encontrados nesta região cerebral. Por outro lado, a perda de receptores D2 poderá constituir um indicador sensível da disfunção neuronal precoce (pré-clínica) que ocorre nos portadores da mutação da DH. A DA pode também induzir stresse oxidativo a nível cerebral através da formação de peróxido de hidrogénio, por degradação da DA pela enzima mono-amino oxidase (mitocondrial), e da formação de quinonas ou semiquinonas de DA e peróxido de hidrogénio ou o anião superóxido, devido à

auto-oxidação da DA. Adicionalmente, as vias de sinalização do glutamato e da DA podem actuar de modo sinergístico, induzindo uma elevação dos sinais de cálcio e a degeneração dos neurónios espinhosos médios do estriado, obtidos de murganhos YAC128 (e.g. Tang et al., 2007).

2.6.6. Activação de proteases e morte neuronal

Apesar de controverso, a activação da morte celular por apoptose parece contribuir para o desenvolvimento da DH. A expansão de poliQ induz a activação da caspase-8, uma caspase iniciadora da via extrínseca da cascata apoptótica. Por outro lado, murganhos YAC que expressam Htt mutante *full-length* resistente à clivagem pela caspase-6 não desenvolvem neurodegenerescência estriatal e são resistentes à excitotoxicidade induzida pelo QA. Por outro lado, a mutação da Serina 536 (situada num domínio da proteína susceptível à proteólise) inibiu a clivagem mediada por calpaínas e diminuiu a toxicidade da Htt mutante. De facto, a Htt possui locais de clivagem pelas caspases 3 e 6 e pela calpaína (Gil e Rego, 2008) (**Figura 3**). A proteólise tende a aumentar na presença de uma longa cauda de poliQ, produzindo fragmentos N-terminais mais tóxicos que agregam mais facilmente e difundem passivamente para o núcleo devido ao seu tamanho reduzido (**Figura 3**). Estes fragmentos podem, por sua vez, recrutar mais proteases para os agregados, favorecendo a sua activação e a morte neuronal.

As mitocôndrias estão no centro do processo de activação de caspases e da apoptose. Estudos anteriores demonstraram que os fragmentos da Htt mutante podem associar-se à membrana mitocondrial externa e induzir a abertura do poro de permeabilidade transitória em mitocôndrias isoladas, um efeito acompanhado pela libertação de citocromo c (**Figura 3**). O 3-NP, utilizado como modelo de disfunção mitocondrial na DH, induz também morte

neuronal por apoptose dependente da mitocôndria através da libertação de citocromo c, e consequente activação de caspases (Rego e Oliveira, 2003).

Igualmente para a DMJ, um dos mecanismos de patogénese sugeridos é a ocorrência de clivagem da ATXN3 expandida, muito provavelmente em estadios primários da doença. E é a formação desse fragmento tóxico C-terminal da ATXN3 (contendo a expansão de poliQ), que potencialmente dará origem aos agregados proteicos que contêm não só a proteína clivada mas também a ATXN3 total, normal e expandida (**Figura 4**). A formação do fragmento de ATXN3 ainda não foi inequivocamente mostrada *in vivo*; de facto a maioria dos estudos que sugerem que a clivagem da ATXN3 poderá ser mediada por caspases (Berke et al., 2004) ou calpaínas (Haacke et al., 2007) foram realizados *in vitro*. O hipotético fragmento da ATXN3 expandida foi detectado em extractos proteicos totais obtidos de cérebro de pacientes *post-mortem* e de um modelo da DMJ em murganho (Goti et al., 2004), mas não de um outro modelo de DMJ representativo de estadios mais precoces da doença (Silva-Fernandes et al., 2010).

Apesar da activação da morte neuronal por apoptose, mediada pela expressão da ATXN3 ou Htt mutantes, parecer contribuir para a doença, este é ainda um assunto controverso, na medida em que estudos recentes sugerem a ocorrência de disfunção neuronal em detrimento de morte celular por apoptose (e.g. Silva-Fernandes et al., 2010). Contudo, foi observado que células neuronais que expressam ATXN3 mutante são mais sensíveis ao tratamento com staurosporina (composto indutor de apoptose), talvez devido a uma diminuição da expressão de factores anti-apoptóticos nestas células, como o Bcl-2. Os níveis de citocromo c libertados pela mitocôndria encontram-se também aumentados em células de doentes DMJ (Tsai et al., 2004). A activação da morte celular programada em células DMJ poderá também ocorrer devido à activação da proteína pró-apoptótica Bax, mais concretamente via acetilação de ku70

(Li et al., 2007), pelo que a utilização de péptidos inibidores de Bax tem sido sugerida como uma estratégia terapêutica na DMJ.

2.7. Estratégias terapêuticas e de Neuroprotecção

O recente avanço no conhecimento sobre os diferentes mecanismos de disfunção neuronal e de neurodegenerescência envolvidos nas doenças de poliglutaminas, nomeadamente na DH e na DMJ, permitiu a identificação de diferentes alvos terapêuticos. Apesar dos tratamentos sintomáticos constituírem a base da terapia usada na prática clínica, vários tratamentos neuroprotectores têm vindo a ser testados em ensaios pré-clínicos e clínicos. Estas terapias neuroprotectoras visam prevenir ou protelar o aparecimento dos primeiros sintomas em portadores assintomáticos da mutação, e retardar a evolução da patologia ou mesmo prevenir o aparecimento de sintomas subsequentes em doentes sintomáticos.

As terapias neuroprotectoras actuam a nível da: (i) modulação da transcrição, (ii) modulação da fosforilação (específico da Htt), (iii) inibição das transglutaminases, (iv) modulação dos receptores de neurotransmissores, (v) redução da disfunção metabólica e mitocondrial, (vi) prevenção ou bloqueio da formação de radicais livres, (vii) activação da autofagia, (viii) inibição da apoptose, e (ix) regeneração neuronal através da acção de factores (neuro)tróficos. Para além disso, o silenciamento da expressão do gene utilizando a tecnologia de RNA de interferência ou oligonucleótidos antisense, e a regeneração neuronal através da terapia celular constituem terapias curativas em fase de desenvolvimento, mas altamente promissoras. Refira-se, por exemplo, que é possível tirar partido da existência de SNPs (do inglês *single nucleotide polymorphisms*) para gerar siRNAs (do inglês *small interfering RNA*) que silenciam exclusivamente o alelo mutante, e que têm sido desenvolvidos oligonucleótidos antisense para o RNA mensageiro que interferem com a expressão da Htt mutante de forma

selectiva (*e.g.* Hu et al., 2009). Na DMJ, verificou-se ainda que o silenciamento do alelo normal da *ATXN3* num modelo em rato, não agrava a patologia e que a utilização de siRNAs não específicos (que actuam sobre o alelo normal e expandido), poderá ser uma estratégia terapêutica eficaz e segura (Alves et al., 2010).

A nível da terapia celular ou de substituição na DH, um estudo publicado após cerca de 10 anos de transplantes em humanos descreve que, de dois doentes transplantados bilateralmente no estriado com tecido cerebral fetal, um deles demonstrou, pela primeira vez, um aumento da ligação a receptores D2 (detectado por tomografia de emissão de positrões) e melhoria clínica ao longo de 5 anos, sugerindo a sobrevivência do tecido transplantado e um benefício potencial dos transplantes estriatais na DH (Reuter et al., 2008).

3. Conclusões

Durante a última década, as doenças de poliglutaminas têm sido alvo de intensa investigação, particularmente após a identificação dos genes envolvidos e da mutação responsável pelas diferentes doenças e da subsequente produção de vários modelos *in vivo*.

A nível neuronal, a perda de função normal das proteínas envolvidas e/ou o ganho de função tóxica conferida pela expansão de poliQ podem contribuir para a patologia associada a estas doenças. As alterações neuronais (e, eventualmente, das células da glia) induzidas pelas proteínas mutantes resultam na disfunção de importantes circuitos neuronais. Por outro lado, os mecanismos celulares e moleculares de neurodegenerescência desenvolvem-se lentamente nos portadores das expansões de poliQ, tornando-se mais evidentes nas fases mais avançadas da doença.

Assim, a identificação de diferentes mecanismos neuropatológicos tem possibilitado a aplicação *in vitro* e *in vivo* de várias terapias na DH e DMJ. Se, por um lado, as terapias que visam suprimir a expressão das proteínas mutantes de forma selectiva (terapia génica), ou que

visam substituir os neurónios lesados e re-estabelecer os circuitos neuronais a nível cerebral (terapia celular ou de substituição, que pode estar associada à terapia génica) se encontram em fase de franco desenvolvimento, tendo como objectivo último a cura destas doenças, por outro lado, as terapias neuroprotectoras podem promover a qualidade de vida dos portadores da mutação. Assim, a protecção neuronal mediada por agentes farmacológicos permitirá não só retardar, como potencialmente prevenir o aparecimento dos sintomas da doença e da sua gravidade, prolongando o tempo de vida dos doentes. Os múltiplos mecanismos neuropatológicos discutidos acima podem ocorrer em paralelo e promover-se mutuamente, sugerindo que a combinação de diferentes terapias neuroprotectoras, que actuam em alvos moleculares distintos, possa ser mais eficaz no combate à lesão neuronal irreversível na DH e na DMJ, e possivelmente noutras doenças neurodegenerativas.

Referências bibliográficas

Alves S, Nascimento-Ferreira I, Dufour N, Hassig R, Auregan G, Nobrega C, Brouillet E, Hantraye P, Pedroso de Lima MC, Deglon N, de Almeida LP Silencing ataxin-3 mitigates degeneration in a rat model of Machado-Joseph disease: no role for wild-type ataxin-3? (2010) Hum Mol Genet 19(12): 2380-2394

Bates G. P., Benn C. (2002) The polyglutamine diseases. *In*: "Huntington's disease" (Bates G., Harper P., Jones L., Eds.), Oxford University Press, New York, 3ª Edição, Cap. 14, pp. 429-472.

Berke SJ, Schmied FA, Brunt ER, Ellerby LM, Paulson HL (2004) Caspase-mediated proteolysis of the polyglutamine disease protein ataxin-3. J Neurochem 89(4): 908-918

Burk K, Globas C, Bosch S, Klockgether T, Zuhlke C, Daum I, Dichgans J (2003) Cognitive deficits in spinocerebellar ataxia type 1, 2, and 3. J Neurol 250(2): 207-211

Costa M. do C., Magalhães P., Ferreirinha F., Guimarães L., Januário C., Gaspar I., Loureiro L., Vale J., Garrett C., Regateiro F., Magalhães M., Sousa A., Maciel P., & Sequeiros J. (2003) Molecular diagnosis of Huntington disease in Portugal: implications for genetic counselling and clinical practice. *Eur. J. Hum. Genet.*, **11**: 872-878.

Coutinho P (1992) Doença de Machado-Joseph: tentativa de definição. Tese-Universidade do Porto.

Coutinho P, Andrade C (1978) Autosomal dominant system degeneration in Portuguese families of the Azores Islands. A new genetic disorder involving cerebellar, pyramidal, extrapyramidal and spinal cord motor functions. Neurology 28(7): 703-709.

Cui, L., Jeong, H., Borovecki, F., Parkhurst, C. N., Tanese, N., & Krainc, D. (2006) Transcriptional repression of PGC-1alpha by mutant huntingtin leads to mitochondrial dysfunction and neurodegeneration. *Cell*, 127, 59-69.

D'Abreu A, Franca M, Jr., Appenzeller S, Lopes-Cendes I, Cendes F (2009) Axonal dysfunction in the deep white matter in Machado-Joseph disease. J Neuroimaging 19(1): 9-12

Gil J. M., Rego A. C. (2008) Mechanisms of neurodegeneration in Huntington's disease. *Eur J Neurosci.* **27** (11): 2803-2820. [Erratum in: *Eur J Neurosci*. 2008; 28 (10): 2156].

Goti D, Katzen SM, Mez J, Kurtis N, Kiluk J, Ben-Haiem L, Jenkins NA, Copeland NG, Kakizuka A, Sharp AH, Ross CA, Mouton PR, Colomer V (2004) A mutant ataxin-3 putative-cleavage fragment in brains of Machado-Joseph disease patients and transgenic mice is cytotoxic above a critical concentration. J Neurosci 24(45): 10266-10279

Haacke A, Hartl FU, Breuer P (2007) Calpain inhibition is sufficient to suppress aggregation of polyglutamine-expanded ataxin-3. J Biol Chem 282(26): 18851-18856

Ho, L. W., Carmichael, J., Swart, J., Wyttenbach, A., Rankin, J., & Rubinsztein, D. C. (2001) The molecular biology of Huntington's disease. *Psychol. Med.*, 31, 3-14.

Hu, J., Matsui, M., Gagnon, K. T., Schwartz, J. C., Gabillet, S., Arar, K., Wu, J., Bezprozvanny, I., & Corey, D. R. (2009) Allele-specific silencing of mutant huntingtin and ataxin-3 genes by targeting expanded CAG repeats in mRNAs. *Nat Biotechnol*., 27, 478-484.

Karpuj, M. V., Garren, H., Slunt, H., Price, D. L., Gusella, J., Becher, M. W., & Steinman, L. (1999) Transglutaminase aggregates huntingtin into nonamyloidogenic polymers, and its enzymatic activity increases in Huntington's disease brain nuclei. *Proc. Natl. Acad. Sci. USA*, 96, 7388-7393.

Kawaguchi Y, Okamoto T, Taniwaki M, Aizawa M, Inoue M, Katayama S, Kawakami H, Nakamura S, Nishimura M, Akiguchi I, et al. (1994) CAG expansions in a novel gene for Machado-Joseph disease at chromosome 14q32.1. Nat Genet 8(3): 221-228.

Leavitt, B. R., Guttman, J. A., Hodgson, J. G., Kimel, G. H., Singaraja, R., Vogl, A. W., & Hayden, M. R. (2001) Wild-type huntingtin reduces the cellular toxicity of mutant huntingtin in vivo. *Am. J. Hum. Genet.*, 68, 313-324.

Li Y, Yokota T, Gama V, Yoshida T, Gomez JA, Ishikawa K, Sasaguri H, Cohen HY, Sinclair DA, Mizusawa H, Matsuyama S (2007) Bax-inhibiting peptide protects cells from polyglutamine toxicity caused by Ku70 acetylation. Cell Death Differ 14(12): 2058-2067

Macedo-Ribeiro S., de Almeida L. P., Carvalho A. L., Rego A. C. (2007) Polyglutamine expansion diseases – the case of Machado-Joseph disease. *In*: "Interaction between neurons and glia in neurons" (Malva J. O., Ed., Rego A. C., Cunha R. A., Oliveira C. R., co-Eds.), Springer, New York., Cap. 18, pp. 391-426.

Matsuishi T, Sakai T, Naito E, Nagamitsu S, Kuroda Y, Iwashita H, Kato H (1996) Elevated cerebrospinal fluid lactate/pyruvate ratio in Machado-Joseph disease. Acta Neurol Scand 93(1): 72-75.

Menalled LB, Chesselet MF (2002) Mouse models of Huntington's disease. Trends Pharmacol Sci. 23(1):32-39.

Menzies FM, Huebener J, Renna M, Bonin M, Riess O, Rubinsztein DC (2010) Autophagy induction reduces mutant ataxin-3 levels and toxicity in a mouse model of spinocerebellar ataxia type 3. Brain 133(Pt 1): 93-104.

Paulson HL, Subramony SH (2003) Spinocerebellar Ataxia 3-Machado-Joseph Disease (SCA3). *In*: "Genetics of Movement Disorders" (Pulst, S-M., Ed.), Academic Press, Cap. 5, pp.57-69.

Perutz, M. F., Johnson, T., Suzuki, M., & Finch, J. T. (1994) Glutamine repeats as polar zippers: their possible role in inherited neurodegenerative diseases. *Proc. Natl. Acad. Sci. USA*, 91, 5355-5358.

Ravikumar, B., Vacher, C., Berger, Z., Davies, J. E., Luo, S., Oroz, L. G., Scaravilli, F., Easton, D. F., Duden, R., O'Kane, C. J., & Rubinsztein, D. C. (2004) Inhibition of mTOR induces autophagy and reduces toxicity of polyglutamine expansions in fly and mouse models of Huntington disease. *Nat. Genet.*, 36, 585-595.

Rego A. C., de Almeida L. P. (2005) Molecular targets and therapeutic strategies in Huntington's disease. *Curr Drug Targets CNS Neurol Disord*. **4**(4):361-381.

Rego, A. C., & Oliveira, C. R. (2003) Mitochondrial dysfunction and reactive oxygen species in excitotoxicity and apoptosis: implications for the pathogenesis of neurodegenerative diseases. *Neurochem. Res.*, 28,1563-1574.

Reina CP, Zhong X, Pittman RN Proteotoxic stress increases nuclear localization of ataxin-3. Hum Mol Genet 19(2): 235-249

Reuter, I., Tai, Y. F., Pavese, N., Chaudhuri, K. R., Mason, S., Polkey, C. E., Clough, C., Brooks, D. J., Barker, R. A., & Piccini, P. (2008) Long-term clinical and positron emission tomography outcome of fetal striatal transplantation in Huntington's disease. *J Neurol Neurosurg Psychiatry*, 79, 948-951.

Riess O, Rub U, Pastore A, Bauer P, Schols L (2008) SCA3: neurological features, pathogenesis and animal models. *Cerebellum* **7**(2)**:** 125-137

Ross, C.A. (1995) When more is less: pathogenesis of glutamine repeat neurodegenerative diseases. Neuron, 15, 493-496.

Seidel K, den Dunnen WF, Schultz C, Paulson H, Frank S, de Vos RA, Brunt ER, Deller T, Kampinga HH, Rub U Axonal inclusions in spinocerebellar ataxia type 3. Acta Neuropathol

Sequeiros J, Coutinho P (1993) Epidemiology and clinical aspects of Machado-Joseph disease. Adv Neurol 61: 139-153.

Silva-Fernandes A, Costa MD, Duarte-Silva S, Oliveira P, Botelho CM, Martins L, Mariz JA, Ferreira T, Ribeiro F, Correia-Neves M, Costa C, Maciel P (2010) Motor uncoordination and neuropathology in a transgenic mouse model of Machado-Joseph disease lacking intranuclear inclusions and ataxin-3 cleavage products. Neurobiol Dis

Tang, T. S., Chen, X., Liu, J., & Bezprozvanny, I. (2007) Dopaminergic signaling and striatal neurodegeneration in Huntington's disease. *J Neurosci.*, 27, 7899-7910.

The Huntington's Disease Collaborative Research Group (1993) A novel gene containing a trinucleotide repeat that is expanded and unstable on Huntington's disease chromosomes. *Cell*, 72, 971-983.

Tsai HF, Tsai HJ, Hsieh M (2004) Full-length expanded ataxin-3 enhances mitochondrial-mediated cell death and decreases Bcl-2 expression in human neuroblastoma cells. Biochem Biophys Res Commun 324(4): 1274-1282

Yu YC, Kuo CL, Cheng WL, Liu CS, Hsieh M (2009) Decreased antioxidant enzyme activity and increased mitochondrial DNA damage in cellular models of Machado-Joseph disease. J Neurosci Res 87(8): 1884-1891.

Lista de abreviaturas:

3-NP, Ácido 3-nitropropiónico;
ATXN3, Ataxina-3;
BDNF, Factor neurotrófico derivado do cérebro (do inglês *brain-derived neurotrophic factor*)
C. elegans, *Caenorhabditis elegans;*
CAG, Citosina-adenina-guanina;
CBP, do inglês *CREB (cyclic-adenosine monophosphate (cAMP) response element (CRE) binding protein)-binding protein;*
DA, Dopamina;
DH, do inglês *Huntington's disease* ou doença de Huntington;
DMJ, do inglês Machado-Joseph disease;
DNA, Ácido desoxirribonucleíco (do inglês *deoxyribonucleic acid*)
DRPLA, do inglês *dentatorubral-pallidoluysian atrophy*;
ERAD, do inglês *endoplasmic reticulum associated protein degradation;*
FT, Factor de transcrição;
GABA, Ácido γ-aminobutírico;
HDAC3, Desacetilase das histonas 3;
Htt, Huntingtina;
$InsP_3R$, Receptor do inositol-(1,4,5)-trifosfato;
IT15, do inglês *Interesting Transcript 15;*
mGluR, Receptor metabotrópico do glutamato
MMP-2, Metaloproteinase 2 da matrix;
mTOR, do inglês *mammalian target of rapamycin;*
NCoR, Receptor nuclear co-repressor;
NII, do inglês *neuronal intranuclear inclusions*
NMDA, *N*-metil-D-aspartato
nNOS, Isoforma neuronal da NOS
NOS, Sintetase do óxico nítrico;
NRSE, do inglês *neuron restrictive silencer element;*
pCAF, Factor Associado a p300/CBP;
PGC-1α, do inglês *peroxisome proliferator-activated receptor-γcoactivator-1α;*
PoliQ, Poliglutaminas
PSD-95, do inglês *postsynaptic density 95*
QA, Ácido quinolínico (do inglês *quinolinic acid*)
RNA, Ácido ribonucleíco (do inglês *ribonucleic acid*)
ROS, Espécies reactivas de oxigénio (do inglês *reactive oxygen species*)
SBMA, do inglês *spinal bulbar muscular atrophy* ou doença de Kennedy;
SCA, Ataxias espinocerebelosas (do inglês *spinocerebellar ataxias)*;
siRNA, do inglês *small interfering RNA*
SNC, Sistema nervoso central;
SNPs, do inglês *single nucleotide polymorphisms*
SOD, Superóxido dismutase
Sp1, do inglês *specific protein-1;*
TAFII130, do inglês *TBP associated factor;*
TBP, do inglês *thymine-adenine-thymine-adenine (TATA)-binding protein*;
UIMs, do inglês ubiquitin interacting motifs;
UPS, do inglês *ubiquitin proteasome system;*
VCP, do inglês *valosin containing protein;*
YAC, do inglês *yeast artificial chromosome*;

GLOSSÁRIO:

Bradicinésia- Dificuldade no iniciar e dar continuidade a movimentos, havendo também a impossibilidade de ajustar a posição do corpo. Habitualmente, aparece como sintoma de doenças neurológicas, particularmente na doença de Parkinson, mas poderá também ser resultante de efeitos secundários de determinados tipos de medicamentos. A palavra bradicinésia e derivada de duas palavras gregas: *bradys*, lento + *kinesis*, movimento= movimento lento.

Caquexia- Desnutrição aguda associada a atrofia muscular, fadiga, fraqueza e perda de apetite. Pode ser um sinal médico de diversos distúrbios, nomeadamente cancro, doenças neurodegenerativas e algumas doenças infecciosas (como tuberculose, SIDA, Leishmaniose Visceral, lesões da parte lateral do hipotálamo, intoxicação por mercúrio e alguns distúrbios autoimunes).

Coreia- Movimentos contínuos do corpo aparentemente coordenados e realizados intencionalmente, mas que na realidade são involuntários. A palavra *chorea* é derivada da palavra grega *khorea* que significa dança.

Defeito cognitivo- Dificuldade no processo de aprendizagem e de aquisição de conhecimento. A cognição envolve atenção, percepção, memória, raciocínio, juízo, imaginação, pensamento e linguagem. A cognição é derivada da palavra latina *cognitione*, que significa a aquisição de um conhecimento através da percepção.

Disartria- Discurso tipicamente lento e não claro, difícil de produzir e de ser entendido. Uma pessoa com disartria terá dificuldade em controlar o volume, o ritmo e qualidade da voz do seu discurso. Disartria é causada por paralisia, fraqueza ou incapacidade de coordenar os músculos da boca. Disartria pode ocorrer como uma incapacidade associada ao desenvolvimento e poderá ser um sinal de doença neuromuscular.

Disfagia- Dificuldade em engolir, que ocorre frequentemente após um acidente vascular cerebral. E associada a problemas de controlo nervoso ou muscular. A disfagia afecta a nutrição e hidratação do indivíduo e poderá levar ao aparecimento de pneumonias e desidratação. Do grego, *Phagein* significa comer, ter dificuldade em comer.

Distonia- Doença associada ao movimento, na qual há contração muscular continua, causando voltas e movimentos repetitivos e posturas anormais. Os movimentos involuntários podem ser dolorosos e podem afectar um único músculo ou um grupo de músculos (braços, pernas ou pescoço) ou mesmo o corpo inteiro.

Fasciculação- Pequena contracção involuntária, localizada e descoordenada de músculos, normalmente visível sob a pele, e advinda de uma descarga espontânea de um feixe de fibras musculares esqueléticas (fascículo muscular). As fasciculações podem ter uma variedade de causas, a maioria das quais é benigna, mas também podem ser resultado de doenças neuro-musculares.

Mosaicismo somático– Presença de populações geneticamente distintas de células somáticas (não germinativas) num dado organismo. É muitas vezes mascarado, mas também pode resultar em grandes alterações fenotípicas e revelar a expressão de mutações genéticas que seriam letais. O mosaicismo pode ser causado por mutações ou alterações epigenéticas no DNA, anormalidades cromossómicas e pela reversão espontânea de mutações hereditárias.

Oftalmoplegia- Paralisia dos músculos do olho. Muitas vezes causada pela mononeuropatia diabética pela lesão no terceiro par craniano (óculo-motor). Pode também ser originada por falta de vitamina B1, como acontece nas hepatites e cirroses hepática. Também está verificada como sintoma de patologias neurodegenerativas do Sistema Nervoso Central, nomeadamente a Esclerose Múltipla.

Legendas das Figuras:

Figura 1- Representação esquemática das principais regiões cerebrais afectadas na DH e DMJ. Vermelho é indicativo de regiões grandemente afectadas e perda neuronal selectiva; Laranja indica perda neuronal variável e moderada. Legenda: CB, córtex cerebeloso; C/P, caudado/*putamen*; Ctx, córtex cerebral; DN, núcleo denteado; GP, *globus pallidus*; LCN, núcleo cuneato lateral; PN, núcleos pônticos; RN, núcleo rubro; SN, *substantia nigra*; STN, núcleos subtalâmicos; VL, núcleos ventrolaterais do tálamo. (Adaptado de Ross, 1995)

Figura 2- Representação do gene da huntingtina (*HTT*) e da ataxina-3 (*ATXN3*) e da influência da expansão do trinucleótido CAG no início dos sintomas da DH **(A)** e da DMJ **(B)**. Repetições CAG entre 8 e 29 são normais; repetições CAG entre 29 e 35 considera-se uma pré-mutação, pois é instável e susceptível de expandir; expansões acima das 36 poderão causar a mutação numa idade mais tardia (penetrância incompleta); se existirem expansões entre 40 e 50, a DH surge invariavelmente na meia-idade; repetições CAG acima das 60 estão associadas às formas juvenis da DH, em que os sintomas geralmente surgem antes dos 20 anos de idade **(A)**. Na DMJ**,** o tamanho do trinucleótido CAG é altamente polimórfico em indivíduos normais variando de 10-51 repetições. Cerca de 90% dos alelos normais apresentam menos de 31 repetições. O aparecimento de sintomas encontra-se associado a expansões acima das 55 repetições CAG **(B)**. Baseado em Rego e de Almeida, 2005. PoliQ, poliglutaminas; *N*, Normal; *D*, Doente.

Figura 3- Mecanismos moleculares neuropatológicos na DH. A huntingtina mutante (mHtt) interfere com vários factores de transcrição (FT), alterando a expressão de BDNF a nível cortical. A mHtt também afecta o transporte axonal, repercutindo-se numa diminuição do BDNF libertado pelos neurónios corticais. Por outro lado, a mHtt induz disfunção sináptica (*e.g.* sinapses cortico-estriatais) e o processo de excitotoxicidade, o aumento da concentração de cálcio intracelular (proveniente da activação do receptor NMDA e/ou do receptor do $InsP_3$ no retículo endoplasmático (ER), em resultado da activação dos receptores metabotrópicos para o glutamato do tipo mGluR5), a disfunção mitocondrial, a desregulação metabólica e o stresse oxidativo; paralelamente, ao interferir com os níveis intracelulares de cálcio e com a mitocôndria, a mHtt promove a activação de calpaínas e de caspases, que clivam a mHtt, potenciando o processo neurodegenerativo; deste modo, a clivagem da proteína promove a formação de fragmentos que mais facilmente atravessam a membrana nuclear e formam

agregados proteicos; este podem ser marcados com moléculas de ubiquitina (Ub) para serem degradados mas, geralmente, o proteossoma é inibido; adicionalmente, o processo autofágico é activado de modo a remover os agregados proteicos.

Figura 4- Mecanismos moleculares neuropatológicos na DMJ. O processo patológico inicia-se provavelmente com a síntese da ataxina-3 (ATXN3) mutante, que contém uma sequência expandida de poliQ, e que altera a conformação nativa da proteína, modelada pela presença de chaperones. Uma parte das proteínas com conformação anormal (*misfolded*) será potencialmente degradada a nível do lisossoma, enquanto que a outra porção será marcada com moléculas de ubiquitina (Ub) e degradada a nível do proteossoma. A ATXN3 mutante tem a capacidade de se auto-associar facilitando assim a formação de espécies oligoméricas e agregados insolúveis. Um mecanismo alternativo, é a potencial clivagem da ATXN3 mutante e a formação de um fragmento tóxico que amplifica o processo de agregação e patogénese. Todas as espécies intermédias formadas ao longo do processo de agregação poderão originar a ocorrência de interacções proteicas anormais no ambiente celular facilitando também deste modo a patogénese da DMJ. Não é claro se estas espécies terão a capacidade de inibir o proteossoma, activar caspases e/ou alterar a função mitocondrial. Intermediários do processo de agregação são translocados para o núcleo, onde recrutam factores nucleares como factores de transcrição (FT), co-activadores e co-repressores, inibindo a sua função normal, resultando numa alteração do processo transcricional.

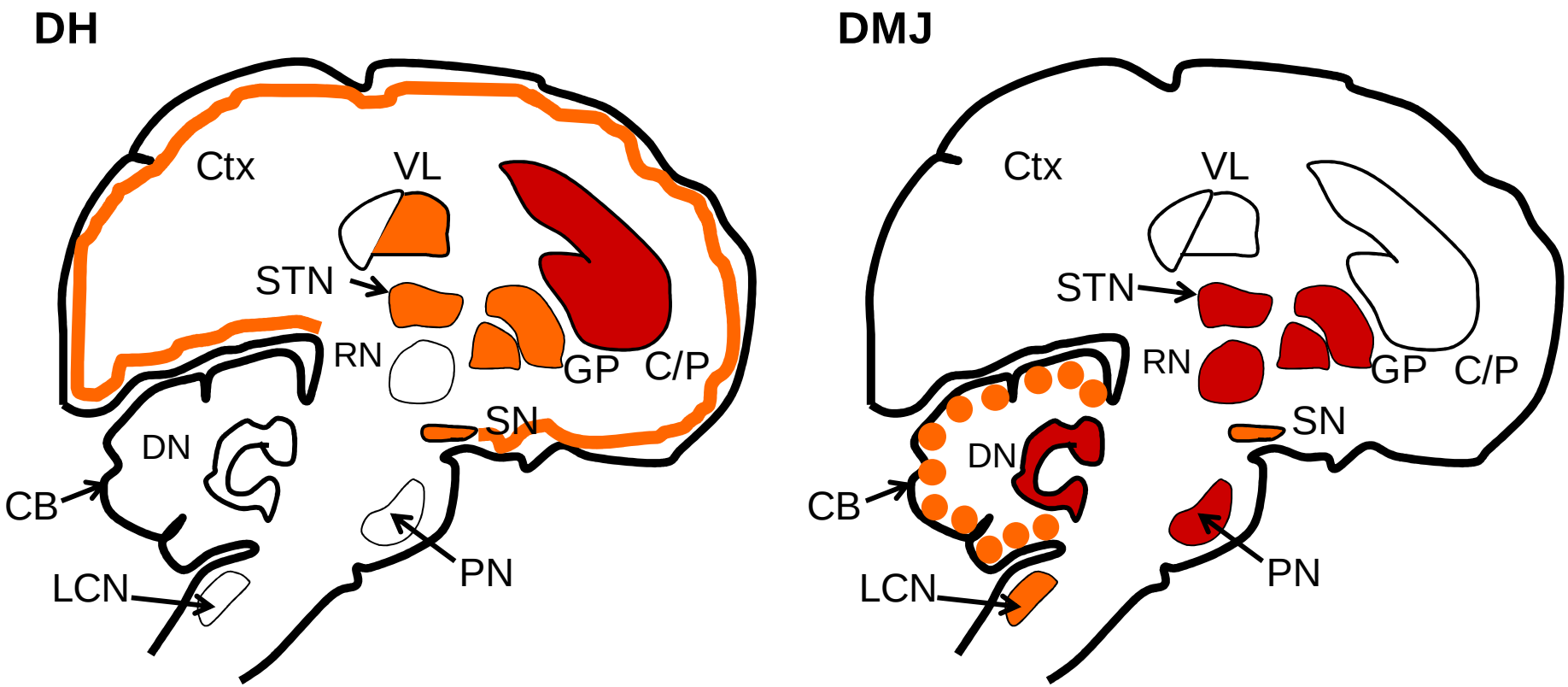
DH
Ctx
VL
STN
RN
GP
C/P
SN
DN
CB
LCN
PN
DMJ
Ctx
VL
STN
RN
GP
C/P
SN
DN
CB
LCN
PN

Figura 1

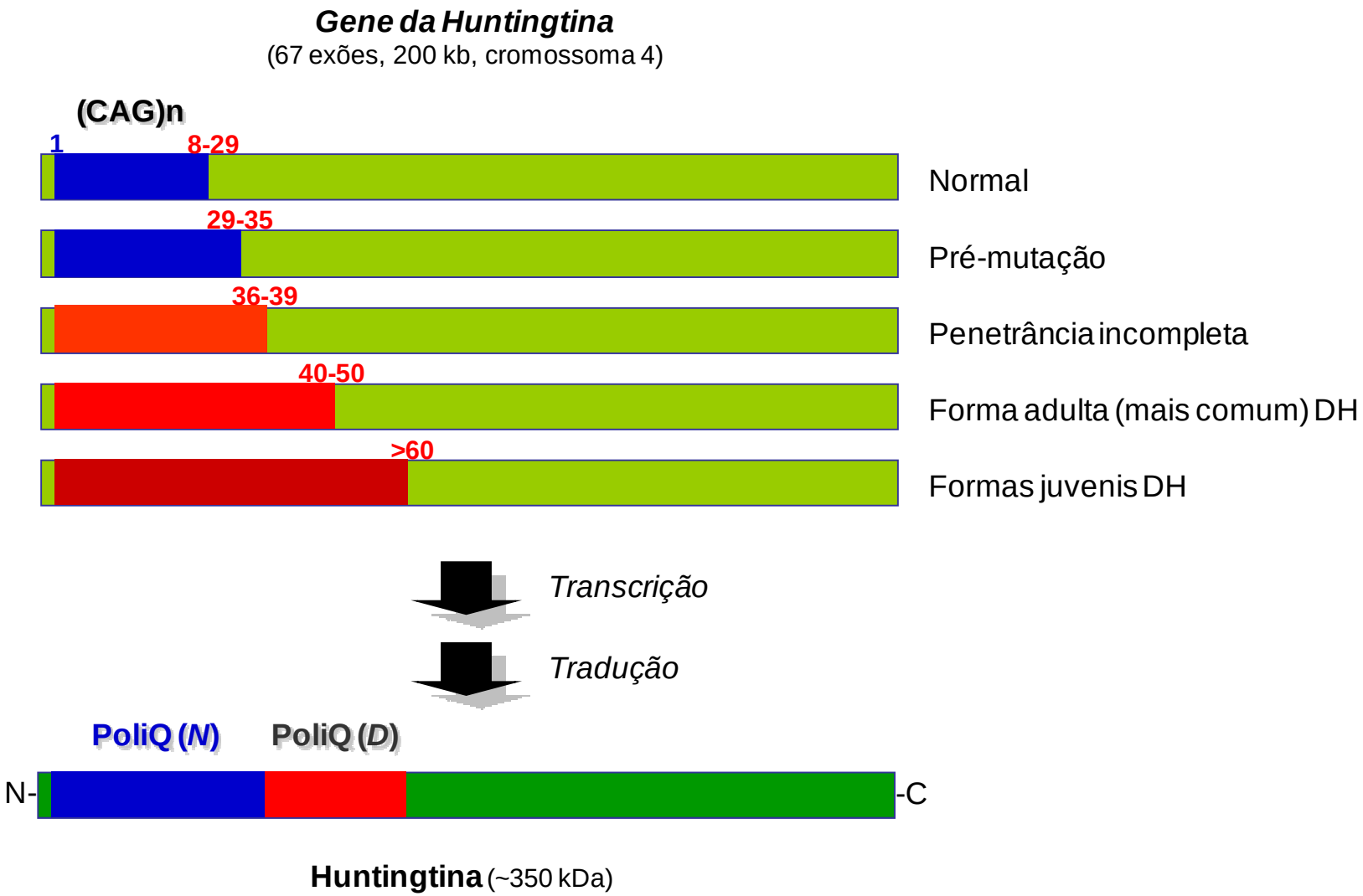
Gene da Huntingtina
(67 exões, 200 kb, cromossoma 4)
(CAG)n
1
8-29
Normal
29-35
Pré-mutação
36-39
Penetrância incompleta
40-50
Forma adulta (mais comum) DH
>60
Formas juvenis DH
Transcrição
Tradução
PoliQ (N)
PoliQ (D)
N-
-C
Huntingtina (~350 kDa)

Figura 2ª

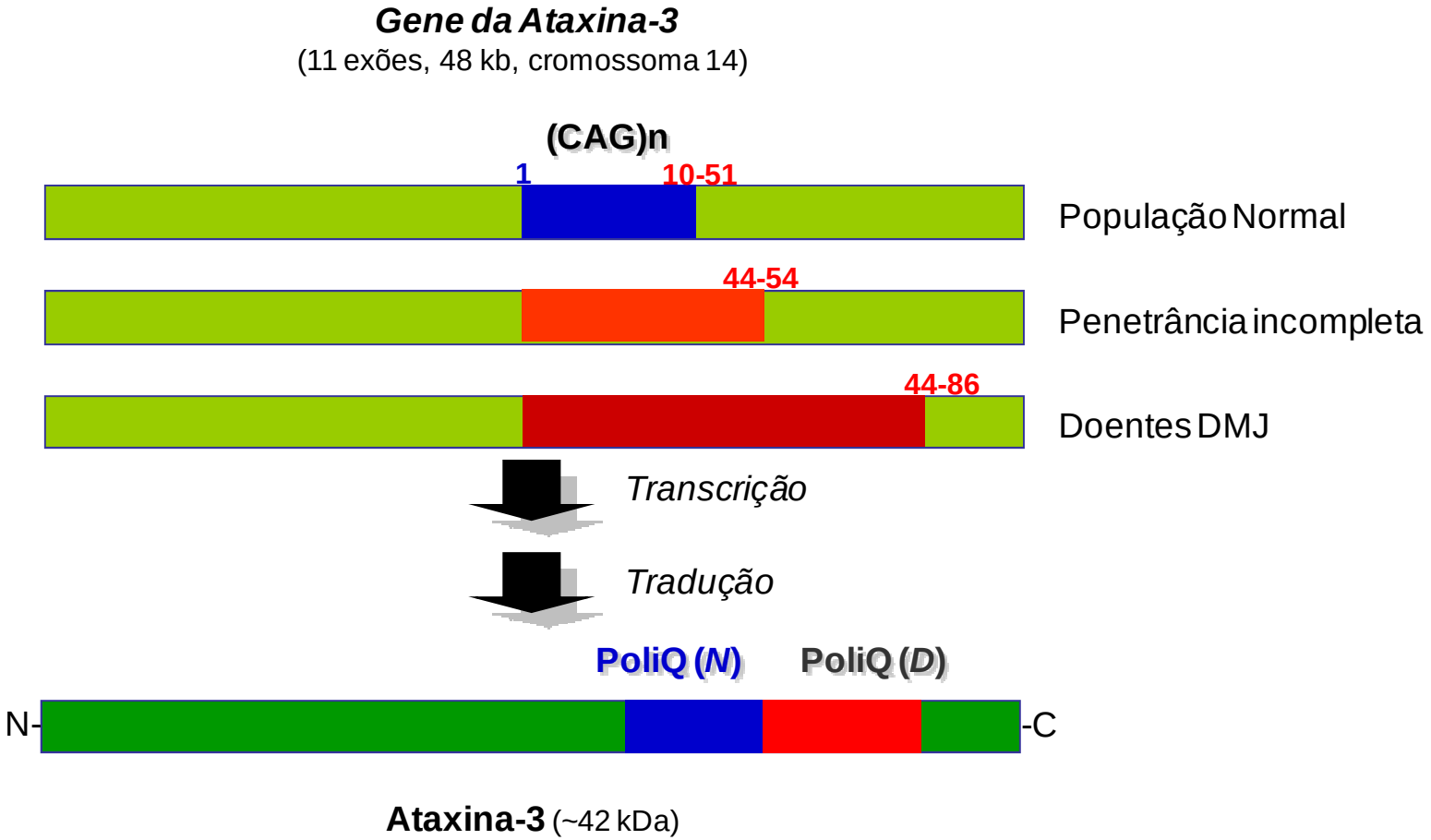
Gene da Ataxina-3
(11 exões, 48 kb, cromossoma 14)
(CAG)n
1
10-51
População Normal
44-54
Penetrância incompleta
44-86
Doentes DMJ
Transcrição
Tradução
PoliQ (N)
PoliQ (D)
N-
-C
Ataxina-3 (~42 kDa)

Figura 2B

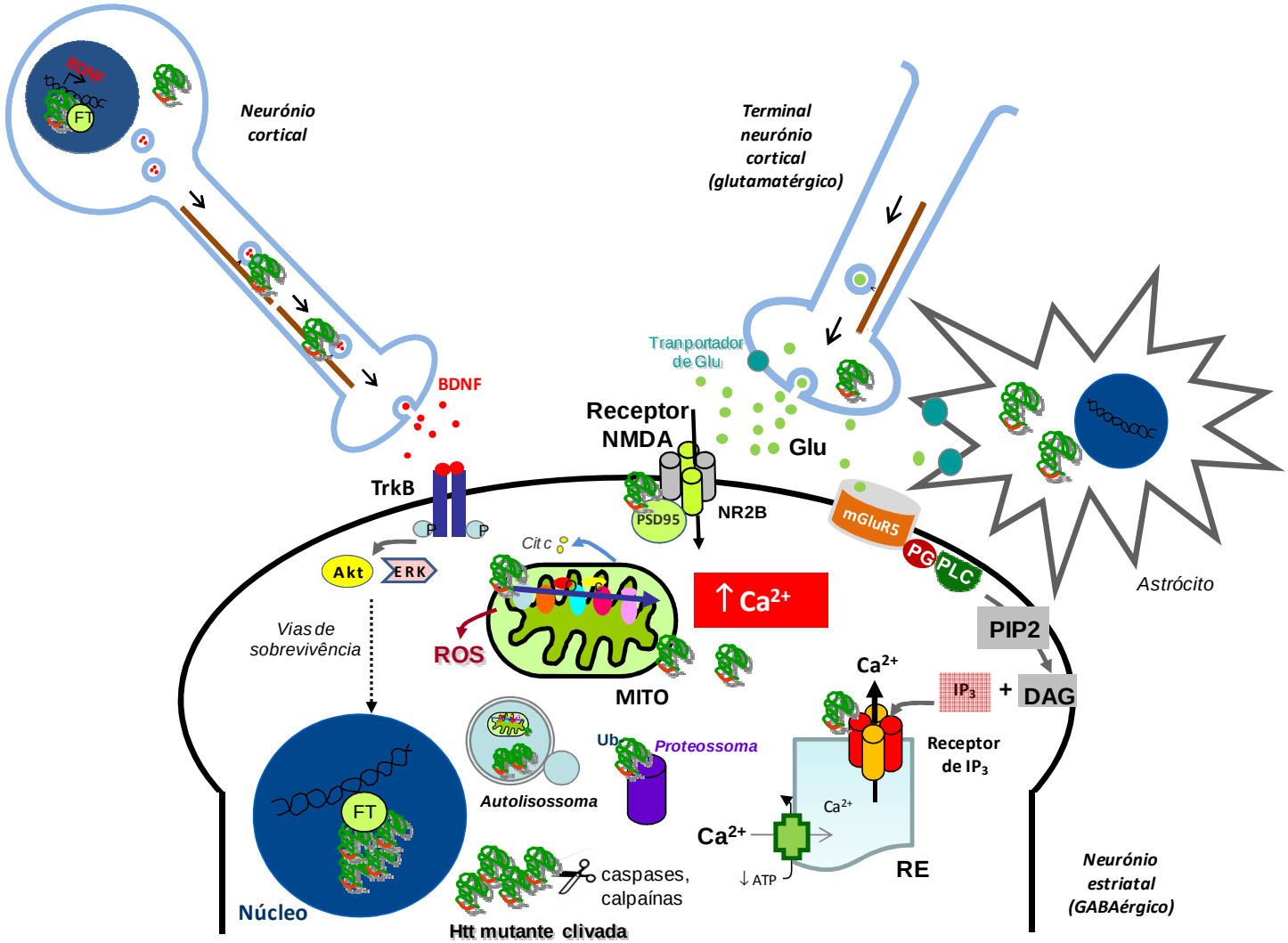
BDNF
FT
Neurónio cortical
Terminal neurónio cortical (glutamatérgico)
Tranportador de Glu
BDNF
Receptor NMDA
Glu
TrkB
PSD95
NR2B
mGluR5
PG
PLC
Astrócito
Cit c
Akt
ERK
↑ Ca2+
PIP2
Vias de sobrevivência
ROS
MITO
Ca2+
IP3
+
DAG
Ub
Proteossoma
Receptor de IP3
Autolisossoma
Ca2+
Ca2+
RE
↓ ATP
FT
caspases, calpaínas
Núcleo
Htt mutante clivada
Neurónio estriatal (GABAérgico)

Figura 3

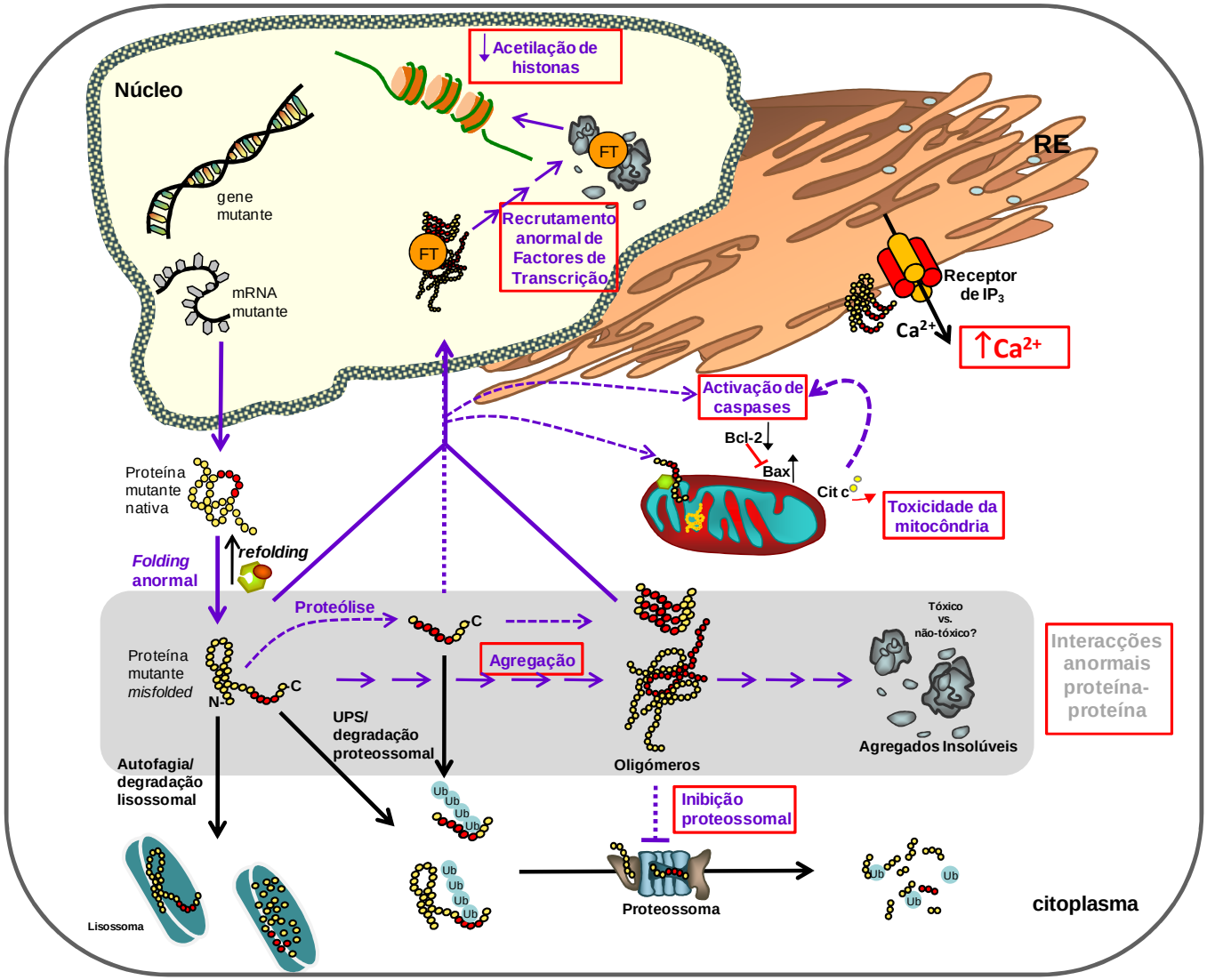
Núcleo
Acetilação de histonas
gene mutante
mRNA mutante
FT
FT
Recrutamento anormal de Factores de Transcrição
RE
Receptor de IP3
Ca2+
↑Ca2+
Activação de caspases
Bcl-2
Bax
Cit c
Toxicidade da mitocôndria
Proteína mutante nativa
refolding
Folding anormal
Proteólise
Proteína mutante misfolded
N-
C
C
Agregação
UPS/ degradação proteossomal
Oligómeros
Tóxico vs. não-tóxico?
Agregados Insolúveis
Interacções anormais proteína-proteína
Autofagia/ degradação lisossomal
Ub
Inibição proteossomal
Proteossoma
Lisossoma
citoplasma

Figura 4

Tabela I – Características das doenças de expansão de poliglutaminas.

Doença (abreviatura)	**Repetição CAG patogénica**	**Gene**	**Proteína afectada**	**Localização intracelular dos agregados proteicos**	**Área(s) cerebral(is) predominantemente afectada(s)**
DH	36-121	4p16.3	Huntingtina	Nuclear/ citoplasmática	Núcleo caudado e *putamen* (estriado), segmento externo do globo pálido, córtex cerebral, alguns neurónios do hipotálamo
SBMA	38-65	Xq11-12	Receptor do androgénio	Nuclear	Neurónios motores do corno anterior da medula espinhal e tronco cerebral
DRPLA	49-88	12p13.31	Atrofina-1	Nuclear	Cerebelo (núcleo denteado), núcleo rubro, segmento externo do globo pálido, núcleos subtalâmicos
SCA1	39-83	6p23	Ataxina-1	Nuclear	Cerebelo, núcleo rubro, oliva inferior, ponte ou protuberância, corno anterior da medula espinhal e via piramidal
SCA2	32-77	12q24.1	Ataxina-2	Nuclear/citoplasmática	Cerebelo, núcleo rubro, oliva inferior, ponte, corno anterior da medula espinhal e via piramidal
SCA3	55-89	14q32.1	Ataxina-3	Nuclear/ Axonal	Cerebelo (núcleo denteado), gânglios da base, tronco cerebral, medula espinhal
SCA6	20-33	19p13.1	CACNA1A	Nuclear/citoplasmática	Cerebelo (células de Purkinje, núcleo denteado), oliva inferior
SCA7	37-306	3p12-13	Ataxina-7	Nuclear	Cerebelo, tronco cerebral, córtex visual, mácula
SCA17	47-63	6q27	TBP	Nuclear	Cerebelo, córtex (atrofia difusa), núcleo caudado e *putamen*.

CACNA1A– Subunidade α_{1A} do canal de cálcio sensível à voltagem do tipo P/Q; DRPLA- do inglês *dentatorubral-pallidoluysian atrophy*; DH–doença de Huntington; SBMA– do inglês *spinal bulbar muscular atrophy* ou doença de Kennedy; SCA– do inglês *spinocerebellar ataxias* ou ataxias espinocerebelosas; TBP– do inglês *thymine-adenine-thymine-adenine (TATA) -binding protein*.
Adaptado de: Macedo-Ribeiro et al., 2007; Rego e de Almeida, 2005.

Tabela II – Principais modelos animais roedores da doença de Huntington.

Roedor e modelos		Promotor	Repetições CAG	Expressão do transgene	Estirpe background	Agregados (NII)	Neurodegeneração	Idade de morte do animal (anos)	Fenótipo	Referência
Mus musculus										
Modelo transgénico 'truncado'	R6/1	*IT15* (exão 1)	~115	31%	CBA x C57BL/6J	Sim	Não (com atrofia cerebral)	32-40 semanas	Défice motor.	Mangiarini et al. (1996) Cell. 87(3):493-506.
	R6/2	*IT15* (exão 1)	~145	75%	CBA x C57BL/6J	Sim	Não (com atrofia cerebral)	10-16 semanas	Rápida deterioração cognitiva e motora.	
	N171-82Q	Proteína prião do murganho	82	10-20%	C3H/HEJ x C57BL/6J	Sim	Disfunção estriatal	24-30 semanas	Défice motor.Diabetes.	Schilling et al. (1999) Hum Mol Genet. 8(3):397-407 [Erratum in: Hum Mol Genet 1999;8(5):943].
	HD94-regulado	CMV, regulado por tetraciclina	94	n.d.	CBA x C57BL/6J	Sim (revertidos por inibição do transgene)	Não (com atrofia cerebral, revertida por inibição do transgene)	Morte prematura	Défice motor, revertido por inibição do transgene.	Yamamoto et al. (2000) Cell. 101(1):57-66.
Modelo transgénico YAC	YAC 72	*IT15*	72	30-50%	FVB/N	Não	Sim (estriado)	> 12 meses	Hipercinésia, seguido de hipocinésia.	Hodgson et al. (1999) Neuron. 23(1):181-92.
	YAC128	*IT15*	128	75%	FVB/N	Sim	Sim (morte e atrofia do estriado e córtex)	< 12 meses	Hipercinésia, seguido de hipocinésia; défice cognitivo.	Slow et al. (2003) Hum Mol Genet. 12(13):1555-67.
Modelo *Knock-in*	Hdh94	*Hdh*	94	100%	129Sv x C57BL/6J	Sim (estriado)	Não	Normal	Hipercinésia, seguido de hipocinésia.	Wheeler et al. (1999) Hum Mol Genet. 8(1):115-22.
	Hdh150	*Hdh*	150	n.d.	129/Ola x C57BL/6J	Sim (cérebro)	Não	> 12 meses	Défice motor.	
Rattus norvegicus										
	HDTg Rat	*Hdh*	51	22%	Sprague Dawley	Sim	Sim (morte e atrofia do estriado)	24 meses	Défice cognitivo e disfunção motora progressiva.	von Hörsten et al. (2003) Hum Mol Genet. 12(6):617-24.

n.d. - não determinado. *IT15* – gene humano da huntingtina completo (*full-length*). NII – do inglês *neuronal intranuclear inclusions*. YAC, do inglês *yeast artificial chromosome*. Adaptado de Menalled e Chesselet, 2002.

Tabela III. Principais modelos animais da doença de Machado-Joseph.

Doença de Machado-Joseph

Organismo	Transgene	Promotor	Tamanho da repetição CAG	Padrão de expressão	Agregados	Neurodegeneração	Início da doença	Fenótipo
C. elegans								
e.g. Khan *et al.* , 2006	MJD1a cDNA total e C-terminal	*unc-119*	17, 19, 63, 127 e 130	ubíquo	sim	não	ND	desccordenação motora
Drosophila								
e.g. Warrick *et al.,* 2005	MJD1a cDNA total e C-terminal	gmr-/ elav-GAL4	27,78 e 84	olho e sistema nervos	sim	sim	ND	disrupção da morfologia do olho; disrupção do fotoreceptor; morte prematura
Mus musculus								
Ikeda *et al.,* 1997	MJD1a cDNA total e C-terminal	L7(Células de Purkinje)	79	Células de Purkinje	não	sim	4 semanas	ataxia; distúrbio da marcha; ausência de elevação das patas anteriores
Cemal *et al.,* 2002	YAC com *ATXN3*	*ATXN3*	64, 67, 72, 76 e 84	ubíquo	sim	sim	4 semanas	perda de peso; pélvis baixa; hipotonia; tremor; deficite na geotaxia negativa
Goti *et al.,* 2004	cDNA MJD1a	PrP	71	ubíquo	sim	↓ número de neurónios TH positivos na SN	8 semanas	descoordenação motora; perda de peso; perda de força nos membros
Bichelmeier U *et al.,* 2007	cDNA MJD1-1	PrP	15, 70 e 148	ubíquo	sim	ND	6 semanas	perda de peso, base alargada das patas posteriores; actividade reduzida;
Chou *et al.,* 2007	MJD1a CDNA total e C-terminal	PrP	79	ubíquo	sim	não	5 semanas	descoordenação motora; hipoactividade; ataxia; perda de peso; redução da elevação pélvica
Boy J *et al.,* 2009	cDNA MJD1-1	PrP/Tet-Off	77	ubíquo	sim	células de purkinje	9 semanas	ansiedade reduzida, hiperactividade, descoordenação motora, menor aumento de peso
Boy *et al.,* 2010	cDNA MJD1-1	huntingtina de rato	148	ubíquo	não	células de purkinje	48 semanas	hiperactividade em estadios precoces da doença, descordenação motora e alteração na aprendizagem motora em estadios avançados da doença
Silva-Fernandes et al., 2010	cDNA MJD1-1	CMV	83 e 94	ubíquo	sim	astrogliose e atrofia neuronal	16 semanas	descoordenação motora
Rattus norvegicus								
e.g. Alves *et al.,* 2008	cDNA MJD1a	Lentivirus (PGK)	27 e 72	Córtex cerebeloso ou estriado ou *Substantia nigra* (injecção)	sim	↓ do número de neurónios TH positivos na SN, degeneração no estriado, morte celular	ND	ND

Legenda: ND- não determinado

Appendix 2

"Screening of therapeutic compounds in a *C. elegans* model of Machado-Joseph disease"

Summary of the research project

Machado-Joseph disease (MJD), also known as spinocerebellar ataxia type 3, is a neurodegenerative disorder caused by the expansion of a polyglutamine (polyQ) tract within the C-terminal of the ataxin-3 protein. Ataxin-3 is known to interact with polyubiquitin chains and to have a deubiquitylase (DUB) activity *in vitro*, however the cellular and physiological role(s) of this protein remain unknown.

The leading hypothesis concerning the pathogenesis of polyQ diseases is that the expanded polyQ tract confers a toxic gain of function to the mutant proteins. These acquire the ability to self associate and form aggregates both with themselves and with other proteins, and form large nuclear and cytoplasmatic inclusions. There are conflicting reports on whether these large inclusions mediate subsequent neuronal dysfunction or if they are rather cytoprotective, being the result of a mechanism by which the cell protects itself against the production of soluble toxic oligomers. In any case, the presence of the expanded ataxin-3 (and potential formation of polyQ-containing fragments) has several pathophysiological consequences for the affected neurons. However, mutated ataxin-3 cannot be considered as a tractable drug target for small molecules itself, mainly due to a lack of knowledge of its in vivo functional activity, unsolved structure, absence of known relevant binding sites for small molecules and ubiquitous expression in many cell types. Alternative approaches using RNAi and intrabodies have shown recent promise in preventing the production of mutant ataxin-3, but toxicity effects have not been sufficiently tested, and delivery to the central nervous system remains an issue. The lack of therapeutic strategies that effectively prevent neurodegeneration in MJD patients prompted us to search for compounds that modulate mutant ataxin-3-related neurological dysfunction. For this purpose, our group has previously generated a transgenic mouse model of MJD which is currently being used by us to test selected compounds as therapeutic approaches to MJD, targeting three main biochemical pathways: inhibition of histone deacetylase activities, activation of Hsp70 and reduction of oxidative stress. Although these mice provide an excellent mammalian system to pre-clinically validate pharmacological strategies for the treatment of human disorders, they are hardly amenable to large-scale drug screenings that could allow the exploration of a much larger number of therapeutical possibilities. In this sense, cell lines are often used as a first-line approach, allowing the screening of libraries of compounds in a hypothesis-free manner, leading to the pre-selection of a smaller number of molecules to be tested *in vivo*, often in rodent and then primate models of a given disorder. In spite of the great advantages of this strategy, it faces the limitations that cell lines often display very specific characteristics, different from the cells they are meant to model – this is particularly true for neurons, which are

highly differentiated cells, that function as part of a network and require permanent interaction with other cellular types for their function.

Recent data from our lab have shown that many aspects of MJD can be properly modeled in the round worm *Caenorhabditis elegans*, and others have shown that it can provide a suitable platform for both the discovery of new bioactive compounds and target identification. This project is based on the idea that the transgenic *C. elegans* MJD model we generated can be used to perform large-scale drug screenings, in which the identification of effective drugs can be accomplished by looking simultaneously at protein aggregation (conformational disorder) in the live neuronal cells, and on its impact on neuron regulated behavior of the whole-animal (neurodegenerative disorder). Our specific goal at this stage is to screen a library of FDA-approved out-of-patent drug molecules for their ability to prevent or delay the formation of fluorescent mutant ataxin-3 aggregates by feeding them to our MJD *C. elegans* model. Additionally, we will address their effect on motor neuron dysfunction by performing an automated motility analysis.

We should be able to identify a number of efficacious compounds that can be tested in higher organisms, including our transgenic mouse model, and eventually enter clinical development. Our work can also contribute to the better understanding of MJD pathogenesis, as we can in the future identify, at the cellular level, the targets of these hit compound(s).

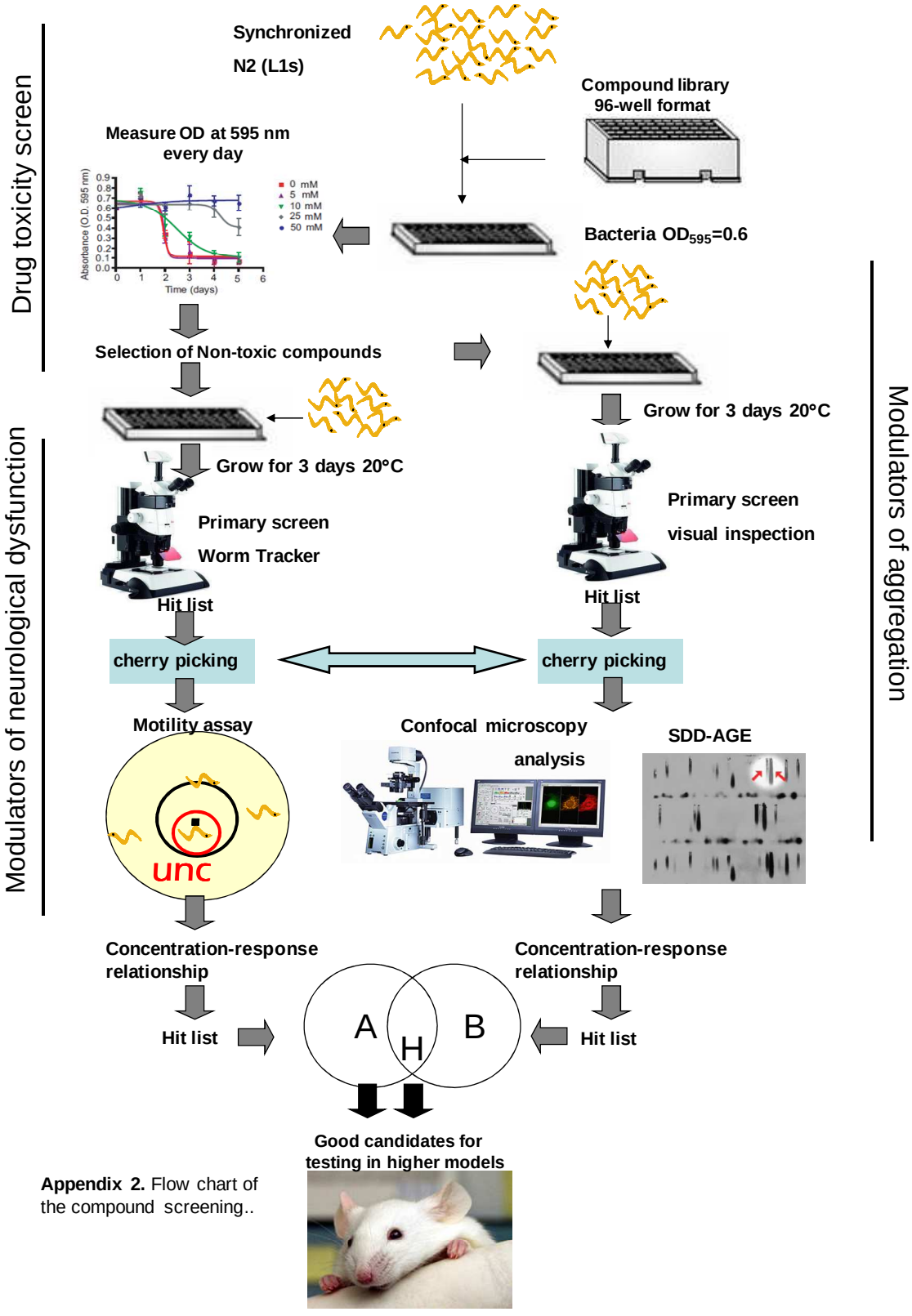

Appendix 2. Flow chart of the compound screening..